THERMOCHEMICAL BIOMASS UPGRADING FOR CO-GASIFICATION WITH COAL

by

Frank Nsaful

Dissertation presented for the Degree

of

DOCTOR OF PHILOSOPHY
(Chemical Engineering)

in the Faculty of Engineering
at Stellenbosch University

The financial assistance of the National Research Foundation (NRF) towards this research is hereby acknowledged. Opinions expressed and conclusions arrived at, are those of the author and are not necessarily attributed to the NRF

Supervisor
Prof. Johann F. Görgens

Co-Supervisor
Dr. François-Xavier Collard

March 2018

Declaration

By submitting this dissertation electronically, I declare that the entirety of the work contained therein is my own, original work, that I am the sole author thereof (save to the extent explicitly otherwise stated), that reproduction and publication thereof by Stellenbosch University will not infringe any third party rights and that I have not previously in its entirety or in part submitted it for obtaining any qualification.

Date: March 2018

This dissertation includes [2] original papers published in peer-reviewed journals or books and [2] unpublished publications. The development and writing of the papers (published and unpublished) were the principal responsibility of myself and, for each of the cases where this is not the case, a declaration is included in the dissertation indicating the nature and extent of the contributions of co-authors.

Abstract

Lignocellulosic biomass is considered as a sustainable and renewable fuel source with the potential to substitute or partially replace coal in applications such as gasification for energy generation due to its sustainable carbon as well as its potential to reduce greenhouse gas emissions. However, raw biomass differs significantly from coal in terms of several important fuel properties, such as low energy density, high moisture, oxygen and volatile matter contents. Due to this the co-utilization of raw biomass with coal in gasification systems has been shown to result in the increase in the production of oxygenated volatile compounds (tar precursors) which impacts negatively on the quality of the gasification products and causes critical operational problems. This challenge has limited the development of biomass-based gasification processes. Hence to ensure the effective and efficient utilization of lignocellulosic biomass with coal, an upgrading process is required to improve some biomass properties to make them more similar to that of coal. The approach of this work consists in a thermal pretreatment in order to generate char products with reduced oxygen and volatile matter contents.

The overall aim of the study therefore was to use thermochemical technologies (torrefaction and slow pyrolysis) as methods to pretreat lignocellulosic biomass feedstocks; pine (PN), bamboo (BB), corn cob (CC) and corn stover (CS) to produce upgraded biomass feedstocks (char), with reduced oxygen content as well as improved fuel properties, comparable to coal for use in co-gasification. For this task the study was divided into several objectives. The initial part focused on the characterization of the lignocellulosic chemical composition of the various biomass feedstocks. Next the types and quantities of oxygenated volatile products produced during the devolatilization of raw biomass feedstocks were studied. For this objective a novel analytical method incorporating the use of Thermogravimetric Analysis, thermal desorption and Gas Chromatography–Mass Spectrometry (herein referred as (TGA-TD/GC-MS) was developed and used to analyse and quantify the oxygenated volatile products. The analysis of the volatile composition data by means of principal components analysis (PCA) showed a clear correlation between lignocellulose chemical composition and the type and quantities of oxygenated volatile compounds produced during biomass devolatilization.

The influence of thermal pretreatment conditions (temperature and time) on the structural transformation of raw biomass and on the volatile evolution mechanism of the resulting char during subsequent char devolatilization was also studied. Thermal pretreatment was done within the temperature range of 250-400 ^{o}C and hold time at pretreatment temperature of 30 and 60 min. It was observed that the temperature had a more profound effect than hold time during thermal pretreatment. The distribution of char devolatilization products was shown to be consistent with the extent of biomass transformation during thermal pretreatment. The biomass composition, particularly cellulose crystallinity, had an impact during thermal pretreatment. It was shown that for biomass feedstock with high degree of crystallinity such as PN a higher temperature (>300 ^{o}C) was required to achieve significant cellulose degradation. Hence char produced from such feedstock at temperature ≤300 ^{o}C generated high amount of anhydrosugar and furan volatiles during the char devolatilization.

With the aim of using pretreated biomass with coal for co-gasification, biomass chars produced at different pretreatment temperatures were compared to coal in terms of fuel properties (proximate and elemental composition and Higher Heating Value), with particular attention given to the composition of oxygenated volatile compounds generated during the devolatilization stage. The result of the study showed that chars produced at temperature ≥350 ^{o}C had fuel properties comparable to that of coal. In addition these chars produced mainly aromatic hydrocarbons and phenolics during devolatilization which were similar to the volatiles generated from coal under identical conditions. Hence the pretreatment temperature of at least 350 ^{o}C is recommended when considering coal substitution, while 400 °C could be considered in the case of samples with high lignin (softwood) or high inorganic contents. Finally, the reactivity of the biomass chars under gasification condition was investigated. The devolatilization characteristics and CO_2 gasification kinetics of biomass/char (produced at 350 ^{o}C) and coal at different blend ratios were studied. The devolatilization characteristics of char were found to follow the profile of coal especially at blend ratios of 10 wt% and 20 wt% with no particular synergy detected, while the kinetic parameters were also comparable. This work confirmed the potential of the use of thermally pretreated biomass chars for coal substitution in gasification process and brought decisive insights for the implementation of future tests at pilot scale.

Opsomming

Lignosellulosiese biomassa word beskou as ’n volhoubare en hernubare bron van brandstof met die potensiaal om steenkool heeltemal of gedeeltelik te vervang in toepassings soos vergassing vir energie generasie. Hierdie beskouing is as gevolg van die lignosellulosiese biomassa se koolstof en sy potensiaal om groenhuisgasuitlate te verminder. Nogtans verskil biomassa van steenkool in terme van verskeie brandstofeienskappe, soos lae energiedigtheid, hoë voginhoud, hoë suurstofinhoud, en hoë vlugtige-materiaal-inhoud. Daarom was dit bevind dat die gesamentlike gebruik van biomassa met steenkool in vergassing sisteme ’n toename in oksigeneerde vlugtige verbindings (teer-voorgangers) tot gevolg het, wat ’n negtiewe impak op die kwaliteit van die vergassingprodukte het en kritiese bedryfsprobleme veroorsaak. Hierdie uitdaging beperk die ontwikkeling van biomassa-baseerde vergassing sisteme. Dus, om die effektiewe en doeltreffende gebruik van biomassa met steenkool te verseker, word ’n opgegradeerde proses benodig om sommige van die biomassa einskappe te verbeter om meer soos die van steenkool te wees. Die benadering in hierdie werk bestaan uit ‘n termiese voorbehandeling om houtskool produkte met verminderde suurstof en vlugtige-materiaal inhoud te genereer.

Die algehele doelwit was dus om termochemiese tegnologie (uitdroging en stadige pirolise) as metodes te gebruik vir die voorbehandeling van lignosellulosiese biomassa grondstowwe: denne (PN), bamboes (BB), mieliestronk (CC), en mieliestrooi (CS) om opgegradeerde biomassa grondstof (houtskool) te produseer, wat verminderde suurstofinhoud sowel as verbeterde brandstofeienskappe vergelykend met die van steenkool het, vir die gebruik in gesamentlike vergassing. Vir die taak is die studie in verskeie doelstellings verdeel. Die aanvanklike gedeelte het gefokus op die karaktarisering van die lignosellulosiese chemiese samestelling van die verskeie biomassa grondstowwe. Volgende is die tipes en hoeveelhede oksigeneerde vlugtige produkte wat tydens die verwydering van vlugtige komponente uit rou biomassa grondstowwe verkry is studeer. Vir hierdie doelstelling was ’n nuwe analitiese metode ontwikkel wat die gebruik van Termogravimetriese Analise, termiese-desorpsie en Gas-Chromatografie-Massaspektrometrie (verwys na as TGA-TD/GC-MS) insluit. Die metode was gebruik om die oksigeneerde vlugtige produkte te analiseer en te kwantifiseer. Die analise van die data oor die vlugtige komponente samestelling is gedoen met hoofkomponente-analise (PCA) en dit het ’n duidelike verwantskap gewys tussen lignosellulosiese-chemiese-samestelling en die tipe en hoeveelhede oksigeneerde

vlugtige verbindings wat produseer word tydens die verwydering van vlugtige komponente uit biomassa uit.

Die invloed van termiese voorbehandeling kondisies (temperatuur en tyd) op die strukturele verandering van rou biomassa en op die vlugtige komponent evolusie meganisme van die resulterende houtskool tydens die opvolgende verwydering van vlugtige komponente uit die houtskool uit, was ook gebestudeer. Termiese voorbehandeling was gedoen binne die temperatuuromvang van 250-400 ^{o}C en hou-tyd by voorbehandelingstemperatuur van 30 en 60 min. Dit was opgemerk dat temperatuur ‘n groter effek as hou-tyd gehad het tydens termiese voorbehandeling. Dit was gewys dat die verspreiding van produkte van die verwydering van vlugtige komponente uit die houtskool uit ooreenstem met die mate van biomassa verandering tydens termiese voorbehandeling. Die biomassa samestelling, veral sellulose kristalliniteit, het ‘n impak gehad tydens termiese voorbehandeling. Dit was bevind dat vir ‘n biomassa grondstof met ‘n hoë graad van kristalliniteit, soos PN, was ‘n hoër temperatuur (>300 ^{o}C) benodig om beduidende sellulose degradasie te behaal. Gevolglik het die houtskool geproduseer van sulke grondstowwe by temperature <300 ^{o}C, hoë hoeveelhede anhidriese suikers en furan vlugtige komponente gegenereer tydens die verwydering van vlugtige komponente vanuit die houtskool.

Met die doelwit om voorbehandelde biomassa te gebruik in die gesamentlike vergassing met steenkool, was biomassa-houtskool, geproduseer by verskillende voorbehandelingstemperature, vergelyk met steenkool in terme van brandstofeienskappe (algemene en elementele samestelling en Hoër Verbrandings Waarde), met spesifieke aandag aan die samestelling oksigeneerde vlugtige verbindings wat gegenereer is tydens die verwydering van vlugtige komponente. Die resultaat van die studie het gewys dat houtskool geproduseer by temperature ≥350 ^{o}C, brandstofeienskappe vergelykbaar met die van steenkool gehad het. Daarbenewens het die houtskole hoofsaaklik aromatiese koolwaterstowwe en fenole geproduseer tydens die verwydering van vlugtige komponente, wat soortgelyk was aan die vlugtige komponente gegenereer van steenkool onder identiese kondisies. Daarom word die voorbehandelingstemperatuur van ten minste 350 ^{o}C aanbeveel wanneer steenkoolvervanging oorweeg word, terwyl 400 ^{o}C oorweeg kan word in die geval van monsters met hoë lignien (sagtehout) of hoë anorganiese inhoud. Laastelik was die reaktiwiteit van biomassa houtskool onder vergassingtoestande ondersoek. Die eienskappe tydens

die verwydering van vlugtige komponente en die CO_2 vergassings-kinetika van biomassa/houtskool (geproduseer by 350 ^oC) en steenkool by verskillende vermengingsverhoudinge was gebestudeer. Dit was gevind dat die eienskappe van houtskool tydens die verwydering van vlugtige komponente dieselfde profiel as steenkool volg veral by vermengingsverhoudinge van 10 wt% en 20 wt% en geen spesifieke sinergie was opgemerk nie, terwyl die kinetiese parameters ook vergelykbaar was. Die werk het die potensiaal van die gebruik van termiese voorbehandelde biomassa houtskool in die vervanging van steenkool in vergassing prosesse bevestig en beslissende insigte voortgebring vir die implementering van toekomstige toetse op toetsskaal.

Declaration of contributions to the work

Declaration by candidate

With regard to the chapters as detailed below, the nature and scope of my contribution were as follows:

Chapter	Pages	Nature of contribution	Contribution (%)
3	46-76	Details provided on page 46	75
4	77-108	Details provided on page 76	80
5	109-137	Details provided on page 107	80
6	138-163	Details provided on page 135	80

The following co-authors have contributed to the following chapters:

Name	e-mail address	Chapters	Pages	Nature of contribution	Contribution (%)
François-Xavier Collard	fcollard@sun.ac.za	3	46-76	Details provided on page 46	10
		4	77-108	Details provided on page 76	15
		5	109-137	Details provided on page 107	15
		6	138-163	Details provided on page 135	15
Johann F. Görgens	jgorgens@sun.ac.za	3	46-76	Details provided on page 46	5
		4	77-108	Details provided on page 76	5
		5	109-137	Details provided on page 107	5
		6	138-163	Details provided on page 135	5
Johannes H. Knoetze	jhk@sun.ac.za	3	46-76	Details provided on page 46	5
Marion Carrier	m.carrier@aston.ac.uk	3	46-76	Details provided on page 46	5

"Declarations(s) with signature(s) are kept with the candidate and supervisor" in respect of declarations on authorship of the papers

Date: ……..……

Declaration by co-authors

The undersigned hereby confirm that:

- the declaration above accurately reflects the nature and extent of the contributions of the candidate and the co-authors to the chapters as specified above,
- no other authors contributed to these chapters besides those specified above, and
- potential conflicts of interest have been revealed to all interested parties and that the necessary arrangements have been made to use the material in this dissertation.

Signature	Institutional affiliation	Date
Declarations(s) with signature(s) are kept with the candidate and supervisor" in respect of declarations on authorship of the papers	Stellenbosch University Stellenbosch University Stellenbosch University Aston University	

Acknowledgement

"Oh for a thousand tongues to sing my great redeemer's praise".

Thank you so much Lord Jesus Christ for seeing me through this PhD journey. I would not have made it this far if not for your righteous right hand that has always held and sustained me.

My appreciation also goes to the following people and institutions:

Professor Johann Görgens my promoter for his supervisory role. Thank you for your invaluable contribution towards this work.

Dr. François-Xavier Collard – indeed words cannot express how much grateful I am to you. I am forever thankful to you for your inputs in this work and most especially for the motivation and encouragement you rendered to me throughout the course of the studies.

Professor Hansie Knoetze and Dr. Marion Carrier – thank you for your involvement and contributions during the initial stages of this work.

Mrs. Hanlie Botha – for introducing me to the field of GC/MS and thermal desorption and for your assistance in the analytical lab. Thank you.

The NRF, Sasol and the Department of Process Engineering – your financial support towards this project is very much appreciated.

My family and friends – thank you for your encouragement and prayer support and for showing me so much love.

Dedication

To the glory of the Almighty God

Table of contents

List of tables

List of figures

Chapter 2

Chapter 3

Chapter 4

Chapter 5

Chapter 6

Chapter 1

Introduction

1.1. Background and context

The overuse of fossil fuels for the production of energy is having negative effect on the environment due to the generation of greenhouse gases from the use of such fuels leading to increased global warming. Additionally these fossil-based fuels are non-renewable and are depleting with time hence the need for an alternative renewable and environmental friendly fuel source for energy production. Lignocellulose biomass is a renewable and a clean energy source with a sustainable carbon [1] and can be converted into energy products for various types of fuel applications (heat, power, transportation fuel, etc.) [2].

Biomass can serve as a feedstock for the production of chemicals, materials, electricity, liquid fuels and heat through thermochemical processes such as combustion, gasification and pyrolysis, and through biochemical processes such as saccharification-fermentation [1,3]. However, compared to fossil fuels, the use of raw biomass comes with problems such as low bulk density, high moisture content and low energy density, which impacts negatively on its potential to act as replacement for fossil fuels such as coal [2,4]. The low bulk density implies higher transport and storage cost which is further compounded by the high moisture content. The high moisture content also leads to reduced heating value of the biomass and makes it susceptible to microbial decay which might result in self-heating/combustion during storage [5–7]. Thus to be able to use biomass in a more efficient and economical way for energy production via any of the above mentioned conversion routes, it is required to address these challenges associated with biomass.

Gasification is seen to be one of the preferred thermochemical conversion routes for producing fuels, chemicals and electricity from biomass, due to its relatively high efficiency [1,8,9]. It involves the conversion of a carbon based feedstock into a fuel gas under partial oxidative conditions at temperatures of about 800 ^{o}C and above [1]. The application of gasification using coal is a well-established technology in South Africa. Coal is converted to syngas and further

processed into liquid fuel by Fisher-Tropsch (FT) in the coal-to-liquid (CTL) process run by Sasol in Sasolburg and Secunda, South Africa. Though coal still remains a dominant solid fuel source in the energy and chemical industry, it is however associated with the emission of high levels of fossil based CO_2 and pollutant emissions in the form of NO_x and SO_2 [10,11], resulting in major production of greenhouse gases (GHG) which contribute to global warming. Hence the potential to introduce renewable biomass with relatively low N and S contents [1], as coal substitute in the CTL process.

Ciferno and Marano [12] in their study proposed three options for the introduction of biomass into already existing CTL processes:

i. Setting up of separate biomass and coal gasification units
ii. Replacing a part of the coal with biomass in existing coal gasification unit
iii. Biomass upgrading by torrefaction/pyrolysis thermal pretreatment for co-feeding with coal into existing coal gasification unit.

Even though dedicated biomass gasification is feasible and has the advantage of ensuring that biomass is gasified at its optimum gasification conditions, thereby producing quality gas from biomass, this option has a major drawback which is the high capital cost required to setup such units [3,13]. There is also the heterogeneous nature of biomass which will require special handling systems [2]. The second option involves the co-gasification of coal and raw biomass in a single gasifier unit. The merits of this option are that it eliminates the cost associated with the setting up of a dedicated biomass facility [10,14,15] and reduces issues regarding biomass supply [3,14,15] as biomass supply is season dependent. In addition, replacing part of the coal with biomass reduces the emission of fossil based CO_2 due to the CO_2 neutrality of biomass [3,10] provided fossil fuel input into the planting, harvesting and transportation of biomass is kept at the barest minimum. Also, NO_x and SO_2 emissions are reduced due to low nitrogen and sulphur contents of biomass [1].

The second option was applied in the study of Aboyade [16] on the co-gasification of coal and agricultural residues in a Lurgi type gasifier used by Sasol for its CTL process. The study concentrated on the upper part of the gasifier, which forms the devolatilization/pyrolysis section,

and analysed the impact of the biomass addition on the yields and composition of gas and volatile compounds in the gasifier during co-pyrolysis/co-gasification. It was observed that the addition of biomass resulted in a significant increase in gas and volatiles production. Similar observation has been reported by other researchers [17–19]. This increase in volatile/tar yield when biomass is co-gasified with coal, compared to gasification of coal alone, is due to the differences in chemical structure of coal and biomass. Biomass structure mostly consists of R-O-R and C-C bonds with lower bond energies (380 – 420 kJ/mol) linking its components together, compared to the strong cross-linked C=C aromatic bonds (bond energy: 1000 kJ/mol) involved in the structure of coal [20]. Therefore, biomass breaks down faster during the pyrolysis step of the gasification process leading to the release of more gas and volatiles. Despite this increase in gas yield, Aboyade [16] found that co-gasification of raw biomass and coal blend impacted negatively on the quality and composition of the volatile fraction. Notably it was found that the raw biomass introduced high levels of oxygenated organic compounds into the volatile stream. This is because biomass has a much higher elemental oxygen content [2,4,21], which leads not only to volatiles production, but also production of oxygenates. Due to their instability and potential to recombine into heavier compounds (known as tar), the presence of these oxygenates result in decreased conversion efficiency and pose both technical and economic challenges during the downstream processing. These oxygenated compounds cause problems such as condensation, fouling and corrosion of process equipment [8,22,23]. Also, they cannot be tolerated in downstream processes, as this would result in fuels that do not meet specifications. Therefore, to be able to introduce them into the condensates stream, there will be the need to install additional costly equipment downstream to remove these oxygenates, to ensure that fuel quality is maintained. However, doing this will also lead to reduced conversion efficiency. That is why pretreating biomass upfront in order to limit the formation of oxygenated volatiles is more recently considered.

Considering this challenge and other negative characteristics of raw biomass such as low bulk density, high moisture content, low energy density, poor grindability, heterogeneity and hygroscopic nature [2,4,21], it is required that a pre-treatment step aimed at reducing such problems mentioned above be applied to raw biomass before its utilization in co-gasification with coal. Several methods have been suggested for use in improving biomass properties for energy conversions. Notably among these are torrefaction and slow pyrolysis which are thermal

pretreatment methods [24]. Both thermal pretreatment methods are usually carried out in an inert atmosphere and at low heating rate (<50 ^{o}C/min) with torrefaction taking place in the temperature range 200-300 ^{o}C [5,25] and slow pyrolysis occurring between 300 and 500 ^{o}C [26]. Previous studies have shown that thermal pretreatment impacts positively on biomass properties producing a solid product (char) with reduced moisture content [24,27], improved grindability [5,28], increased energy density [29] and is homogenous [30] and hydrophobic in nature [31,32], resulting in a material more similar to coal. Moreover, the char tends to have a reduced O/C ratio thus giving improved co-gasification efficiency when compared to raw biomass [33]. Additionally, the thermal pretreatment leads to a significant removal of oxygenated groups as a result of the degradation of biomass components. Thus the char produced will have a reduced oxygen content and hence will generate less oxygenated compounds when blended with coal as fuel for co-gasification.

In this study thermal pretreatment (torrefaction/slow pyrolysis) was used to upgrade the properties of selected lignocellulosic biomass feedstocks (pine, bamboo, corn residues) for co-gasification with coal. More specifically biomass samples were pretreated to produce upgraded biomass (char) with reduced oxygen content and other acceptable fuel properties for coal substitution. The study first examines the lignocellulosic chemical composition and fuel properties of raw biomass samples. Then raw biomass samples were devolatilized and the generated volatiles were analysed to identify and quantify the oxygenated compounds, which was achieved through the development of an appropriate analytical method. Following this biomass samples were pretreated at varying conditions and the char products were analysed to establish the impact of the pretreatment on the transformation and evolution mechanism during char devolatilization. Subsequently chars were characterized and compared to coal in terms of fuel properties (proximate and elemental analysis and higher heating value) and volatile composition with emphasis placed on identifying the best pretreatment condition. Finally, the upgraded biomass (char) samples were blended with coal for co-gasification which was simulated in a thermogravimetric analyser (TGA). The impact of the biomass addition was established through kinetics study.

1.2. Motivation

Lignocellulosic biomass is a sustainable fuel with the potential of replacing coal in energy generation systems such as gasification due to its renewable carbon and low environmental emissions. However, it is characterized by negative attributes such as high oxygen content leading to decreased conversion efficiency and the increased production of oxygenated volatiles/tars during gasification conversion, which causes operational problems. Biomass could be upgraded through thermal pretreatment (torrefaction/slow pyrolysis) to produce char with improved fuel quality and reduced oxygen content thus serving as potential feedstock for co-gasification. Though studies on thermal pretreatment methods for char production is gaining attention recently, only few have focused on the extensive characterization of the char, and more particularly on the impact of the pretreatment on the composition of oxygenated volatiles generated during the subsequent conversion of the char. Hence, the need to bridge the information gap. Also limited information exist on the use of pretreated biomass in co-gasification and the effects thereof.

1.3. Aim and objectives

The overall aim of the study was to use thermal pretreatment (torrefaction/slow pyrolysis) as a means of upgrading lignocellulosic biomass to produce a char with required fuel properties for use with coal in co-gasification which will also result in the generation of a limited amount of oxygenated volatiles during the pyrolysis/devolatilization stage of gasification. In order to understand the impact of the pretreatment conditions and biomass composition, a particular attention was given to the mechanisms occurring during biomass pretreatment and char devolatilization.

The following research questions were therefore defined:

- What types and quantities of oxygenated volatile compounds are produced during the devolatilization of raw biomass and how does these relate to the lignocellulosic composition of biomass?
- What are the effects of thermal pretreatment conditions on biomass transformation and on the evolution of oxygenated volatile compounds generated during char conversion?

- How does thermally pretreated biomass (char) compare with coal in terms of fuel properties (proximate and elemental analysis and higher heating value) and oxygenated volatiles composition at the preferred pretreatment condition?
- What are the impacts of pretreated biomass on devolatilization characteristics and gasification kinetics when blended with coal?

The aim and the questions were realised through the following objectives:

1. Characterization of lignocellulosic biomass

Lignocellulosic biomass comes from several sources ranging from hardwood to softwood, herbaceous plants and grass. The type and origin of biomass largely determines their lignocellulosic composition which in turn affects their behaviour during thermal conversion and the composition of the devolatilization products. It is therefore essential to determine the lignocellulosic composition of various biomass feedstocks in order to determine their potential for fuel application and also to be able to draw the relationship between the lignocellulosic composition and volatiles products.

This objective was achieved using standard laboratory analytical procedures outlined in literature. The details of this are found in chapter 3 while the results are also utilised in chapters 4-6.

2. Devolatilization and analysis of oxygenated volatiles through the development of an appropriate volatiles analysis method

Given that biomass is a complex mixture of polymers, several compounds covering a wide range of molecular weight are produced during thermal conversion. Hence an appropriate analytical method is required for the determination and quantification of the range of oxygenated volatile compounds.

A novel method incorporating the use of thermogravimetric analysis (TGA), capture of the volatiles using thermal desorption tubes, thermal desorption and Gas Chromatography/Mass Spectrometry (GC/MS) was developed for the analysis of the devolatilization products. The method was used to study the oxygenated volatiles composition from the devolatilization of raw biomass and the data used to establish the influence of biomass component on volatile distribution through principal component analysis (PCA) in chapter 3. The method was also applied in chapter 4 and 5 for the analysis of oxygenated volatiles produced during char and coal devolatilization.

3. Thermal pretreatment of biomass feedstocks and analysis of oxygenated volatiles from char

The severity of the pretreatment conditions will have different transformational effects on biomass. Depending on the type of biomass and lignocellulosic composition, different biomass feedstocks will be transformed differently when pretreated at the same condition thereby influencing the volatile composition during char devolatilization.

The effect of thermal pretreatment conditions on biomass transformation and evolution profile of volatiles were therefore studied. Biomass feedstocks were pretreated at various conditions of temperature and time. The chars were then devolatilized and the composition of oxygenated volatiles quantified using the developed analytical method. The study is detailed in chapter 4.

4. Comparison of fuel properties and devolatilization volatiles of coal and chars

For this objective, coal as well as biomass chars were analysed for oxygenated volatiles composition, proximate and elemental analysis and HHV with the aim of determining char with appropriate properties for co-gasification. The study is detailed in chapter 5.

5. Devolatilization characteristics and gasification of coal and biomass char blends

The impact of char blending ratio on devolatilization characteristics and CO_2 gasification was studied under atmospheric conditions simulated in a TGA. Subsequently the data was used to generate kinetic parameters to compare the performance of the gasification conversion (chapter 6).

1.4. Dissertation layout

This dissertation is divided into seven (7) chapters. Chapter 1 is the introductory chapter and provides information on the context and background to the study as well as the study objectives. A literature review is given in chapter 2. Chapters 3, 4, 5 and 6 are a compilation of journal articles/manuscripts covering the objectives of this work. Chapter 3 is focused on the characterization of lignocellulose biomass; the devolatilization, identification and quantification of oxygenated volatiles from raw biomass. The development of a novel analytical method for the analysis of oxygenates is also detailed in chapter 3. Chapter 4 is about the pretreatment of biomass and subsequent devolatilization of the resulting char with in-situ oxygenates analysis thereby providing information on the evolution mechanism of volatiles as following pretreatment. In

chapter 5, pretreated biomass (char) is compared with coal on the basis of oxygenated volatile composition and fuel properties (proximate and elemental analysis and heating value. Chapter 6 studies the devolatilization characteristic and gasification kinetics of pretreated biomass and coal blends. Conclusion and recommendations are given in chapter 7.

References

[1] M.J.C. van der Stelt, H. Gerhauser, J.H.A. Kiel, K.J. Ptasinski, Biomass upgrading by torrefaction for the production of biofuels: A review, Biomass and Bioenergy. 35 (2011) 3748–3762.

[2] D. Medic, M. Darr, A. Shah, B. Potter, J. Zimmerman, Effects of torrefaction process parameters on biomass feedstock upgrading, Fuel. 91 (2012) 147–154.

[3] L. Emami-Taba, M.F. Irfan, W.M.A. Wan Daud, M.H. Chakrabarti, Fuel blending effects on the co-gasification of coal and biomass – A review, Biomass and Bioenergy. 57 (2013) 249–263.

[4] M. Phanphanich, S. Mani, Impact of torrefaction on the grindability and fuel characteristics of forest biomass, Bioresour. Technol. 102 (2011) 1246–1253.

[5] B. Arias, C. Pevida, J. Fermoso, M.G. Plaza, F. Rubiera, J.J. Pis, Influence of torrefaction on the grindability and reactivity of woody biomass, Fuel Process. Technol. 89 (2008) 169–175.

[6] E.S. Lipinsky, J.R. Arcate, T.B. Reed, Enhanced wood fuels via torrefaction, ACS Div. Fuel Chem. Prepr. 47 (2002) 408–409.

[7] T.G.G. Bridgeman, J.M.M. Jones, I. Shield, P.T.T. Williams, Torrefaction of reed canary grass, wheat straw and willow to enhance solid fuel qualities and combustion properties, Fuel. 87 (2008) 844–856.

[8] F.J. Wang, S. Zhang, Z.D. Chen, C. Liu, Y.G. Wang, Tar reforming using char as catalyst during pyrolysis and gasification of Shengli brown coal, J. Anal. Appl. Pyrolysis. 105 (2014) 269–275.

[9] Q. Chen, J.S. Zhou, B.J. Liu, Q.F. Mei, Z.Y. Luo, Influence of torrefaction pretreatment on biomass gasification technology, Chinese Sci. Bull. 56 (2011) 1449–1456.

[10] A. Smoliński, N. Howaniec, Application of gas chromatography in the study of steam gasification and co-gasification of hard coal and biomass chars, Acta Chromatogr. 25 (2013) 317–330.

[11] A. Demirbaş, Sustainable cofiring of biomass with coal, Energy Convers. Manag. 44 (2003) 1465–1479.

[12] J.P. Ciferno, J.J. Marano, Benchmarking biomass gasification technologies for fuels, chemicals and hydrogen production, US Dep. Energy. Natl. Energy. (2002) 58.

[13] R.H. Williams, E.D. Larson, G. Liu, T.G. Kreutz, Fischer-Tropsch fuels from coal and biomass: Strategic advantages of once-through ("polygeneration") configurations, Energy Procedia, 1 (2009) 4379–4386.

[14] N. Koukouzas, A. Katsiadakis, E. Karlopoulos, E. Kakaras, Co-gasification of solid waste and lignite - A case study for Western Macedonia, Waste Manag. 28 (2008) 1263–1275.

[15] A.O. Aboyade, M. Carrier, E.L. Meyer, H. Knoetze, J.F. Görgens, Slow and pressurized co-pyrolysis of coal and agricultural residues, Energy Convers. Manag. 65 (2013) 198–207.

[16] A.O. Aboyade, Co - Gasification of Coal and Biomass : Impact on Condensate and Syngas Production, 2012. Phd thesis submitted to Stellenbosch University.

[17] T. Sonobe, N. Worasuwannarak, S. Pipatmanomai, Synergies in co-pyrolysis of Thai lignite and corncob, Fuel Process. Technol. 89 (2008) 1371–1378.

[18] C. Meesri, B. Moghtaderi, Lack of synergetic effects in the pyrolytic characteristics of woody biomass/coal blends under low and high heating rate regimes, Biomass and Bioenergy. 23 (2002) 55–66.

[19] M.W. Seo, J.H. Goo, S.D. Kim, S.H. Lee, Y.C. Choi, Gasification characteristics of coal/biomass blend in a dual circulating fluidized bed reactor, Energy and Fuels. 24 (2010)

3108–3118.

[20] B. Moghtaderi, C. Meesri, T.F. Wall, Pyrolytic characteristics of blended coal and woody biomass, in: Fuel, 2004: pp. 745–750.

[21] Q. Lu, X.C. Yang, C.Q. Dong, Z.F. Zhang, X.M. Zhang, X.F. Zhu, Influence of pyrolysis temperature and time on the cellulose fast pyrolysis products: Analytical Py-GC/MS study, J. Anal. Appl. Pyrolysis. 92 (2011) 430–438.

[22] L.F. de Diego, F. García-Labiano, P. Gayán, A. Abad, T. Mendiara, J. Adánez, M. Nacken, S. Heidenreich, Tar abatement for clean syngas production during biomass gasification in a dual fluidized bed, Fuel Process. Technol. 152 (2016) 116–123.

[23] J. Han, H. Kim, The reduction and control technology of tar during biomass gasification/pyrolysis: An overview, Renew. Sustain. Energy Rev. 12 (2008) 397–416.

[24] P. Rousset, C. Aguiar, N. Labbé, J.-M. Commandré, Enhancing the combustible properties of bamboo by torrefaction., Bioresour. Technol. 102 (2011) 8225–31.

[25] M. Broström, A. Nordin, L. Pommer, C. Branca, C. Di Blasi, Influence of torrefaction on the devolatilization and oxidation kinetics of wood, J. Anal. Appl. Pyrolysis. 96 (2012) 100–109.

[26] A.V. Bridgwater, Renewable fuels and chemicals by thermal processing of biomass, Chem. Eng. J. 91 (2003) 87–102.

[27] J.H. Peng, H.T. Bi, C.J. Lim, S. Sokhansanj, Study on density, hardness, and moisture uptake of torrefied wood pellets, Energy and Fuels. 27 (2013) 967–974.

[28] A. Ohliger, M. Förster, R. Kneer, Torrefaction of beechwood: A parametric study including heat of reaction and grindability, Fuel. 104 (2013) 607–613.

[29] W. Yan, T.C. Acharjee, C.J. Coronella, V.R. Vásquez, Thermal pretreatment of lignocellulosic biomass, Environ. Prog. Sustain. Energy. 28 (2009) 435–440.

[30] C. Couhert, S. Salvador, J.-M. Commandré, Impact of torrefaction on syngas production

from wood, Fuel. 88 (2009) 2286–2290.

[31] F.F. Felfli, C.A. Luengo, J.A. Suárez, P.A. Beatón, Wood briquette torrefaction, Energy Sustain. Dev. 9 (2005) 19–22.

[32] H. Li, X. Liu, R. Legros, X.T. Bi, C.J. Lim, S. Sokhansanj, Torrefaction of sawdust in a fluidized bed reactor, Bioresour. Technol. 103 (2012) 453–458.

[33] M.J. Prins, K.J. Ptasinski, F.J.J.G. Janssen, Torrefaction of wood. Part 2. Analysis of products, J. Anal. Appl. Pyrolysis. 77 (2006) 35–40.

Chapter 2

Literature

This chapter presents firstly the compositional characteristics of lignocellulosic biomass. Secondly, the advantages of thermal pretreatment to improve the fuel properties of lignocellulosic biomass are described. Finally, this review focusses on the properties of pretreated biomass in the context of gasification, the technology of interest in this study, with a particular attention given to the volatiles released during the pyrolysis/devolatilization stage.

2.1. Lignocellulosic biomass

Lignocellulosic biomass is produced by living organisms (excluding micro-organisms such as micro-algae) that utilizes the energy of the sun through the process of photosynthesis to store energy. It is composed of three main chemical components; hemicellulose, cellulose and lignin. In addition to this are other minor components such as extractives and inorganic materials [1–4]. Sources of lignocellulosic biomass include waste and by-products from agro-processing, forest products, crop residues and energy crops and can be generally classified into softwood, hardwood, and non woody (some agricultural residues, herbaceous plants, etc.) biomass. The chemical composition of lignocellulosic biomass is dependent on specie and factors such as environmental conditions, maturity, geographic location, variety, harvesting period and season [5]. Table 2-1 gives the chemical compositions of some selected biomass feedstocks [6]. Generally woody based biomass feedstocks tend to contain more cellulose (40-50 wt.%, dry basis) than the agricultural residues and herbaceous plants. Also softwoods contain more lignin than hardwoods. The three main chemical components of lignocellulosic biomass are described below.

Table 2-1: Cellulose, hemicellulose and lignin composition of lignocellulose feedstocks (wt%, dry basis) [6]

Lignocellulose feedstock	Cellulose	Hemicellulose	Lignin
Softwoods			
Douglas fir	50	2.4 – 3.4	28.3
Pine	44.6	5.3 – 8.8	27.7
Spruce	45	6.6	27.9
Hardwoods			
Black locust	41.6	17.7	26.7
Hybrid poplar	44.7	18.6	26.4
Eucalyptus	49.5	13.1	27.7
Populous tristis	40 – 49.9	13 – 17.4	18.1 - 20
Crop residues			
Corn cobs	45	35	15
Corn stover	36.8 – 39	14.8 – 25	15.1 – 23.1
Cotton gin trash	20	4.6	17.6
Rice hults	36.1	14	19.4
Wheat straw	30 – 38	21 – 50	20 – 23.4
Herbaceous materials			
Bermuda grass	25	35.7	6.4
Switch grass	31 – 38	20.4 – 25.2	14.5 – 18.1

2.1.1. Cellulose

Cellulose is by far the most abundant component of biomass forming about 40-50% of wood based feedstocks [7,8]. Figure 2-1 is an illustration of cellulose polymer. It is a polymer of D-glucose units linked by β-(1-4) glucosidic bonds and has a high degree of polymerization (500-10000) and molecular weight ($\geq 10^6$ amu) [9]. Cellulose is insoluble in most solvents and the molecules are joined together by inter and intra-molecular hydrogen bonds between OH groups resulting in an organized structure [8,10]. The highly organized fraction, named crystalline cellulose, is responsible for the strength of cellulose and makes up for 60-70% of total cellulose with the remainder being amorphous cellulose [3,8].

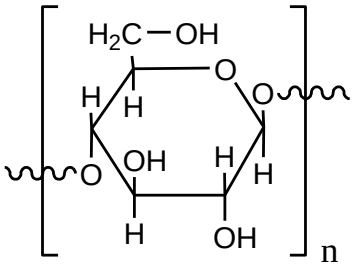

Figure 2-1: An illustration of cellulose polymer

2.1.2. Hemicellulose

Hemicellulose also known as polyose is the next most predominant component of lignocellulosic biomass after cellulose. It constitutes 20-35% and 20-30% of herbaceous and woody biomass feedstocks respectively [8]. Hemicellulose is located in plant cell wall and is bound to cellulose by hydrogen bonds and lignin by covalent bonds. Its degree of polymerization ranges from 100 to 200 units [11] and the molecules are characterized by highly branched and amorphous structures[3,8]. Hemicellulose is a polysaccharide polymer made up of monomers of hexose (six-carbon) and pentose (five-carbon) sugars. The pentose monomers consist of xylose, arabinose and rhamnose while the hexose monomers are mannose, glucose and galactose [12] as illustrated in Figure 2-2. Depending on the biomass type the amount of these sugar units might differ significantly. While hardwood, herbaceous and agricultural residues hemicellulose is predominantly xylan (main chain composed of xylose), softwood on the other hand mostly contain galactoglucomannan (a polymer made up of glucose, galactose and mannose monomers) [11,13,14]. Aside the sugar monomer units, hemicellulose also contains galacturonic acid, 4-O-methyle-D-glucuronic acid, glucuronic acid and acetyl substituents.

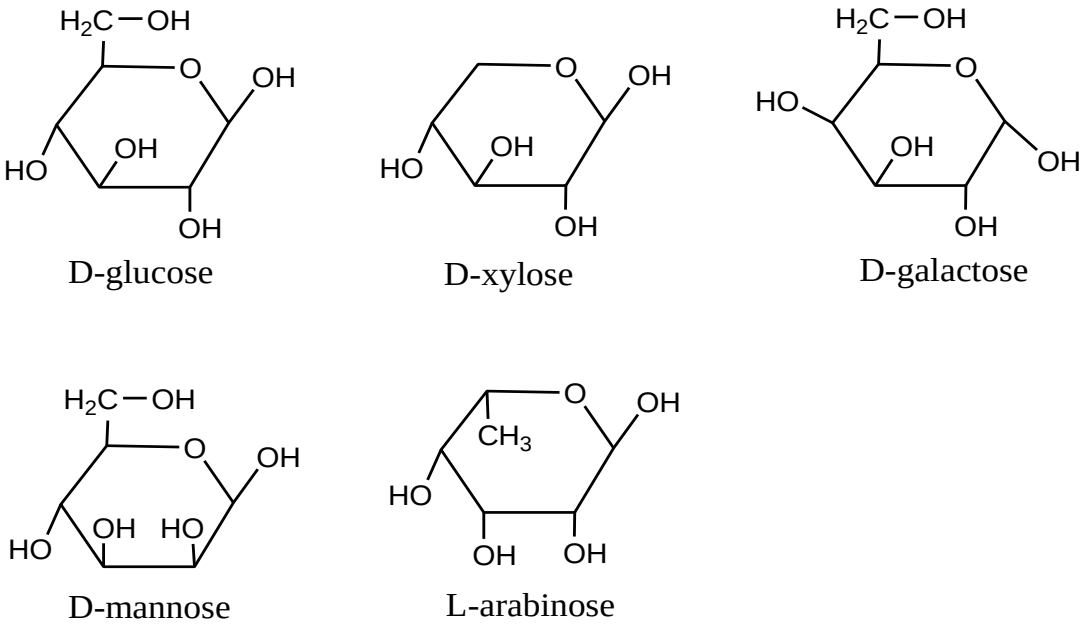

Figure 2-2: Hemicellulose monomer units

2.1.3. Lignin

Lignin provides structural support to plants and acts as a binder for cellulose and hemicellulose fractions of biomass [3]. A typical woody biomass contains 18-35% lignin [8]. Lignin is a cross-linked amorphous polymer consisting of three main phenylpropane units namely guaiacyl (coniferyl alcohol), p-hydroxyphenyl (p-coumaryl alcohol) and syringyl (sinapyl alcohol) which are linked together by carbon-carbon and ether bonds. Figure 2-3 gives the structure of the various phenylpropane units. Lignin has a high molecular weight and is highly branched and complex with no definitive repetitive structure. The degree of polymerization of lignin is in the range of 400-500 units [15]. Syringyl and guaiacyl are the main units of hardwood lignin with a small amount of p-hydroxyphenyl units. Lignin from herbaceous plants has a higher content of p-hydroxyphenyl units together with syringyl and guaiacyl units. Softwood lignin is composed mainly of guaiacyl units with a small amount of p-hydroxyphenyl units [16,17].

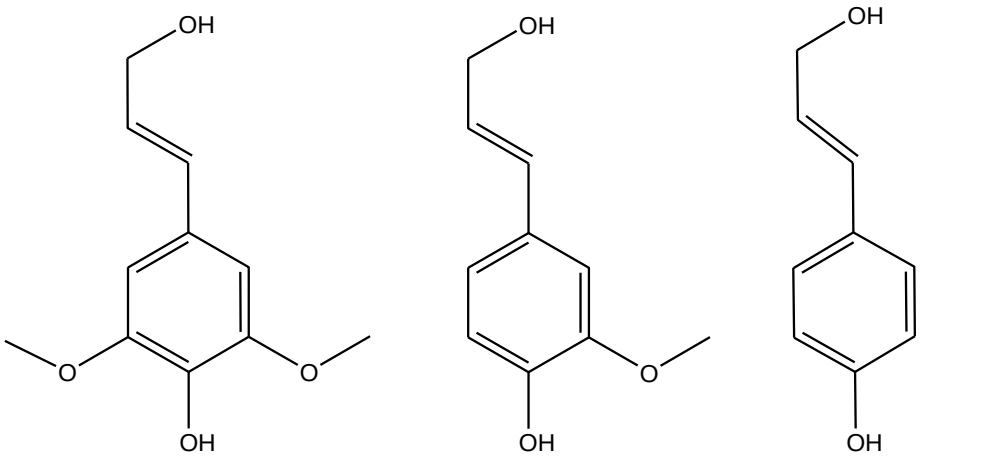

Figure 2-3: Phenylpropane units of lignin

2.2. Thermal pretreatment

In general biomass is a clean and renewable energy source and has the potential to replace fossil fuels like coal in coal gasifiers and boilers for the production of energy due to its carbon neutrality [18]. However, there exist differences between biomass and coal which hinder the utilization of biomass. Lignocellulosic biomass exhibits characteristics such as high moisture content, high oxygen content, heterogeneity, low bulk and energy density, hydrophilicity, susceptibility to microbial decay and difficulty in grinding [19–21]. These characteristics have a negative impact and hinders the efficient and full utilization of biomass. Hence, for many applications, biomass needs to be pretreated to enhance its efficient usage.

To improve on the properties of biomass a thermal pretreatment process is highly recommended. Torrefaction and slow pyrolysis (also known as carbonisation) are pretreatment methods used to improve biomass properties for energy conversion and co-utilization with coal [22]. Due to their similarities they are referred herein as thermal pretreatment processes. Both thermal pretreatment processes involve the treatment of biomass usually in an inert atmosphere and low heating rates (<50 ^{o}C/min) with torrefaction occurring at 200-300 ^{o}C [23,24] and slow pyrolysis between 300 and 500 ^{o}C [25]. After undergoing thermal pretreatment raw biomass is transformed into a solid product (char) alongside the release of some volatile compounds such as CO_2, H_2O, CO and

organic compounds such as acetic acid, alcohols, aldehydes and ketones [26,27]. The char product is characterised by the following qualities: reduced moisture content [22,28], reduced O/C ratio [26], hydrophobicity [29,30], increased energy density [31], improved grindability [23,32] and uniformity of the solid fuel product [33].

These positive effects are as a result of the thermal transformation of biomass components. Hemicellulose is the most reactive component of biomass and is the component that is mostly degraded during thermal pretreatment at low temperature (200-250 ^{o}C). As temperature increases to 300 ^{o}C, hemicellulose degrades substantially while cellulose degrades to a certain extent. At > 300 ^{o}C, hemicellulose degrades completely while cellulose degradation is also greatly enhanced. Lignin is the most stable component and degrades progressively over a wide range of temperature (200-500 °C) [22]. The degradation of these components leads to the removal of moisture and volatiles in the raw biomass which results in the formation of a char with improved fuel properties.

2.2.1. Properties of thermally pretreated biomass

In the context of this study, where the main interest is the use of biomass char for coal substitution, a particular attention is given to the influence of the pretreatment conditions on the properties of the char product.

2.2.1.1. Moisture

The moisture content of fuel is very important as it leads to the loss of energy during the burning of the fuel [27]. Generally biomass contains about 10-50% moisture [34] and it is therefore essential to reduce the moisture in biomass to ensure efficient conversion. Reducing the moisture will also reduce the storage and handling cost and make it less susceptible to biological decay[35]. Biomass is hydrophilic in nature and therefore absorbs moisture from the environment which binds to the hydroxyl groups in the cell wall of biomass through hydrogen bonds [35]. The hydrophilic nature of biomass has been attributed to its hemicellulose fraction. This is because hemicellulose is richer in hydroxyl groups [14,36]. The equilibrium moisture content of rice straw, cotton gin waste and wheat straw were reduced by 49.4, 48.8 and 70.5 wt% respectively following torrefaction pretreatment at 260 ^{o}C [37]. Li et al [30] found an improvement in the hydrophobic nature of torrefied sawdust with increase in temperature.

Some hydroxyl groups are converted during thermal pretreatment by torrefaction/slow pyrolysis through dehydration reactions [31] hence limiting the potential of hydrogen bond formation [38]. The condensation of some volatiles due to recombination reactions (secondary char) inside biomass pores during torrefaction could also reduce the equilibrium moisture content. This prevents the flow of moist air through the biomass pore, therefore preventing the condensation of water [29].

2.2.1.2. Proximate and elemental analysis

Proximate analysis of biomass characterizes a fuel in terms of volatile matter (VM), fixed carbon (FC) and ash. In comparison with coal (FC of 40-98 wt.%), raw biomass contains a low FC (10-21 wt%) and a high VM in the range 70-88 wt% [27]. After undergoing thermal pretreatment the VM decreases while the FC increases. This is due to dehydration and other devolatilization reactions [39]. The VM and FC profiles of biomass before and after torrefaction pretreatment is shown in Figure 2-4.

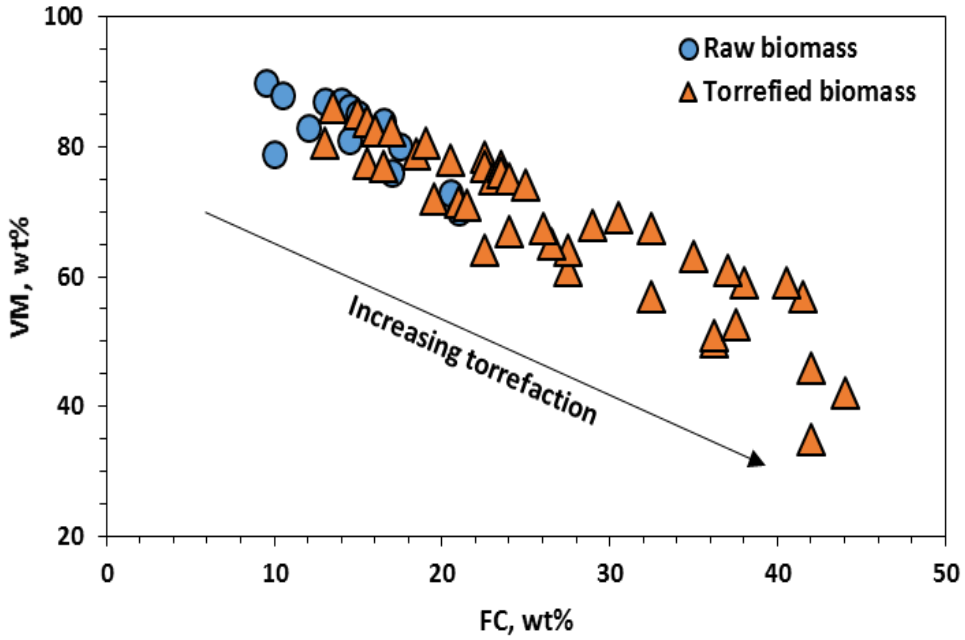

Figure 2-4: Profile of VM and FC of biomass undergoing thermal pretreatment (redrawn from Chen et al. [27])

Among the chemical groups found in biomass, the oxygenated groups are particularly unstable and mostly react at relatively low temperatures to generate some oxygenated volatile compounds. The release of H_2O and volatiles during thermal pretreatment results in the removal of hydrogen (H) and oxygen (O) elements. Thus the O/C and H/C ratios of biomass are reduced significantly after thermal pretreatment. Torrefied biomass therefore becomes more similar to coal (oxygen content lower than 15 wt.%) in terms of chemical composition. Figure 2-5 shows the O/C and H/C plot of biomass after torrefaction pretreatment.

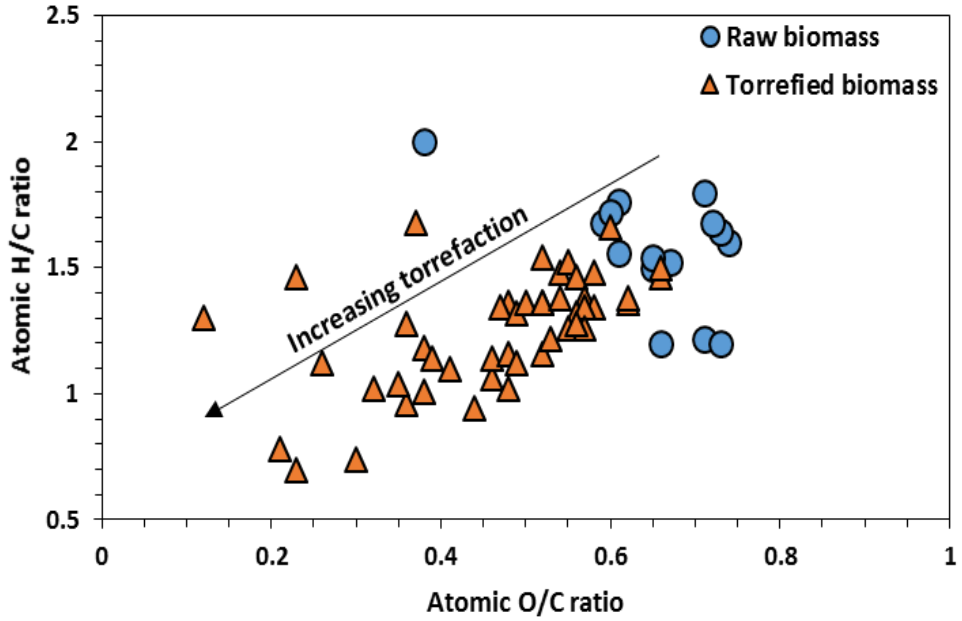

Figure 2-5: van Krevelen diagram of biomass undergoing thermal pretreatment (redrawn from Chen et al. [27])

2.2.1.3. Grindability

To be able to use biomass as fuel in boilers or gasifiers alone or blended with coal, the biomass needs to be milled [40,41]. The polymeric microstructure of biomass shows cellulose is embedded in a hemicellulose matrix and then densely packed by layers of lignin [42]. Due to this the grinding

of biomass becomes difficult and requires high energy. After thermal pretreatment, the microstructure of biomass is destroyed thus improving its grindability and reducing the energy consumption. The grindability of beechwood has been reported to increase with the mass loss of the solid biomass during torrefaction [32]. Bergman and Kiel [38] observed a 70-90 % reduction in grinding energy when biomas was torrefied in comparison to raw biomass. Improvement in grindability was also observed through an increase in the percentage of fines during grinding [43].

2.2.1.4. Mass and energy yields

The mass yield of solid product is correlated to the extent of thermal degradation of biomass during torrefaction/slow pyrolysis pretreatment. The mass yield is defined as the mass ratio of the solid product after thermal pretreatment and the initial raw biomass. Previous studies have suggested that the mass loss during thermal pretreatment was first from hemicellulose, then cellulose and lignin [14]. Mass yield is very much dependent on lignocellulosic composition together with temperature and residence time. For example the mass yield for pine wood during torrefaction at 250 or 300 °C with conversion time between 0.25 and 8 h was observed to be in the range 37-95 wt%, with the higher yields obtained at low temperature and short conversion time [44].

As the energy content (calorific value) of a solid fuel product is known to increase with increased carbon content and decreased oxygen content, a higher degree of conversion during pretreatment generally results in a more extensive deoxygenation and a fuel sample with increased energy density [45].

The energy yield, which is defined as the ratio of the energy content of the solid product to the energy content of the raw biomass, is a measure of the total energy retained after thermal pretreatment [12]. The energy yield is also dependent on temperature and residence time. The energy yield obtained for pine pretreated between 250 and 300 °C (0.25 – 8h conversion time) has been reported to be 52.4-99.8 % with HHV in the range 21.22-32.34 MJ/kg [44].

2.2.2. Potential uses of thermally pretreated biomass

Some potential applications of pretreated biomass are given below;

2.2.2.1. Gasification

When lignocellulosic biomass is considered for gasification, a critical issue is associated to its high volatile matter content. Some of the produced volatiles called tar easily condense resulting in major operational issues. Due to its low moisture and volatile contents, improved grindability and heating value, pretreatment significantly improves the fuel properties of biomass for gasification as it will improve the gasification efficiency and reduce tar formation [27]. In a previous gasification study [46] raw biomass was found to be more reactive than torrefied biomass. However, the high moisture content of raw biomass caused biomass to be over oxidised leading to higher thermodynamic loss. Torrefied biomass on the other hand had a lower moisture and O/C ratio hence giving it a low thermodynamic loss during gasification. The use of torrefied biomass in another gasification process was found to reduce the tar content of the gas product [47]. The potential of using torrefied sawdust for gasification in an entrained flow gasifier was studied by Chen et al [48]. The cold gas efficiency and the quality of the gas were improved compared to the use of raw biomass. Thermal pretreatment of biomass therefore could ensure a more efficient utilization of biomass in gasification systems. The benefit and optimisation of thermal pretreatment in the context of gasification application are the main interest of this study.

2.2.2.2. Blast furnace

The use of coal in blast furnaces during iron production releases high volumes of anthropogenic CO_2 into the atmosphere [49,50]. Being a renewable fuel, biomass pretreated by torrefaction can be blended with coal and used in blast furnace to reduce CO_2 emissions [51].

2.2.2.3. Co-firing

Pulverized coal combustors are used in power plants for energy generation. Improved grindability, high heating value and low moisture content of torrefied biomass makes it a good fuel for use in pulverized coal combustor. Studies have shown that torrefied biomass can be co-utilized with coal in coal combustor without major changes to the design of the plant [41,52].

2.2.2.4. Bio-oil production

The use of torrefied biomass for bio-oil production is another potential way of utilizing pretreated biomass. Bio-oil from torrefied biomass tend to have lower moisture content, high energy content and lower acidity[18,53,54].

2.2.2.5. Production of pellet

Thermally pretreated biomass can be converted into pellets. However, the process is characterised by some disadvantages. Torrefied biomass have improved grindability and therefore can be milled easily but the pellet production require higher energy [55,56]. The thermal softening ability of lignin is reduced during thermal pretreatment, hence high operating temperature and sometimes the addition of binders will be required to produce the pellets [18,56].

2.2.3. Effects of thermal pretreatment conditions

According to literature, the main parameters influencing the properties of the char products are the temperature, the conversion time (residence time), the particle size of the material and the atmosphere composition.

2.2.3.1. Temperature and residence time

Both temperature and residence time have impact on the mass and energy yields of the solid product during thermal pretreatment. Figure 2-6 shows the effect of temperature and residence time on torrefaction. Generally an increase in temperature and residence time leads to more pronounced mass loss and lower yield of the torrefied biomass. However, the effect of temperature has been shown to be more drastic than residence time [57]. This trend can be observed in Figure 2-6. While conversion at 250 °C for various residence times up to 6 h resulted in char yield higher than 60 wt.%, the yields obtained from the samples converted at 300 °C were lower than 50 wt.% even for residence time as low as 0.5 h.

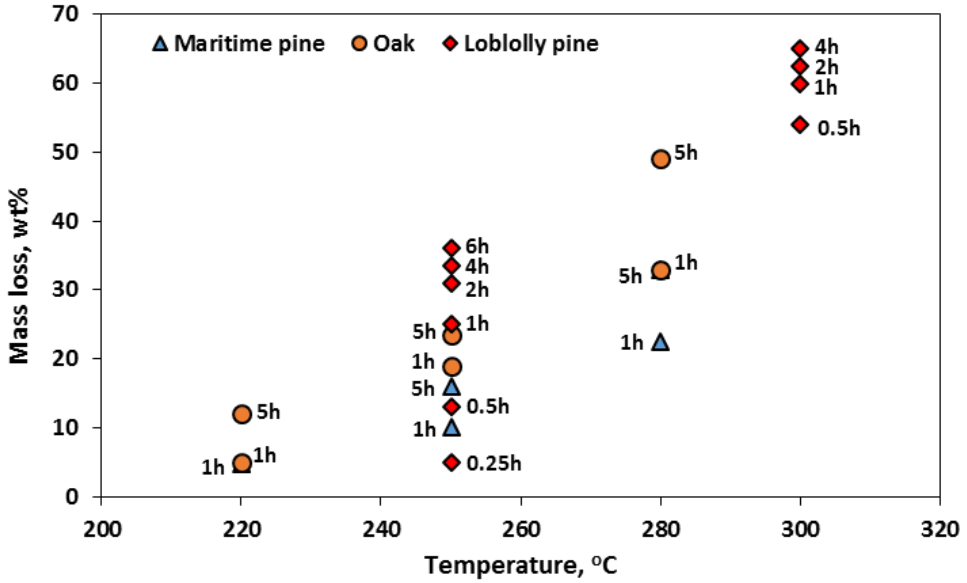

Figure 2-6: Impact of temperature and residence time on mass loss during torrefaction (data: loblolly pine [44], maritme pine and oak [58])

2.2.3.2. Particle size

Increase in particle size will lead to an increase in the mass yield of the solid product due to heat and mass transfer effects. In smaller particles volatiles are released easily and leave the particle quickly hence limiting secondary reactions [14]. In larger particles, longer time is required for the volatiles to leave the particle matrix, thus increasing the probability of secondary reactions and formation of secondary char.

2.2.3.3. Reaction atmosphere

Torrefaction is usually done in an inert atmosphere. However the use of other gases such as air, O_2, CO_2 and H_2O have also been investigated [14,18]. The use of an oxidative atmosphere produces increased mass loss during thermal pretreatment [59,60]. Lu et al [61] found that the mass loss of palm fibre torrefied at 250 ^oC increased by 33.1% when nitrogen was replaced with air. CO_2 the main non-condensable gas generated during torrefaction can be utilized as the reactive medium. The effect of CO_2 during torrefaction has been studied by some researchers [62,63]. There was an improvement in grindability of wood while the mass loss increased by 4.3% when Juniper hardwood was torrefied in CO_2 atmosphere instead of an inert atmosphere [62].

2.3. Gasification

Gasification is a partial oxidation process used to convert carbonaceous materials (coal, biomass, and plastics) into a gas product in the presence of a gasifying agent which can be air, steam, oxygen, carbon dioxide or a mixture [64]. It is a versatile technology and is deemed to have a relatively high efficiency among other thermochemical processes [65,66]. The process of gasification occurs at high temperature (500-1400 ^{o}C) and the pressure can range from atmospheric to 33 bar [64].

The gas product is made up of mainly CO and H_2. In addition other compounds such as CO_2, CH_4, tars (oxygenated volatiles), ash and some particulates are likely to be found. After cleaning and purification the gas can be used directly in gas engines and turbines to generate electricity or upgraded in order to be used for the synthesis of chemicals or liquid fuels via Fischer-Tropsch process [66,67]. While coal gasification is well established, biomass gasification is yet to attain maturity [65], one of the main issue being the high concentration of tar, making the gas cleaning very challenging.

2.3.1. Stages of gasification

The gasification process can be classified into four (4) stages namely: drying, pyrolysis, oxidation/combustion and reduction/gasification [68]:

2.3.1.1. Drying

Drying of the solid fuel is required prior to feeding into the gasifier. Drying is essential in reducing the moisture content of the fuel and improving the gasification efficiency. However, complete drying is not practical. When the particles are introduced in the hot reactor, water originating from the moisture in the sample is the first compound to be released.

2.3.1.2. Pyrolysis

The pyrolysis stage takes place during the heating of the particles and generates the char and volatiles [68]. The volatile fraction consists of H_2O, CO_2, CO, CH_4, H_2 and organic compounds

(tar precursors). The presence of tars in the gas produced by gasification present operational problems and therefore tars need to be avoided or reduced to a lower level [66,67].

2.3.1.3. Oxidation

In this stage some volatiles and char particles are oxidized by the gasification agent producing H_2O, CO_2 and CO. This exothermic stage provides the energy required for the pyrolysis and reduction/gasification stage.

2.3.1.4. Reduction

Here the char generated from the pyrolysis stage is converted through partial oxidation into CO, H_2 and CH_4 by reacting with the gasifying agent.

2.3.2. Types of gasification reactors

The gasifier is the main unit within a gasification plant. Gasifiers are classified based on the manner in which the feedstock and gasifying agent come into contact within the reactor [69]. The design highly influences the concentration of tar in the gas product. The classification includes:

2.3.2.1. Fixed bed gasifier

Fixed bed gasifiers or reactors are also known as moving bed reactors. In the reactor a bed of feedstock moves very slowly down the reactor and contacts the gasifying agent. Based on the direction of flow of the gasifying agent fixed bed reactors can further be classified into updraft or counter current and downdraft or co-current reactors [64].

In updraft reactors the feedstock is fed from the top of the reactor while the gasifying agent is fed from the bottom. The gasifying agent comes into contact with the feed as it rises up the reactor through a bed of descending feedstock. The gas produced also leaves though the top of the reactor. In downdraft reactors, the feedstock is fed from the top and moves down the reactor. The gasifying agent is fed from the side and mixes with the pyrolysis gases and then flow concurrently with the feedstock down the reactor [68]. Downdraft gasifiers produce less tar than updraft gasifiers but are less efficient and difficult to scale up. Updraft gasifiers are normally easy to scale up and are more

efficient [64,70]. In general fixed bed reactors have high carbon conversion, low ash carry-over and are easy to construct and operate compared to other reactors [70].

2.3.2.2. Entrained flow reactors

Entrained flow gasifiers operate at high temperature (1400 ^{o}C) and high pressure (20-70 bar and require very fine particle size feedstock (<75 µm) [64]. The flow of feed and gasifying agent (usually oxygen) are in the co-current direction. In the gasifier the reaction of oxygen with char and volatiles happens very quickly and is highly exothermic. As such the reactor temperature is raised above the ash melting temperature and results in more efficient destruction of tars and oils [68]. The gas from entrained flow gasifier is therefore of a relatively high quality. A high carbon conversion is also a characteristic of this type of gasifier.

2.3.2.3. Fluidized bed reactors

In fluidized bed gasifier the feedstock is fed from the top of the reactor while the gasifying agent is supplied in the form of a fluidizing gas from the bottom. The fluidizing action of the gasifying agent ensures rapid mixing of the arrived feed particles with the bed of hot solids. This raises the particles temperature to the bed temperature so they can undergo gasification [64]. This type of gasifier operates at temperatures of 800-1000 ^{o}C and prevent the build-up of ash [71]. Fluidized bed gasifier is therefore suitable for low grade fuels such as biomass and lignite. Carbon conversion in fluidized bed gasifier is low and the loss of unconverted feedstock leads to reduced efficiency. This gasifier is however preferred because it can easily be scaled up.

2.3.3. Pyrolysis/devolatilization in the context of gasification

As stated above, pyrolysis or devolatilization is an essential step during gasification. It is responsible for generating the char and volatiles (tar precursors), and determining the nature of the intermediates for the gasification step. It is therefore important to have a good understanding of the feedstock pyrolysis process as this will directly impact on the fuel reactivity, gas quality and yield, and overall efficiency of the gasification process. In this section, attention is given to the devolatilization of coal and biomass.

Pyrolysis or devolatilization is the thermal degradation of materials in an environment deprived of oxygen. In the gasification reactor, most of the volatiles are released when the particles temperature is between 200 and 600 °C. The products of devolatilization are gas, liquid (gases that are condensable at ambient temperature) and a solid product (char). Depending on the heating rate of the particles, pyrolysis can be classified as either slow or fast. For fast pyrolysis a higher heating rate (10^3-10^5 ^{o}C/min) is used and the process promotes the production of volatiles. Slow pyrolysis uses low heating rate (<50 ^{o}C/min) and is more suited for char production [25]. The type of gasification reactor determines the pyrolysis condition within the reactor. Usually entrained flow and fluidized bed reactors experience fast pyrolysis while lower heating rates are obtained in a fixed bed reactor due to the slow movement of the bed [72]. The design of the reactor also influences the residence time of the volatiles in the hot part of the reactor, where secondary reactions can occur.

2.3.3.1. Coal devolatilization

Coal is a sedimentary rock that is combustible in nature. It is a fossil formed as a result of the slow decomposition of plants and animals remains under high pressures and temperatures over a very long time period (several million years) [73]. It has a complex chemical structure held together by very strong C═C aromatic bonds [74,75]. The process of coal formation over time is called the coalification series and the level at which coal has reached on this series is referred to as the rank. Based on the rank coal is classified as lignite, sub-bituminous, bituminous, semi-anthracite, anthracite and graphite with lignite and graphite at the lower and upper ends of the coalification series respectively [73].

Coal devolatilization or pyrolysis starts with the depolymerization of the chemical structure to form an intermediate product that is meta-stable. Depolymerization occurs as a result of the scission of methylene or ether bonds between the aromatic structures [76–79]. This reaction leads to the release of volatiles. Some of these volatiles are free radicals and are stabilized through the rearrangement of atoms or by collision with other species. These stabilized structures either remain as volatiles (tar) or form part of a char product depending on vapour pressure [76–79].

The cracking of the coal during pyrolysis leads to the formation of char. As mentioned above, some char is also formed from repolymerisation of the intermediate volatiles [76,77,79]. The char

tends to retain the aromatic structure of the parent coal and its pore structure is dependent on the origin of the coal. The liquid product (condensable volatiles) is a mixture of several compounds with varying molecular weights, most of them being composed of a benzene or phenol ring (toluene, benzene, phenol, cresols, xylene, etc.) [80].

The gas products are formed throughout the pyrolysis process during char formation and from secondary reactions of the condensable volatiles. The gas includes CO_2, CH_4, H_2, CO and light hydrocarbons [81,82].

2.3.3.2. Effects of operating parameters

Feedstock

Different coals have different devolatilization characteristics. Hence the product distribution during the pyrolysis is affected by coal rank. For example, a significant amount of tar is produced from the devolatilization of bituminous coal. However for low rank coals such as sub-bituminous and lignite the quantity of non-condensable gases in the volatile product increases while tar is reduced [83].

Reaction temperature

The temperature regime during coal devolatilization is a critical parameter. In general low temperature favours the formation of char, primary tars and gases. Increasing temperature promotes the release of more gases and the secondary reactions of the primary tars. For coal, devolatilization starts at around 300-400 ^oC producing primary volatiles and light hydrocarbons as a result of primary reactions [81,84]. As temperature is increased above 600 ^oC, secondary cracking and repolymerisation reactions of primary volatiles become dominant leading to the formation of secondary char and more gases, particularly H_2, and cracking of some hydrocarbons [81].

Pressure

Increase in pressure limits the rate at which volatiles are released from within the coal particle to the surface [85]. As a consequence an increase in pressure decreases the production of volatiles

and tars. Also an increase in pressure increases the volatile residence time within the reaction environment. This promotes cracking and repolymerisation of the volatiles leading to the formation of additional secondary char and gases.

Reactor type

Different reactor types have different influences on the devolatilization characteristics within the reaction environment. Entrained flow and fluidized bed reactors require the use of smaller particle size and are designed to provide shorter residence time. The smaller particle size ensures faster heat transfer rates and promotes devolatilization and release of volatiles. With shorter residence time, secondary reactions are limited compared to fixed bed reactors [81].

2.3.3.3. Biomass pyrolysis/devolatilization

Lignocellulosic biomass is composed of three (3) main component; cellulose, hemicellulose and lignin. Though some interactions between constituents and volatile products have been observed, the overall devolatilization characteristic of biomass is generally comparable with a combination of that of the three components [86].

The devolatilization of cellulose starts at around 250 ^{o}C where its degree of polymerisation is reduced (up to 200) [87] forming an activated cellulose (also called anhydrocellulose) and the release of H_2O (74). When relatively low heating rates are experienced, a significant fraction of anhydrocellulose then decomposes to form char through cross-linking and aromatization reactions. The decomposition of the anhydrocellulose also produces additional H_2O as well as carbon oxides by decarboxylation and decarbonylation reactions [88,89]. CH_4 and other permanent gases are also formed from the further conversion of the char. As particle temperature increases beyond 300 ^{o}C depolymerization of the cellulose occurs forming mainly oligomers, levoglucosan and other heterocyclic molecules containing 6-carbon atoms [90]. Secondary reaction of levoglucosan occurs as pyrolysis proceeds. This leads to the formation of H_2O and condensable volatiles (tar precursors) such as furan derivatives and aldehydes. Secondary reaction of levoglucosan can also produce secondary char and permanent gases such as CO_2 [91,92]. The yield of condensable volatiles increases with pyrolysis temperature reaching a maximum at 400-550 ^{o}C after which the

yield is reduced owing to the formation of permanent gases from secondary cracking reactions. Figure 2-7 shows some of the devolatilization products of cellulose.

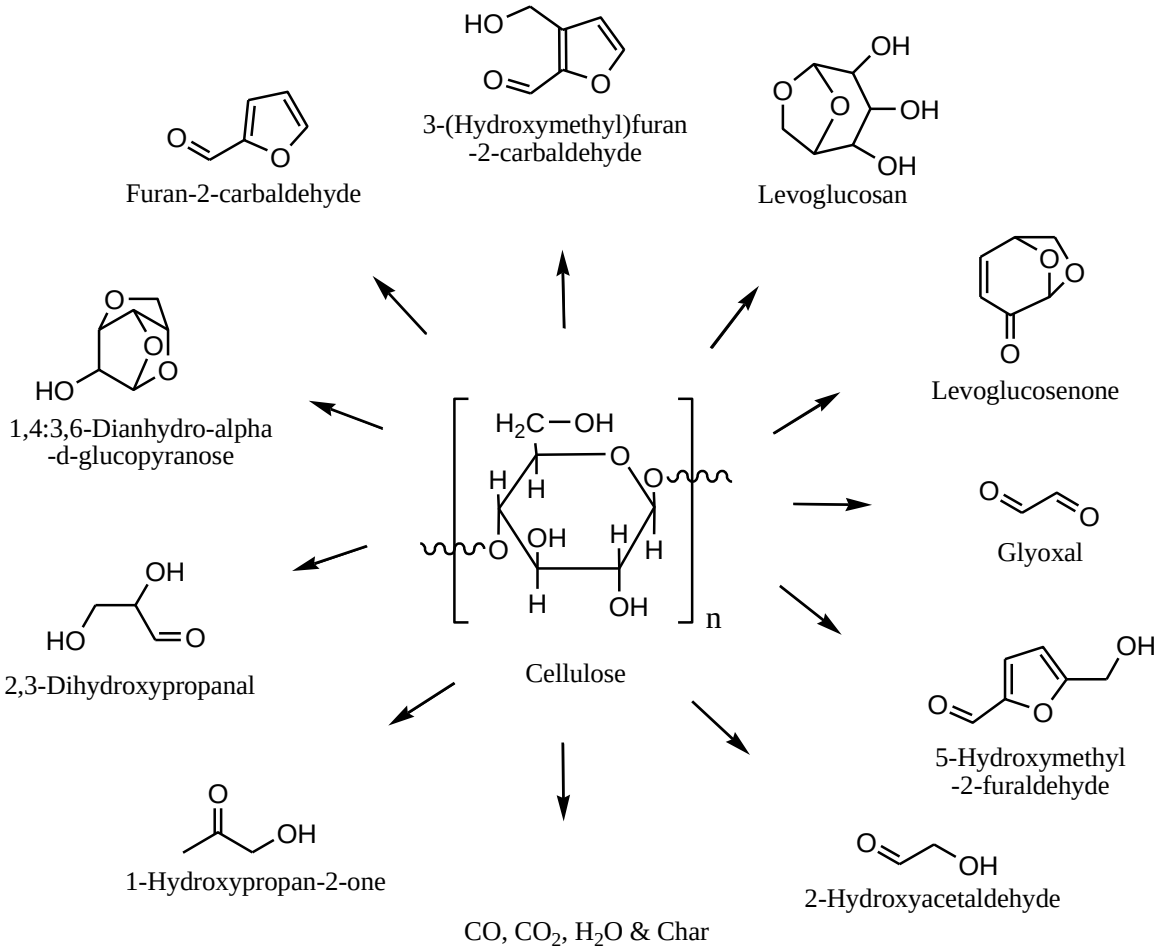

Figure 2-7: Cellulose pyrolysis products (redrawn from Kanaujia et al. [86])

As the most reactive component of biomass, hemicellulose decomposition starts at a lower temperature (200-250 ^{o}C) [93]. The devolatilization characteristic of hemicellulose is much similar to that of cellulose. Hemicellulose also undergoes depolymerisation reactions during pyrolysis producing heterocyclic molecules (5 or 6-carbon atoms depending on sugar composition) [90]. Rearrangement reactions of hemicellulose produces CO_2 and H_2O [91,92]. Some major pyrolysis products from xylan hemicellulose are shown in Figure 2-8.

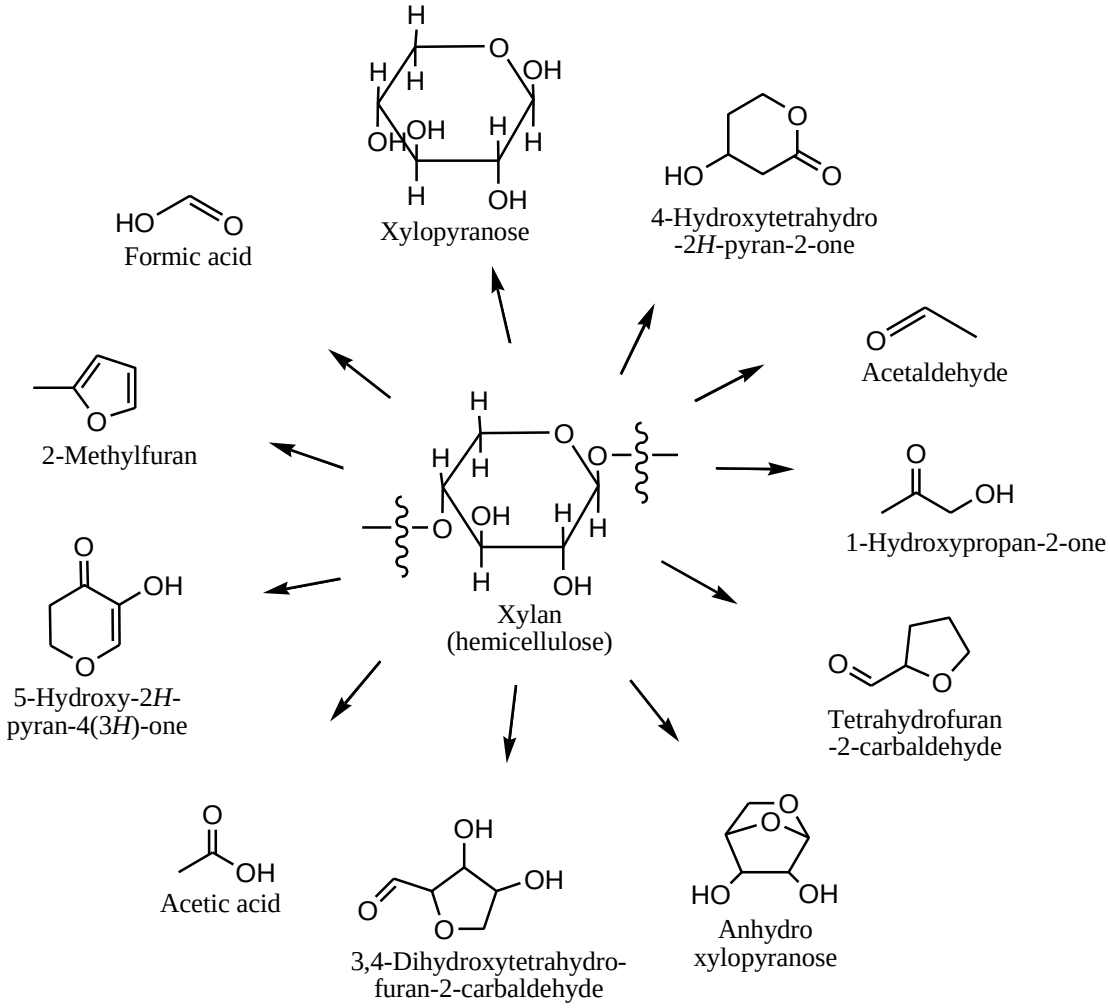

Figure 2-8: Hemicellulose pyrolysis products (redrawn from Kanaujia et al. [86])

Lignin is more stable due to its aromatic rings and produces more char than cellulose and hemicellulose during devolatilization [94,95]. The devolatilization of lignin proceeds through depolymerisation, fragmentation and rearrangement reactions. The depolymerisation reactions involve the breakage of bonds between the lignin monomer units and produce mainly aromatic compounds such as guaiacols, syringols, and phenols [94]. The fragmentation of the propyl chain produces permanent gases and small chain organic compounds [90,96]. Rearrangement reactions between the aromatic rings produce char [97]. Some pyrolysis products from lignin are shown in Figure 2-9.

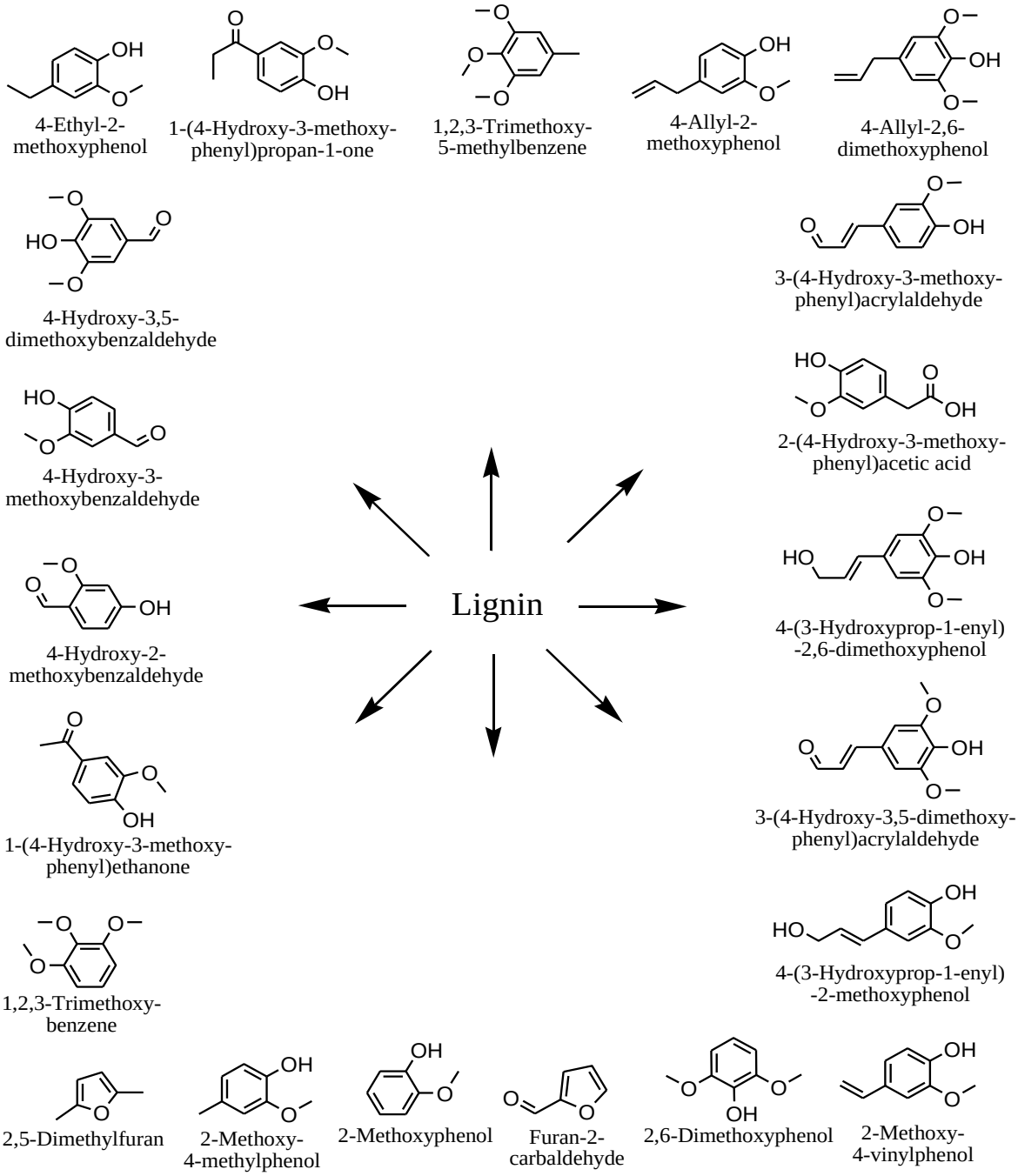

Figure 2-9: Lignin pyrolysis products (redrawn from Kanaujia et al. [86])

In general it can be said that each biomass component contributes towards the final pyrolysis product distribution in varying amounts. The condensable volatile products can be classified as

primary, secondary or tertiary tar products, depending on their degree of conversion, as given below [82]:

Primary tars: cellulose-derived products (levoglucosan, furfural, hydroxyacetaldehyde), lignin-derived methoxy phenols.

Secondary tars: phenols and olefins

Alkyl tertiary tars: methyl derivative of aromatics (toluene, methylnaphthalene and methyl acenaphthylene)

Condensed tertiary tars: polycyclic aromatic hydrocarbons (PAH) without substituents (indene, anthracene, naphthalene, benzene, pyrene, phenanthrene, acenaphthylene)

The effects of operating conditions on biomass devolatilization are similar to that of coal. Increasing temperature favours secondary reactions and produces permanent gases while the tar yield is reduced. An increase in pressure also promotes char and gas yields while reducing the production of tars. It must be emphasised that due to the structural differences between biomass and coal, biomass produces more oxygenated compounds and tar precursors than coal.

2.3.4. Char gasification

Char from both coal and biomass devolatilization follow similar gasification reactions as given below in Table 2-2:

Table 2-2: Gasification reactions

R1 (Boudouard)	$C + CO_2 \rightarrow 2CO$	$\Delta H = 159.7$ kJ/mol
R2 (Steam gasification)	$C + H_2O \rightarrow CO + H_2$	$\Delta H = 118.9$ kJ/mol
R3 (Partial combustion)	$C + 0.5O_2 \rightarrow CO$	$\Delta H = -123.1$ kJ/mol
R4 (Hydrogasification)	$C + 2H_2 \rightarrow C + CH_4$	$\Delta H = -187.4$ kJ/mol
R5 (Water gas shift)	$CO + H_2O \rightarrow CO_2 + H_2$	$\Delta H = -40.9$ kJ/mol
R6 (Methanation)	$CO + 3H_2 \rightarrow CH_4 + H_2O$	$\Delta H = -206.3$ kJ/mol
R7 (Combustion)	$C + O_2 \rightarrow CO_2$	$\Delta H = -405.9$ kJ/mol

These reactions determine the extent to which char is converted during gasification and the composition of the gas product. They however depend on the characteristics of the char as well as gasifier operating conditions. Char characteristic has to do with its structure and reactivity. Pore structure, hydrogen and mineral contents of char determine the concentration of active reactive sites within the char and hence its reactivity during gasification [98]. Pores within the char allow for the mass transfer of reactive gases into the internal matrix of the char and provide an escape route for product gases from inside the char to the surrounding. Based on the size, pores can be classified as micropores (<2 nm), mesopores (2-50 nm) and macropores (>50 nm) [99]. The bigger the pore size the faster the rate of mass transfer and the more reactive the char is. Also high mineral and hydrogen contents increase the reactivity of the char [99]. Usually low rank coal like lignite produces chars with higher proportions of mesopores and macropores than bituminous coal. Additionally these chars have high hydrogen and mineral contents, hence more reactive sites. Biomass char also tends to have a high proportion of reactive sites [100]. In particular, the relatively high oxygen content is considered as a characteristic increasing the char reactivity.

The temperature and the pressure of the gasifier system determine the equilibrium positions of the gasification reactions [99,101]. For reactions R1 and R2, the equilibrium shifts towards products formation when temperature is increased. On the other hand reactions R4, R5 and R6 favour reactant formation when temperature is increased. Increasing pressure favours products formation in reactions R4 and R6 while R1 and R2 shift towards the reactant side [99].

2.3.5. Co-gasification

Co-gasification involves the combined use of both coal and biomass in the gasification process. For most studies the focus has been on the effect of operating conditions on possible synergy, product composition and yield.

The impact of biomass addition on the quantity and quality of products has widely been studied. In general biomass addition to coal was found to increase tar and hydrocarbon contents of the syngas [102–104] due to the high volatile matter of biomass. Pan et al [104] in their study blended biomass with low grade coal and found that the gas yield and heating value were increased when the biomass fraction in the feed was increased. However, in another study using a fluidized bed reactor a reduction in the heating value of the gas was observed [105]. By using a fluidized bed

reactor several studies [102–104] reported an increase in tar and light hydrocarbons yield while H_2 yield decreased when the biomass fraction was increased. However, the addition of catalyst and increase in reaction temperature and oxygen input reduced the tar and hydrocarbons yield. Co-pyrolysis study of agricultural residues and coal by Aboyade et al [106] in a pressurised fixed bed reactor reported an increase in tar yield with increase in biomass fraction. The composition of the tar was also found to increase in oxygenates content due to the addition of biomass. The presence of oxygenates could cause downstream operational difficulties such as fouling, corrosion and blockage of equipment pipes.

Regarding synergy during biomass and coal co-gasification, there has been conflicting reports in the literature. In a co-gasification study of coal and wood in a pressurised fluidized bed reactor, Mclendon et al [107] observed no synergy effect on the yield of products. Similar effect was also observed when operating at atmospheric pressure [108–110]. Using char from co-pyrolysis of bituminous coal and biomass for gasification no synergy in char reactivity was observed [108]. However, Lapuerta et al [109] gasified biomass and low grade coal in a circulating fluidized bed reactor at atmospheric pressure and reported synergy in the heat content of the producer gas.

References

[1] B. Prabis, Biomass Gasification and Pyrolysis - A practical guide, 2010.

[2] M.O.S. Dias, A.V. Ensinas, S.A. Nebra, R. Maciel Filho, C.E.V Rossell, M.R.W. Maciel, Production of bioethanol and other bio-based materials from sugarcane bagasse: Integration to conventional bioethanol production process, Chem. Eng. Res. Des. 87 (2009) 1206–1216

[3] D. Mohan, C.U. Pittman, P.H. Steele, C.U. Pittman,, P.H. Steele, Pyrolysis of Wood/Biomass for Bio-oil: A Critical Review, Energy & Fuesl. 20 (2006) 848–889.

[4] A. Sluiter, B. Hames, R. Ruiz, C. Scarlata, J. Sluiter, D. Templeton, D. Crocker, Determination of Structural Carbohydrates and Lignin in Biomass Determination of Structural Carbohydrates and Lignin in Biomass, (2012).

[5] Y. Kim, N.S. Mosier, M.R. Ladisch, V. Ramesh Pallapolu, Y.Y. Lee, R. Garlock, V.

Balan, B.E. Dale, B.S. Donohoe, T.B. Vinzant, R.T. Elander, M. Falls, R. Sierra, M.T. Holtzapple, J. Shi, M.A. Ebrik, T. Redmond, B. Yang, C.E. Wyman, R.E. Warner, Comparative study on enzymatic digestibility of switchgrass varieties and harvests processed by leading pretreatment technologies, Bioresour. Technol. 102 (2011) 11089–11096

[6] S. Kumar, S.K. Shukla, A Review on Recent Gasification Methods for Biomethane Gas Production, Int. J. Energy Eng. 6 (2016) 32–43.

[7] R. Pettersen, The chemical composition of wood, Chem. Solid Wood. (1984) 1–9.

[8] R. Alen, Structure and chemical composition of wood, in: Papermak. Sci. Technol., 2000: pp. 11–57.

[9] D. Klemm, B. Heublein, H.P. Fink, A. Bohn, Cellulose: Fascinating biopolymer and sustainable raw material, Angew. Chemie - Int. Ed. 44 (2005) 3358–3393.

[10] H.B. Goyal, D. Seal, R.C. Saxena, Bio-fuels from thermochemical conversion of renewable resources: A review, Renew. Sustain. Energy Rev. 12 (2008) 504–517.

[11] R.C. Sun, Cereal Straw as a Resource for Sustainable Biomaterials and Biofuels, 2010.

[12] D. Fengel, G. Wegener, Wood—chemistry, ultrastructure, reactions, J. Polym. Sci. Polym. Lett. Ed. 23 (1984) 601–602.

[13] D. Fengel, G. Wegener, Wood: chemistry, ultrastructure, reactions., 1989.

[14] M.J. Prins, K.J. Ptasinski, F.J.J.G. Janssen, Torrefaction of wood. Part 1. Weight loss kinetics, J. Anal. Appl. Pyrolysis. 77 (2006) 28–34.

[15] A. Gandini, T.M. Lacerda, From monomers to polymers from renewable resources: Recent advances, Prog. Polym. Sci. 48 (2015) 1–39.

[16] L.V.G. Ros, C. Gabaldón, F. Pomar, F. Merino, M.A. Pedreño, A.R. Barceló, Structural motifs of syringyl peroxidases predate not only the gymnosperm-angiosperm divergence but also the radiation of tracheophytes, New Phytol. 173 (2007) 63–78.

[17] L.A. Donaldson, Lignification and lignin topochemistry — an ultrastructural view, Phytochemistry. 57 (2001) 859–873.

[18] M.J.C. van der Stelt, H. Gerhauser, J.H.A. Kiel, K.J. Ptasinski, Biomass upgrading by torrefaction for the production of biofuels: A review, Biomass and Bioenergy. 35 (2011) 3748–3762.

[19] Q. Lu, X.C. Yang, C.Q. Dong, Z.F. Zhang, X.M. Zhang, X.F. Zhu, Influence of pyrolysis temperature and time on the cellulose fast pyrolysis products: Analytical Py-GC/MS study, J. Anal. Appl. Pyrolysis. 92 (2011) 430–438.

[20] M. Phanphanich, S. Mani, Impact of torrefaction on the grindability and fuel characteristics of forest biomass, Bioresour. Technol. 102 (2011) 1246–1253.

[21] D. Medic, M. Darr, A. Shah, B. Potter, J. Zimmerman, Effects of torrefaction process parameters on biomass feedstock upgrading, Fuel. 91 (2012) 147–154.

[22] P. Rousset, C. Aguiar, N. Labbé, J.-M. Commandré, Enhancing the combustible properties of bamboo by torrefaction., Bioresour. Technol. 102 (2011) 8225–8231.

[23] B. Arias, C. Pevida, J. Fermoso, M.G. Plaza, F. Rubiera, J.J. Pis, Influence of torrefaction on the grindability and reactivity of woody biomass, Fuel Process. Technol. 89 (2008) 169–175.

[24] M. Broström, A. Nordin, L. Pommer, C. Branca, C. Di Blasi, Influence of torrefaction on the devolatilization and oxidation kinetics of wood, J. Anal. Appl. Pyrolysis. 96 (2012) 100–109.

[25] A.V . Bridgwater, Renewable fuels and chemicals by thermal processing of biomass, Chem. Eng. J. 91 (2003) 87–102.

[26] M.J. Prins, K.J. Ptasinski, F.J.J.G. Janssen, Torrefaction of wood. Part 2. Analysis of products, J. Anal. Appl. Pyrolysis. 77 (2006) 35–40.

[27] W.H. Chen, J. Peng, X.T. Bi, A state-of-the-art review of biomass torrefaction,

densification and applications, Renew. Sustain. Energy Rev. 44 (2015) 847–866.

[28] J.H. Peng, H.T. Bi, C.J. Lim, S. Sokhansanj, Study on density, hardness, and moisture uptake of torrefied wood pellets, Energy and Fuels. 27 (2013) 967–974.

[29] F.F. Felfli, C.A. Luengo, J.A. Suárez, P.A. Beatón, Wood briquette torrefaction, Energy Sustain. Dev. 9 (2005) 19–22.

[30] H. Li, X. Liu, R. Legros, X.T. Bi, C.J. Lim, S. Sokhansanj, Torrefaction of sawdust in a fluidized bed reactor, Bioresour. Technol. 103 (2012) 453–458.

[31] W. Yan, T.C. Acharjee, C.J. Coronella, V.R. Vásquez, Thermal pretreatment of lignocellulosic biomass, Environ. Prog. Sustain. Energy. 28 (2009) 435–440.

[32] A. Ohliger, M. Förster, R. Kneer, Torrefaction of beechwood: A parametric study including heat of reaction and grindability, Fuel. 104 (2013) 607–613.

[33] C. Couhert, S. Salvador, J.-M. Commandré, Impact of torrefaction on syngas production from wood, Fuel. 88 (2009) 2286–2290.

[34] J.S. Tumuluru, S. Sokhansanj, J.R. Hess, C.T. Wright, R.D. Boardman, A review on biomass torrefcation process and product properties for energy applications, Ind. Biotechnol. 7 (2011) 384–401.

[35] M. Andersson, A. Tillman, M. Marie, Acetylation of jute: Effects on strength, rot resistance, and hydrophobicity, J. Appl. Polym. Sci. 37 (1989) 3437–3447.

[36] H. Li, X. Liu, R. Legros, X.T. Bi, C. Jim Lim, S. Sokhansanj, Pelletization of torrefied sawdust and properties of torrefied pellets, Appl. Energy. 93 (2012) 680–685.

[37] S. Sadaka, S. Negi, Improvements of Biomass Physical and Thermochemical Characteristics via Torrefaction Process, 28 (2009) 427–434.

[38] P.C. A. Bergman, J.H.A. Kiel, Torrefaction for biomass upgrading, Proc. 14th Eur. Biomass Conf. Paris, France, (2005) 17–21.

[39] J.J. Chew, V. Doshi, Recent advances in biomass pretreatment – Torrefaction fundamentals and technology, Renew. Sustain. Energy Rev. 15 (2011) 4212–4222.

[40] T.G. Bridgeman, J.M. Jones, A. Williams, D.J. Waldron, An investigation of the grindability of two torrefied energy crops, Fuel. 89 (2010) 3911–3918.

[41] J. Li, A. Brzdekiewicz, W. Yang, W. Blasiak, Co-firing based on biomass torrefaction in a pulverized coal boiler with aim of 100% fuel switching, Appl. Energy. 99 (2012) 344–354.

[42] Z. Hu, Z. Wen, Enhancing enzymatic digestibility of switchgrass by microwave-assisted alkali pretreatment, Biochem. Eng. J. 38 (2008) 369–378.

[43] B. Arias, C. Pevida, J. Fermoso, M.G. Plaza, F. Rubiera, J.J. Pis, Influence of torrefaction on the grindability and reactivity of woody biomass, Fuel Process. Technol. 89 (2008) 169–175.

[44] H. Ben, A.J. Ragauskas, Torrefaction of Loblolly pine, Green Chem. 14 (2012) 72–76.

[45] S.A. Channiwala, P.P. Parikh, A unified correlation for estimating HHV of solid, liquid and gaseous fuels, Fuel. 81 (2002) 1051–1063.

[46] M.J. Prins, K.J. Ptasinski, F.J.J.G. Janssen, More efficient biomass gasification via torrefaction, Energy. 31 (2006) 3458–3470.

[47] P.-C. Kuo, W. Wu, W.-H. Chen, Gasification performances of raw and torrefied biomass in a downdraft fixed bed gasifier using thermodynamic analysis, Fuel. 117 (2014) 1231–1241.

[48] W.H. Chen, C.J. Chen, C.I. Hung, C.H. Shen, H.W. Hsu, A comparison of gasification phenomena among raw biomass, torrefied biomass and coal in an entrained-flow reactor, Appl. Energy. 112 (2013) 421–430.

[49] C. Wang, C. Ryman, J. Dahl, Potential CO2 emission reduction for BF-BOF steelmaking based on optimised use of ferrous burden materials, Int. J. Greenh. Gas Control. 3 (2009) 29–38.

[50] S. Jahanshahi, J.G. Mathieson, M.A. Somerville, N. Haque, T.E. Norgate, A. Deev, Y. Pan, D. Xie, P. Ridgeway, P. Zulli, Development of Low-Emission Integrated Steelmaking Process, J. Sustain. Metall. 1 (2015) 94–114.

[51] S.W. Du, W.H. Chen, J.A. Lucas, Pretreatment of biomass by torrefaction and carbonization for coal blend used in pulverized coal injection, Bioresour. Technol. 161 (2014) 333–339.

[52] P.C.A Bergman, A.R. Boersma, R.W.R. Zwart, J.H.A. Kiel, Torrefaction for biomass co-firing in existing coal-fired power stations, Energy Res. Cent. Netherlands ECN ECNC05013. (2005) 71.

[53] A. Zheng, Z. Zhao, S. Chang, Z. Huang, X. Wang, F. He, H. Li, Effect of torrefaction on structure and fast pyrolysis behavior of corncobs, Bioresour. Technol. 128 (2013) 370–377.

[54] D. Chen, Z. Zheng, K. Fu, Z. Zeng, J. Wang, M. Lu, Torrefaction of biomass stalk and its effect on the yield and quality of pyrolysis products, Fuel. 159 (2015) 27–32.

[55] W. Stelte, C. Clemons, J.K. Holm, A.R. Sanadi, J. Ahrenfeldt, L. Shang, U.B. Henriksen, Pelletizing properties of torrefied spruce, Biomass and Bioenergy. 35 (2011) 4690–4698.

[56] L. Shang, N.P.K. Nielsen, J. Dahl, W. Stelte, J. Ahrenfeldt, J.K. Holm, T. Thomsen, U.B. Henriksen Quality effects caused by torrefaction of pellets made from Scots pine, Fuel Process. Technol. 101 (2012) 23–28.

[57] M. Wilk, A. Magdziarz, I. Kalemba, Characterisation of renewable fuels' torrefaction process with different instrumental techniques, Energy. 87 (2015) 259–269.

[58] F. Pierre, G. Almeida, J.O. Brito, P. Perré, Influence of torrefaction on some chemical and energy properties of maritime pine and pedunculate oak, BioResources. 6 (2011) 1204–1218.

[59] W.H. Chen, K.M. Lu, W.J. Lee, S.H. Liu, T.C. Lin, Non-oxidative and oxidative torrefaction characterization and SEM observations of fibrous and ligneous biomass, Appl. Energy. 114 (2014) 104–113.

[60] C. Wang, J. Peng, H. Li, X.T. Bi, R. Legros, C.J. Lim, S. Sokhansanj, Oxidative torrefaction of biomass residues and densification of torrefied sawdust to pellets, Bioresour. Technol. 127 (2013) 318–325.

[61] K.-M. Lu, W.-J. Lee, W.-H. Chen, S.-H. Liu, T.-C. Lin, Torrefaction and low temperature carbonization of oil palm fiber and eucalyptus in nitrogen and air atmospheres, Bioresour. Technol. 123 (2012) 98–105.

[62] D. Eseltine, S.S. Thanapal, K. Annamalai, D. Ranjan, Torrefaction of woody biomass (Juniper and Mesquite) using inert and non-inert gases, Fuel. 113 (2013) 379–388.

[63] S.S. Thanapal, W. Chen, K. Annamalai, N. Carlin, R.J. Ansley, D. Ranjan, Carbon dioxide torrefaction of woody biomass, Energy and Fuels. 28 (2014) 1147–1157.

[64] M.P. Morales, P. Mun, J.A. Ruiz, M.C. Jua, Biomass gasification for electricity generation : Review of current technology barriers, Renew. Sustain. Energy Rev. 18 (2013) 174–183.

[65] L.F. de Diego, F. García-Labiano, P. Gayán, A. Abad, T. Mendiara, J. Adánez, M. Nacken, S. Heidenreich, Tar abatement for clean syngas production during biomass gasification in a dual fluidized bed, Fuel Process. Technol. 152 (2016) 116–123.

[66] F.J. Wang, S. Zhang, Z.D. Chen, C. Liu, Y.G. Wang, Tar reforming using char as catalyst during pyrolysis and gasification of Shengli brown coal, J. Anal. Appl. Pyrolysis. 105 (2014) 269–275.

[67] J. Han, H. Kim, The reduction and control technology of tar during biomass gasification/pyrolysis: An overview, Renew. Sustain. Energy Rev. 12 (2008) 397–416.

[68] P. Basu, Biomass Gasification, Pyrolysis and Torrefaction: Practical Design and Theory, 2013.

[69] M. Balat, M. Balat, E. Kirtay, H. Balat, Main routes for the thermo-conversion of biomass into fuels and chemicals. Part 1: Pyrolysis systems, Energy Convers. Manag. 50 (2009) 3147–3157.

[70] C. Di Blasi, Modeling wood gasification in a countercurrent fixed-bed reactor, AIChE J. 50 (2004) 2306–2319.

[71] P. Teixeira, H. Lopes, I. Gulyurtlu, N. Lapa, P. Abelha, Evaluation of slagging and fouling tendency during biomass co-firing with coal in a fluidized bed, Biomass and Bioenergy. 39 (2012) 192–203.

[72] A. Zabaniotou, O. Ioannidou, E. Antonakou, A. Lappas, Experimental study of pyrolysis for potential energy, hydrogen and carbon material production from lignocellulosic biomass, Int. J. Hydrogen Energy. 33 (2008) 2433–2444.

[73] B.G. Miller, D.A. Tillman, Coal Characteristics, in: Combust. Eng. Issues Solid Fuel Syst., 2008: pp. 33–81.

[74] Ö. Onay, E. Bayram, Ö.M. Koçkar, Copyrolysis of Seyitömer−Lignite and Safflower Seed: Influence of the Blending Ratio and Pyrolysis Temperature on Product Yields and Oil Characterization, Energy & Fuels. 21 (2007) 3049–3056.

[75] R.M. Soncini, N.C. Means, N.T. Weiland, Co-pyrolysis of low rank coals and biomass: Product distributions, Fuel. 112 (2013) 74–82.

[76] F. Ferrara, A. Orsini, A. Plaisant, A. Pettinau, Pyrolysis of coal, biomass and their blends: Performance assessment by thermogravimetric analysis, Bioresour. Technol. 171 (2014) 433–441.

[77] H. Kobayashi, J.B. Howard, A.F. Sarofim, Coal devolatilization at high temperatures, Symp. Combust. 16 (1977) 411–425.

[78] P.R. Solomon, T.H. Fletcher, R.J. Pugmire, Progress in coal pyrolysis, Fuel. 72 (1993) 587–597.

[79] M.V. Kok, Coal pyrolysis: Thermogravimetric study and kinetic analysis, Energy Sources. 25 (2003) 1007–1014.

[80] J. Cheng, Y. Zhang, T. Wang, P. Norris, W.-Y. Chen, W.-P. Pan, Thermogravimetric–

Fourier Transform Infrared Spectroscopy–Gas Chromatography/Mass Spectrometry Study of Volatile Organic Compounds from Coal Pyrolysis, Energy & Fuels. 31 (2017) 7042–7051.

[81] R. Kandiyoti, A.A. Herod, K.D. Bartle, Pyrolysis: Thermal Breakdown of Solid Fuels in a Gaseous Environment, in: Solid Fuels Heavy Hydrocarb. Liq., 2006: pp. 36–90.

[82] R.J. Evans, T.A. Milne, Molecular characterization of pyrolysis of biomass. 1. Fundamentals, Energy & Fuels. 1 (1987) 123–138.

[83] C.Z. Li, K.D. Bartle, R. Kandiyoti, Characterization of tars from variable heating rate pyrolysis of maceral concentrates, Fuel. 72 (1993) 3–11.

[84] J.R. Gibbins, Z.S. Gonenc, R. Kandiyoti, Pyrolysis and hydropyrolysis of coal: comparison of product distributions from a wire-mesh and a hot-rod reactor, Fuel. 70 (1991) 621–626.

[85] H. Yang, H. Chen, F. Ju, R. Yan, S. Zhang, Influence of pressure on coal pyrolysis and char gasification, Energy and Fuels. 21 (2007) 3165–3170.

[86] P.K. Kanaujia, Y.K.K. Sharma, M.O.O. Garg, D. Tripathi, R. Singh, Review of analytical strategies in the production and upgrading of bio-oils derived from lignocellulosic biomass, J. Anal. Appl. Pyrolysis. 105 (2014) 55–74.

[87] A. Dufour, P. Girods, E. Masson, S. Normand, Y. Rogaume, A. Zoulalian, Comparison of two methods of measuring wood pyrolysis tar, J. Chromatogr. A. 1164 (2007) 240–247.

[88] M.J. Antal, G. Varhegyi, Cellulose Pyrolysis Kinetics - the Current State Knowledge, Ind. Eng. Chem. Res. 34 (1995) 703–717.

[89] G. Várhegyi, M. Antal, E. Jakab, P. Szabó, Kinetic modeling of biomass pyrolysis, J. Anal. Appl. Pyrolysis. 42 (1997) 73–87.

[90] R. Alén, E. Kuoppala, P. Oesch, Formation of the main degradation compound groups from wood and its components during pyrolysis, J. Anal. Appl. Pyrolysis. 36 (1996) 137–148.

[91] A. Pappa, K. Mikedi, N. Tzamtzis, M. Statheropoulos, Chemometric methods for studying the effects of chemicals on cellulose pyrolysis by thermogravimetry-mass spectrometry, J. Anal. Appl. Pyrolysis. 67 (2003) 221–235.

[92] A.M. Azeez, D. Meier, J. Odermatt, Temperature dependence of fast pyrolysis volatile products from European and African biomasses, J. Anal. Appl. Pyrolysis. 90 (2011) 81–92.

[93] E. Biagini, F. Barontini, L. Tognotti, Devolatilization of biomass fuels and biomass components studied by TG/FTIR technique, Ind. Eng. Chem. Res. 45 (2006) 4486–4493.

[94] T. Hosoya, H. Kawamoto, S. Saka, Pyrolysis behaviors of wood and its constituent polymers at gasification temperature, J. Anal. Appl. Pyrolysis. 78 (2007) 328–336.

[95] K. Raveendran, A. Ganesh, K.C. Khilar, Pyrolysis characteristics of biomass and biomass components, Fuel. 75 (1996) 987–998.

[96] T. Hosoya, H. Kawamoto, S. Saka, Secondary reactions of lignin-derived primary tar components, J. Anal. Appl. Pyrolysis. 83 (2008) 78–87.

[97] D. Ferdous, A.K. Dalai, S.K. Bej, R.W. Thring, Production of H2 and medium heating value gas via steam gasification of lignins in fixed-bed reactors, Can J Chem Eng. 79 (2001) 913–922.

[98] C. Di Blasi, Combustion and gasification rates of lignocellulosic chars, Prog. Energy Combust. Sci. 35 (2009) 121–140.

[99] H.H. Schobert, C. Song, Chemicals and materials from coal in the 21st century, Fuel. 81 (2002) 15–32.

[100] I. Rafiqul, B. Lugang, Y. Yan, T. Li, Study on co-liquefaction of coal and bagasse by Factorial Experiment Design Method, Fuel Process. Technol. 68 (2000) 3–12.

[101] D. Klass, Thermal Conversion : Pyrolysis and liquefaction, Biomass Renew. Energy, Fuels, Chem. (1998) 651.

[102] R.N. André, F. Pinto, C. Franco, M. Dias, I. Gulyurtlu, M.A.A. Matos, I. Cabrita, Fluidised

bed co-gasification of coal and olive oil industry wastes, Fuel. 84 (2005) 1635–1644.

[103] F. Pinto, C. Franco, H. Lopes, R. André, I. Gulyurtlu, I. Cabrita, Effect of used edible oils in coal fluidised bed gasification, in: Fuel, 2005: pp. 2236–2247.

[104] Y.G. Pan, E. Velo, X. Roca, J.J. Manyà, L. Puigjaner, Fluidized-bed co-gasification of residual biomass/poor coal blends for fuel gas production, Fuel. 79 (2000) 1317–1326.

[105] K. Li, R. Zhang, J. Bi, Experimental study on syngas production by co-gasification of coal and biomass in a fluidized bed, Int. J. Hydrogen Energy. 35 (2010) 2722–2726.

[106] A.O. Aboyade, M. Carrier, E.L. Meyer, H. Knoetze, J.F. Görgens, Slow and pressurized co-pyrolysis of coal and agricultural residues, Energy Convers. Manag. 65 (2013) 198–207.

[107] T.R. McLendon, A.P. Lui, R.L. Pineault, S.K. Beer, S.W. Richardson, High-pressure co-gasification of coal and biomass in a fluidized bed, Biomass and Bioenergy. 26 (2004) 377–388.

[108] W. Zhu, W. Song, W. Lin, Catalytic gasification of char from co-pyrolysis of coal and biomass, Fuel Process. Technol. 89 (2008) 890–896.

[109] M. Lapuerta, J.J. Hernández, A. Pazo, J. López, Gasification and co-gasification of biomass wastes: Effect of the biomass origin and the gasifier operating conditions, Fuel Process. Technol. 89 (2008) 828–837.

[110] K. Kumabe, T. Hanaoka, S. Fujimoto, T. Minowa, K. Sakanishi, Co-gasification of woody biomass and coal with air and steam, Fuel. 86 (2007) 684–689.

Chapter 3

Lignocellulose pyrolysis with condensable volatiles quantification by thermogravimetric analysis–thermal desorption/gas chromatography–mass spectrometry method

This chapter has been published in "*Journal of Analytical and Applied Pyrolysis 116 (2015) 86–95"* and is been reproduced in this dissertation with copyright permission from Elsevier publishers.

Title: *"Lignocellulose pyrolysis with condensable volatiles quantification by thermogravimetric analysis–thermal desorption/gas chromatography–mass spectrometry method"*

Authors: *Frank Nsaful, François-Xavier Collard, Marion Carrier, Johann F. Görgens, Johannes H. Knoetze*

Objective of dissertation in this chapter and summary of findings

This chapter focussed on the identification, analysis and quantification of condensable volatile products from raw biomass devolatilization (objective 2). As part of this objective an analytical method for volatiles analysis was developed which incorporates the use of TGA in conjunction with thermal desorption unit and a GC-MS. The TGA was used for sample devolatilization while the evolved volatile products were captured unto a thermal desorber tube and analysed by means of a thermal desorption GC-MS. Biomass chemical composition was also studied in order to understand their impacts on volatiles evolution (objective 1).

The analytical technique developed in this chapter is original and has never been reported for the quantification of lignocellulose pyrolysis products. From the conversion of 4 different lignocellulose feedstocks, a total of 15-19 wt% (dry weight) of pyrolysis products were quantified

by the analytical technique. The average Relative Standard Deviation on the high concentration volatiles yield was 6.45% (an improvement on what is usually reported in literature), showing the versatility of the technique in quantifying pyrolysis volatile products even at trace levels. The chemical composition of volatiles was statistically analysed using Principal Component Analysis (PCA). The first two principal components accounted for 89.37% of the variance in the data and enable to clearly identify 4 different clusters, corresponding to the four biomasses. The chemical composition of volatiles showed clear correlations with the original lignocellulose content and the composition of the constituents (type of lignin and hemicellulose).

The analytical method developed in this chapter was subsequently applied in the evaluation of torrefaction/pyrolysis process conditions, as well as characterisation of char products from different thermal treatment conditions, to identify those most suitable for co-gasification with coal.

Summary of authors' contributions

Frank Nsaful planned and conducted all the experimental work. In addition he did the analysis and interpretation of the experimental data and wrote the chapter. *François-Xavier Collard* contributed to the experimental planning and also reviewed the chapter. *Johann F. Görgens* also assisted with data interpretation and reviewed the chapter. Both *Marion Carrier* and *Johannes H. Knoetze* also reviewed the chapter.

Abstract

A thermogravimetric analysis technique coupled to an evolved gas analysis, namely the thermal desorption/gas chromatography–mass spectrometry method (TGA–TD/GC–MS) was developed, to identify and quantify condensable volatile compounds produced during the pyrolysis of lignocellulose. Four lignocellulose samples of different origins (i.e., pine, bamboo, corn cob and corn stover) were pyrolysed using a TGA system. Condensable volatiles released during pyrolysis were captured onto thermal desorption tubes and subsequently identified and quantified using a TD/GC–MS method. Chemical composition of condensable volatiles was statistically correlated with the original lignocellulose composition, using Principal Component Analysis (PCA). A total of 15–19 wt% (dry weight) of biomass pyrolysis products were quantified by the method, with an average Relative Standard Deviation on the high concentration condensable volatiles yield of 6.4%, a significant improvement to what has been reported in literature. The first two principal components accounted for 89.4% of the variance in the data and showed clear correlations between evolved condensable volatile compounds and compositional differences among the four biomass samples. The origin of most lignin-derived compounds could be determined, due to the limitation of secondary reactions under slow pyrolysis. The yield of levoglucosan and 5-hydroxymethylfurfural were consistent with the initial content of C_6 sugars in the feedstock, but also negatively correlated with the ash content. The quantification of acetic acid, the highest yielding condensable volatile product, can be used as an indicator of the number of acetyl groups in biomass.

Keywords: Pyrolysis; Thermogravimetric analysis; Thermal desorption; Condensable volatiles; GC–MS; Biomass

3.1. Introduction

The over dependence on fossil based fuels for energy have resulted in the depletion of such resources. Coupled to this is the issue of global warming caused by the greenhouse gases (GHG) releases associated with the consumption of these fuels. To curtail these effects, research has focussed on the search for renewable and clean alternative sources of energy such as wind, solar, tidal wave, geothermal and biomass. Among these sources, biomass is the only renewable and sustainable carbon carrier [1], with the potential to be converted into fossil-fuel-replacing liquid fuels, chemicals and synthetic materials [2].

The conversion of biomass into chemicals and fuels through thermochemical processes such as pyrolysis, combustion and gasification has gained much attention in recent years. Bio-oil, char and gas are the main products of pyrolysis and gasification processes [3,4]. Beside the use of pyrolysis for bio-oil and char production, the process is also a very critical first step in all thermochemical processes, including gasification and combustion [5]. For this reason, an understanding of feedstock pyrolysis properties and its impact on the conversion process is essential. This will lead to the effective design of competitive thermochemical processes for the production of fuels and chemicals from biomass, or biomass in combination with other feedstock such as coal.

Many studies have been conducted on the optimization of operating conditions (temperature, pressure, heating rate, residence time and particle size) for the efficient pyrolysis of lignocellulose. Others have focussed on thermal decomposition properties and conversion pathways of the various biomass components [6–11]. At the milligram scale, the thermogravimetric analysis (TGA) method has been used to determine the pyrolysis kinetics and thermal stability of biomass, both important for large scale applications. The mechanisms of pyrolysis conversion have been studied with analytical techniques such as TGA coupled with mass spectroscopy (MS) or Fourier transform infrared spectroscopy (FTIR) [12–16]. These techniques have led to the continuous identification of functional groups that are present in the volatiles released during biomass pyrolysis. These, however, are only useful as qualitative results, without accurate quantification of the yields of volatile components from various feedstocks. Given the complex nature of biomass [17,18], many volatiles are produced at the same time during its thermal conversion, thus making quantification very difficult.

At the lab scale, the quantification of the pyrolysis bio-oil product is usually done by gas chromatography–mass spectroscopy (GC–MS) after dilution of the bio-oil in an organic solvent. However, for study at milligram scale with small biomass sample sizes, the use of solvents to recover volatiles would lead to trace amount which would be hard to quantify. The application of pyrolysis coupled to gas chromatography-mass spectroscopy (Py-GC/MS) method has proven to effectively analyse the volatiles generated from such small sample mass without the use of solvent [19]. However, Py-GC/MS does not allow one to combine volatiles production with the kinetics of biomass pyrolysis, as captured in time-wise mass loss.

The precise quantification of bio-oil requires the preparation of individual calibration curves for all the compounds of interest to be quantified. This is a tedious task and explains why in most bio-oil analyses using GC–MS or Py-GC/MS the quantification is done based on the surface areas/normalised surface areas of the peaks corresponding to the main compounds and not on calibration curves of these compounds, which is the only method to determine the actual yields. No absolute quantities of evolved volatiles components are provided thus the need of a quantification method for the effective analysis of biomass pyrolysis volatile components even on small sample sizes.

Thermal desorption/gas chromatography–mass spectrometry (TD/GC–MS) is a technique that allows for the analysis of small sample sizes of volatile compounds and eliminates the need for solvent [20,21]. It has found wide application in several environmental and workplace air monitoring studies [22–25] as well as wood thermodegradation studies [19, 20] for the analysis of volatile organic compounds (VOCs). Although the coupling of TD/GC–MS to TGA for the characterisation of VOCs has been reported [26], the application of this technique to lignocellulose pyrolysis and quantification of volatile products, is limited. The merits of the method include adaptability to smaller sample sizes (milligram scale), and provision of additional TGA information regarding the thermal stability and mass loss kinetics during the main steps of thermal conversion [26]. Other advantages are that it eliminates the effect of solvent signal on analyte peaks in sample chromatograms and it is compatible with both polar and non-polar thermally stable compounds [24]. The disadvantages are that it is ineffective for analysing thermally unstable compounds and high boiling point (>300 ^{o}C) compounds, due to reduced desorption efficiencies

on thermal desorption (TD) tubes, and generation of artefacts possibly due to sorbent degradation that might influence the analysis [24].

In this study we developed a method coupling thermogravimetric analysis with thermal desorption/gas chromatography–mass spectrometry herein referred to as TGA–TD/GC–MS. This was used to study the pyrolysis profiles of four biomass feedstocks (i.e. pine, bamboo, corn cobs and corn stover) and to quantify the distribution of condensable volatile compounds from these feedstocks. TGA was used to pyrolyse the biomass and the evolved volatiles were trapped on-line into TD tubes. The tubes were then analysed off-line by TD/GC–MS, enabling the identification and quantification of condensable volatile compounds (with internal calibration). The data generated were used to establish correlations between biomass composition and volatile yield among the four biomasses by means of principal component analysis (PCA).

3.2. Materials and methods

3.2.1. Feedstock preparation

The lignocellulosic biomasses used in this study were bamboo *(Bambusa balcooa)* (BB), pine *(Pinus radiata)* (PN), and two corn *(Zea mays)* residues; corn cobs (CC) and corn stover (CS). BB is often considered for energy applications because it is a fast growing species [27]. CC and CS are agricultural residues produced in large amounts in South Africa [28], while PN is also widely available in South Africa. BB was supplied from the Western Cape Province of South Africa. It was received wet and was air dried to moisture content of less than 10 wt% and then chipped into chips sizes of approximately 2 cm x 0.5 cm for further preparation. CC and CS were obtained from farms in the Northern Cape Province of South Africa. CC was obtained in whole pieces, while CS was shredded; both were received dried with about 7 wt% moisture. Pine was obtained in pellet form (5–25 mm length and 6–12 mm diameter, 4–8 wt% moisture) from EC Biomass Fuel Pellets (Pty) Limited, Eastern Cape, South Africa. The coning-and-quartering method (DD CEN/TS 14780:2005) was used to obtain sub-samples from each feedstock for experimental work. The biomass feedstocks were milled over a 2 mm screen in a Retsch mill (model ZM100) and sieved into various particle size ranges using a vibratory sieve shaker (model AS200). The 250–450 µm particle size range was selected for all TGA runs.

3.2.2. Biomass characterisation

Elemental and proximate analyses were done for all four biomass samples. A Leco TruSpec Micro CHNS was used to determine the elemental content of the samples, while proximate (volatile matter (VM), fixed carbon (FC) and ash content (AC) analysis was determined by the ASTM method E1131 using TGA/DSC 1-LF1100 system (Mettler Toledo).

The chemical component of biomass consists of extractives, lignin and carbohydrates (mainly C_6 and C_5 sugar moieties). The standard methods NREL/TP-510-42619 and NREL/TP-510-42618 (http://www.nrel.gov/biomass/analytical_procedures.html) were used to determine extractives and lignin and carbohydrates respectively. For extractives, about 5 g of sample was extracted with distilled water in a Soxhlet apparatus for 24 hours, after which the water extractive free sample was extracted with 95% ethanol solution (Scientific World SA) for a further 24 hours. After extractives removal, approximately 0.3 g of the extractive-free sample was hydrolysed with approximately 3 mL of 72% (w/w) sulphuric acid (H_2SO_4) (Fluka Analytical, Sigma-Aldrich) in a water bath at a temperature of 30 ^oC for an hour. The mixture was stirred intermittently at 10 minute intervals. The hydrolysed sample was then diluted to a final concentration of 4% w/w H_2SO_4 using 84 mL of distilled water. The resulting mixture was autoclaved at 121 ^oC and then filtered through a porous crucible to separate the solid residue from the hydrolysis liquor. The solid residue remaining on the porous crucible was dried at 105 ^oC in an oven overnight and then cooled and weighed to determine the acid insoluble lignin (AIL). The AIL was corrected for ash content according to the ISO 1762 standard procedure by combusting the solid residue in a muffle furnace at 575 ± 25 ^oC for a minimum of 4 hours and subtracting the weight of the resulting ash from the estimated AIL. The hydrolysis liquor was used for acid soluble lignin (ASL), monomeric sugars and acetyl content determination. The ASL was measured by a UV spectrophotometer (Varian Cary 50 Bio UV–visible spectrophotometer) at a wavelength of 240 nm (absorptivity of 12 L/(gcm)), except for CS which was measured at a wavelength of 320 nm (absorptivity of 30 L/(gcm)) as set out for this specific biomass in the analysis method. Monomeric sugars (xylose, glucose, mannose, and arabinose) were determined by HPLC (Thermo Separation Products) and converted to their polymeric sugars (glucan, xylan, arabinan, and mannan) concentrations using a correction factor of 0.88 for C_5 sugars (xylose and arabinose) and 0.90 for C_6 sugars (glucose and mannose). Acetic acid content was also determined by HPLC and converted to acetyl content using

a correction factor of 0.983. The completeness of the biomass hydrolysis process was established by HPLC determination of cellobiose concentration in the hydrolysis liquor (concentration of more than 3.0 mg/mL indicated that the hydrolysis was not complete, necessitating the hydrolysis of a new sample for analysis). Before HPLC analysis the hydrolysis liquor was neutralised to a pH of 7 using a 8.25M potassium hydroxide (KOH) solution (115.52 g KOH pellets (Merck) in 250 mL distilled water) and then filtered through a 20 µL filter (Kimix). The neutralised hydrolysis liquor (30 µL) was injected into the HPLC for products separation and quantification (based on standard calibration curves of the pure monomeric sugars). The HPX-87H ion exclusion column (300 mm x 7.8 mm, Bio-Rad) was used. The mobile phase used was 5 mM sulphuric acid at 0.6 mL/min flow rate and the column was maintained at a constant temperature of 65 ^{o}C.

3.2.3. Volatiles Analysis

The analysis of condensable volatile products was made possible in this study by use of a TGA/DSC 1-LF1100 system (Mettler Toledo) connected offline via a TD tube to a thermal desorber/gas chromatography–mass spectroscopy system, hereinafter referred to as TGA–TD/GC–MS. Volatiles generation and capturing was possible using the TGA and TD tube, respectively, while the identification and quantification was done by TD/GC–MS. The following sections describe the technique.

3.2.3.1. Volatile generation by TGA and capture of the condensable organic compounds

Volatiles were produced from various feedstocks by pyrolysis using TGA from 30 ^{o}C to 600 ^{o}C at a heating rate of 10 ^{o}C/min in an inert atmosphere. Evolved gases were quickly swept out from the TGA oven chamber by an argon (baseline 5.0, Afrox SA) flow of 70 mL/min passing through a sampling TD tube, connected at the exit point of the TGA. Condensable volatile compounds were captured onto the TD tube sorbent material. Due to the low flow volumes in the TGA and the short sampling period, active sampling as opposed to passive/diffusive sampling was used for the sampling of volatiles, which was achieved by use of a low flow vacuum pump (ACTI-VOC pump, Markes International, USA) set to constant flow of 70 mL/min (±3 mL/min flow control accuracy). Figure 3-1 shows the volatiles generation and capturing setup.

Multi-sorbent tubes containing Tenax TA, Carbograph 1TD and Carboxen 1003 sorbents materials were used for volatiles capturing. TD tubes were supplied by Markes International, USA, pre-packed into standard stainless steel TD tubes (3.5 in L x 0.5 in O.D) and were already conditioned and capped. TD tubes were blank tested (according to tube desorption procedure outlined in section 3.2.3.2) before first use. After each use TD tubes were reconditioned according to supplier guidelines: 15 min of heating at 100 ^{o}C, 200 ^{o}C, 300 ^{o}C and 325 ^{o}C each, using the UNITY 2 thermal desorption system (Markes International, USA) at helium (baseline 5.0, Afrox SA) carrier gas flow of 50 mL/min. Reconditioned tubes were blank tested before use for volatile sampling. Prior to the first volatiles sampling, the breakthrough volume of the multi-sorbent tube was determined under the sampling conditions, to establish the maximum mass of feedstock required to avoid the breakthrough of volatiles in the tube. To do this, two TD tubes were connected in series to the exit of the TGA and different feedstock masses (5, 10, 12 and 15 mg) were introduced into the TGA and pyrolysed according to conditions described above, with volatiles drawn through the 2 TD tube assembly for capture. Both tubes were thermally desorbed and analysed by TD/GC-MS (Section 3.2.3.2), with the second tube checked for any breakthroughs from the first tube. Breakthrough of compound/s >5% of the amount found on the first tube was deemed significant. Feedstock sample mass of 10 mg and below in the TGA did not result in any significant breakthrough from the first tube and hence 10 mg was chosen as sample size.

3.2.3.2. Volatiles analysis by TD/GC–MS

TD tubes after sampling were analysed by TD/GC–MS. TD was used to release the captured volatile compounds from the tube sorbent material onto the GC/MS for identification and quantification. TD was carried out by use of UNITY 2 thermal desorption system (Markes International, USA) and involved 2 steps: (1) tube desorption (Figure 3-2A) and (2) trap desorption (Figure 3-2B). In the tube desorption step TD tube was rapidly heated to 300 ^{o}C for 10 min to ensure complete desorption using helium (baseline 5.0, Afrox SA) as carrier gas at 10 mL/min and split flow of 30 mL/min (split ratio of 4). Released volatiles were then trapped onto a general purpose cold trap at -10 ^{o}C. In the trap desorption stage the cold trap was desorbed at 320 ^{o}C for 10 min and 1.5 mL/min helium flow through the transfer line to the GC–MS with 30 mL/min split flow. The transfer line was maintained at 200 ^{o}C to prevent volatile condensation. To avoid irreversible adsorption of low volatile compounds by strong sorbent material in the TD tubes, the

flow of carrier gas in both the tube and trap desorption stages was in the reverse direction, from the rear end to the sampling end of the TD tube/trap. A 3 min pre-purge of the system at 1 mL/min helium flow and room temperature was done before each analysis to rid the system of oxygen and/or moisture.

The identification and quantification of released volatile compounds from TD was performed with Agilent Technologies 7890A gas chromatography system coupled with an Agilent Technologies 5975C inert mass spectrometer with Triple-Axis detector. The GC was equipped with Zebron ZB-1701 capillary column (14%-cyanopropylphenyl – methylpolysiloxane, 60 m x 0.25 mm x 0.25 µm dimension – Agilent Technologies). The carrier gas used was helium (baseline 5.0, Afrox SA) at a flow rate of 1.5 mL/min and 25 psi constant pressure and was operated in the splitless mode. The following oven program was used: initial at 45 ^{o}C for 10 min and then from 45 to 100 ^{o}C at 2 ^{o}C/min followed by 100–260 ^{o}C at 7 ^{o}C/min and held for 14 min. 2-Octanol was used as the internal standard. The MS was operated in the scan acquisition mode (20–500 amu). The MS source and MS quadruple temperatures were 230 ^{o}C and 150 ^{o}C respectively while the transfer line temperature was 280 ^{o}C. The identification of compounds was done using the NIST library (2011) and by comparing the retention time of standard compounds.

Calibration was done by preparing 5 standard solutions of each compound of interest (see Table 2) at different concentration ranges (compounds bought from Sigma Aldrich at minimum purity of 97%). Methanol (99.99%, Chromasol grade, Sigma-Aldrich) was used as solvent except for compounds containing carboxylic acid group where acetone (99.8%, Fluka, Riedel-de Haën, Sigma-Aldrich) was used. Each standard solution plus internal standard was introduced into the GC–MS by first loading them onto clean conditioned TD tubes using the calibration solution loading rig, CSLR (Markes International, USA). The sampling end of a TD tube was attached to the CSLR by ¼" brass nut fitted with a PTFE ferrule. Helium carrier gas at 80 mL/min was set to sweep through the injection port of the CSLR down through the TD tube to vent. A GC syringe was used to inject the standard solution through the injection septum of the CSLR. Compounds were then carried by the carrier gas stream to the sampling end of the TD tube to reach the sorbent material. TD tubes were thermally desorbed using conditions outlined above and volatiles transferred to the GC/MS for analysis. A five-point calibration curve ($R^2 \geq 0.97$) was then plotted for each compound of interest. The same loading procedure was used to add the internal standard

solution to sampled TD tubes from TGA before TD/GC–MS analysis. Internal calibration using the calibration curve of each compound was used to quantify and calculate its yield on a dry feedstock basis (wt %).

3.2.4. Principal component analysis (PCA)

PCA was used to study the variability in the data generated by the TGA–TD/GC–MS analysis method for all feedstocks using the Statistica software (V12).

PCA has been used in several studies to chemometrically evaluate a large data set from different origins, thus making it possible for variations in the data to be drawn [19,29–32]. It reduces the dimensionality of the data by replacing a large set of observed variables into a smaller set of new variables. In this study the PCA was performed using the 3 replicate runs from each of four biomass feedstocks as cases (12 cases). Active variables used for the analysis were the yields of char and quantified volatile compounds obtained with significant yields (> 0.1%) (Table 3-2).

3.3. Results and discussion

3.3.1. Feedstock characterization

The properties and chemical compositions of PN, BB, CC and CS biomass samples are presented in Table 3-1. PN contained the highest volatile matter (VM) and the lowest fixed carbon (FC) and ash content (AC), compared to the non-woody biomasses. The low AC was in agreement with previous reports for wood based samples (≤3 wt%) [33]. The chemical compositions showed that PN had the highest C_6 sugars and lignin contents. The cellulose content generally within the range of 40–46 % [34,35] and the hemicelluloses composition (mainly glucomannan) explains the relatively high C_6 sugars content in PN**.** High lignin content of PN was characteristic of softwoods, with values between 25 and 30 wt% previously reported for pine [36].

Among the non-woody biomasses, as xylan is the main hemicelluloses component C_5 and C_6 sugars contents are expected to be similar to hemicelluloses and cellulose contents respectively. In a recent review of bamboo as a source of carbohydrates [37] the composition ranges of 37–47%, 15–30% and 23–31% were reported for cellulose, hemicelluloses and lignin contents, respectively, consistent with the results of this study. In comparison to CS, CC contained less ash and more C_5

sugars (Table 3-1). A similar composition was reported previously for CS [28]. In particular, ash content of CS was relatively high (approx. 7%), which may be attributed to mineral matter from soil contamination during harvesting. A direct correlation was observed between the FC and the lignin contents of BB, CC and CS. Although pine was the biomass with the highest content of lignin (29.9 wt% daf), which is known to be main source of char and FC, it contained the lowest amount of FC, an indication that the other biomass polymers (cellulose and hemicelluloses) also contribute to the overall FC content. This may also be as a result of the nature of lignins and their respective thermal stabilities. The lignin present in angiosperm monocots like BB, CC and CS is evenly distributed among guaiacyl (G) and syringyl (S) units with small amounts of *p*-hydroxyphenyl (H) units [38,39], while that occurring in gymnosperms such as PN consists predominantly of G unit [39,40].

3.3.2. Thermogravimetric analysis

Thermal analyses (mass loss and dTG curves) of the biomass samples are shown in Figure 3-3. The mass loss for PN occurred much later, at higher temperatures, than for the other three biomass samples. As expected the PN, which contained the lowest AC and FC, had the lowest char yield (22.3 wt% db), followed by CC (23.2 wt% db). Higher char yields observed for CS and BB were due to high AC and FC, respectively.

The thermal stabilities of biomass polysaccharides depend on their composition, structure and the presence of inorganic compounds that can have a catalytic effect, shifting the pyrolysis conversion to lower temperatures. Glucomannan as the main component of softwood hemicellulose, has been reported to be more stable than xylan, which is the main component of angiosperm hemicellulose [41]. These observations were consistent with the starting temperatures of conversion observed in the present study, i.e. 260 ^{o}C for PN and approx. 230 ^{o}C for the other samples. While the main peak on the dTG curve is attributed to cellulose depolymerisation, a shoulder attributed to hemicelluloses conversion is sometimes observed around 300 ^{o}C, depending on the heating rate applied. Previous studies [42–45] have shown that hemicelluloses decomposition occur at 220–315 ^{o}C with 250–300 ^{o}C as the temperature range where maximum mass loss rate is observed.

Differences between the temperatures of maximum degradation (as observed in the dTG curves) could be attributed to the variations in the cellulose crystallinity index: higher crystallinity index

is known to shift conversion to a higher temperature and increase the conversion rate [46]. In the case of PN, the temperature of maximum degradation could also be attributed to the negligible catalytic effect of the inorganics, due to its low content (2.1wt% db).

3.3.3. Volatiles analysis

The selection of an appropriate sorbent material is essential in an analysis based on thermal desorption. The sorbent material must be able to capture or trap the compounds of interest from the flow of sampling gas and should be able to release these compounds during heating/desorption, when the flow of gas is reversed. Biomass is a complex material and produces a wide range of volatile compounds from highly volatile (generally with low molecular weight) to less volatile (oligomers with generally high molecular weight). Since no single sorbent can cover this range of compounds, multi-bed sorbent tubes were used to collect analytes of the widest possible range of volatilities. Three sorbent materials, namely Tenax TA, Carbograph 1TD and Carboxen 1003, arranged in order of increasing sorbent strength from the sorbent tube sampling end, were combined in the TD tube. This combination allowed the capture of volatiles in the range from n-C_2–n-C_{30}. Tenax TA is made of porous polymer and is weak strength sorbent suitable for compounds in the range of n-C_7–n-C_{30}. Carbograph 1TD is a medium strength sorbent material made of graphitised carbon black and suitable for compounds of volatility range n-$C_{5/6}$–n-C_{14}. Carboxen 1003, which is a carbonised molecular sieve sorbent, was selected for its strong sorbent strength and hence its ability to trap ultra-light volatiles from ethane – n-C_5.

The yields of condensable pyrolysis volatiles captured onto TD tubes and quantified by the TGA–TD/GC–MS method are presented in Table 3-2 and an example chromatogram in the case of CC is shown in Figure 3-4. Compounds were grouped into classes based on their origin. The values presented for each compound are the averages of 3 measurements. Considering the relative standard deviation (RSD), measurements were found reproducible except for few discrepancies for low yield compounds. The average RSD was 6.4% for compounds with high yields (>0.1 wt%) and 15.6% for compounds with low yields (<0.1 wt%). High RSD for low yield compounds has been reported previously for GC–MS analysis [47], which might be due to baseline noise affecting chromatograph peak integration.

The amount of bio-oil from slow pyrolysis of various biomasses was estimated as 30–45% by Neves et al. [33], with an averaged water content of 10–15% – implying a tar yield of 15%–35%. For most studies reporting the precise quantification of bio-oil by internal calibration using GC-MS, less than 50% of this tar, representing 7–16% [48,49] and 6–16% [47,50] of biomass weight, have been quantified under slow and fast pyrolysis respectively. The difficulty in full quantification of bio-oil on GC–MS has been attributed to the non-detection of high molecular weight oligomers by GC–MS [31,51,52]. Although the analytical strategy TGA–TD/GC–MS did not allow the quantification of water, nor the determination of bio-oil yields, this method was able to account for condensable volatile release representing 15–19 wt% (dry basis) of the lignocellulose feedstock (Table 3-2). The volatile quantification by TGA–TD/GC–MS was thus a significant improvement to previous reports [47–50], in particular under slow pyrolysis conditions which are supposed to give relatively low yield of volatiles, making the method a versatile tool for the analysis and quantification of volatiles produced by pyrolysis.

As seen from Table 3-2, BB had the highest yield of (quantified) volatiles, followed by PN, CS and CC in decreasing order. In particular, the yields of polysaccharide depolymerisation products were higher for PN than for the other lignocelluloses. This result was mostly due to high yields of 5-hydroxymethylfurfural (5-HMF; 0.74 wt% db) and levoglucosan (2.1 wt% db), both of which are products of C_6 sugars degradation [19,21,29], which is consistent with the high C_6 sugars content of pine.

The yield of G lignin derived compounds was observed to be higher for PN than for the other biomasses, again characteristic of softwood lignins [53,54]. On the other hand, low levels of H lignin derived compounds were obtained from PN pyrolysis, while significantly higher for BB, CC and CS. The measured composition of the phenol-derived compounds (G and S units) in the volatile fraction from pyrolysis, indicated that methoxyl groups remained intact, giving evidence of a limited number of secondary, methoxyl conversion reactions. (Methoxyl groups are often substituted by methyl group during pyrolysis at higher heating rates [55]). The limitations to secondary conversion reactions was confirmed by comparison of the yields of guaiacol and *o*-cresol (produced from guaiacol by secondary reactions [55]). The guaiacol to *o*-cresol ratio were estimated from Table 3-2 to be 13.8, 5.1, 10.5 and 3.5, respectively, for PN, BB, CC and CS. These ratios are significantly higher than values obtained from fast pyrolysis, where secondary reactions

result in ratios that are often smaller than 0.5 [31,47] . It is also interesting to note that the guaiacol to *o*-cresol ratio was the lowest for CS, the biomass with the highest ash content (Table 3-1), which could indicate that these secondary reactions were catalyzed at the surface of the inorganics. The limitation of secondary pyrolysis reactions in the TGA–TD/GC–MS runs, renders this method as suitable for studying the composition of biomass polymers.

Figure 3-5 shows the PCA score and correlation loading plots for the chemical compositions of volatiles obtained from the four biomass samples, with regards to the first two principal components PC1 and PC2. PCA allowed for the determination of similarities and non-similarities in volatile products as a result of the compositional differences in the biomasses, by visualizing such correlations. The two selected principal components described 89.4 % of the total variance, with PC1 and PC2 describing respectively 64.0 % and 25.3% of the total variance (Figure 3-5). The PCA analysis clearly identified 4 different clusters, corresponding to the four biomasses (Figure 3-5A). This indicated statistically significant differences in volatiles composition produced from the four biomasses, as a result of differences in characteristics and composition. A good reproducibility of data for the triplicate runs with the analysis method was observed in the score plot (Figure 3-5A), which is in support of the relatively low RSD. PN products correlated very positively with PC1 and negatively with PC2, and were positioned distinctly from the other biomasses. This indicated that the mechanisms of conversion of gymnosperm woody biomass were significantly different in comparison with the other biomasses. Similarly, the BB cluster was distinctly separated from the other angiosperms and correlated negatively with both PC1 and PC2. Although CC and CS correlated positively and negatively with respect to PC1, respectively, they both had a positive correlation with PC2 (Figure 3-5A), which might probably be due to the common origin of these two angiosperm biomasses.

The correlation loading plot (Figure 3-5B) depicted the relationship between the volatile compounds formed from the four biomasses and PC1 and PC2. For convenience the compounds originating from G and H lignins (Table 3-2) were gathered in groups referred to as G lignin and H lignin, respectively (Figure 3-5B). Lignocellulosic composition and proximate analysis were also plotted as supplementary variables, to highlight the correlations between product yield and biomass composition, although these were not used for statistical analysis. The position of PN was mostly due to its high C_6 sugars and lignin contents, while the CS position was mostly influenced

by ash content (Figure 3-5B). From the correlation matrix (Table A-1, Appendix A) a very high correlation (0.99) was observed between levoglucosan and 5-HMF yields, due to the common origin of these compounds (i.e. C_6 sugars degradation). However it is worth noting that the correlation between C_6 sugars and levoglucosan is only 0.88. This result can be related to the negative correlation between levoglucosan and ash content. Indeed it is well known that ash has a catalytic effect on pyrolysis, which generally limits levoglucosan production [32,56]. An illustration of this is the lower levoglucosan yield obtained from CS in comparison with CC, although CS has a higher cellulose content.

In this study the acetyl content of the samples is clearly correlated positively (0.93) with their C_5 sugars composition (Table A-1, Appendix A). This trend is certainly influenced by the low content of acetyl groups in softwood hemicelluloses as observed in Table 3-1. Acetyl substitution of hemicelluloses is known to be an important source of acetic acid production during pyrolysis [41,56]. Hence the lower yield of acetic acid (6.2 wt% db) obtained for PN compared to the other lignocelluloses (Table 3-2). Based on the hypothesis that acetyl groups are exclusively converted into acetic acid, the acetyl content of the biomasses in Table 3-1 were compared to their corresponding yield of acetic acid in Table 3-2. It could be seen that acetyl content contribution to acetic acid yield was between 30.4–43.5%, indicating that acetic acid was also produced from other components of the biomass. Indeed acetic acid has also been reported as a product of lignin and cellulose pyrolysis [47]. In particular, the presence of acetyl group observed on the ɣ-C of BB lignin [57] could explain the higher yields of acetic acid obtained from this sample.

3.4. Conclusion

The pyrolysis of biomass and the subsequent quantification of the generated volatiles were studied through the application of the TGA–TD/GC–MS analytical method. The chemical composition of released volatiles could be correlated with the lignocellulosic composition of the feedstock. PCA confirmed the variability in the chemical compositions of volatiles from the analytical methods, as well as similarities and dissimilarities among different biomass constituents.

While most previous studies on the quantification of bio-oil fraction of biomass have quantified less than 15 wt% fraction of the dry biomass volatile components, especially under slow pyrolysis conditions, the method developed in this study was able to quantify 15–19 wt% dry biomass, which

was particularly high especially under slow pyrolysis conditions. PCA (first two principal components) showed a good repeatability of the analytical method and could explain 89.4% of total variability in the generated data, proving the versatility of the method in the analysis of pyrolysis products from biomass. Lignocellulose composition in comparison to volatile composition showed that biomass type had a direct effect on the type of compounds produced during pyrolysis. With the method developed (low heating rate) it appeared that secondary pyrolysis/cracking reactions due to thermal instabilities were limited. As a consequence it was possible to determine the origin of most of the lignin derived compounds. The yields of the products of cellulose depolymerization were consistent with cellulose content of the feedstocks, but also depended on the ash content. Such findings are of significant interest for optimization of the production of specific chemicals from biomass, or to study the composition of oxygenated compounds released during biomass pyrolysis.

References

[1] M.J.C. van der Stelt, H. Gerhauser, J.H.A. Kiel, K.J. Ptasinski, Biomass upgrading by torrefaction for the production of biofuels: A review, Biomass and Bioenergy. 35 (2011) 3748–3762.

[2] D. Medic, M. Darr, A. Shah, B. Potter, J. Zimmerman, Effects of torrefaction process parameters on biomass feedstock upgrading, Fuel. 91 (2012) 147–154.

[3] Q. Lu, W.M. Xiong, W.Z. Li, Q.X. Guo, X.F. Zhu, Catalytic pyrolysis of cellulose with sulfated metal oxides: A promising method for obtaining high yield of light furan compounds, Bioresour. Technol. 100 (2009) 4871–4876.

[4] S. Czernik, A.V. Bridgwater, Overview of applications of biomass fast pyrolysis oil, Energy & Fuels. 18 (2004) 590–598.

[5] Q. Ren, C. Zhao, X. Chen, L. Duan, Y. Li, C. Ma, NOx and N2O precursors (NH3 and HCN) from biomass pyrolysis: Co-pyrolysis of amino acids and cellulose, hemicellulose and lignin, Proc. Combust. Inst. 33 (2011) 1715–1722.

[6] J.L. Banyasz, S. Li, J. Lyons-Hart, K.H. Shafer, Gas evolution and the mechanism of cellulose pyrolysis, Fuel. 80 (2001) 1757–1763.

[7] V. Mamleev, S. Bourbigot, J. Yvon, Kinetic analysis of the thermal decomposition of cellulose: The main step of mass loss, J. Anal. Appl. Pyrolysis. 80 (2007) 151–165.

[8] S. Wang, H. Lin, B. Ru, W. Sun, Y. Wang, Z. Luo, Comparison of the pyrolysis behavior of pyrolytic lignin and milled wood lignin by using TG-FTIR analysis, J. Anal. Appl. Pyrolysis. 108 (2014) 78–85.

[9] C. Lu, W. Song, W. Lin, Kinetics of biomass catalytic pyrolysis, Biotechnol. Adv. 27 (2009) 583–587.

[10] P.R. Patwardhan, D.L. Dalluge, B.H. Shanks, R.C. Brown, Distinguishing primary and secondary reactions of cellulose pyrolysis, Bioresour. Technol. 102 (2011) 5265–5269.

[11] M. Zhang, F.L.P. Resende, A. Moutsoglou, D.E. Raynie, Pyrolysis of lignin extracted from prairie cordgrass, aspen, and Kraft lignin by Py-GC/MS and TGA/FTIR, J. Anal. Appl. Pyrolysis. 98 (2012) 65–71.

[12] O. Fasina, B. Littlefield, TG-FTIR analysis of pecan shells thermal decomposition, Fuel Process. Technol. 102 (2012) 61–66.

[13] E. Mészáros, E. Jakab, G. Várhegyi, TG/MS, Py-GC/MS and THM-GC/MS study of the composition and thermal behavior of extractive components of Robinia pseudoacacia, J. Anal. Appl. Pyrolysis. 79 (2007) 61–70.

[14] D. Shen, J. Hu, R. Xiao, H. Zhang, S. Li, S. Gu, Online evolved gas analysis by Thermogravimetric-Mass Spectroscopy for thermal decomposition of biomass and its components under different atmospheres: Part I. Lignin, Bioresour. Technol. 130 (2013) 449–456.

[15] N. Gao, A. Li, C. Quan, L. Du, Y. Duan, TG–FTIR and Py–GC/MS analysis on pyrolysis and combustion of pine sawdust, J. Anal. Appl. Pyrolysis. 100 (2013) 26–32.

[16] P. Fu, S. Hu, J. Xiang, P. Li, D. Huang, L. Jiang, A. Zhang, J. Zhang, FTIR study of pyrolysis products evolving from typical agricultural residues, J. Anal. Appl. Pyrolysis. 88 (2010) 117–123.

[17] H. V. Lee, S.B.A. Hamid, S.K. Zain, Conversion of Lignocellulosic Biomass to Nanocellulose: Structure and Chemical Process, Sci. World J. 2014 (2014) 1–20.

[18] F.-X. Collard, J. Blin, A review on pyrolysis of biomass constituents: Mechanisms and composition of the products obtained from the conversion of cellulose, hemicelluloses and lignin, Renew. Sustain. Energy Rev. 38 (2014) 594–608.

[19] S.-S. Liaw, V. Haber Perez, S. Zhou, O. Rodriguez-Justo, M. Garcia-Perez, Py-GC/MS studies and principal component analysis to evaluate the impact of feedstock and temperature on the distribution of products during fast pyrolysis, J. Anal. Appl. Pyrolysis. 109 (2014) 140–151.

[20] K. Candelier, M. Chaouch, S. Dumarçay, A. Pétrissans, M. Pétrissans, P. Gérardin, Utilization of thermodesorption coupled to GC–MS to study stability of different wood species to thermodegradation, J. Anal. Appl. Pyrolysis. 92 (2011) 376–383.

[21] K. Candelier, S. Dumarçay, A. Pétrissans, M. Pétrissans, P. Kamdem, P. Gérardin, Thermodesorption coupled to GC–MS to characterize volatiles formation kinetic during wood thermodegradation, J. Anal. Appl. Pyrolysis. 101 (2013) 96–102.

[22] R. Lindahl, A.S. Claesson, M.A. Khan, J.O. Levin, Development of a method for the determination of naphthalene and phenanthrene in workplace air using diffusive sampling and thermal desorption GC-MS analysis, Ann. Occup. Hyg. 55 (2011) 681–687.

[23] M.R. Ras-Mallorquí, R.M. Marcé-Recasens, F. Borrull-Ballarín, Determination of volatile organic compounds in urban and industrial air from Tarragona by thermal desorption and gas chromatography-mass spectrometry, Talanta. 72 (2007) 941–950.

[24] N. Ramírez, A. Cuadras, E. Rovira, F. Borrull, R.M. Marcé, Comparative study of solvent extraction and thermal desorption methods for determining a wide range of volatile organic compounds in ambient air, Talanta. 82 (2010) 719–727.

[25] S.M. Alston, A.D. Clark, J.C. Arnold, B.K. Stein, Environmental impact of pyrolysis of mixed WEEE plastics part 1: Experimental pyrolysis data, Environ. Sci. Technol. 45 (2011) 9380–9385.

[26] P. Tsytsik, J. Czech, R. Carleer, G. Reggers, A. Buekens, Thermogravimetric desorption and de novo tests I: Method development and validation, Chemosphere. 73 (2008) 113–119.

[27] J. He, S. Cui, S.Y. Wang, Preparation and crystalline analysis of high-grade bamboo dissolving pulp for cellulose acetate, J. Appl. Polym. Sci. 107 (2008) 1029–1038.

[28] A.O. Aboyade, T.J. Hugo, M. Carrier, E.L. Meyer, R. Stahl, J.H. Knoetze, J.F. Görgens, Non-isothermal kinetic analysis of the devolatilization of corn cobs and sugar cane bagasse in an inert atmosphere, Thermochim. Acta. 517 (2011) 81–89.

[29] A. Pattiya, J.O. Titiloye, A.V. Bridgwater, Evaluation of catalytic pyrolysis of cassava rhizome by principal component analysis, Fuel. 89 (2010) 244–253.

[30] C.J. Gómez, E. Mészáros, E. Jakab, E. Velo, L. Puigjaner, Thermogravimetry/mass spectrometry study of woody residues and an herbaceous biomass crop using PCA techniques, J. Anal. Appl. Pyrolysis. 80 (2007) 416–426.

[31] A.M. Azeez, D. Meier, J. Odermatt, Temperature dependence of fast pyrolysis volatile products from European and African biomasses, J. Anal. Appl. Pyrolysis. 90 (2011) 81–92.

[32] A. Khelfa, A. Bensakhria, J.V. Weber, Investigations into the pyrolytic behaviour of birch wood and its main components: Primary degradation mechanisms, additivity and metallic salt effects, J. Anal. Appl. Pyrolysis. 101 (2013) 111–121.

[33] D. Neves, H. Thunman, A. Matos, L. Tarelho, A. Gómez-Barea, Characterization and prediction of biomass pyrolysis products, Prog. Energy Combust. Sci. 37 (2011) 611–630.

[34] R. Capart, L. Khezami, A.K. Burnham, Assessment of various kinetic models for the pyrolysis of a microgranular cellulose, Thermochim. Acta. 417 (2004) 79–89.

[35] Y. Huang, L. Wei, J. Julson, Y. Gao, X. Zhao, Converting pine sawdust to advanced biofuel over HZSM-5 using a two-stage catalytic pyrolysis reactor, J. Anal. Appl. Pyrolysis. 111 (2015) 148–155.

[36] F. Huang, P.M. Singh, A.J. Ragauskas, Characterization of milled wood lignin (MWL) in loblolly pine stem wood, residue, and bark, J. Agric. Food Chem. 59 (2011) 12910–12916.

[37] M. He, J. Wang, H. Qin, Z. Shui, Q. Zhu, B. Wu, F. Tan, K. Pan, Q. Hu, L. Dai, W. Wang, X. Tang, G. Hu, Bamboo: a new source of carbohydrate for biorefinery., Carbohydr. Polym. 111 (2014) 645–54.

[38] X. Bai, P. Johnston, R.C. Brown, An experimental study of the competing processes of evaporation and polymerization of levoglucosan in cellulose pyrolysis, J. Anal. Appl. Pyrolysis. 99 (2013) 130–136.

[39] L.A. Donaldson, Lignification and lignin topochemistry — an ultrastructural view, Phytochemistry. 57 (2001) 859–873.

[40] L.V.G. Ros, C. Gabaldón, F. Pomar, F. Merino, M.A. Pedreño, A.R. Barceló, Structural motifs of syringyl peroxidases predate not only the gymnosperm-angiosperm divergence but also the radiation of tracheophytes, New Phytol. 173 (2007) 63–78.

[41] S. Wang, B. Ru, H. Lin, W. Sun, Pyrolysis behaviors of four O-acetyl-preserved hemicelluloses isolated from hardwoods and softwoods, Fuel. 150 (2015) 243–251.

[42] D.K. Shen, S. Gu, K.H. Luo, S.R. Wang, M.X. Fang, The pyrolytic degradation of wood-derived lignin from pulping process, Bioresour. Technol. 101 (2010) 6136–6146.

[43] H. Yang, R. Yan, H. Chen, D.H. Lee, C. Zheng, Characteristics of hemicellulose, cellulose and lignin pyrolysis, Fuel. 86 (2007) 1781–1788.

[44] S. Zhou, M. Garcia-Perez, B. Pecha, S.R.A. Kersten, A.G. McDonald, R.J.M. Westerhof, Effect of the fast pyrolysis temperature on the primary and secondary products of lignin, Energy and Fuels. 27 (2013) 5867–5877.

[45] G. Di Nola, W. de Jong, H. Spliethoff, TG-FTIR characterization of coal and biomass single fuels and blends under slow heating rate conditions: Partitioning of the fuel-bound nitrogen, Fuel Process. Technol. 91 (2010) 103–115.

[46] Z. Wang, A.G. McDonald, R.J.M. Westerhof, S.R.A. Kersten, C.M. Cuba-Torres, S. Ha, B. Pecha, M. Garcia-Perez, Effect of cellulose crystallinity on the formation of a liquid intermediate and on product distribution during pyrolysis, J. Anal. Appl. Pyrolysis. 100 (2013) 56–66.

[47] F.X. Collard, J. Blin, A. Bensakhria, J. Valette, Influence of impregnated metal on the pyrolysis conversion of biomass constituents, J. Anal. Appl. Pyrolysis. 95 (2012) 213–226.

[48] Z. Wang, J. Cao, J. Wang, Pyrolytic characteristics of pine wood in a slowly heating and gas sweeping fixed-bed reactor, J. Anal. Appl. Pyrolysis. 84 (2009) 179–184.

[49] C. Branca, P. Giudicianni, C. Di Blasi, GC/MS characterization of liquids generated from low-temperature pyrolysis of wood, Ind. Eng. Chem. Res. 42 (2003) 3190–3202.

[50] M. Melzer, J. Blin, A. Bensakhria, J. Valette, F. Broust, Pyrolysis of extractive rich agroindustrial residues, J. Anal. Appl. Pyrolysis. 104 (2013) 448–460.

[51] Q. Lu, X.C. Yang, C.Q. Dong, Z.F. Zhang, X.M. Zhang, X.F. Zhu, Influence of pyrolysis temperature and time on the cellulose fast pyrolysis products: Analytical Py-GC/MS study, J. Anal. Appl. Pyrolysis. 92 (2011) 430–438.

[52] C.A. Mullen, A.A. Boateng, Catalytic pyrolysis-GC/MS of lignin from several sources, Fuel Process. Technol. 91 (2010) 1446–1458.

[53] J. Rencoret, G. Marques, A. Gutiérrez, L. Nieto, J. Jiménez-Barbero, Á.T. Martínez, J.C. del Río, Isolation and structural characterization of the milled-wood lignin from Paulownia fortunei wood, Ind. Crops Prod. 30 (2009) 137–143.

[54] C.A. Nunes, C.F. Lima, L.C.A. Barbosa, J.L. Colodette, A.F.G. Gouveia, F.O. Silvério, Determination of Eucalyptus spp lignin S/G ratio: a comparison between methods., Bioresour. Technol. 101 (2010) 4056–61.

[55] T. Hosoya, H. Kawamoto, S. Saka, Secondary reactions of lignin-derived primary tar components, J. Anal. Appl. Pyrolysis. 83 (2008) 78–87.

[56] O.D. Mante, S.P. Babu, T.E. Amidon, A comprehensive study on relating cell-wall components of lignocellulosic biomass to oxygenated species formed during pyrolysis, J. Anal. Appl. Pyrolysis. 108 (2014) 56–67.

[57] S.-N. Sun, M.-F. Li, T.-Q. Yuan, F. Xu, R.-C. Sun, Sequential extractions and structural characterization of lignin with ethanol and alkali from bamboo (Neosinocalamus affinis), Ind. Crops Prod. 37 (2012) 51–60.

Tables

Table 3-1: Characteristic properties of biomass feedstocks

Property	Feedstock			
	Pine (PN)	Bamboo (BB)	Corn cob (CC)	Corn Stover (CS)
Proximate analysis (wt%), db[a]				
Volatile Matter (VM)	81.85	76.11	78.91	75.30
Fixed Carbon (FC)	16.01	21.45	18.49	16.85
Ash Content (AC)	2.14	2.44	2.61	7.85
Ultimate analysis (wt%), daf[b]				
C	45.60	44.41	43.80	41.88
H	6.47	6.32	6.49	6.40
N	0.02	0.44	0.33	0.59
S	0.08	0.14	0.00	0.20
O[c]	47.83	48.69	49.38	50.93
Lignocellulose composition (wt%), daf[b]				
Lignin	29.9	25.5	17.8	16.5
Extractives	5.2	12.0	10.5	17.5
C_6 sugars	46.1	39.3	34.3	36.7
C_5 sugars	6.7	16.3	26.0	21.3
Acetyl	1.9	3.3	3.9	3.1

[a] Dry basis
[b] Dry ash free basis
[c] Determined by difference

Table 3-2: Yields of volatile compounds and char from pyrolysis of pine (PN), bamboo (BB), corn cob (CC) and corn stover (CS) (wt% dry biomass)

Compound Name	Bamboo (BB)		Pine (PN)		Corn stover (CS)		Corn cob (CC)	
Carbohydrates-derived/Short chain compounds	Yield	SD	Yield	SD	Yield	SD	Yield	SD
Levoglucosan	0.09	0.01	2.1	0.2	0.23	0.02	0.26	0.01
5-Hydroxymethylfurfural	0.34	0.01	0.74	0.02	0.36	0.02	0.40	0.02
Furfural	0.39	0.02	0.96	0.02	0.63	0.09	0.66	0.05
2-Methylfuran	0.18	0.01	0.17	0.01	0.13	0.01	0.14	0.01
2(5H)-Furanone	0.40	0.02	0.61	0.03	0.49	0.01	0.38	0.08
Methyl acetate	0.19	0.01	0.02	0.01	0.10	0.01	0.04	0.01
Formic acid	1.1	0.1	2.7	0.1	1.1	0.1	2.2	0.1
Acetic acid	9.6	0.1	6.2	0.1	9.0	0.4	7.1	0.9
Acetol	3.4	0.1	2.2	0.1	3.2	0.2	1.8	0.1
Propanoic acid	0.49	0.01	0.26	0.01	0.62	0.04	0.61	0.05
Butanoic acid	0.09	0.02	0.05	0.01	0.09	0.01	0.06	0.01
Sub-total	**16.27**	**0.41**	**16.01**	**0.61**	**15.95**	**0.91**	**13.65**	**1.34**
Lignin-derived compounds								
Guaiacyl units (G)								
Guaiacol	0.32	0.02	0.24	0.01	0.19	0.02	0.23	0.03
Creosol	0.06	0.01	0.24	0.02	0.03	0.01	0.04	0.01
2-Methoxy-4-vinylphenol	0.46	0.01	0.36	0.05	0.33	0.03	0.57	0.06
Eugenol	0.01	0.01	0.04	0.02	0.01	0.01	0.01	0.01
4-Propyl guaiacol	0.007	0.001	0.01	0.01	0.002	0.001	0.004	0.004
o-Cresol	0.06	0.01	0.02	0.01	0.05	0.01	0.02	0.01
trans-Isoeugenol	0.17	0.01	0.50	0.02	0.07	0.01	0.06	0.01
Isoeugenol	0.03	0.02	0.11	0.03	0.01	0.01	0.02	0.01
Sub-total	**1.12**	**0.09**	**1.52**	**0.17**	**0.69**	**0.10**	**0.95**	**0.14**
Syringyl units (S)								
Phenol, 2,6-dimethoxy-	0.55	0.03	0.50	0.07	0.17	0.01	0.13	0.01
Sub-total	**0.55**	**0.03**	**0.50**	**0.07**	**0.17**	**0.01**	**0.13**	**0.01**
p-Hydroxyphenyl units (H)								
Phenol	0.54	0.02	0.05	0.02	0.30	0.02	0.22	0.02
p-Cresol	0.05	0.01	0.005	0.001	0.02	0.01	0.01	0.01
Phenol, 4-ethyl-	0.08	0.01	0.009	0.004	0.05	0.01	0.03	0.01
Sub-total	**0.67**	**0.04**	**0.06**	**0.02**	**0.37**	**0.04**	**0.26**	**0.04**
Other aromatic compounds								
Naphthalene	0.002	0.001	0.002	0.001	0.003	0.001	0.003	0.002
Ethylbenzene	0.007	0.001	<0.001	0.001	0.005	0.001	0.003	0.004
Dibenzyl ether	<0.001	0.000	<0.001	0.000	0.003	0.000	<0.000	0.000
m-Cresol	0.06	0.01	0.006	0.001	0.03	0.001	0.02	0.01
2,4-Xylenol	<0.001	0.000	0.002	0.001	<0.001	0.000	<0.001	0.000
Benzofuran	0.002	0.000	0.002	0.001	0.000	0.000	0.002	0.001

Sub-total	**0.07**	**0.01**	**0.01**	**0.005**	**0.04**	**0.003**	**0.028**	**0.017**
Total	**18.68**	**0.58**	**18.10**	**0.87**	**17.22**	**1.06**	**15.02**	**1.55**
Char yield	**28.58**		**22.34**		**27.68**		**23.21**	

SD – standard deviation

Figures

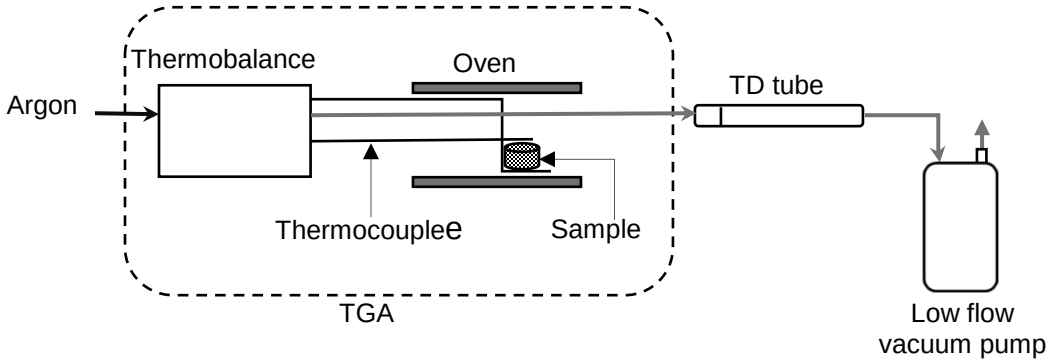

Figure 3-1: TGA volatiles generation and capturing

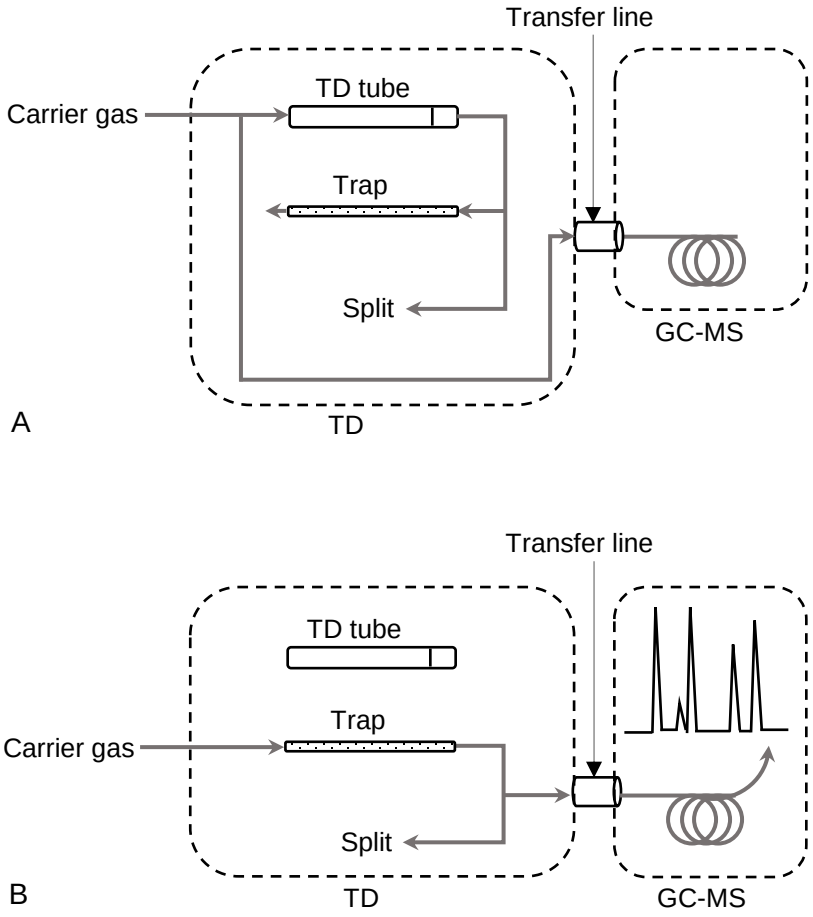

Figure 3-2: TD/GC-MS volatiles analysis setup - (A) tube desorption, (B) trap desorption

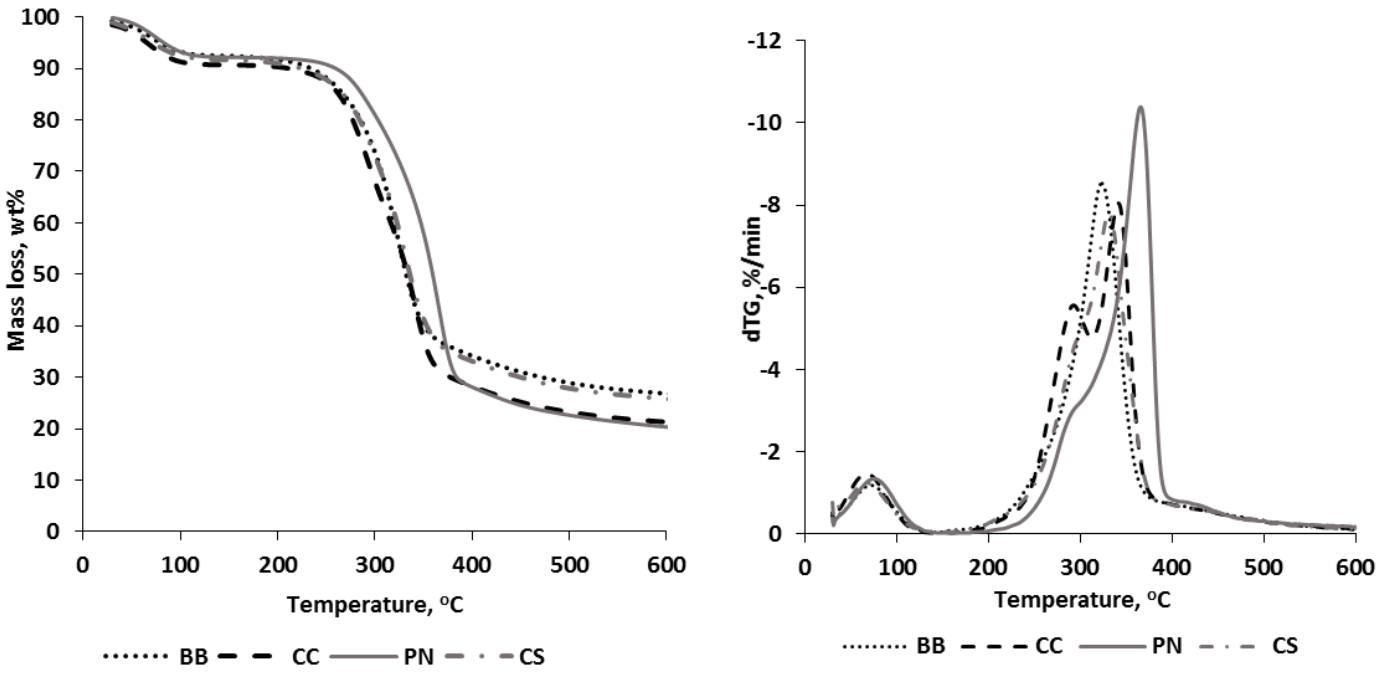

Figure 3-3: Mass loss and DTG curves of pine (PN), bamboo (BB), corn cob (CC) and corn stover (CS) at 10 °C/min

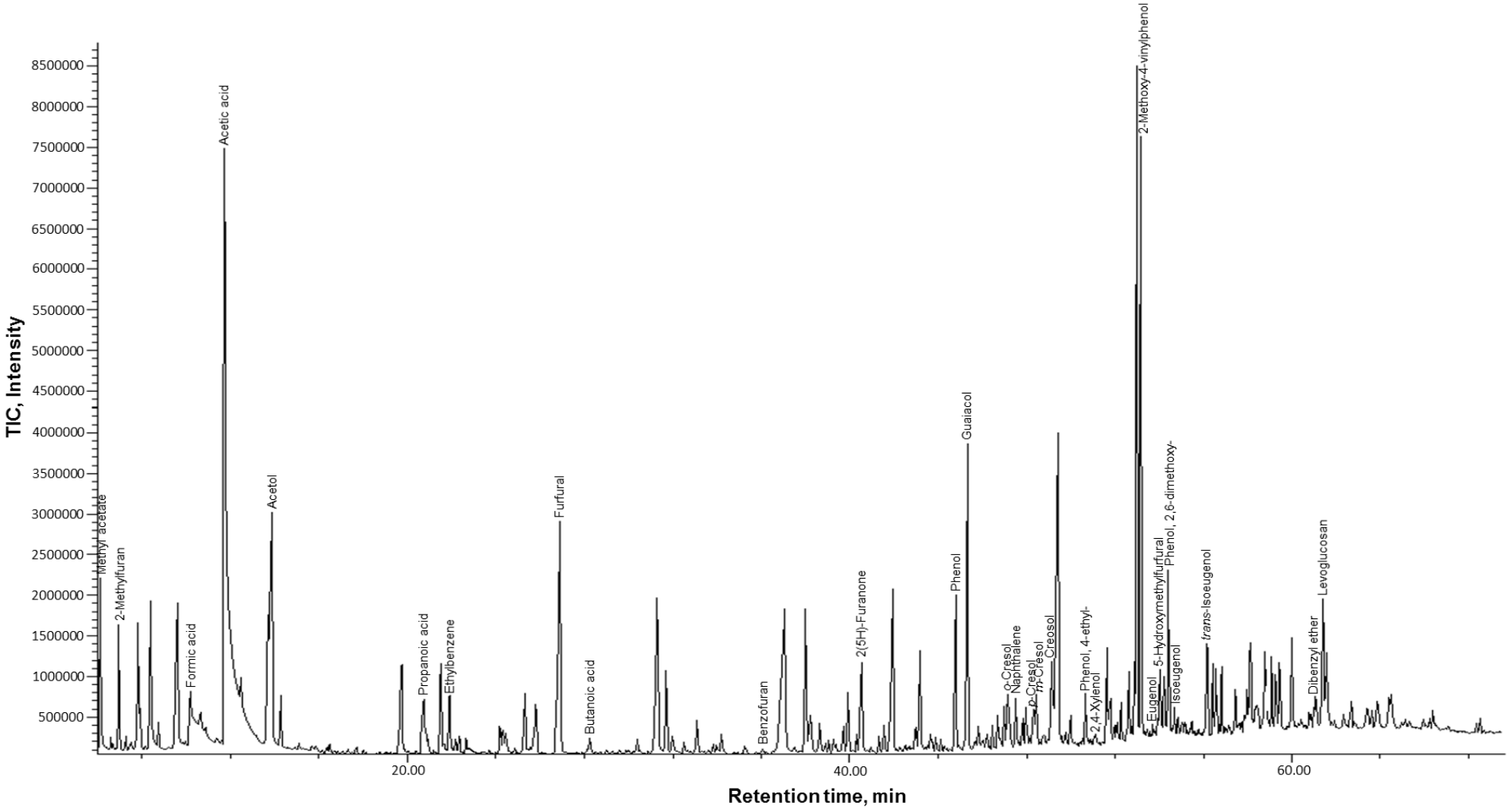

Figure 3-4: GC-MS chromatogram with identification of some main compounds produced from corn cob (CC) pyrolysis

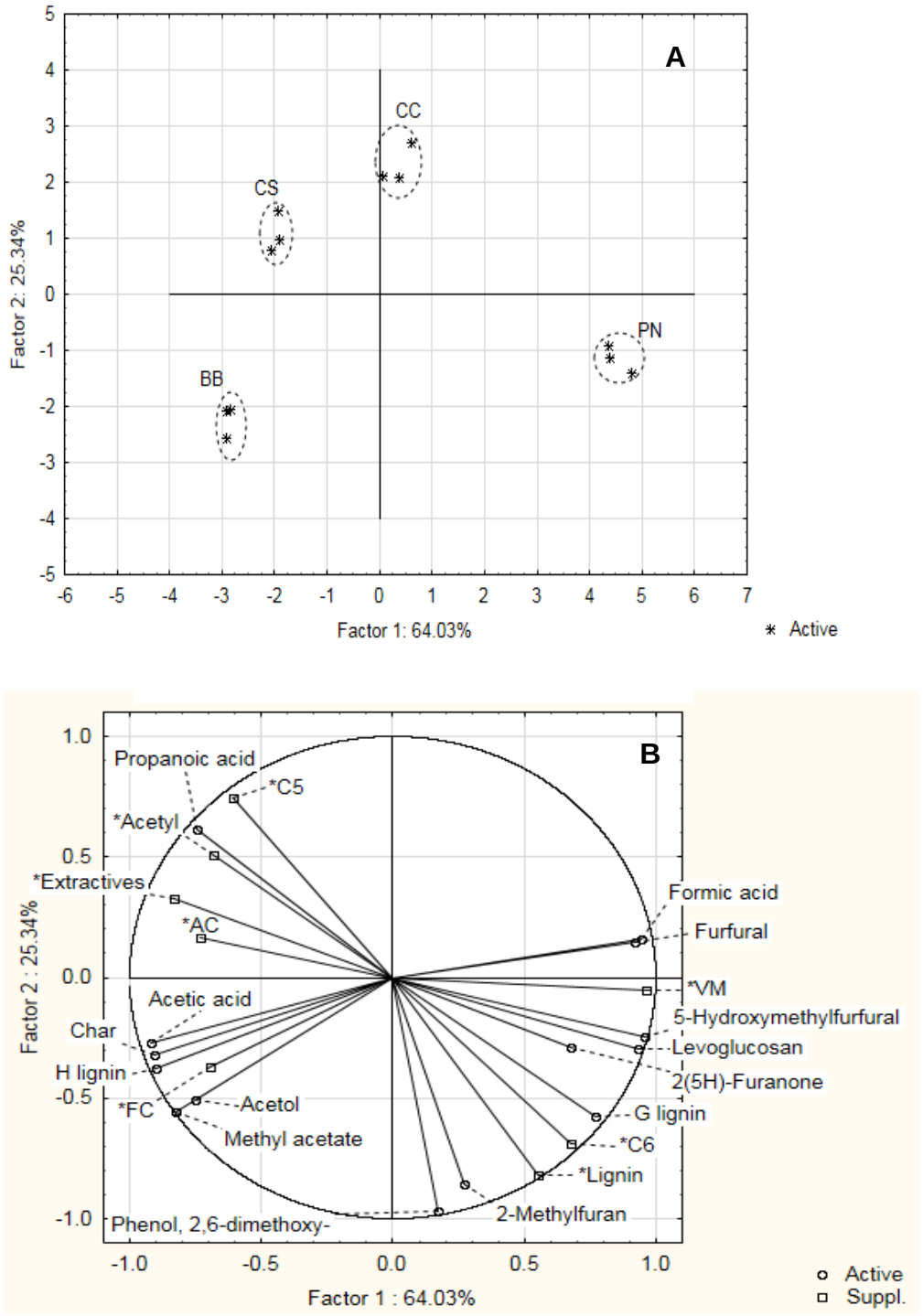

Figure 3-5: PCA score (A) and correlation loading (B) plots of factor 1 (PC1) and factor 2 (PC2) of TGA-TD/GC-MS volatiles data from four biomass feedstocks

Chapter 4

Influence of lignocellulose thermal pretreatment on the composition of condensable products obtained from char devolatilization by means of thermogravimetric analysis-thermal desorption/gas chromatography-mass spectrometry

This chapter has been published in "*Journal of Analytical and Applied Pyrolysis 127 (2017) 99–108"* and is been reproduced in this dissertation with copyright permission from Elsevier publishers.

Title: "*Influence of lignocellulose thermal pretreatment on the composition of condensable products obtained from char devolatilization by means of thermogravimetric analysis-thermal desorption/gas chromatography-mass spectrometry"*

Authors: *Frank Nsaful, François-Xavier Collard, Johann F. Görgens*

Objective of dissertation in this chapter and summary of findings

In this chapter the impact of thermal pretreatment conditions (250–400 ºC temperature and 30 or 60 min hold times) on biomass structural transformation and on the volatile evolution mechanism of char during subsequent devolatilization was studied (objective 3). In addition the effect of the lignocellulosic chemical composition of biomass (objective1) during the pretreatment was also established. Biomass thermal pretreatment and char devolatilization were done at the milligram scale using TGA.

The novel approach of the chapter consists in the yield quantification of condensable volatile products from char devolatilization, achieved via volatiles capture and analysis by thermal desorption, gas chromatography-mass spectroscopy technique (objective 2; Chapter 3). The results were consistent with the steps of biomass degradation as confirmed by thermogravimetric analysis (TGA) curves. There was correlation between biomass constituents' degradation during thermal pretreatment and char devolatilization products. Hemicelluloses and cellulose degradation during thermal pretreatment resulted in reduced yields of acids, ketones, furans and levoglucosan from subsequent char devolatilization. Interestingly, it was found that pretreatment temperature to convert cellulose was dependent on biomass nature and in particular on cellulose crystallinity. Char devolatilization of samples pretreated at 350 ^{o}C and above produced mainly aromatic hydrocarbons due to the formation of more condensed aromatic structures in the char during pretreatment. Based on the work completed in the present chapter, thermal treatment at 350 ^{o}C and above could be selected as appropriate for biomass pretreatment before co-gasification with coal.

Summary of authors' contributions

Frank Nsaful was responsible for the planning and execution of the experimental work. He also did the data analysis and interpretation and wrote the chapter. *François-Xavier Collard* contributed towards the experimental planning and also reviewed the chapter. *Johann F. Görgens* also assisted with data interpretation and reviewed the chapter.

Abstract

Four lignocellulosic biomass types, i.e. pine, bamboo, corn cob and corn stover were converted at varying temperatures (250–400 ^{o}C) and hold times (30 or 60 min). Chars produced were devolatilized in a thermogravimetric analyser (TGA) and evolved condensable volatile products were captured and quantified by thermal desorption/gas chromatography-mass spectrometry. Based on the mass loss rate curves (dTG), char devolatilization products distribution was consistent with the extent of biomass modification by thermal pretreatment. It was evident that pretreatment at 250 and 275 ^{o}C led to significant conversion of hemicelluloses, the latter resulting in a 2–3 factor decrease in acids yield from char devolatilization. Except for pine (with more crystalline structure), significant cellulose conversion was achieved at 300 ^{o}C resulting in a decreased levoglucosan yield and at least a 10 factor reduction in furans production from char devolatilization compared to raw biomass. Most of the oxygenated groups were converted during pretreatment at a temperature of 350 ^{o}C while the char became a more condensed aromatic structure. Therefore the condensable organic products were obtained in low yields (< 1 wt%) and were characterized by a majority of aromatic hydrocarbons and the absence of most of the oxygenated compounds, except for the phenolic products.

Keywords: Biomass; Char; Torrefaction; Pyrolysis; Volatile analysis; TGA

4.1. Introduction

Fossil-based fuels play a major role in the global energy supply chain. However, the use of such fuels poses environmental problems such as air pollution and global warming [1]. In addition these fuels are non-renewable and hence, the need for an alternative fuel source that is both renewable and environmentally friendly. Lignocellulosic biomass has the potential to replace fossil-based fuels, given that it is a renewable carbon carrier and offers environmental benefits such as CO_2 neutrality, and low SO_x and NO_x emissions [2,3].

Several methods exist for the conversion of biomass into energy and/or energy carriers. Prominent among these are the thermochemical processes such as gasification, combustion and pyrolysis generating energy products including, bio-fuels and power from biomass [4,5]. However untreated lignocellulose exhibits characteristics such as high moisture content, high oxygen content, heterogeneity, low bulk and energy density, hydrophilicity, susceptibility to microbial decay and difficulty in grinding [3,6,7]. These characteristics impact adversely on the processing/conversion efficiency and the quality of the products obtained when lignocellulose is utilized in the above mentioned processes. Improvement of the characteristics of untreated lignocellulose would ensure more efficient utilization in energy conversions.

Torrefaction and slow pyrolysis are among the thermal pretreatments used to improve biomass properties for energy conversions [8]. Torrefaction is a mild form of pyrolysis usually in the temperature range of 200-300 ^oC [9,10], while slow pyrolysis is typically undertaken between 300 and 500 ^oC [11], in an inert atmosphere. Compared to other thermochemical processes they are characterized by low heating rates (<50 ^oC) and long volatiles residence time. Thermal pretreatment processes provide lignocellulose with several added advantages such as reduced moisture content [8,12], reduced O/C ratio [13], hydrophobicity [14,15], increased energy density [16], improved grindability [9,17] and uniformity of the solid fuel product [18]. Due to the above advantages research on thermal pretreatment has increased over the last few decades [2]. Most of these studies, however, have focused on the impact of thermal pretreatment conditions (temperature and hold time (HT)) on the mass yield [19,20], heating value [20] and grindability [9,21] of the solid product. Temperature is usually reported to be the factor with the most pronounced effect. Char yields ranging from 75 to 90 wt% with an HHV increase of 1-3 MJ/kg

have been reported for torrefied biomass at 250 °C, while char yields of 40–60 wt% and an HHV increase of 3–7 MJ/kg were obtained at 300 °C [3,13]. At higher temperatures, for instance 400 °C and above char yields of less than 40 wt% [22] and an HHV greater than 25 MJ/kg [23] has been reported. The effect of HT had been observed, especially during torrefaction, with longer HT resulting in improved HHV and reduced char yields. For instance a 13.5 wt% reduction in char yield and 2.6 MJ/kg increase in HHV were obtained for wood at 280 °C when HT was increased from 25 to 80 min [20].

Depending on the lignocellulosic composition of biomass, the yield and fuel properties of the char product as influenced by temperature during thermal pretreatment can vary significantly. For example using two woody biomasses (*Lantana Camara* and *Mimosa Pigra*) with similar initial HHV (≈ 18 MJ/kg), Mundike et al [20] obtained 43.4 wt% char yield and 27.1 MJ/kg HHV for *Lantana Camara* and 52.1 wt% char yield and 24.5 MJ/kg HHV for *Mimosa Pigra* when both were torrefied at 303 °C. This difference was attributed to the relatively high hemicellulose content in *Lantana Camara*. While hemicellulose conversion occur at 200-350 °C, lignin conversion occurs at a slow rate over a wide range (200–600 °C) with the maximum rate usually at 400 °C [24,25].

The extent of cellulose conversion has a critical influence on char yield and composition as cellulose is the main lignocellulose constituent. While slow conversion can occur for temperatures lower than 300 °C, cellulose depolymerization becomes very fast at higher temperatures as evidenced by the presence of a narrow peak with a maximum usually observed between 320 and 380 °C on the dTG curve of thermogravimetric analysis (TGA) [26]. The main factors identified as influencing the maximum temperature are the cellulose crystallinity [27,28], the catalytic effect of inorganics [26] and some interactions due to the decomposition of the other constituents [29]. An interesting illustration is a study of the conversion of washed and unwashed grasses [26]. As a consequence, in case a significant conversion of the cellulose constituent is required, the temperature of the thermal pretreatment must be adapted to the type of biomass considered. The temperature of the thermal pretreatment is thus based on a compromise. Increasing temperature leads to more extensive conversion which results in higher char heating value, but lower char yield. For temperatures higher than 400 °C, the conversion of the lignocellulosic constituents is more limited, thus such temperatures are avoided in order to limit the energy demand of pretreatment.

The use of biomass char as substitute fuel for coal in combustion and gasification processes is envisioned to increase in the future as research strives towards sustainable and environmental friendly sources of energy. For such applications, a critical factor is the composition of the volatile organic compounds released from biomass char during the devolatilization step. For combustion, the presence of reactive volatiles can significantly modify the combustion performance of a fuel [30,31]. In the case of gasification applications, some volatiles called tar cause several operational problems such as corrosion or deactivation of catalysts used during syngas conversion [32]. While several studies about the composition of volatiles released during biomass torrefaction or pyrolysis can be found (though it is still a challenge due to the complexity of bio-oil), similar studies about char devolatilization are limited. Previous work [33,34] reported torrefaction of biomass up to 290 ^{o}C with subsequent pyrolysis of the torrefied biomass (char) to study the effect of the pretreatment on the bio-oil and concluded that the bio-oil properties were greatly improved. Regarding thermal pretreatment to produce char for combustion and gasification applications a more severe pretreatment temperature is required. For such experiments, especially when thermal pretreatment was realized at relatively high temperature, low yields of organic compounds are expected. As a consequence, the use of a solvent to recover the organic compounds is not recommended and an analytical method such as thermogravimetric analysis with quantification of captured evolved volatile products by thermal desorption/gas chromatography-mass spectrometry (referred to as TGA–TD/GC–MS) recently developed [35] appears as particularly suitable.

In the current work, the influence of thermal pretreatment on the characteristics of four different lignocellulosic feedstocks was explored. The aim of the study was to assess the impact of torrefaction and slow pyrolysis on the chemical properties of biomass, and the effect of pretreatment conditions on the mechanisms of devolatilization of the generated chars, evaluated through analysis of the volatile products' chemical composition. Thermal pretreatment experiments and the subsequent devolatilization of the chars were performed at milligram-scale in TGA. The volatiles products from devolatilization of chars were captured onto thermal desorption tubes and analyzed by thermal desorption/GC–MS for identification and quantification by internal calibration. The combination of thermal degradation with compositional analysis of volatile products provided insights into the mechanisms and pathways for specific volatiles evolution.

4.2. Materials and methods

4.2.1. Feedstock

Four types of biomass from different provinces of South Africa were used for this study. These include two corn *(Zea mays)* residues; corn stover (CS) and corncob (CC), pine *(Pinus radiata)* (PN) and bamboo *(Bambusa balcooa)* (BB), which were obtained from the Northern, Eastern and Western provinces, respectively. Prior to further analysis, sub-samples of each feedstock for experiments were obtained by the standard method DD CEN/TS 14780:2005. The biomass feedstocks were ground and sieved to a particle size range of 250–450 μm using Retsch mill (model ZM100) and a vibratory sieve shaker (model AS200). Both corn residues had a moisture content of less than 7 wt% (as received), while PN was obtained in the form of pellets (5–25 mm length and 6–12 mm diameter, EC Biomass Fuel Pellets (Pty) Limited, Eastern Cape, South Africa) and had a moisture content of 4–8 wt%. BB was air dried to less than 10 wt% moisture and cut into chips (about 2 cm x 0.5 cm).

4.2.2. Chemical analysis

The lignocellulose chemical composition (extractives, acetyl, lignin and structural carbohydrates) of raw biomass feedstocks were determined according to the standard laboratory analytical procedures (LAPs) 002, 003, 017 and 019, as developed by the National Renewable Energy Laboratory (NREL) (http://www.nrel.gov/biomass/analytical_procedures.html). Proximate analysis was conducted to determine the percentages of ash, fixed carbon (FC) and volatile matter (VM) present in feedstock according to ASTM method E1131, by means of thermogravimetric analysis (TGA) (TGA/DSC 1-LF1100 system, Mettler Toledo). Elemental analysis was determined using a Leco TruSpec Micro elemental analyzer.

4.2.3. TGA thermal pretreatment

The thermal pretreatment (torrefaction or slow pyrolysis) of biomass samples was achieved by the use of TGA (TGA/DSC 1-LF1100 system, Mettler Toledo). About 180–400 mg per sample of raw biomass (depending on the bulk density of biomass feedstock) was pretreated in an inert atmosphere at an argon (baseline 5.0, Afrox SA) flow rate of 70 ml/min. The following heating

program was followed: dynamic heating at 10 ^{o}C/min from 30 ^{o}C to the appropriate pretreatment temperature, followed by isothermal condition for a specific hold time. The pretreatment temperatures were 250, 275, 300, 350, and 400 ^{o}C, while the hold times were fixed at 30 min or 60 min. Biomass pretreatment was performed in at least triplicate to generate sufficient quantities of char product, which was stored in air tight containers until further analysis. The TGA ensured efficient temperature control during pretreatment and allowed for the measurement of the weight loss dynamics of the biomass as a function of temperature, hold time and heating time.

4.2.4. TGA devolatilization and condensable volatiles analysis

The production and analysis of volatiles from pretreated/raw biomass samples were done following the TGA–TD/GC–MS (thermogravimetric analysis-thermal desorption/gas chromatography-mass spectrometry) method of Nsaful et al [35]. The method makes use of a thermogravimetric analyzer (to pyrolyse and release volatiles from samples) which is connected offline to a thermal desorber/GC-MS assemble (for the analysis, separation, identification and quantification of volatiles) via a thermal desorption (TD) tube. A schematic diagram of the method is shown in Figure 4-1. Pyrolysis volatiles products are collected and analyzed in the gaseous form, thus avoiding the use of solvents as is typically required for GC-MS analysis of pyrolysis liquids. The effect of solvent signal on analyte peaks is eliminated, therefore making the method suitable for smaller sample sizes.

The devolatilization of raw/pretreated biomass was conducted as follows: A 10 mg sample was added to a 70 µl alumina crucible and pyrolysed using a TGA/DSC 1-LF1100 system (Mettler Toledo) according to the following heating programme: dynamic heating at 10 ^{o}C/min from 30 ^{o}C to 600 ^{o}C. Pure argon (baseline 5.0, Afrox SA) at a flowrate of 70 mL/min was used as carrier gas to create an inert atmosphere within the TGA oven. Evolved volatiles were immediately carried out from the oven chamber in the flow of hot argon gas to a pre-conditioned standard stainless steel TD tube (3.5 in L x 0.5 in O.D, Markes international, USA) connected at the TGA exit, where they were adsorbed onto the surface of TD tube sorbent materials. TD tubes contained a combination of three sorbent materials: Tenax TA, Carbograph 1TD and Carboxen 1003 (in order of increasing strength from the tube inlet), which cover volatiles in the range n-C_2–n-C_{30} (excluding water and some non-condensable volatiles).

After devolatilization the TD tubes were immediately transferred to a UNITY 2 thermal desorber (Markes International, USA), where a 3 µl of internal standard (2-octanol dissolved in methanol solvent) solution of known concentration was added, using a standard GC syringe and a calibration solution loading rig (CSLR). Tubes were then thermally desorbed and volatiles transferred to a GC–MS (Agilent Technologies 7890A gas chromatography system coupled with an Agilent Technologies 5975C mass spectrometer) for separation, identification and quantification. For thermal desorption the following conditions were used: 3 min system pre-purge at 1 mL/min helium (baseline 5.0, Afrox SA) flow; primary/tube desorption at 300 ^{o}C for 10 min using helium at 10 mL/min tube flow and 30 mL/min split flow (split ratio of 4) with general purpose cold trap maintained at -10 ^{o}C; secondary/trap desorption at 320 ^{o}C for 10 min with 1.5 mL/min column flow and 30 mL/min split flow; 200 ^{o}C transfer line temperature. The GC was operated in a splitless mode and conditions were as follows: oven program – 10 min isothermal at 45 ^{o}C followed by a 2 ^{o}C/min ramp from 45 to 100 ^{o}C and 7 ^{o}C/min from 100 to 260 ^{o}C and then 14 min hold at 260 ^{o}C; carrier gas – helium (baseline 5.0, Afrox SA) at a flow of 1.5 mL/min and 172.37 kPa constant pressure; column type – Zebron ZB-1701 capillary column (14%-cyanopropylphenyl – methylpolysiloxane, 60 m x 0.25 mm x 0.25 µm dimension - Agilent Technologies). The MS source and quadrupole temperatures were 230 ^{o}C and 150 ^{o}C respectively, and the detector was operated in the scan acquisition mode (20–500 amu). The GC and MS interface was maintained at 280 ^{o}C. The NIST library (2011) together with the retention times of standard compounds were used to identify compounds. Quantification was done using a five-point calibration curve ($R^2 \geq 0.97$) of each compound. Curves were obtained by injecting known concentrations of pure standard compounds (97% minimum purity from Sigma Aldrich), together with a known amount of internal standard, directly onto TD tubes using standard GC syringe and the CSLR. Tubes were then analyzed using the same thermal desorption and GC–MS conditions stated above to plot the calibration curves.

4.2.5. Crystallinity analysis

To study the impact of the pretreatment conditions (specifically temperature) on chemical transformation and cellulose degradation, a crystallinity analysis was done on selected samples. For this study, samples of each raw biomass as well as their chars produced at temperatures of 275 ^{o}C, 300 ^{o}C and 350 ^{o}C and a hold time of 30 min were analyzed for the presence of a crystalline

phase. Crystallinity was determined by X-ray Diffraction (XRD), using a PANalytical X'Pert Pro MPD instrument with Bragg-Brentano geometry, Cu-Kα radiation (λ = 1.5418 Å) and an X'Celerator detector. The accelerating voltage and current were 45 kV and 40 mA respectively. Samples were scanned at 2ɵ in the range 5–35^{o} with a step size of 0.0167. Several methods exist for estimating the degree of crystallinity present in a sample such as the multi-peak resolution method and profile fitting of XRD data [36,37]. However, a qualitative approach was used in this study, hence the presence of the principal cellulose peak (I_{002}) located at 2ɵ = 22.7^{o} [36,37] and its relative intensity was deemed to show the crystallinity of the material.

4.3. Results and discussion

4.3.1. Feedstock characterization

The compositional characteristics of the lignocellulosic feedstocks used in the study are detailed in Table 4-1. All four feedstocks had similar compositions of organic elements in the range 41.88–45.60 wt% (daf) for carbon (C), 47.83–50.93 wt% (daf) for oxygen (O) and 6.32–6.49 wt% (daf) for hydrogen (H). The variation in C content can be attributed to the biomass chemical composition specifically lignin. Lignin is higher in carbon than the polysaccharides [38], hence a higher lignin content often results in a higher C content, as observed in Table 4-1.

Regarding proximate analysis, PN was richer in volatile matter (VM) at 81.81 wt% db, followed by CC (78.91), BB (76.11) and CS (75.30). From Table 4-1, the ash content (AC) was in the following sequence: PN < BB < CC < CS. This was in agreement with previous studies [22,38], which showed that woody biomasses (PN, BB) have lower AC than non-woody biomass, especially agricultural residues (CC and CS). The high AC of CS (7.85 wt%, db) may be as a result of contamination with mineral matter during harvesting, which report to the ash during AC determination. From the lignocellulose composition (Table 4-1) the extractives content varied from 5.19 wt% to 17.53 wt% for CS. Extractives from biomass could be anything from small molecules to starches, soluble sugars and even inorganics [38]. Hence the high extractive content of CS could be due to the contribution of some inorganic materials from contamination, in addition to the expected extractive components. As seen in Table 4-1, PN contained a higher proportion of lignin (29.87 wt%), compared to the non-woody biomass. This phenomenon is characteristic of

softwood (eg. Pine) [39]. Also PN had the highest cellulose content (40.94 wt%), while the agricultural residues CC and CS had relatively low proportions (Table 4-1).

4.3.2. Weight loss characteristic of biomass during thermal pretreatment

The total (final) weight losses observed for each of the lignocellulosic biomass, as a consequence of various pretreatment conditions, are shown in Figure 4-2. For all biomass types the weight loss constantly increased with an increase in the pretreatment temperature and hold time (HT), although temperature clearly had a more pronounced effect than HT (Figure 4-2). The effect of HT on weight loss was only significant at lower temperatures (≤ 300 ^{o}C). For instance, at 275 ^{o}C when HT was increased from 30 min to 60 min, increment in weight loss for the different types of biomass was in the range 4–8 wt%. However, at higher pretreatment temperatures (>300 ^{o}C), only minor increments in weight losses were observed with similar increase in HT. For instance less than 1.3 wt.% increment in weight loss was observed for all biomass types at 350 ^{o}C.

From Figure 4-2 it can be seen that, up to 300 ^{o}C the softwood sample (PN) was the least susceptible biomass to pretreatment temperature, irrespective of the HT. For example at HT of 30 min and pretreatment temperatures of 250 and 275 ^{o}C, PN experienced weight loss of 10.42 wt% and 19.78 wt% as opposed to a weight loss of at least 17 and 31wt% respectively for the other biomass samples. This temperature range (< 300 ^{o}C) is specifically associated with hemicellulose degradation, which is more pronounced than lignin and cellulose degradation [40,41]. The low hemicellulose content of PN (see Table 4-1) therefore resulted in a lower conversion of PN in this temperature range. Moreover, the three biomass types BB, CC and CS are angiosperms containing xylan as the main hemicellulose while PN being a gymnosperm mostly contains glucomannan. Xylan is known to be more reactive than glucomannan [42,43], thereby increasing the reactivity of the three biomass types in comparison with PN. At temperatures higher than 300 ^{o}C, the weight loss characteristics of all the biomasses were more similar (Figure 4-2) due to significant conversion of the different constituents (see Section 4.3.3). The maximum mass loss difference between two biomass types was 3.8 wt% and 4.3 wt% at 350 ^{o}C and 400 ^{o}C respectively.

4.3.3. Thermal behaviour of pretreated biomass

The thermogravimetric analysis (TGA) and derivative thermogravimetric (dTG) curves obtained from the devolatilization of raw and pretreated biomass samples are presented in Figures 4-3 and 4-4. In both Figures 4-3 and 4-4 only curves for char produced at preceding pretreatment HT of 30 min are presented and discussed (curves for 60 min HT which follow similar trends are presented in Appendix B as Figures B-1 and B-2). As expected, the masses of residues of thermally treated biomass that remained at the end of devolatilization increased with an increase in the temperature of the preceding pretreatment, for all biomass types (Figure 4-3). For BB, CC and CS, following a pretreatment at a temperature in the range 300–400 ^{o}C, the devolatilization resulted in mass loss systematically lower than 40 wt% (Figure 4-3a–c). For PN, the trend was different with a substantial mass loss (63 wt%) of the sample pretreated at 300 ^{o}C (Figure 4-3d).

Considering the dTG thermograms (Figure 4-4), the major thermal decomposition of raw BB, CC and CS biomass occurred in the temperature range 200–380 ^{o}C, while raw PN was degraded from 230 to 380 ^{o}C. As expected it was observed that the starting temperature of thermal decomposition increased with an increase in the biomass pretreatment temperature (Figure 4-4). The thermal degradation peak/shoulder attributed to hemicelluloses decomposition could be clearly observed for raw CS, CC and PN at around 290 ^{o}C as usually reported in literature [24]. Following biomass thermal pretreatment, this peak/shoulder completely disappeared from the dTG profile of the chars, even when pretreated at a temperature as low as 250 ^{o}C. This indicated that even if the degradation is slower than at higher temperature, substantial thermal decomposition of hemicelluloses can be achieved through a pretreatment at 250 ^{o}C. It is well accepted that the main peak on the dTG thermogram, observed in the temperature range 320–360 ^{o}C, can be attributed to cellulose degradation [24]. As seen from Figure 4-4a–d, biomass pretreatment at 250 ^{o}C had a relatively small impact on the thermal degradation of the cellulose. With an increase in the pretreatment temperature to 275 ^{o}C, a reduction in cellulose thermal degradation peak was observed except for PN. This suggested that cellulose decomposition had already started at pretreatment temperature of 275 ^{o}C for all the biomass types with the exception of PN. At a thermal pretreatment of 300 ^{o}C, the cellulose peak disappeared for the non-softwood biomass and could only be identified in the char from PN (Figure 4-4d), implying that the cellulose in PN was the most resistant to thermal

decomposition, among the considered biomass types. For pretreatment above 300 ^{o}C, cellulose peak was not observed for any of the four biomass feedstocks (Figure 4-4).

To understand the effect of thermal pretreatment on the crystallinity of the different cellulose structures, XRD analysis was performed on selected samples of pretreated biomass. Figure 4-5 shows the obtained XRD patterns. As stated in Section 4.2.5, a qualitative approach was used in this study, where the presence of the principal crystalline peak (I_{002}) located at $2\theta = 22.7^{o}$ [36,37] and its relative intensity was deemed to estimate the crystallinity of the material. It could be seen that for raw biomass samples the I_{002} peak was present in all biomass types with PN and BB showing narrower peaks. When pretreated at 275 ^{o}C the I_{002} peak was still present in all samples but at a lower intensity (as compared to the raw biomass samples), especially for BB and CS (Figures 4-5a and 4-5c). This observation was consistent with the respective decreases of the cellulose peaks observed in the dTG curves (Figure 4-4a–d). At thermal pretreatment temperature of 300 ^{o}C, the I_{002} peak could be seen for only the PN sample (Figure 4-5d) while no observable peaks could be seen in the patterns of BB, CC and CS (Figure 4-5a–c). This shows that the cellulose crystalline structure of BB, CC and CS were completely degraded at 300 ^{o}C which was consistent with the dTG result of biomass pretreatment at 300 ^{o}C (Figure 4-4) above where cellulose peak was only present for PN char sample. From Figure 4-5 no crystallinity peak could be seen for all biomass samples pretreated at 350 ^{o}C which also agrees with a significant degradation of cellulose for all the biomass types as observed from the dTG results (Figure 4-4). When studying cellulose chars prepared at different temperatures, Pastorova et al. [44] and Yu et al. [45] found that the major part of the crystalline structure was altered between 270 ^{o}C and 300 ^{o}C. Also in a NMR study of various biomass samples treated at varying temperatures, Alonso et al. [46], found that cellulose crystalline structure was still present for wood at 300 ^{o}C while it is was degraded for grasses thus consistent with the result of this study.

The differences in cellulose degradation could be due to the nature of cellulose present in biomass. Cellulose is composed of an amorphous phase (disordered) and a crystalline phase (ordered). The relative proportion of these phases in biomass therefore determines its thermal stability which in turn affects the devolatilization characteristics and products. The temperature and the rate of cellulose conversion have been shown to increase with increasing degree of crystallinity [30].

4.3.4. Analysis of volatiles obtained during devolatilization of pretreated biomass

The condensable volatile products were quantified by thermal desorption GC-MS, with yields expressed per mass of dry sample introduced in TGA (raw biomass or char devolatilization). Table 4-2 presents the yields of individual compounds for the bamboo biomass (data for the other biomass samples are presented as Table B-1 – Appendix B). The yields of the products, grouped based on functional groups, which included acids, ketones, phenolics, furans, aromatic hydrocarbons and anhydrosugar, as obtained during the devolatilization of raw and pretreated biomass (char), are presented in Figure 4-6. In general, the composition of products from devolatilization of the chars were significantly different to that obtained from devolatilization of the raw biomass samples. In most cases (Figure 4-6a–e) the mass yields of volatiles tended to decrease with an increase in the pretreatment temperature, due to the conversion of more thermally unstable chemical groups, resulting in the production of chars with decreased volatile matter content.

The yield of acids declined progressively with an increase in temperature and HT, for all biomass types, until complete disappearance for samples pretreated at 350 ^{o}C (Figure 4-6a). The yield was reduced by a factor of at least 2–3 for samples pretreated at ≥275 ^{o}C compared to the untreated biomass. The major compound in this group was acetic acid (Table 4-2), which has been reported in previous studies [47] to be one of the main volatile products from torrefaction thermal pretreatment. In particular acetic acid is significantly produced by the deacetylation of hemicelluloses. Acetic acid has also been reported to be produced from cellulose conversion [48], explaining its presence amongst the volatiles produced from chars generated at temperatures of 275 and 300 ^{o}C. Following hemicelluloses and cellulose significant degradation by pretreatment at 350 and 400 ^{o}C, no acetic acid was produced during subsequent devolatilization of the chars. Figure 4- 6b shows the distribution of ketones from devolatilization of chars from the various biomass samples, in relation to the pretreatment temperature. The ketones include hydroxy acetone (the main observed product), 2,3-butanedione and 2-cyclopenten-1-one. These compounds are formed from the decomposition of sugar rings (i.e. carbohydrates) in biomass [49]. As seen in Figure 4-6b, compared to raw biomass, the ketone yield from char devolatilization was similar or slightly enhanced for chars produced at 250 ^{o}C. For CS their proportion decreased significantly from as high as 53 µg/mg at 250 ^{o}C to as low as 5 µg/mg at 300 ^{o}C. For the four types of biomass,

no ketone was detected from the devolatilization of chars produced at temperatures higher than 300 °C. Based on acids and ketones evolutions, it appeared that C=O bonds became particularly unstable when pretreatment temperature was increased to more than 300 °C.

Furans and anhydrosugars are typical products obtained from hemicelluloses and cellulose depolymerization [23,48], which occurs through the breakage of β-1,4-glycosidic bonds between monomer units. Formation of furans such as 5-hydroxymethylfurfural (5-HMF) and furfural was described as the consequence of the contraction of the pyran ring [23,48]. The production of furans from devolatilization of chars decreased with an increase in pretreatment temperature (Figure 4-6c), due to the increasing breakdown of the carbohydrate structures during biomass pretreatment. With the exception of PN the yield of furans from char devolatilization decreased by at least a factor of 10 at pretreatment temperature of 300 °C compared to the untreated biomass. Following pretreatment at temperatures higher than 300 °C, no furan was produced during char devolatilization. At 300 °C, the yield of furans obtained from PN char was more than 8 times higher than for the other biomass feedstocks. This was seen as the result of differences in cellulose crystallinity as also confirmed by the yield distribution of levoglucosan (Figure 4-6d).

As the main anhydrosugar generated from cellulose conversion [23,48], levoglucosan can be used as an indicator of the progress of cellulose degradation. The proportion of crystalline amount in biomass influences the extent to which glycosidic bonds in cellulose are broken during thermal treatment, as crystalline cellulose is more stable than amorphous cellulose and is therefore not easily degraded at lower temperatures [27,28]. As observed from the XRD analysis (Figure 4-5), PN showed a greater proportion of crystalline cellulose structure, resulting in greater thermal stability than the other three biomass types during thermal pretreatment. From levoglucosan yields (Figure 4-6d) obtained from raw biomass and chars produced in the temperature range 250–300 °C, it can be observed that levoglucosan yields were at least 8 times higher for PN than for the other feedstocks. It was interpreted as a result of its higher cellulose crystallinity [27,28] and lower ash content. Indeed inorganics are known to have a catalytic effect limiting levoglucosan yield [26]. The stability of the crystalline structure of PN cellulose could thus explain why the yield remained relatively high irrespective of the thermal pretreatment temperature even at 300 °C (Figure 4-6d), as opposed to the other biomass feedstocks where a rapid decline in yield was observed in response to pretreatment temperature of 300 °C (Figure 4-6d). Thus while a

pretreatment temperature of 300 ºC may be enough to remove carbohydrate derived oxygenated volatiles from biomass, a higher temperature will be required for samples with more stable cellulose.

The yields of phenolic products from the devolatilization of raw and pretreated biomass are presented in Figure 4-6e. As phenolics are primarily the products of lignin degradation, the yields of phenolic products were in agreement with biomass lignin content, with higher values obtained from PN and BB (see Table 4-1; Figure 4-6e). From NMR studies [49,50], it has been shown that the quantity of etherified linkages in lignin decreased with an increase in torrefaction pretreatment temperature, while the content of non-etherified linkages increased, implying the cleavage of aryl ether bonds is involved in the production of phenolics during biomass torrefaction. For each biomass the phenolic product yield from devolatilization of char remained relatively high at a pretreatment temperature of 250 ºC. At such temperature, mass loss was mostly due to hemicellulose decomposition, resulting in the production of chars with increased percentage of the lignin content. As the pretreatment temperature increased the decomposition of lignin was accelerated leading to the observed reduction in phenolics as shown in Figure 4-6e. However due to the presence of various types of chemical groups with different thermal stabilities, lignin degradation is known to occur over a wide range of temperatures 200–600 ºC [24,25], this explains the detection of phenolic products from char produced at pretreatment temperatures of 350 and 400 ºC. From Table 4-2 it can be seen that for the chars pretreated at 250 and 275 °C, the phenolic compounds obtained in relatively high yields (> 0.2 wt.%) were the same as for the raw biomasses, i.e. syringol (2,6-dimethoxyphenol), guaiacol (2-methoxyphenol) and vinylguaiacol (2-methoxy-4-vinylphenol), as reported in another study using rice husk torrefied at temperatures in the range of 200–290 °C [33]. They were characterised by a structure close to the primary lignin monomer units, which evidenced limited lignin degradation at such pretreatment temperatures. From devolatilization of the chars pretreated at 300 °C, the yields of such compounds significantly decreased. Following pretreatments at 350 or 400 °C, the yield of phenolic compounds containing a methoxy group dropped and the compounds obtained in significant yields (> 0.05 wt.%) were mostly phenol and other compounds characteristic of more extensive lignin conversion such as cresols as observed in Table 4-2.

The distributions of aromatic hydrocarbon products from devolatilization of chars are shown in Figure 4-6f. Toluene, benzene and *p*-xylene were the products obtained with higher yields as seen in Table 4-2. The yields of aromatic hydrocarbons were low at 250 ^{o}C, followed by a substantial increase at temperatures of 275 ^{o}C and 300 ^{o}C (Figure 4-6f). For chars produced at 400 ^{o}C, aromatic hydrocarbons were found to be the main volatile products. This suggests that thermal pretreatment of biomass led to the formation of more condensed solid structures which were aromatic in nature. This was due to the rearrangement of some benzene rings present in lignin structure [50], and also to the formation of additional rings during polysaccharide degradation as observed for cellulose char produced at pretreatment temperature as high as 270 ^{o}C [44].

4.4. Conclusion

Lignocellulose biomass thermal pretreatment and its effect on the products distribution resulting from subsequent devolatilization of chars, were studied. Four lignocellulosic biomass feedstocks, i.e. pine (PN), bamboo (BB), corn cob (CC) and corn stover (CS), were converted at varying temperatures (250–400 ^{o}C) and hold times (30 or 60 min) followed by the devolatilization of the chars in TGA and quantification of captured evolved volatile products by thermal desorption–gas chromatography–mass spectrometry. Weight loss during biomass thermal pretreatment increased with temperature for all biomass feedstocks with PN being the least reactive especially at temperatures of 300 ^{o}C and below due to a high lignin content and more stable crystalline cellulose structure as evidenced through XRD analysis of the chars. Analysis of char devolatilization products provided insight into the biomass structure modification induced by thermal pretreatment. From dTG curves pretreatment temperature of 275 ^{o}C resulted in significant conversion of hemicelluloses leading to a 2–3 factor decline in acids yield from char devolatilization. Other than PN, a pretreatment temperature of 300 ^{o}C was found to significantly degrade cellulose leading to reductions in furans (by at least a factor of 10) and levoglucosan production from char devolatilization when compared to the untreated biomass. However, it was found that PN required a higher pretreatment temperature (>300 ^{o}C) for cellulose conversion which has been attributed to a more stable crystalline cellulose structure. Thus indicating that the pretreatment temperature required for polysaccharide conversion, to remove a large fraction of the oxygenated volatiles, is dependent on biomass structure. Pretreatment at temperatures > 300 ^{o}C resulted in the concentration of condensed aromatic structures in the char. Therefore, phenolics and aromatic

hydrocarbons were the main compounds detected from devolatilization of char produced at temperatures higher than 350 ^{o}C.

References

[1] A. Franco, A.R. Diaz, The future challenges for "clean coal technologies": Joining efficiency increase and pollutant emission control, Energy. 34 (2009) 348–354.

[2] M.J.C. van der Stelt, H. Gerhauser, J.H.A. Kiel, K.J. Ptasinski, Biomass upgrading by torrefaction for the production of biofuels: A review, Biomass and Bioenergy. 35 (2011) 3748–3762.

[3] D. Medic, M. Darr, A. Shah, B. Potter, J. Zimmerman, Effects of torrefaction process parameters on biomass feedstock upgrading, Fuel. 91 (2012) 147–154.

[4] T. Pröll, H. Hofbauer, H2 rich syngas by selective CO2 removal from biomass gasification in a dual fluidized bed system — Process modelling approach, Fuel Process. Technol. 89 (2008) 1207–1217.

[5] H.B. Goyal, D. Seal, R.C. Saxena, Bio-fuels from thermochemical conversion of renewable resources: A review, Renew. Sustain. Energy Rev. 12 (2008) 504–517.

[6] Q. Lu, X.C. Yang, C.Q. Dong, Z.F. Zhang, X.M. Zhang, X.F. Zhu, Influence of pyrolysis temperature and time on the cellulose fast pyrolysis products: Analytical Py-GC/MS study, J. Anal. Appl. Pyrolysis. 92 (2011) 430–438.

[7] M. Phanphanich, S. Mani, Impact of torrefaction on the grindability and fuel characteristics of forest biomass, Bioresour. Technol. 102 (2011) 1246–1253.

[8] P. Rousset, C. Aguiar, N. Labbé, J.-M. Commandré, Enhancing the combustible properties of bamboo by torrefaction., Bioresour. Technol. 102 (2011) 8225–31.

[9] B. Arias, C. Pevida, J. Fermoso, M.G. Plaza, F. Rubiera, J.J. Pis, Influence of torrefaction on the grindability and reactivity of woody biomass, Fuel Process. Technol. 89 (2008) 169–175.

[10] M. Broström, A. Nordin, L. Pommer, C. Branca, C. Di Blasi, Influence of torrefaction on the devolatilization and oxidation kinetics of wood, J. Anal. Appl. Pyrolysis. 96 (2012) 100–109.

[11] A.V. Bridgwater, Renewable fuels and chemicals by thermal processing of biomass, Chem. Eng. J. 91 (2003) 87–102.

[12] J.H. Peng, H.T. Bi, C.J. Lim, S. Sokhansanj, Study on density, hardness, and moisture uptake of torrefied wood pellets, Energy and Fuels. 27 (2013) 967–974.

[13] M.J. Prins, K.J. Ptasinski, F.J.J.G. Janssen, Torrefaction of wood. Part 2. Analysis of products, J. Anal. Appl. Pyrolysis. 77 (2006) 35–40.

[14] F.F. Felfli, C.A. Luengo, J.A. Suárez, P.A. Beatón, Wood briquette torrefaction, Energy Sustain. Dev. 9 (2005) 19–22.

[15] H. Li, X. Liu, R. Legros, X.T. Bi, C.J. Lim, S. Sokhansanj, Torrefaction of sawdust in a fluidized bed reactor, Bioresour. Technol. 103 (2012) 453–458.

[16] W. Yan, T.C. Acharjee, C.J. Coronella, V.R. Vásquez, Thermal pretreatment of lignocellulosic biomass, Environ. Prog. Sustain. Energy. 28 (2009) 435–440.

[17] A. Ohliger, M. Förster, R. Kneer, Torrefaction of beechwood: A parametric study including heat of reaction and grindability, Fuel. 104 (2013) 607–613.

[18] C. Couhert, S. Salvador, J.-M. Commandré, Impact of torrefaction on syngas production from wood, Fuel. 88 (2009) 2286–2290.

[19] W. Yan, J.T. Hastings, T.C. Acharjee, C.J. Coronella, V.R. Vásquez, Mass and Energy Balances of Wet Torrefaction of Lignocellulosic Biomass, Energy & Fuels. 24 (2010) 4738–4742.

[20] J. Mundike, F.-X. Collard, J.F. Görgens, Torrefaction of invasive alien plants: Influence of heating rate and other conversion parameters on mass yield and higher heating value, Bioresour. Technol. 209 (2016) 90–99.

[21] V. Repellin, A. Govin, M. Rolland, R. Guyonnet, Energy requirement for fine grinding of torrefied wood, Biomass and Bioenergy. 34 (2010) 923–930.

[22] D. Neves, H. Thunman, A. Matos, L. Tarelho, A. Gómez-Barea, Characterization and prediction of biomass pyrolysis products, Prog. Energy Combust. Sci. 37 (2011) 611–630.

[23] F. Collard, J. Blin, A review on pyrolysis of biomass constituents : Mechanisms and composition of the products obtained from the conversion of cellulose , hemicelluloses and lignin, Renew. Sustain. Energy Rev. 38 (2014) 594–608.

[24] H. Yang, R. Yan, H. Chen, D.H. Lee, C. Zheng, Characteristics of hemicellulose, cellulose and lignin pyrolysis, Fuel. 86 (2007) 1781–1788.

[25] D.K. Shen, S. Gu, K.H. Luo, S.R. Wang, M.X. Fang, The pyrolytic degradation of wood-derived lignin from pulping process, Bioresour. Technol. 101 (2010) 6136–6146.

[26] R. Fahmi, A.V. Bridgwater, L.I. Darvell, J.M. Jones, N. Yates, S. Thain, I.S. Donnison, The effect of alkali metals on combustion and pyrolysis of Lolium and Festuca grasses, switchgrass and willow, Fuel. 86 (2007) 1560–1569.

[27] Z. Wang, A.G. McDonald, R.J.M.M. Westerhof, S.R.A.A. Kersten, C.M. Cuba-Torres, S. Ha, B. Pecha, M. Garcia-Perez, Effect of cellulose crystallinity on the formation of a liquid intermediate and on product distribution during pyrolysis, J. Anal. Appl. Pyrolysis. 100 (2013) 56–66.

[28] J. Zhang, J. Luo, D. Tong, L. Zhu, L. Dong, C. Hu, The dependence of pyrolysis behavior on the crystal state of cellulose, Carbohydr. Polym. 79 (2010) 164–169.

[29] Q. Liu, Z. Zhong, S. Wang, Z. Luo, Interactions of biomass components during pyrolysis: A TG-FTIR study, J. Anal. Appl. Pyrolysis. 90 (2011) 213–218.

[30] J.M. Jones, T.G. Bridgeman, L.I. Darvell, B. Gudka, A. Saddawi, A. Williams, Combustion properties of torrefied willow compared with bituminous coals, Fuel Process. Technol. 101 (2012) 1–9.

[31] C. Di Blasi, Combustion and gasification rates of lignocellulosic chars, Prog. Energy Combust. Sci. 35 (2009) 121–140.

[32] S. Anis, Z.A. Zainal, Tar reduction in biomass producer gas via mechanical, catalytic and thermal methods: A review, Renew. Sustain. Energy Rev. 15 (2011) 2355–2377.

[33] D. Chen, J. Zhou, Q. Zhang, Effects of torrefaction on the pyrolysis behavior and bio-oil properties of rice husk by using TG-FTIR and Py-GC/MS, Energy & Fuels. 28 (2014) 5857-5863.

[34] D. Chen, Z. Zheng, K. Fu, Z. Zeng, J. Wang, M. Lu, Torrefaction of biomass stalk and its effect on the yield and quality of pyrolysis products, Fuel. 159 (2015) 27–32.

[35] F. Nsaful, F.X. Collard, M. Carrier, J.F. Görgens, J.H. Knoetze, Lignocellulose pyrolysis with condensable volatiles quantification by thermogravimetric analysis - Thermal desorption/gas chromatography-mass spectrometry method, J. Anal. Appl. Pyrolysis. 116 (2015) 86–95.

[36] Y.-L. Hsieh, X.-P. Hu, A. Nguyen, Strength and Crystalline Structure of Developing Acala Cotton, Text. Res. J. 67 (1997) 529–536.

[37] S. Park, J.O. Baker, M.E. Himmel, P.A. Parilla, D.K. Johnson, Cellulose crystallinity index: measurement techniques and their impact on interpreting cellulase performance., Biotechnol. Biofuels. 3 (2010) 10.

[38] D. Da Silva Perez, C. Dupont, A. Guillemain, S. Jacob, F. Labalette, S. Briand, S. Marsac, O. Guerrini, F. Broust, J.M. Commandre, Characterisation of the most representative agricultural and forestry biomasses in france for gasification, Waste and Biomass Valorization. 6 (2015) 515–526.

[39] F. Huang, P.M. Singh, A.J. Ragauskas, Characterization of Milled Wood Lignin (MWL) in Loblolly Pine Stem Wood, Residue, and Bark, J. Agric. Food Chem. 59 (2011) 12910–12916.

[40] M.J. Prins, K.J. Ptasinski, F.J.J.G. Janssen, Torrefaction of wood, J. Anal. Appl. Pyrolysis.

77 (2006) 28–34.

[41] W.-H. Chen, P.-C. Kuo, Isothermal torrefaction kinetics of hemicellulose, cellulose, lignin and xylan using thermogravimetric analysis, Energy. 36 (2011) 6451–6460.

[42] M. V. Ramiah, Thermogravimetric and differential thermal analysis of cellulose, hemicellulose, and lignin, J. Appl. Polym. Sci. 14 (1970) 1323–1337.

[43] K. Werner, L. Pommer, M. Broström, Thermal decomposition of hemicelluloses, J. Anal. Appl. Pyrolysis. 110 (2014) 130–137.

[44] I. Pastorova, R.E. Botto, P.W. Arisz, J.J. Boon, Cellulose char structure: A combined analytical Py-GC-MS, FTIR, and NMR study, Carbohydr. Res. 262 (1994) 27–47.

[45] Y. Yu, D. Liu, H. Wu, Characterization of water-soluble intermediates from slow pyrolysis of cellulose at low temperatures, Energy and Fuels. 26 (2012) 7331–7339.

[46] E. Rodriguez Alonso, C. Dupont, L. Heux, D. Da Silva Perez, J.M. Commandre, C. Gourdon, Study of solid chemical evolution in torrefaction of different biomasses through solid-state 13C cross-polarization/magic angle spinning NMR (nuclear magnetic resonance) and TGA (thermogravimetric analysis), Energy. 97 (2016) 381–390.

[47] T. Nocquet, C. Dupont, J.M. Commandre, M. Grateau, S. Thiery, S. Salvador, Volatile species release during torrefaction of biomass and its macromolecular constituents: Part 2 - Modeling study, Energy. 72 (2014) 188–194.

[48] S.D. Stefanidis, K.G. Kalogiannis, E.F. Iliopoulou, C.M. Michailof, P.A. Pilavachi, A.A. Lappas, A study of lignocellulosic biomass pyrolysis via the pyrolysis of cellulose, hemicellulose and lignin, J. Anal. Appl. Pyrolysis. 105 (2014) 143–150.

[49] S. Wang, B. Ru, G. Dai, H. Lin, L. Zhang, Influence mechanism of torrefaction on softwood pyrolysis based on structural analysis and kinetic modeling, Int. J. Hydrogen Energy. (2016) 2–9.

[50] J.-L. Wen, S.-L. Sun, T.-Q. Yuan, F. Xu, R.-C. Sun, Understanding the chemical and

structural transformations of lignin macromolecule during torrefaction, Appl. Energy. 121 (2014) 1–9.

Tables

Table 4-1: Compositional characteristics of lignocellulose feedstocks

Property	Feedstock			
	Pine (PN)	Bamboo (BB)	Corn cob (CC)	Corn Stover (CS)
Proximate analysis (wt%), db[a]				
Volatile Matter (VM)	81.85	76.11	78.91	75.30
Fixed Carbon (FC)	16.01	21.45	18.49	16.85
Ash Content (AC)	2.14	2.44	2.61	7.85
Ultimate analysis (wt%), daf[b]				
C	45.60	44.41	43.80	41.88
H	6.47	6.32	6.49	6.40
N	0.02	0.44	0.33	0.59
S	0.08	0.14	0.00	0.20
O[c]	47.83	48.69	49.38	50.93
Lignocellulose composition (wt%), daf[b]				
Lignin	29.87	25.48	17.76	16.53
Cellulose	40.94	39.39	34.34	36.70
Hemicelluloses	11.82	16.34	26.02	21.28
Extractives	5.19	12.96	10.49	17.53
Acetyl	1.89	3.32	3.91	3.06

[a] Dry basis
[b] Dry ash free basis,
[c] Determined by difference

Table 4-2: Yields (µg/mg, dry basis) of devolatilization volatile products from raw and thermally pretreated Bamboo (nq: not quantified)

Compound	Raw	Char									
		250 °C		275 °C		300 °C		350 °C		400 °C	
		30 min	60 min	30 min	60 min	30 min	60 min	30 min	60 min	30 min	60 min
Acids											
Formic acid	10.54	11.37	8.52	0.00	0.00	0.00	0.00	0.00	0.00	0.00	0.00
Acetic acid	96.36	71.18	50.19	36.55	31.98	23.39	22.21	0.00	0.00	0.00	0.00
Propanoic acid	4.94	5.17	4.47	4.25	4.18	0.00	0.00	0.00	0.00	0.00	0.00
Sub-total	**111.84**	**87.71**	**63.18**	**40.80**	**36.16**	**23.39**	**22.21**	**0.00**	**0.00**	**0.00**	**0.00**
Ketones											
2,3-Butanedione	6.57	7.95	6.94	4.55	4.11	1.34	1.40	0.00	0.00	0.00	0.00
Hydroxy acetone	34.03	35.09	30.13	9.05	0.00	0.00	0.00	0.00	0.00	0.00	0.00
2-Cyclopenten-1-one	3.78	4.54	4.00	3.79	3.93	1.00	1.15	0.00	0.00	0.00	0.00
2-Hydroxy-3-methyl-2-cyclopentene	3.53	3.21	2.91	1.86	1.49	0.13	0.00	0.00	0.00	0.00	0.00
Sub-total	**47.91**	**50.80**	**43.98**	**19.24**	**9.53**	**2.47**	**2.55**	**0.00**	**0.00**	**0.00**	**0.00**
Furans											
2-Methylfuran	1.76	4.05	3.52	3.55	3.87	1.07	1.01	0.13	0.12	0.00	0.00
Furfural	3.87	7.50	6.34	5.25	4.81	0.00	0.00	0.00	0.00	0.00	0.00
Furfuryl alcohol	15.13	11.83	8.66	4.06	0.00	0.00	0.00	0.00	0.00	0.00	0.00
Benzofuran	0.02	0.14	0.12	0.11	0.12	0.13	0.13	0.11	0.11	0.00	0.00
5-Methyl furfural	0.71	0.51	0.41	0.31	0.30	0.00	0.00	0.00	0.00	0.00	0.00
2(5H)-Furanone	4.01	5.01	4.30	2.38	1.36	0.00	0.00	0.00	0.00	0.00	0.00
5-Hydroxymethylfurfural	3.36	0.48	1.76	0.48	0.00	0.00	0.00	0.00	0.00	0.00	0.00
Sub-total	**28.87**	**29.51**	**25.11**	**16.14**	**10.47**	**1.20**	**1.14**	**0.24**	**0.23**	**0.00**	**0.00**
Anhydrosugar											
Levoglucosan	0.85	1.30	0.46	0.57	0.53	0.18	0.00	0.00	0.00	0.00	0.00
Phenolics											
Phenol	5.42	6.64	5.95	6.20	7.65	3.77	5.34	1.58	2.09	0.40	0.13
Guaiacol	3.17	3.31	2.77	2.59	2.72	0.91	1.07	0.05	0.06	0.00	0.00
o-Cresol	0.62	1.30	1.22	1.43	1.86	0.85	1.42	0.35	0.59	0.07	0.02
Maltol	0.96	0.35	0.74	0.63	0.43	0.00	0.00	0.00	0.00	0.00	0.00
m&*p*-Cresol	1.19	1.26	1.24	1.49	1.87	0.83	1.25	0.34	0.49	0.08	0.02
Creosol	0.57	0.88	0.79	0.82	0.91	0.31	0.37	0.01	0.01	0.00	0.00
4-Ethyl-phenol	0.84	0.87	0.91	1.00	1.17	0.37	0.56	0.12	0.12	0.02	0.01
2,4-Xylenol	0.00	0.09	0.10	0.12	0.15	0.06	0.09	0.00	0.00	0.01	0.00
2-Methoxy-4-vinylphenol	4.63	2.39	1.84	1.07	0.82	0.11	0.09	0.00	0.00	0.00	0.00
Eugenol	0.08	0.05	0.04	0.00	0.00	0.00	0.00	0.00	0.00	0.00	0.00
4-Propyl guaiacol	0.07	0.08	0.07	0.10	0.11	0.03	0.03	0.00	0.00	0.00	0.00
2,6-Dimethoxy-phenol	5.54	4.84	3.48	2.67	2.01	0.28	0.34	0.15	0.08	0.02	0.01

trans-Isoeugenol	1.70	2.18	1.76	1.46	0.00	0.00	0.00	0.00	0.00	0.00	0.00
Isoeugenol	0.31	1.40	0.92	0.72	0.64	0.10	0.12	0.00	0.00	0.00	0.00
Apocynin	0.19	0.13	0.09	0.08	0.08	0.02	0.00	0.00	0.00	0.00	0.00
Sub-total	**25.30**	**25.78**	**21.94**	**20.39**	**20.42**	**7.63**	**10.68**	**2.61**	**3.44**	**0.60**	**0.20**
Aromatic hydrocarbons											
Benzene	0.45	0.48	0.42	0.52	0.61	0.53	0.49	0.46	0.44	0.43	0.38
Toluene	0.99	nq	nq	1.96	2.42	1.62	1.97	1.18	1.41	0.89	0.57
Ethylbenzene	0.07	0.13	0.13	0.14	0.16	0.12	0.14	0.09	0.10	0.07	0.06
p-xylene	0.29	0.62	0.57	0.71	0.88	0.51	0.72	0.36	0.48	0.25	0.17
o-xylene	0.06	0.12	0.11	0.13	0.18	0.09	0.13	0.05	0.07	0.03	0.02
Naphthalene	0.02	0.07	0.06	0.08	0.10	0.09	0.08	0.07	0.08	0.06	0.10
Sub-total	**1.88**	**1.41**	**1.28**	**3.53**	**4.34**	**2.97**	**3.54**	**2.22**	**2.58**	**1.73**	**1.30**
Total Volatile Yield	**216.64**	**196.52**	**155.95**	**100.68**	**81.45**	**37.93**	**40.22**	**5.08**	**6.26**	**2.33**	**1.50**

Figures

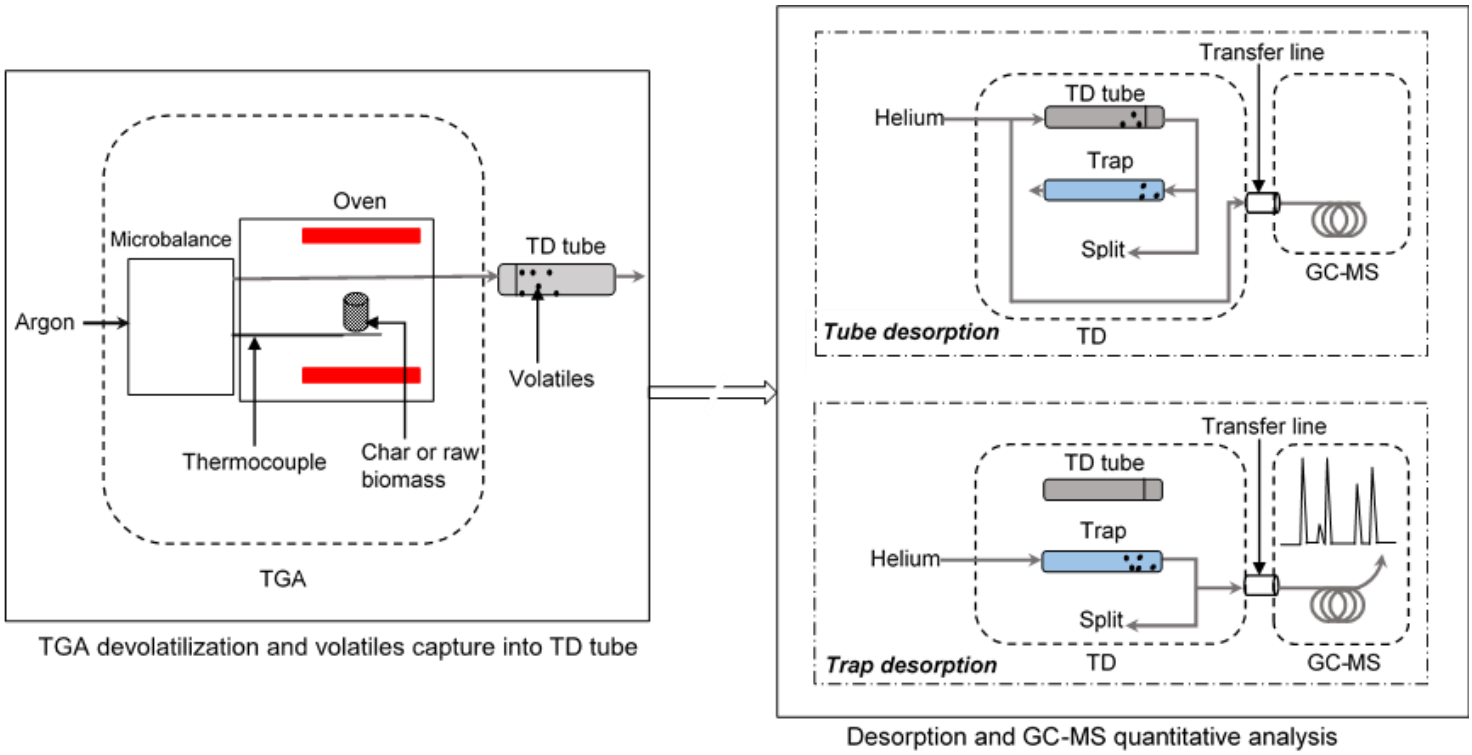

Figure 4-1: Schematic diagram of the thermogravimetric analysis–thermal desorption/gas chromatography–mass spectrometry (TGA-TD/GC-MS) method

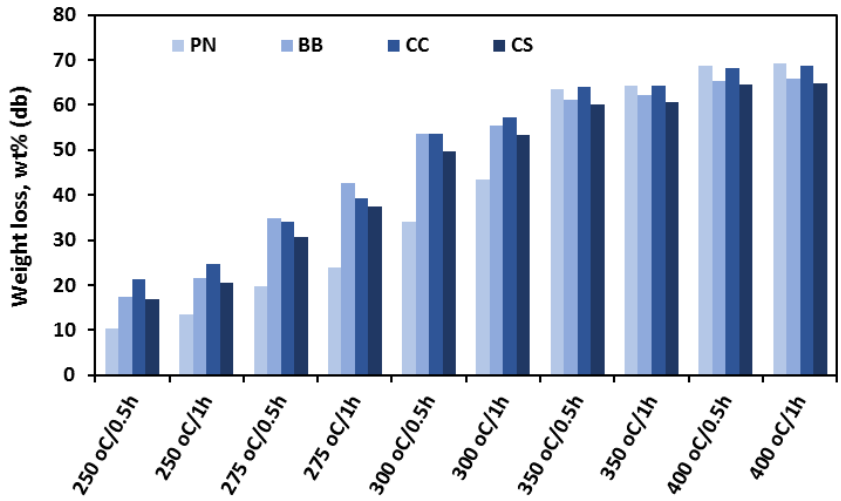

Figure 4-2: Weight loss characteristics of biomass samples at various pretreatment conditions (db: dry basis)

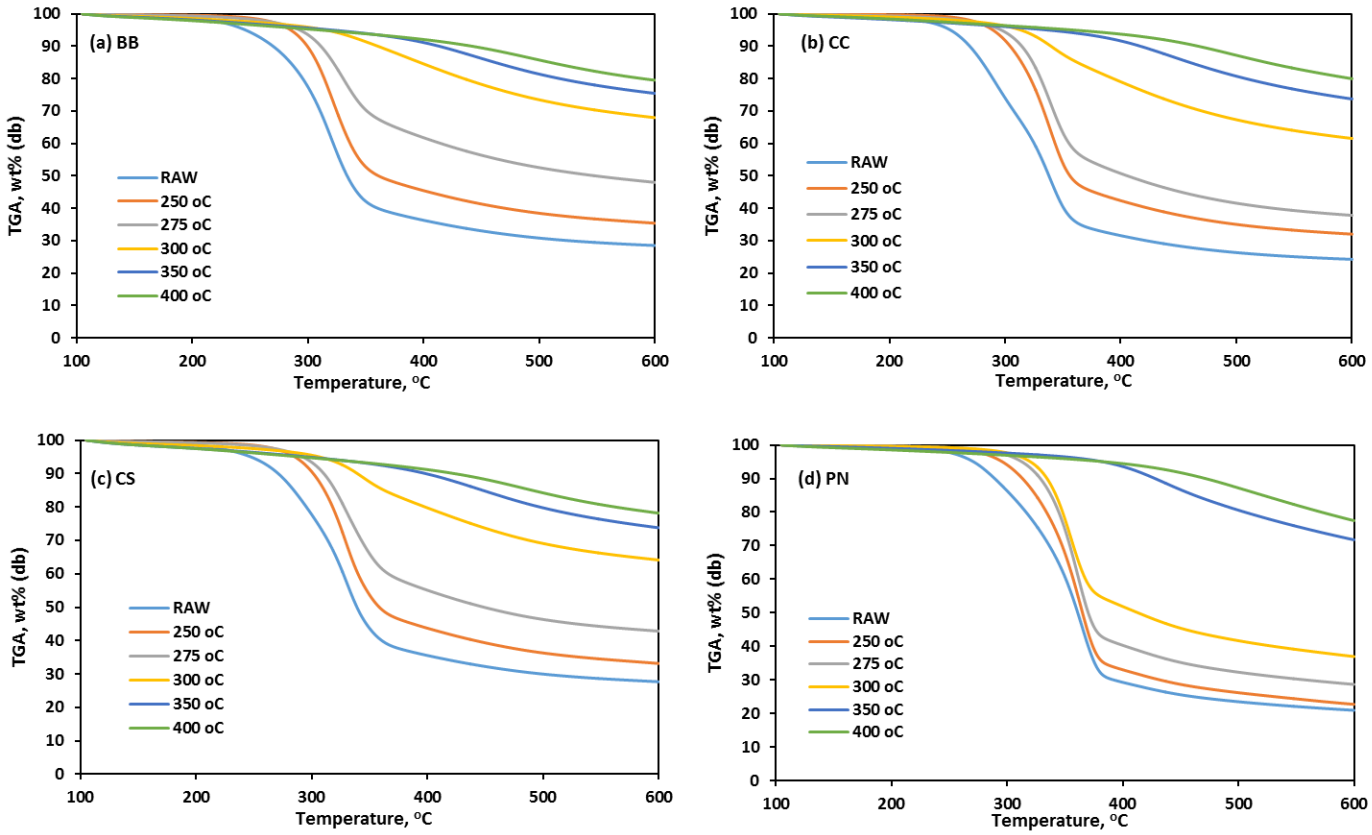

Figure 4-3: Thermogravimetric Analysis (TGA) of biomass samples pretreated at different temperatures (30 min Hold Time) during devolatilization (db: dry basis)

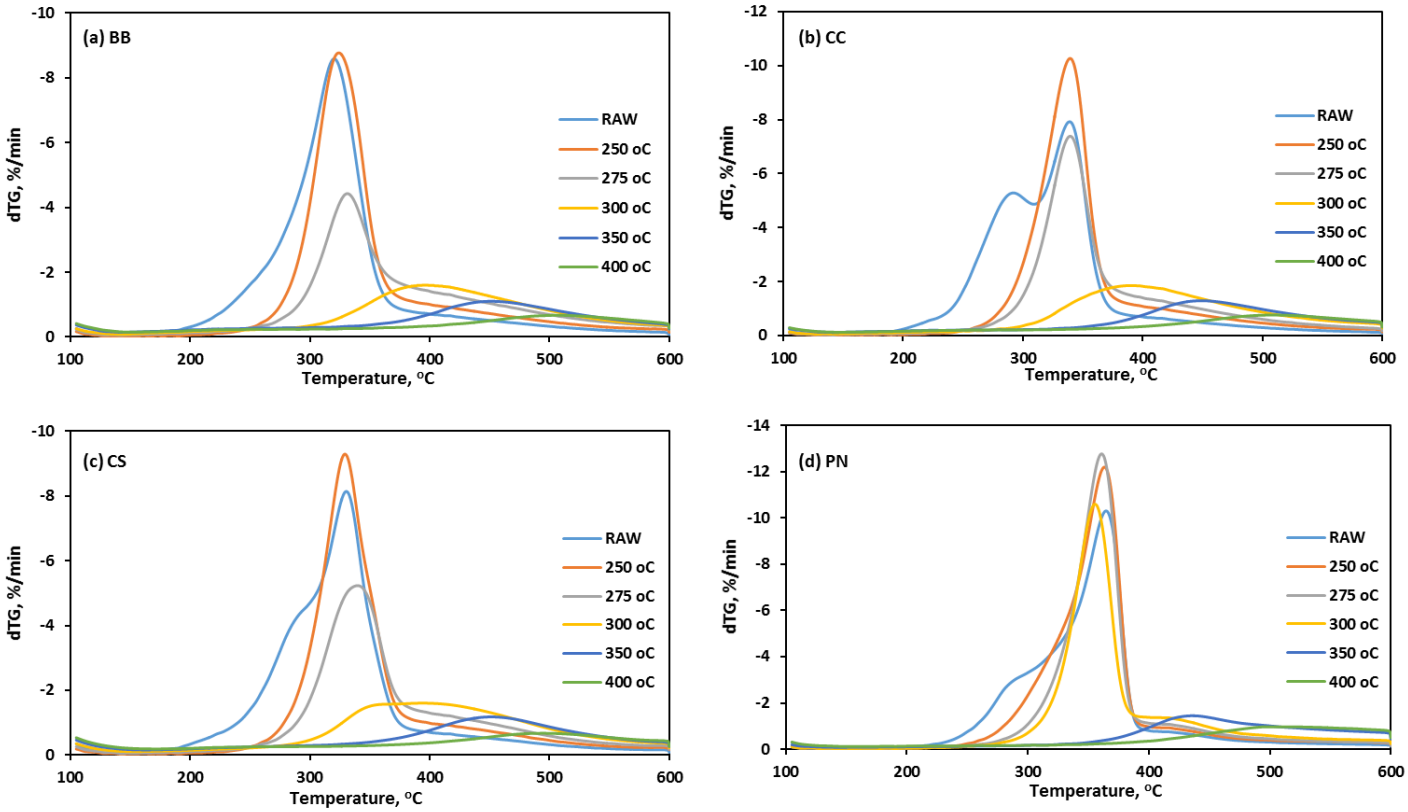

Figure 4-4: Derivative thermogravimetric (dTG) curves of biomass samples pretreated at different temperatures (30 min Hold Time) during devolatilization

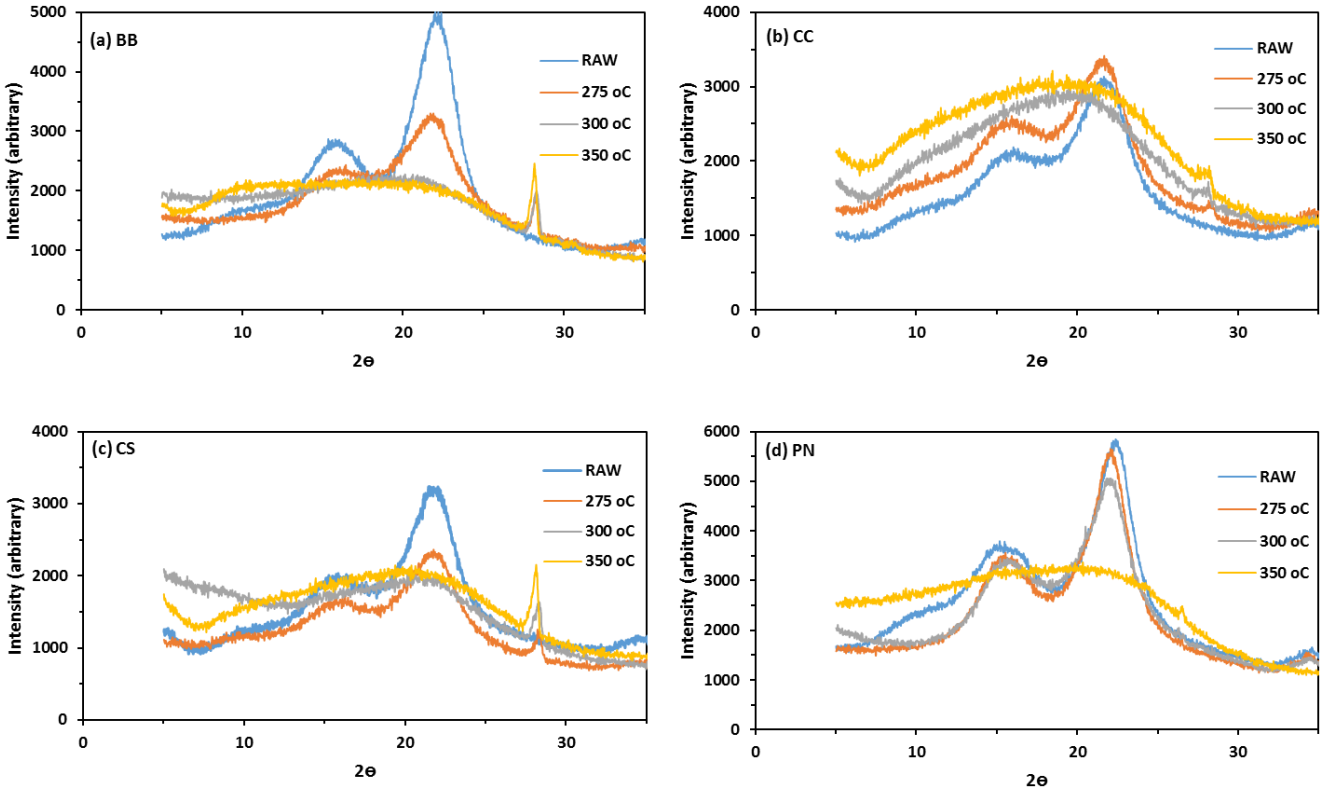

Figure 4-5: X-Ray Diffraction (XRD) patterns of raw biomass and chars (275, 300 and 350 ^{o}C; 30 min Hold Time)

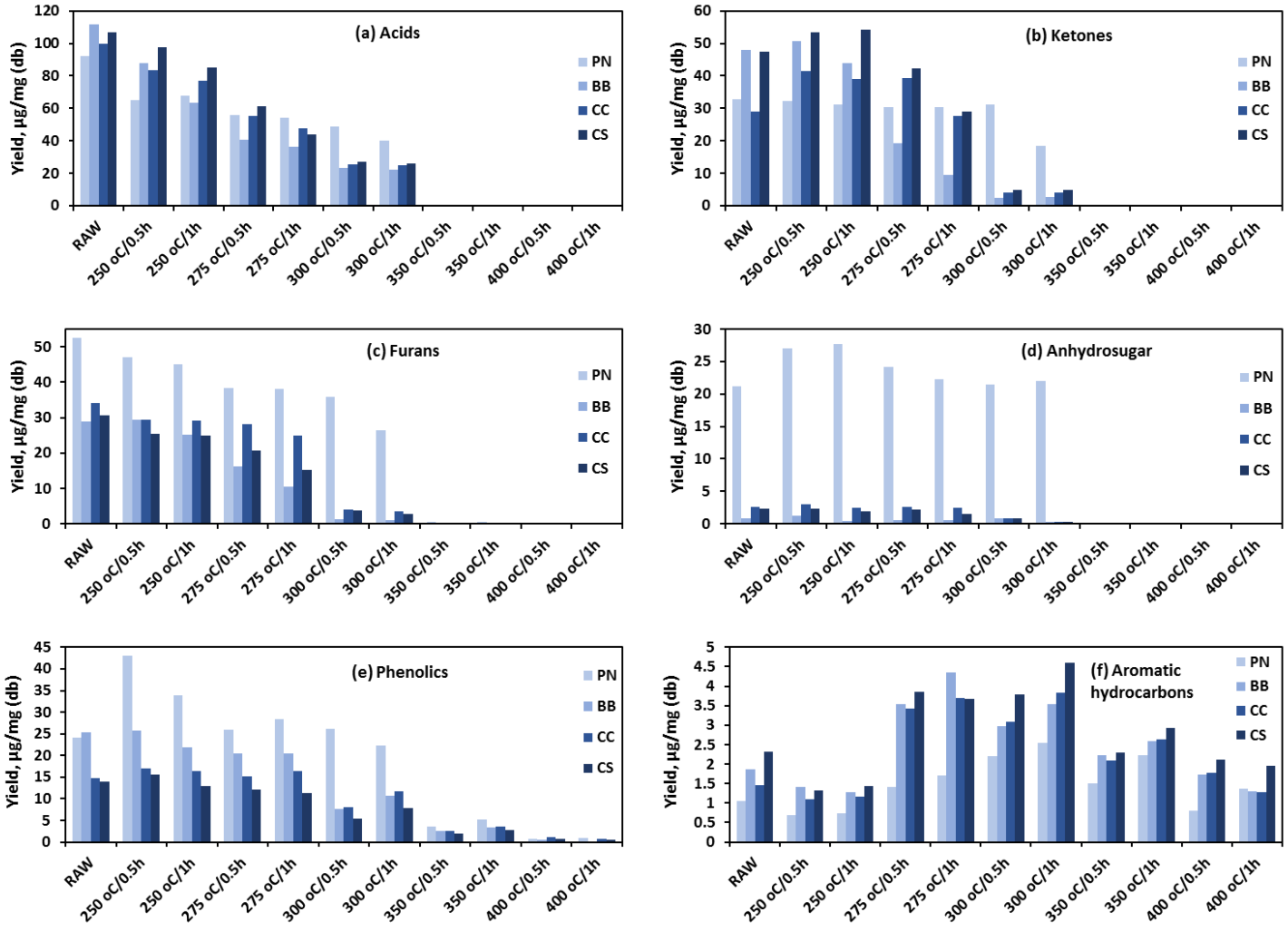

Figure 4-6: Yields of devolatilization products from raw and thermally pretreated biomass (db: dry basis)

Chapter 5

Lignocellulose thermal pretreatment and its effect on char devolatilization product composition and fuel properties in comparison to coal

This chapter is prepared as a manuscript for submission to the journal of Fuel

Title: "*Lignocellulose thermal pretreatment and its effect on the char devolatilization product composition and fuel properties in comparison to coal"*

Authors: *Frank Nsaful, François-Xavier Collard, Johann F. Görgens*

Objective of dissertation in this chapter and summary of findings

This chapter mainly addresses the fourth objective of the study which is the comparison of pretreated biomass (char) and coal in terms of critical fuel properties and devolatilization products (tar precursors) composition. This was to confirm that the thermal pretreatments selected in Chapter 4, were appropriate for producing char of an acceptable quality. Following the thermal pretreatment study in the previous chapter, the char products were subjected to further analysis with the aim of determining their suitability for use with coal in co-gasification process leading to the establishment of an appropriate biomass pretreatment temperature. Biomass chars were therefore characterised for their fuel properties (proximate and elemental composition and Higher Heating Value) and oxygenated volatiles composition. These parameters were then compared to those of coal and through this, pretreatment conditions capable of producing char with acceptable properties for co-gasification with coal were determined. Char production again was done at the milligram scale (250 – 400 ^{o}C and 30 min) while volatiles analysis was also done by use of the thermal desorption and GC-MS (objective 2). Proximate analysis was done in the TGA and higher

heating value determination was done by means of oxygen bomb calorimeter. Elemental composition was determined using a Leco TruSpec Micro elemental analyser.

It was shown that char properties were consistently transformed towards that of coal with increasing pretreatment temperature. Fixed carbon content and higher heating value of chars were significantly improved following pretreatment at 300 ^{o}C and above while oxygen content was decreased due to the reduction in volatile matter content of the chars. Considering the evolution of the devolatilization products, the yield of condensable volatiles from char were from 21.5 to < 0.5 wt.% (dry basis) depending on char pretreatment temperature. In comparison with coal, tar precursors particularly phenolics quantified from chars produced at 350 and 400 ^{o}C were similar and at lower amounts respectively. Based on the analysis of results with a particular attention given to the production of tar precursors, a pretreatment temperature of ≥350 ^{o}C could be recommended for coal replacement.

Summary of authors' contributions

Frank Nsaful planned and conducted all the experimental work for this chapter. He also did the analysis and interpretation of the experimental data and wrote the chapter. *François-Xavier Collard* contributed to the experimental planning and also reviewed the chapter. *Johann F. Görgens* also assisted with data interpretation and reviewed the chapter.

Abstract

To establish the potential of thermally pretreated biomass as fuel for coal replacement in applications such as gasification, the fuel properties (Higher Heating Value, elemental and proximate analyses) and the composition of char devolatilization products were analyzed and compared to those of coal. Samples of pine, bamboo, corn cob and corn stover were pretreated at 250, 300, 350 and 400 ^{o}C with a hold time of 30 min. The devolatilization experiments were done in a TGA while captured volatiles were analyzed by thermal desorption/Gas Chromatography–Mass Spectrometry. The results showed that an increase in pretreatment temperature constantly led to a decrease in oxygen and volatile matter contents while the fixed carbon content and the Higher Heating Value of the samples increased, with a drastic evolution from 300 °C onwards. Analysis of the devolatilization products confirmed a major modification of the polysaccharides structure as only traces of depolymerisation products were observed following pretreatment at 350 °C. Regarding the evolution of the tar precursors, especially the phenolics, in comparison with coal, similar and lower amounts were quantified from chars pretreated at 350 and 400 °C respectively. Overall, a pretreatment temperature of 350 °C would be recommended for coal substitution, while 400 °C could be considered for species with high lignin or inorganic contents.

Keywords: Biomass; Coal; Char; Pyrolysis; Volatile analysis; TGA

5.1. Introduction

Fossil based fuels continue to be major sources of the world's energy supply. However such fuels are non-renewable and their quantities are currently on the decline due to increased growth in global industrialization. The use of fossil-based fuels is also known to release high levels of greenhouse gases such as CO_2 and other pollutant emissions into the environment leading to global warming and other environmental issues such as SO_x and NO_x air pollution [1]. On the other hand, lignocellulosic biomass is a renewable source of energy and is considered to be environmentally friendly due to its CO_2 neutrality and low contents of S and N elements in comparison to fossil-based fuels [2,3].

Thermochemical processes such as combustion, pyrolysis and gasification are technologies used to convert materials like biomass and coal into energy and fuel products [4,5]. Among these thermochemical processes, gasification is more efficient and is considered to be the most promising route for utilizing coal and biomass on a large scale [6–8]. Fuel gas is the main product of gasification and can be combusted directly in gas turbines and gas engines for the generation of electricity or upgraded to syngas for conversion into liquid fuels and chemicals through Fischer-Tropsch synthesis [7]. Coal gasification is an already mature technology while the gasification of biomass is still under development. In order to reduce greenhouse gas emissions from coal and take advantage of the environmental benefits from the use of biomass, recent research on gasification has been focused on the co-utilization of coal and biomass [9,10]. It has been shown that the addition of biomass to coal during gasification can result in significant increase in the yield of gas due to the high volatile content of biomass [9–11]. However, in addition to the gas there is also an increased production of oxygenated volatile compounds (tar precursors) during the devolatilization step which impacts negatively on the quality of the syngas product and needs to be limited. In particular, the phenolic volatiles were identified to be problematic due to their thermal stability and potential to recombine [12].

Biomass tar condensation leads to the blockage and fouling of process equipment and catalyst deactivation during syngas production and conversion [7,8,13]. The problem of tar removal is therefore a challenge that needs to be overcome to ensure effective utilization of biomass in gasification. Traditionally processes such as the use of electrostatic precipitators, granular beds

and scrubbers have been employed to deal with the tar problem. Others include thermal cracking, catalytic cracking and plasma methods but these are expensive and energy intensive [7]. In the case of tar scrubbing there is also the production of contaminated water which needs proper disposal thereby adding to the cost [7].

Given the increase in the demand for renewable energy, there is a need to limit the formation of tar precursors during the devolatilization (pyrolysis) step of the co-gasification process. An approach to this consists in pretreating biomass to alter its properties to be closer to that of coal. This will ensure more efficient gasification of the two fuels and in addition address the problem of tar/oxygenated volatiles generation.

Among the processes used to pretreat biomass for energy conversion applications are torrefaction and slow pyrolysis [14]. These two thermal pretreatment processes are carried out at temperatures of 200–300 ^{o}C for torrefaction [15,16] and between 300 and 500 ^{o}C for slow pyrolysis [17] with both processes generally taking place in an inert atmosphere and at low heating rate (< 50 ^{o}C/min). During thermal pretreatment of biomass, a significant part of the volatile matter is released from the sample, resulting in a solid product (char) with several improved characteristics such as lower moisture content [14,18], increased energy density [19], improved grindability [15,20], hydrophobicity [21,22], reduced oxygen content leading to lower O/C ratio [23] and a homogeneous solid fuel product [24]. Though several studies have been done on biomass thermal pretreatment, most of these focused on the effect of the pretreatment process on the physico-chemical properties of the char. Studies on the subsequent conversion of the char are limited and need to be explored further especially if char is to be used for coal substitution in gasification applications. Since devolatilization/pyrolysis is a critical step of gasification during which volatiles/tar are generated, it is important to investigate this step and quantify the devolatilization products generated during the conversion of char in comparison to coal.

Therefore in this study torrefaction/slow pyrolysis as thermal pretreatment method is used to pretreat lignocellulosic biomass with the aim of producing char with improved properties for co-gasification with coal, both in terms of devolatilization product composition and fuel properties (composition and energy content). Series of thermal pretreatment experiments were performed on four biomass feedstocks (pine, bamboo, corn cob and corn stover) at temperatures between 250

and 400 ^{o}C. Chars and coal were devolatilized/pyrolyzed and the volatiles products were quantified and compared. In addition, chars were compared to coal in terms of fuel properties such as proximate analysis, elemental composition and heating value.

5.2. Materials and methods

5.2.1. Feedstock

The coal used in this study was a typical South African low grade sub-bituminous coal with a relatively high ash content. Prior to its use, the coal was pulverized and then sieved to a particle size range of 160–450 μm (Vibratory sieve shaker – model AS200). The biomass feedstocks used were two corn (*Zea mays*) residues; corn stover (CS) and corn cob (CC), pine (*Pinus radiata*) (PN) and bamboo (*Bambusa balcooa*) (BB), which were sourced from the Northern, Eastern and Western provinces, respectively. All biomass feedstocks were dried to less than 10 wt% moisture content and were milled and sieved to 250–450 μm particle size range by means of Retsch mill (model ZM100) and a vibratory sieve shaker (model AS200). Table 5-1 lists the lignocellulosic chemical composition of the biomass feedstocks as determined by use of the standard laboratory analytical procedures (LAPs) 002, 003, 017 and 019 of the National Renewable Energy Laboratory (NREL) (http://www.nrepriorl.gov/biomass/analytical_procedures.html). The standard method DD CEN/TS 14780:2005 was used to obtain sub-samples of each feedstock.

5.2.2. Thermal pretreatment

Torrefaction or slow pyrolysis thermal pretreatment of biomass feedstocks was performed in a TGA (TGA/DSC 1-LF1100 system, Mettler Toledo). Approximately 180–400 mg mass of raw biomass (depending on biomass bulk density) was used for each pretreatment. Thermal pretreatment was done as follows: dynamic heating at 10 ^{o}C/min from 30 ^{o}C to the appropriate pretreatment temperature (250, 300, 350, and 400 ^{o}C), followed by isothermal condition for a hold time of 30 min. Argon (baseline 5.0, Afrox SA) at a flow rate of 70 ml/min was used to provide an inert atmosphere during pretreatment. Pretreatment was performed in triplicate runs and the generated char product stored for further analysis.

5.2.3. Chemical analysis

Proximate and elemental analyses as well as higher heating value (HHV) determination were performed on coal and raw/thermally treated biomass samples to determine their fuel properties. Proximate analysis was conducted according to the ASTM method E1131, by means of thermogravimetric analysis (TGA) (TGA/DSC 1-LF1100 system, Mettler Toledo) to determine the percentage composition of volatile matter (VM), fixed carbon (FC) and ash in each sample. Elemental analysis (C, H, N, and S) of samples was done using a Leco TruSpec Micro elemental analyser and O content was determined by difference. HHV was measured by oxygen bomb calorimetry (CAL2K ECO bomb calorimeter – model 2013) and was determined according to the ASTM standard D5865-11a.

5.2.4. Devolatilization and quantification analysis of condensable volatiles

To study and compare the types and quantities of condensable volatiles generated during devolatilization of coal and biomass (raw/treated) samples, a method coupling thermogravimetric-analysis and thermal desorption/gas chromatography-mass spectrometry (TGA–TD/GC–MS) was used. Details of the analytical method can be found in Nsaful et al [25]. Samples were pyrolysed in a TGA and evolved volatiles captured into thermal desorption (TD) tube which were then analyzed offline using a thermal desorber/GC-MS system for the separation, identification and quantification of pyrolysis condensable volatiles.

For devolatilization, a 10 mg sample was pyrolysed in an inert atmosphere from 30 ^{o}C to 600 ^{o}C at a heating rate of 10 ^{o}C/min using a TGA/DSC 1-LF1100 system (Mettler Toledo). Argon (baseline 5.0, Afrox SA) carrier gas at a flow rate of 70 mL/min was used to swiftly transfer evolved pyrolysis volatiles to the TGA exit end. A pre-conditioned standard stainless steel TD tube (3.5 in L x 0.5 in O.D, Markes international, USA) containing a combination of Tenax TA, Carbograph 1TD and Carboxen 1003 (in order of increasing strength from the tube inlet) sorbent materials was connected to the exit of the TGA to adsorb evolved volatiles emanating from the TGA oven chamber. The TD tube sorbent combination was designed to capture most of the pyrolysis volatiles (except water and non-condensable volatiles) in the range n-C_2–n-C_{30}.

Soon after devolatilization TD tube was thermally desorbed using a UNITY 2 thermal desorber (Markes International, USA) to release the captured pyrolysis volatiles which were then transferred to a GC–MS (Agilent Technologies 7890A gas chromatography system coupled with an Agilent Technologies 5975C mass spectrometer) for separation, identification and quantification by internal calibration. A 3 µl volume of internal standard (2-octanol dissolved in methanol solvent) solution was added to the TD tube before thermal desorption. Internal standard was introduced to the TD tube by means of a standard GC syringe and a calibration solution loading rig (CSRL). Thermal desorption was performed as follows: initial system pre-purge with 1 mL/min helium (baseline 5.0, Afrox SA) flow for 3 min; primary/tube desorption at 300 ^{o}C for 10 min using helium at 10 mL/min tube flow and 30 mL/min split flow (split ratio of 4) with general purpose cold trap maintained at -10 ^{o}C; secondary/trap desorption at 320 ^{o}C for 10 min with 1.5 mL/min column flow and 30 mL/min split flow; 200 ^{o}C transfer line temperature. The GC was operated in a splitless mode. The oven was held at 45 ^{o}C for 10 min followed by a 2 ^{o}C/min ramp from 45 to 100 ^{o}C and 7 ^{o}C/min from 100 to 260 ^{o}C and then held at 260 ^{o}C for 14 min. Helium (baseline 5.0, Afrox SA) was used as the carrier gas at a flow of 1.5 mL/min and 172.37 kPa constant pressure and the column type was Zebron ZB-1701 capillary column (14%-cyanopropylphenyl – methylpolysiloxane, 60 m x 0.25 mm x 0.25 µm dimension - Agilent Technologies). The GC and MS interface was maintained at 280 ^{o}C whilst the quadrupole and the MS source temperatures were 150 ^{o}C and 230 ^{o}C respectively. The detector was operated in the scan acquisition mode (20–500 amu). The identification of compounds was done by the use of the NIST library (2011) and comparison with the retention times of standard compounds. Quantification was done using a five-point calibration curve ($R^2 \geq 0.97$) of each compound. Calibration curves were obtained by injecting known concentrations of pure standard compounds (97% minimum purity from Sigma Aldrich), together with a known amount of internal standard, directly onto TD tubes using standard GC syringe and the CSLR. Tubes were then analyzed using the same thermal desorption and GC–MS conditions stated above to plot the calibration curves.

5.3. Results and discussion

5.3.1. Mass yield of solid products (char) during thermal pretreatment

The lignocellulosic composition of the raw biomass feedstocks are presented in Table 5-1. Among the biomass types PN and BB contained the highest percentage of cellulose (40.94 and 39.39 wt% respectively) while that of the agricultural residues CS and CC was lower than 37 wt.%. Also PN had the highest lignin content in comparison to the other feedstocks, a characteristic typical of softwood biomass (eg. Pine) [26]. From Table 5-1 the extractives content was in the range 5.19–17.53 wt% with CS having the highest amount. This could be as a result of contamination from inorganic materials such as silica during harvesting which adds to the extractives content of CS [27]. This assumption was consistent with the relatively high ash content (7.85 wt.%) measured in CS. Hemicellulose contents of BB, CC and CS were higher than that of PN.

The char yields obtained from the biomass samples at various pretreatment temperatures are shown in Figure 5-1. The mass yield was estimated as a ratio of residual solid mass after pretreatment to the initial raw biomass mass expressed on percentage dry basis (wt% db). Overall, mass yield decreased with increase in pretreatment temperature with a pronounced effect at higher temperatures (>300 ^{o}C). Previous studies [28,29] have reported the thermal decomposition of hemicellulose, cellulose and lignin to occur at the temperature ranges of 200–315 ^{o}C, 300–400 ^{o}C and 200–600 ^{o}C respectively. It can be seen from Figure 5-1 that at pretreatment temperature of 250 ^{o}C, the mass yield of BB, CC and CS solid products were less than that of PN. This result was consistent with the relatively high hemicellulose content of BB, CC and CS (Table 5-1). Indeed, thermal decomposition is known to be much severe for hemicellulose than for cellulose and lignin in this temperature range [30,31]. In addition, BB, CC and CS being angiosperms contain xylan as the predominant hemicellulose component as opposed to glucomannan which is mainly found in softwoods such as pine [30]. Xylan has been shown to be more reactive than glucomannan [32,33], thus the increased reactivity of BB, CC and CS leading to lower mass yield of solid products. For pretreatment at 300 ^{o}C, the degree of conversion of the samples increased with devolatilization representing around 50 wt.%, except for PN which was characterised by a particular high char yield (66 wt.%). This difference can be attributed to its high lignin and cellulose contents (Table 5-1) and to some extent to the structure of the cellulose present in PN. In a previous study using

X-ray diffraction analysis [34] it was found that the crystalline cellulose in PN was more stable than for the other samples and required a higher temperature for conversion. From 350 °C onward, significant conversion of the three constituents was achieved and similar char yields were observed for the samples, with CS having the highest yield due to its relatively high inorganic content (Table 5-2).

5.3.2. Fuel properties in terms of elemental composition, proximate analysis and HHV

The proximate (on dry basis) and elemental (on dry ash free basis) analyses results of coal and biomass thermally pretreated at various temperatures are presented in Table 5-2. In general volatile matter (VM) decreased with pretreatment temperature whereas fixed carbon (FC) and ash content increased. This behaviour was as expected and in agreement with what has been reported in previous studies [24,35]. An increase in the degree of devolatilization resulted with a char with a lower VM content, while FC and inorganic material were further concentrated in the char residue. A high ash content is not desired as it will reduce the gas yield (based on dry basis feed) and increase the risk of process operational issues (gas cleaning, ash disposal) [36]. The highest ash content observed in the lignocellulosic chars, which was 18.11 wt.% for CS pretreated at 400 °C (Table 5-2), was found to be lower than for the coal sample (25.96 wt.%). For PN, BB and CC, ash contents were even observed to be lower than 6 wt.% irrespective of the pretreatment temperature. For pretreatment at 250 °C, VM was still the main component (≥ 70 wt.%) of the chars. A drastic change in proximate composition was observed at 300 °C, which was consistent with the char yield evolution described in the previous section. The VM of the sample decreased to less than 46 wt.%, except for pine. It resulted in a FC content comparable with that of coal for BB and CC, as values higher than 50 wt.% were measured (Table 5-2). The value was lower for CS (43.4 wt.%) due to the relatively high ash content of the biomass. The lower FC content observed for PN pretreated at 300 °C was due to the relatively high stability of PN structure (Figure 5-1) and a pretreatment of 350 °C was required to obtain a FC content of 60.99 wt.%, higher than for coal. A similar temperature was also necessary to obtain a CS char with a FC content similar to that of coal. Based on a comparison in terms of ash and FC, a pretreatment of 300 °C could be sufficient for some lignocellulosic samples, while 350 °C would be required for samples with particularly resistant cellulose structure or high inorganic content. However, the VM was found to represent more than 25 wt.% for all the obtained chars, which was higher than the value of 22.39

wt.% for the coal sample. As some of the volatiles are the precursors of the tar products, an analysis of the volatile composition is required prior to recommendation.

The elemental analysis results (Table 5-2) confirmed the relatively low sulphur (S) and nitrogen (N) contents of lignocellulosic biomass-derived fuels, when compared to coal [37]. While the N content of coal was 1.95 wt.%, the biomass chars were characterized by contents lower than 1 wt.% irrespective of the pretreatment temperature, except for CS (up to 1.17 wt.%). Regarding the S content, the highest measured content in the different chars was 0.23 wt.%, almost 10 times lower than for the coal sample (2.25 wt.%). This result highlighted the potential of reducing NO_x and SO_x emissions through the substitution of coal with biomass chars. A gradual reduction in hydrogen (H) and oxygen (O) contents of the char samples was observed with an increase in pretreatment temperature. This was due to the conversion of several types of unstable oxygenated groups (hydroxyl, acetyl, etc.) and the release of oxygenated volatiles such as H_2O, CO_2, formic acid, acetic acid, etc. Such reactions resulted in an increase of the carbon content of the chars. For pretreatment temperatures of 250 and 300 °C, the carbon content of the char samples were around 51 wt.% and ≤70 wt.% respectively, which was found to be lower than for the coal sample (75.92 wt.%). At pretreatment temperatures of 350 and 400 °C, the carbon content of the chars from the different samples was found to be in the range of 72.59-77.07. The H content of the char samples pretreated at 350 °C was in the range of 4.56-4.92 wt.%, while values for pretreatment at 400 °C (4.00-4.42 wt.%) were more similar to that of the coal sample (4.02 wt.%). From Table 5-2 the oxygen (O) content of the raw biomass samples was in the range 47.83–50.93 wt%, which was much higher than the O content of the coal sample (15.86 wt%). From literature, values lower than 20 wt.% are usually reported, and sometimes even 15 wt.% for coal of sub-bituminous and higher rank [37]. Upon thermal pretreatment of biomass samples, the O content dropped to around 42 wt.% at 250 °C and less than 27 wt.% at 300 °C (except for PN due to limited conversion of the crystalline cellulose). Values lower than 20 wt.% were obtained for pretreatment at 350 °C (only CC) and 400 °C (BB, PN and CC). However, as the lowest recorded O content (17.85 wt.%) was still higher than for coal, biomass char samples are still likely to produce more oxygenated compounds through devolatilization, thus the need to investigate the composition of the devolatilization products.

Figure 5-2 shows the van Krevelen diagram (H/C versus O/C molar ratios) for coal, raw biomass and char samples. The molar H/C and O/C ratios of raw biomass samples were larger than 1.70 and 0.78 respectively, which was much higher than the H/C and O/C ratios of the coal sample (ie. 0.64 and 0.16 respectively). Thermal pretreatment led to a reduction in H/C and O/C ratios of chars which moved towards the values observed for coal as temperature was increased. The H/C and O/C ratios of char were in the range of 1.39–1.48 and 0.59–0.63 respectively when pretreatment temperature was 250 ^{o}C and in the range of 0.89-1.19 and 0.28-0.45 respectively for 300 °C. When pretreated at temperatures ≥350 ^{o}C, the H/C and O/C ratios of char were less than 0.81 and 0.23 respectively and were situated in the region of coal (Figure 5-2). This result suggests that a temperature of at least 350 ^{o}C is required for biomass pretreatment when considering coal replacement.

The HHV profiles of coal and biomass samples are shown in Figure 5-3. It could be seen that HHVs of biomass samples intensified with increase in pretreatment temperature. This was due to the decreased content of oxygen element and the enrichment in FC content. The HHVs of the raw biomass samples and chars pretreated at 250 °C were lower than 20 MJ/kg, which corresponds to lignite coal quality. At a pretreatment temperature of 300 ^{o}C, the HHVs of BB and CC chars were higher than for the coal sample, while a pretreatment temperature of 350 °C was required for PN, due to its more resistant cellulose structure. When pretreated at 350 ^{o}C and 400 ^{o}C, BB, CC and PN biomass chars had HHVs higher than 25 MJ/kg, which corresponds to sub-bituminous A rank coal. The relatively high ash content of CS was detrimental to the energy content of the chars, which was constantly lower than 22 MJ/kg. Only pretreatment at 350 and 400 °C resulted in CS char with HHV close to that of the coal sample.

5.3.3. Analysis of condensable volatiles

The yields (per mass, on dry basis) of individual condensable volatile products generated during the devolatilization of coal, raw biomass and thermally pretreated biomass samples are compiled in Table 5-3. Samples were devolatilized in a TGA and the generated volatiles analyzed and quantified by thermal desorption/GC-MS. Condensable products were categorized into four groups; low molecular weight compounds (acids and ketones), polysaccharide depolymerization

products (furans and anhydrosugar), phenolics and aromatic hydrocarbons. Figure 5-4 illustrates the evolution of the various groups as a function of pretreatment temperature.

In Table 5-3 the total quantified condensable volatile/tar yields from untreated biomass samples were significantly higher than that from coal (ie. 18.19–22.37 versus 0.49 wt.%). These values were significantly lower than the VM contents of the samples because the method did not quantify the amount of permanent gases and water (especially for biomass samples) generated during devolatilization. When biomass feedstocks were pretreated the total volatile yields decreased with increase in pretreatment temperature (Table 5-3), which was consistent with the evolution of volatile matter content (Table 5-2). However, different trends were observed for the four groups.

The contribution of the light acids and ketones to the tar condensation issue is expected to be limited, as such compounds have relatively low boiling points. Moreover, in the gasification reactor the acid and ketone groups are likely to react, resulting in the formation of CO_2 or CO and the production of even lighter compounds [38]. The yield of the acids and ketones shown in Figure 5-4a for biomass samples declined with the increase in pretreatment temperature. Particularly, there was a major drop in yield when pretreatment temperature was at 300 ^{o}C, while no detection was observed for char produced at ≥350 ^{o}C. Acetic acid was the main acid compound produced during char devolatilization (Table 5-3). It was reported to be a product of hemicelluloses deacetylation reaction as well as cellulose conversion [39,40] . Amongst the ketones, the main compound was hydroxyacetone, which is also a typical product from the decomposition of biomass sugar rings [41]. The absence of ketones and acids following pretreatment at temperatures higher than 300 °C confirmed the relatively low thermal stability of the C=O bond.

The formation of the depolymerization products (furans and anhydrosugars) proceeds through the degradation of glucosidic bonds between sugar monomers [38,40]. The contraction of the pyran ring has been reported to lead to the formation of furans such as furfural and 5-hydroxymethylfurfural (5-HMF) [38,40]. From the yield evolution of furan and anhydrosugar shown in Figure 5-4b. It appears that pretreatment at 250 ^{o}C had minimal effect on the formation of polysaccharide depolymerisation products. Following pretreatment at 300 ^{o}C the production of furans and anhydrosugar during subsequent char devolatilization reduced drastically especially for BB, CC and CS feedstocks. The yields of the depolymerization products from PN char remained

relatively high even after pretreatment at 300 ^{o}C, due to the stability of the cellulose crystalline structure as discussed in section 5.3.1. The formation of furans and anhydrosugar was not observed after biomass pretreatment at ≥350 ^{o}C, except for the production of very small quantities of benzofuran and 2-methylfuran (Table 5-3). This indicates that pretreatment temperature of 350 ^{o}C is sufficient enough to remove most of the condensable volatiles originating from biomass polysaccharide fraction. Though some phenolic compounds were identified from cellulose and hemicelluloses pyrolysis studies [42], the contribution of polysaccharides-derived compounds to tar formation is probably less significant than for the lignin-derived compounds.

The degradation of lignin is known to be the main source of phenolics during lignocellulosic biomass pyrolysis. The phenolics yield evolution shown in Figure 5-4c was in agreement with the lignin content of biomass samples (Table 5-1), with higher yields observed for the PN and BB samples. For pretreatment at 250 ^{o}C, lignin degradation is limited, especially in comparison with hemicelluloses [28,29]. Such pretreatment resulted in an increase of the lignin content in the sample, ultimately generating a higher yield of phenolics through devolatilization, when compared to raw biomass. At higher temperature, significant lignin degradation occurred and was found to be more pronounced with increasing temperature, hence the observed trend in phenolic products in Figure 5-4c. Due to the increasing content of aromatic rings during char formation, a pretreatment of 300 °C led to a significant increase in the production of aromatic hydrocarbons through subsequent devolatilization. With an increment in pretreatment temperature, the devolatilization resulted in decreased yield of aromatic hydrocarbons due to the reduced volatile matter content of the char samples. However, the decrease was less pronounced than for the other groups and, for pretreatment at 400 °C, the highest volatile yields were observed for the aromatic hydrocarbons group (Figure 5-4).

Contrary to what was observed for biomass, coal devolatilization produced virtually no acids, ketones and anhydrosugars, while only traces of furan compounds were detected Coal generated mainly aromatic hydrocarbons and phenolics, which was consistent with its strong C═C aromatic structure [43,44]. The compounds obtained in higher yields were phenol, cresols, toluene and benzene (Table 5-3), which was consistent with the study of Cheng et al. [45] based on surface area comparison.

Phenolic volatiles are considered as a major source of the problematic tar condensation issue observed during biomass gasification [12]. Through recombination, they can be converted into Polycyclic Aromatic Hydrocarbons (PAH), which condense at relatively high temperature [36]. From Figure 5-4c it can be seen that the devolatilization yields of phenolics from raw biomass and low temperature (≤ 300 °C) chars were much higher than from coal. It is worth noting that most of the phenolics were characterized by the presence of methoxy groups (guaiacol, 2-methoxy-4-vinylphenol and 2,6-dimethoxyphenol, etc.). Such groups increase the reactivity of the phenols and could be responsible of an increased risk of recombination reactions and condensation [46]. Following pretreatment at 350 °C, the yields of phenolics were in the range of 0.20-0.35 wt.%, which is comparable with the yields of 0.29 wt.% observed for the coal sample. For all the chars pretreated at 400 °C, the yields of phenolics decreased to values lower than 0.11 wt.%. Interestingly, a drastic change in phenolics distribution with a decreased proportion of compounds with methoxy group was observed. In this study, PN was the sample with the highest lignin content and softwood lignin is known to be more thermally stable than in other biomass species. For pretreatment at 350 °C it was only for the PN char that the yields of methoxyphenols were found to be higher than for coal (Table 5-3). In the case of BB, the yields were found to be similar for pretreatment at 350 °C (0.02 wt.%) while only traces were detected for 400 °C char. For the two corn residues, both chars pretreated at 350 and 400 °C produced less methoxyphenols than the coal sample.

From Figure 5-4d it can be seen that the yields of aromatic hydrocarbons from coal were similar to that from biomass chars produced at 350 °C and 400 °C. Compared to the phenolics, the aromatic hydrocarbons are more stable and these light aromatics are not suspected to pose any major condensation issue [36]. Finally, Table 5-3 shows that the total quantified volatile yield from coal (4.93 µg/mg) was within the range 4.52–5.43 µg/mg obtained from biomass chars produced at 350 °C. Therefore, when considering coal replacement, based on volatiles yield and composition a char production temperature of 350 °C could be sufficient for some lignocellulosic samples while a temperature of 400 °C would be recommended for the samples with high lignin content, especially softwoods.

When considering these recommendations for pilot scale, a limitation of this study is that it was not possible to characterise the oligomer-derived compounds produced during devolatilization. As

these heavy compounds cannot be analyzed with GC instrument due to limited volatility, it is clear they are likely to contribute to the tar condensation issue. However, these compounds are typically produced during the main devolatilization stage of biomass, around 350 °C, which is the same temperature where the maximum peak for cellulose depolymerisation occurs. With low heating rate, the main lignin depolymerisation stage is usually observed at similar temperature [38]. In addition, char formation process leads to a higher degree of reticulation of the residue, which is expected to limit the production of oligomer-derived compounds during subsequent devolatilization. This assumption is consistent with the minimal mass loss and the composition of volatiles produced from biomass at temperatures higher than 400 °C, which is characterized by a majority of permanent gases. Based on the similarities between coal and chars prepared at 350 and 400 °C in terms of elemental composition, proximate analysis and composition of the quantified devolatilization products, a significant difference in the production of oligomer-derived compounds is not expected. The higher VM content of the biomass chars could appear as a cause of concern. However, it is worth noting that it was a consequence of lower ash content in biomass chars. When considering only the organic composition, the ratio FC/VM was found to be higher for the chars pretreated at 400 °C than for coal (2.3), except for CS the sample with the highest ash content. This result means that on a dry ash free basis, when comparing the amount of organic material fed to the gasification process, lower or similar quantities of volatiles are expected from the biomass chars pretreated at 400 °C.

5.4. Conclusion

The potential of thermally pretreated biomass as coal substitute has been evaluated. Four lignocellulosic biomass feedstocks (pine, bamboo, corn cob and corn stove) thermally pretreated at varying temperatures (250–400 ^{o}C) were compared to coal in terms of fuel properties and char devolatilization products, using a TGA coupled with thermal desorption/GC-MS. From the results it was shown that increasing the pretreatment temperature resulted in a char with a composition more similar to that of coal. The oxygen content was particularly reduced for pretreatment temperatures ≥ 300 °C due to the significant degradation of the cellulose structure. The analysis of the char devolatilization products confirmed the absence of polysaccharides depolymerization products for pretreatment at 350 and 400 °C. In comparison with coal, as the composition and the yields of the phenolics volatiles were similar, a pretreatment temperature of 350 °C could be

sufficient prior to gasification. For lignocellulosic species with high lignin or inorganic contents, an increase to 400 °C could be more suitable.

References

[1] A. Franco, A.R. Diaz, The future challenges for "clean coal technologies": Joining efficiency increase and pollutant emission control, Energy. 34 (2009) 348–354.

[2] M.J.C. van der Stelt, H. Gerhauser, J.H.A. Kiel, K.J. Ptasinski, Biomass upgrading by torrefaction for the production of biofuels: A review, Biomass and Bioenergy. 35 (2011) 3748–3762.

[3] D. Medic, M. Darr, A. Shah, B. Potter, J. Zimmerman, Effects of torrefaction process parameters on biomass feedstock upgrading, Fuel. 91 (2012) 147–154.

[4] T. Pröll, H. Hofbauer, H2 rich syngas by selective CO2 removal from biomass gasification in a dual fluidized bed system — Process modelling approach, Fuel Process. Technol. 89 (2008) 1207–1217.

[5] H.B. Goyal, D. Seal, R.C. Saxena, Bio-fuels from thermochemical conversion of renewable resources: A review, Renew. Sustain. Energy Rev. 12 (2008) 504–517.

[6] Q. Chen, J.S. Zhou, B.J. Liu, Q.F. Mei, Z.Y. Luo, Influence of torrefaction pretreatment on biomass gasification technology, Chinese Sci. Bull. 56 (2011) 1449–1456.

[7] J. Han, H. Kim, The reduction and control technology of tar during biomass gasification/pyrolysis: An overview, Renew. Sustain. Energy Rev. 12 (2008) 397–416.

[8] F.J. Wang, S. Zhang, Z.D. Chen, C. Liu, Y.G. Wang, Tar reforming using char as catalyst during pyrolysis and gasification of Shengli brown coal, J. Anal. Appl. Pyrolysis. 105 (2014) 269–275.

[9] M.W. Seo, J.H. Goo, S.D. Kim, S.H. Lee, Y.C. Choi, Gasification characteristics of coal/biomass blend in a dual circulating fluidized bed reactor, Energy and Fuels. 24 (2010) 3108–3118.

[10] Y. Pan, E. Velo, X. Roca, J.. Manyà, L. Puigjaner, Fluidized-bed co-gasification of residual biomass/poor coal blends for fuel gas production, Fuel. 79 (2000) 1317–1326.

[11] A.O. Aboyade, M. Carrier, E.L. Meyer, H. Knoetze, J.F. Görgens, Slow and pressurized co-pyrolysis of coal and agricultural residues, Energy Convers. Manag. 65 (2013) 198–207.

[12] C. Li, K. Suzuki, Tar property, analysis, reforming mechanism and model for biomass gasification-An overview, Renew. Sustain. Energy Rev. 13 (2009) 594–604.

[13] L.F. de Diego, F. García-Labiano, P. Gayán, A. Abad, T. Mendiara, J. Adánez, M. Nacken, S. Heidenreich, Tar abatement for clean syngas production during biomass gasification in a dual fluidized bed, Fuel Process. Technol. 152 (2016) 116–123.

[14] P. Rousset, C. Aguiar, N. Labbé, J.-M. Commandré, Enhancing the combustible properties of bamboo by torrefaction., Bioresour. Technol. 102 (2011) 8225–31.

[15] B. Arias, C. Pevida, J. Fermoso, M.G. Plaza, F. Rubiera, J.J. Pis, Influence of torrefaction on the grindability and reactivity of woody biomass, Fuel Process. Technol. 89 (2008) 169–175.

[16] M. Broström, A. Nordin, L. Pommer, C. Branca, C. Di Blasi, Influence of torrefaction on the devolatilization and oxidation kinetics of wood, J. Anal. Appl. Pyrolysis. 96 (2012) 100–109.

[17] A.V. Bridgwater, Renewable fuels and chemicals by thermal processing of biomass, Chem. Eng. J. 91 (2003) 87–102.

[18] J.H. Peng, H.T. Bi, C.J. Lim, S. Sokhansanj, Study on density, hardness, and moisture uptake of torrefied wood pellets, Energy and Fuels. 27 (2013) 967–974.

[19] W. Yan, T.C. Acharjee, C.J. Coronella, V.R. Vásquez, Thermal pretreatment of lignocellulosic biomass, Environ. Prog. Sustain. Energy. 28 (2009) 435–440.

[20] A. Ohliger, M. Förster, R. Kneer, Torrefaction of beechwood: A parametric study including heat of reaction and grindability, Fuel. 104 (2013) 607–613.

[21] F.F. Felfli, C.A. Luengo, J.A. Suárez, P.A. Beatón, Wood briquette torrefaction, Energy Sustain. Dev. 9 (2005) 19–22.

[22] H. Li, X. Liu, R. Legros, X.T. Bi, C.J. Lim, S. Sokhansanj, Torrefaction of sawdust in a fluidized bed reactor, Bioresour. Technol. 103 (2012) 453–458.

[23] M.J. Prins, K.J. Ptasinski, F.J.J.G. Janssen, Torrefaction of wood. Part 2. Analysis of products, J. Anal. Appl. Pyrolysis. 77 (2006) 35–40.

[24] C. Couhert, S. Salvador, J.-M. Commandré, Impact of torrefaction on syngas production from wood, Fuel. 88 (2009) 2286–2290.

[25] F. Nsaful, F.X. Collard, M. Carrier, J.F. Görgens, J.H. Knoetze, Lignocellulose pyrolysis with condensable volatiles quantification by thermogravimetric analysis - Thermal desorption/gas chromatography-mass spectrometry method, J. Anal. Appl. Pyrolysis. 116 (2015) 86–95.

[26] F. Huang, P.M. Singh, A.J. Ragauskas, Characterization of Milled Wood Lignin (MWL) in Loblolly Pine Stem Wood, Residue, and Bark, J. Agric. Food Chem. 59 (2011) 12910–12916.

[27] D. Da Silva Perez, C. Dupont, A. Guillemain, S. Jacob, F. Labalette, S. Briand, S. Marsac, O. Guerrini, F. Broust, J.M. Commandre, Characterisation of the most representative agricultural and forestry biomasses in france for gasification, Waste and Biomass Valorization. 6 (2015) 515–526.

[28] H. Yang, R. Yan, H. Chen, D.H. Lee, C. Zheng, Characteristics of hemicellulose, cellulose and lignin pyrolysis, Fuel. 86 (2007) 1781–1788.

[29] D.K. Shen, S. Gu, K.H. Luo, S.R. Wang, M.X. Fang, The pyrolytic degradation of wood-derived lignin from pulping process, Bioresour. Technol. 101 (2010) 6136–6146.

[30] M.J. Prins, K.J. Ptasinski, F.J.J.G. Janssen, Torrefaction of wood, J. Anal. Appl. Pyrolysis. 77 (2006) 28–34.

[31] W.-H. Chen, P.-C. Kuo, Isothermal torrefaction kinetics of hemicellulose, cellulose, lignin and xylan using thermogravimetric analysis, Energy. 36 (2011) 6451–6460.

[32] M.V. Ramiah, Thermogravimetric and differential thermal analysis of cellulose, hemicellulose, and lignin, J. Appl. Polym. Sci. 14 (1970) 1323–1337.

[33] K. Werner, L. Pommer, M. Broström, Thermal decomposition of hemicelluloses, J. Anal. Appl. Pyrolysis. 110 (2014) 130–137.

[34] F. Nsaful, F.-X. Collard, J.F. Görgens, Influence of lignocellulose thermal pretreatment on the composition of condensable products obtained from char devolatilization by means of thermogravimetric analysis-thermal desorption/gas chromatography-mass spectrometry, J. Anal. Appl. Pyrolysis. 127 (2017) 99–108.

[35] K.M. Lu, W.J. Lee, W.H. Chen, S.H. Liu, T.C. Lin, Torrefaction and low temperature carbonization of oil palm fiber and eucalyptus in nitrogen and air atmospheres, Bioresour. Technol. 123 (2012) 98–105.

[36] S. Anis, Z. A. Zainal, Tar reduction in biomass producer gas via mechanical, catalytic and thermal methods: A review, Renew. Sustain. Energy Rev. 15 (2011) 2355–2377.

[37] P. McKendry, Energy production from biomass (part 1): overview of biomass, Bioresour. Technol. 83 (2002) 37–46.

[38] F. Collard, J. Blin, A review on pyrolysis of biomass constituents : Mechanisms and composition of the products obtained from the conversion of cellulose , hemicelluloses and lignin, Renew. Sustain. Energy Rev. 38 (2014) 594–608.

[39] T. Nocquet, C. Dupont, J.M. Commandre, M. Grateau, S. Thiery, S. Salvador, Volatile species release during torrefaction of biomass and its macromolecular constituents: Part 2 - Modeling study, Energy. 72 (2014) 188–194.

[40] S.D. Stefanidis, K.G. Kalogiannis, E.F. Iliopoulou, C.M. Michailof, P.A. Pilavachi, A.A. Lappas, A study of lignocellulosic biomass pyrolysis via the pyrolysis of cellulose, hemicellulose and lignin, J. Anal. Appl. Pyrolysis. 105 (2014) 143–150.

[41] S. Wang, B. Ru, G. Dai, H. Lin, L. Zhang, Influence mechanism of torrefaction on softwood pyrolysis based on structural analysis and kinetic modeling, Int. J. Hydrogen Energy. (2016) 2–9.

[42] F.X. Collard, J. Blin, A. Bensakhria, J. Valette, Influence of impregnated metal on the pyrolysis conversion of biomass constituents, J. Anal. Appl. Pyrolysis. 95 (2012) 213–226.

[43] Ö. Onay, E. Bayram, Ö.M. Koçkar, Copyrolysis of Seyitömer−Lignite and Safflower Seed: Influence of the Blending Ratio and Pyrolysis Temperature on Product Yields and Oil Characterization, Energy & Fuels. 21 (2007) 3049–3056.

[44] R.M. Soncini, N.C. Means, N.T. Weiland, Co-pyrolysis of low rank coals and biomass: Product distributions, Fuel. 112 (2013) 74–82.

[45] J. Cheng, Y. Zhang, T. Wang, P. Norris, W.-Y. Chen, W.-P. Pan, Thermogravimetric–Fourier Transform Infrared Spectroscopy–Gas Chromatography/Mass Spectrometry Study of Volatile Organic Compounds from Coal Pyrolysis, Energy & Fuels. 31 (2017) 7042–7051.

[46] T. Hosoya, H. Kawamoto, S. Saka, Role of methoxyl group in char formation from lignin-related compounds, J. Anal. Appl. Pyrolysis. 84 (2009) 79–83.

Tables

Table 5-1: Lignocellulosic composition (wt% daf: dry ash-free basis) of biomass feedstocks

Component	Feedstock			
	Pine (PN)	Bamboo (BB)	Corn cob (CC)	Corn Stover (CS)
Lignin	29.87	25.48	17.76	16.53
Cellulose	40.94	39.39	34.34	36.70
Hemicelluloses	11.82	16.34	26.02	21.28
Extractives	5.19	12.96	10.49	17.53
Acetyl	1.89	3.32	3.91	3.06

Table 5-2: Proximate and Elemental analysis of coal and raw/treated biomasses

Feedstock	Proximate analysis (wt%), db[a]			Elemental analysis (wt%), daf[b]				
	VM	FC	Ash	C	H	N	S	O[c]
Coal	22.39	51.64	25.96	75.92	4.02	1.95	2.25	15.86
PN								
Raw	81.85	16.01	2.14	45.60	6.47	0.02	0.08	47.83
250	78.77	19.06	2.17	51.47	6.08	0.24	0.01	42.20
300	67.78	29.91	2.31	58.48	5.81	0.12	0.00	35.60
350	35.78	60.99	3.22	74.36	4.59	0.23	0.00	20.82
400	28.98	67.32	3.70	76.78	4.00	0.25	0.01	18.95
BB								
Raw	76.11	21.45	2.44	44.41	6.32	0.44	0.14	48.69
250	70.19	27.03	2.78	51.96	6.07	0.59	0.03	41.35
300	37.60	57.97	4.43	68.72	5.14	0.74	0.13	25.28
350	29.64	65.52	4.84	72.59	4.56	0.79	0.11	21.96
400	26.48	68.23	5.29	75.22	4.14	0.90	0.10	19.63
CC								
Raw	78.91	18.49	2.61	43.80	6.49	0.33	0.00	49.38
250	72.34	24.79	2.86	51.65	6.00	0.48	0.06	41.82
300	45.24	50.38	4.37	68.00	5.23	0.80	0.00	25.97
350	30.49	64.82	4.69	75.00	4.60	0.95	0.12	19.32
400	27.13	68.05	4.82	77.07	4.10	0.93	0.06	17.85
CS								
Raw	75.30	16.85	7.85	41.88	6.40	0.59	0.20	50.93
250	69.95	21.03	9.02	50.54	6.23	0.77	0.03	42.42
300	41.79	43.40	14.81	66.15	5.54	1.06	0.04	27.21
350	31.11	51.74	17.15	72.84	4.92	1.17	0.23	20.83
400	26.31	55.58	18.11	74.13	4.42	1.11	0.16	20.18

[a] Dry basis
[b] Dry ash-free basis
[c] Determined by difference

Table 5-3: Yields (µg/mg, dry basis) of devolatilization volatile products (nq: not quantified)

Compound	PN					BB					CC					CS					Coal
	Raw	Char				Raw	Char				Raw	Char				Raw	Char				
		250 ºC	300 ºC	350 ºC	400 ºC		250 ºC	300 ºC	350 ºC	400 ºC		250 ºC	300 ºC	350 ºC	400 ºC		250 ºC	300 ºC	350 ºC	400 ºC	
Acids																					
Formic acid	27.43	10.22	8.14	0.00	0.00	10.54	11.37	0.00	0.00	0.00	22.48	22.78	0.00	0.00	0.00	10.86	16.02	0.00	0.00	0.00	0.00
Acetic acid	62.01	52.41	40.79	0.00	0.00	96.36	71.18	23.39	0.00	0.00	71.33	56.52	25.45	0.00	0.00	89.90	77.30	26.81	0.00	0.00	0.00
Propanoic acid	2.61	2.57	0.00	0.00	0.00	4.94	5.17	0.00	0.00	0.00	6.10	3.99	0.00	0.00	0.00	6.15	4.34	0.00	0.00	0.00	0.00
Sub-total	**92.05**	**65.20**	**48.93**	**0.00**	**0.00**	**111.84**	**87.71**	**23.39**	**0.00**	**0.00**	**99.91**	**83.29**	**25.45**	**0.00**	**0.00**	**106.91**	**97.66**	**26.81**	**0.00**	**0.00**	**0.00**
Ketones																					
2,3-Butanedione	4.77	3.63	3.14	0.00	0.00	6.57	7.95	1.34	0.00	0.00	5.13	6.91	1.71	0.00	0.00	6.88	8.93	1.95	0.00	0.00	0.00
Hydroxy acetone	21.62	21.97	21.93	0.00	0.00	34.03	35.09	0.00	0.00	0.00	18.48	28.03	0.00	0.00	0.00	31.80	36.71	0.00	0.00	0.00	0.00
2-Cyclopenten-1-one	1.58	2.38	2.56	0.00	0.00	3.78	4.54	1.00	0.00	0.00	2.47	4.11	1.83	0.00	0.00	4.20	4.89	2.54	0.00	0.00	0.00
2-Hydroxy-3-methyl-2-cyclopentene	4.76	4.37	3.47	0.00	0.00	3.53	3.21	0.13	0.00	0.00	3.00	2.47	0.40	0.00	0.00	4.47	2.93	0.39	0.00	0.00	0.00
Sub-total	**32.73**	**32.36**	**31.10**	**0.00**	**0.00**	**47.91**	**50.80**	**2.47**	**0.00**	**0.00**	**29.08**	**41.51**	**3.95**	**0.00**	**0.00**	**47.35**	**53.45**	**4.88**	**0.00**	**0.00**	**0.00**
Furans																					
2-Methylfuran	1.74	4.78	4.30	0.32	0.00	1.76	4.05	1.07	0.13	0.00	1.39	3.89	2.02	0.22	0.00	1.28	3.52	1.57	0.19	0.00	0.03
Furfural	9.55	10.12	8.35	0.00	0.00	3.87	7.50	0.00	0.00	0.00	6.58	8.02	0.00	0.00	0.00	6.25	8.64	0.00	0.00	0.00	0.00
Fufuryl alcohol	25.94	15.91	11.42	0.00	0.00	15.13	11.83	0.00	0.00	0.00	17.82	11.31	0.71	0.00	0.00	13.67	4.63	0.76	0.00	0.00	0.00
Benzofuran	0.02	0.11	0.14	0.13	0.11	0.02	0.14	0.13	0.11	0.00	0.02	0.13	0.13	0.12	0.00	0.00	0.13	0.12	0.00	0.00	0.00
5-Methyl furfural	1.82	1.13	1.29	0.00	0.00	0.71	0.51	0.00	0.00	0.00	0.86	0.71	0.45	0.00	0.00	1.02	0.72	0.42	0.00	0.00	0.00
2(5H)-Furanone	6.06	10.63	6.44	0.00	0.00	4.01	5.01	0.00	0.00	0.00	3.37	4.83	0.67	0.00	0.00	4.90	7.06	0.85	0.00	0.00	0.08
5-Hydroxymethylfurfural	7.39	4.29	3.82	0.00	0.00	3.36	0.48	0.00	0.00	0.00	4.00	0.60	0.00	0.00	0.00	3.58	0.62	0.00	0.00	0.00	0.00
Sub-total	**52.51**	**46.96**	**35.76**	**0.44**	**0.11**	**28.87**	**29.51**	**1.20**	**0.24**	**0.00**	**34.05**	**29.49**	**4.00**	**0.34**	**0.00**	**30.68**	**25.31**	**3.72**	**0.19**	**0.00**	**0.11**
Anhydrosugar																					
Levoglucosan	21.20	26.99	21.51	0.00	0.00	0.85	1.30	0.18	0.00	0.00	2.59	2.99	0.84	0.00	0.00	2.29	2.38	0.79	0.00	0.00	0.00
Sub-total	**21.20**	**26.99**	**21.51**	**0.00**	**0.00**	**0.85**	**1.30**	**0.28**	**0.00**	**0.00**	**2.59**	**2.99**	**0.84**	**0.00**	**0.00**	**2.29**	**2.38**	**0.79**	**0.00**	**0.00**	**0.00**

Table 5-3 continued

Compound	PN					BB					CC					CS					Coal
	Raw	Char				Raw	Char				Raw	Char				Raw	Char				
		250 °C	300 °C	350 °C	400 °C		250 °C	300 °C	350 °C	400 °C		250 °C	300 °C	350 °C	400 °C		250 °C	300 °C	350 °C	400 °C	
Phenolics																					
Phenol	0.54	1.01	1.32	0.97	0.38	5.42	6.64	3.77	1.58	0.40	2.22	4.13	3.14	1.47	0.71	3.01	3.50	2.31	1.19	0.54	1.09
Guaiacol	2.35	4.00	3.96	0.64	0.04	3.17	3.31	0.91	0.05	0.00	2.25	2.69	1.09	0.08	0.00	1.88	1.90	0.60	0.02	0.00	0.02
o-Cresol	0.17	0.49	0.71	0.41	0.06	0.62	1.30	0.85	0.35	0.07	0.21	0.72	0.68	0.35	0.14	0.53	0.70	0.67	0.34	0.12	0.49
Maltol	2.67	2.25	2.89	0.00	0.00	0.96	0.35	0.00	0.00	0.00	1.23	0.87	0.27	0.00	0.00	1.42	0.85	0.10	0.00	0.00	0.00
m&p-Cresol	0.12	0.44	0.63	0.39	0.08	1.19	1.26	0.83	0.34	0.08	0.26	0.81	0.85	0.40	0.16	0.47	0.68	0.63	0.32	0.12	0.92
Creosol	2.39	4.94	4.83	0.48	0.05	0.57	0.88	0.31	0.01	0.00	0.40	0.92	0.51	0.03	0.00	0.32	0.55	0.27	0.01	0.00	0.01
4-Ethylphenol	0.09	0.12	0.13	0.07	0.02	0.84	0.87	0.37	0.12	0.02	0.33	0.64	0.46	0.15	0.03	0.48	0.49	0.33	0.13	0.03	0.10
2,4-Xylenol	0.02	0.05	0.09	0.06	0.01	0.00	0.09	0.06	0.00	0.01	0.00	0.06	0.07	0.03	0.01	0.00	0.06	0.05	0.02	0.01	0.10
2-Methoxy-4-vinylphenol	3.63	6.16	2.34	0.06	0.02	4.63	2.39	0.11	0.00	0.00	5.65	3.27	0.33	0.00	0.00	3.34	2.44	0.16	0.00	0.00	0.00
Eugenol	0.43	0.50	0.18	0.00	0.00	0.08	0.05	0.00	0.00	0.00	0.05	0.00	0.00	0.00	0.00	0.04	0.05	0.00	0.00	0.00	0.00
4-Propyl guaiacol	0.13	0.20	0.17	0.02	0.00	0.07	0.08	0.03	0.00	0.00	0.04	0.03	0.02	0.00	0.00	0.02	0.04	0.01	0.00	0.00	0.00
2,6-Dimethoxyphenol	5.01	7.58	6.60	0.31	0.00	5.54	4.84	0.28	0.15	0.02	1.31	2.08	0.37	0.02	0.00	1.69	2.01	0.20	0.01	0.00	0.15
trans-Isoeugenol	5.00	9.19	0.00	0.00	0.00	1.70	2.18	0.00	0.00	0.00	0.56	0.00	0.00	0.00	0.00	0.66	1.42	0.00	0.00	0.00	0.00
Isoeugenol	1.13	5.99	1.98	0.06	0.03	0.31	1.40	0.10	0.00	0.00	0.17	0.59	0.11	0.00	0.00	0.11	0.85	0.08	0.00	0.00	0.00
Apocynin	0.53	0.16	0.34	0.02	0.02	0.19	0.13	0.02	0.00	0.00	0.18	0.09	0.04	0.01	0.00	0.06	0.09	0.02	0.00	0.00	0.00
Sub-total	**24.21**	**43.07**	**26.16**	**3.47**	**0.72**	**25.30**	**25.78**	**7.63**	**2.61**	**0.60**	**14.83**	**16.91**	**7.94**	**2.54**	**1.05**	**14.04**	**15.61**	**5.43**	**2.03**	**0.82**	**2.89**
Aromatics																					
Benzene	0.32	0.36	0.43	0.32	0.25	0.45	0.48	0.53	0.46	0.43	0.37	0.40	0.45	0.44	0.38	0.48	0.49	0.66	0.44	0.50	0.38
Toluene	0.54	nq	1.18	0.74	0.34	0.99	nq	1.62	1.18	0.89	0.79	nq	1.78	1.08	0.91	1.31	nq	2.14	1.06	1.03	1.05
Ethylbenzene	0.00	0.08	0.10	0.08	0.07	0.07	0.13	0.12	0.09	0.07	0.03	0.13	0.12	0.10	0.08	0.05	0.14	0.15	0.10	0.08	0.04
p-xylene	0.13	0.18	0.35	0.23	0.10	0.29	0.62	0.51	0.36	0.25	0.18	0.43	0.43	0.31	0.27	0.35	0.51	0.57	0.38	0.35	0.28
o-xylene	0.04	0.05	0.07	0.05	0.02	0.06	0.12	0.09	0.05	0.03	0.05	0.11	0.10	0.07	0.04	0.09	0.13	0.14	0.09	0.07	0.08
Naphthalene	0.02	0.03	0.07	0.09	0.03	0.02	0.07	0.09	0.07	0.06	0.03	0.05	0.20	0.09	0.08	0.03	0.06	0.11	0.22	0.09	0.10
Sub-total	**1.04**	**0.70**	**2.20**	**1.51**	**0.80**	**1.88**	**1.41**	**2.97**	**2.22**	**1.73**	**1.46**	**1.11**	**3.09**	**2.09**	**1.77**	**2.31**	**1.33**	**3.78**	**2.30**	**2.11**	**1.93**
TOTAL YIELD	**223.74**	**215.28**	**165.66**	**5.43**	**1.63**	**216.64**	**196.52**	**37.93**	**5.08**	**2.33**	**181.92**	**175.29**	**45.27**	**4.97**	**2.82**	**203.59**	**195.74**	**45.41**	**4.52**	**2.93**	**4.93**

Figures

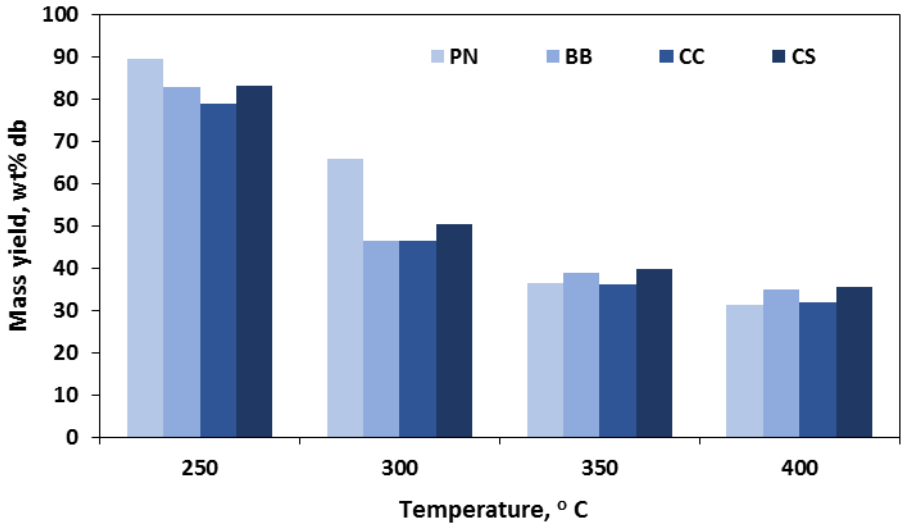

Figure 5-1: Mass yield during char preparation

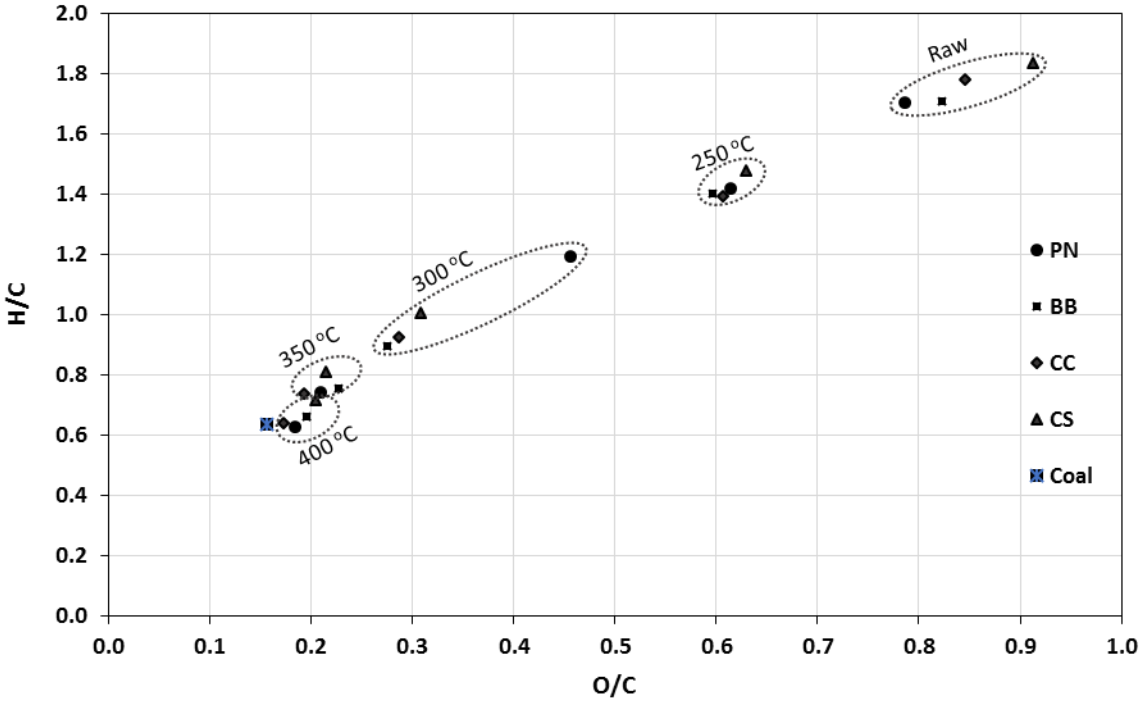

Figure 5-2: H/C and O/C molar ratio of chars and coal

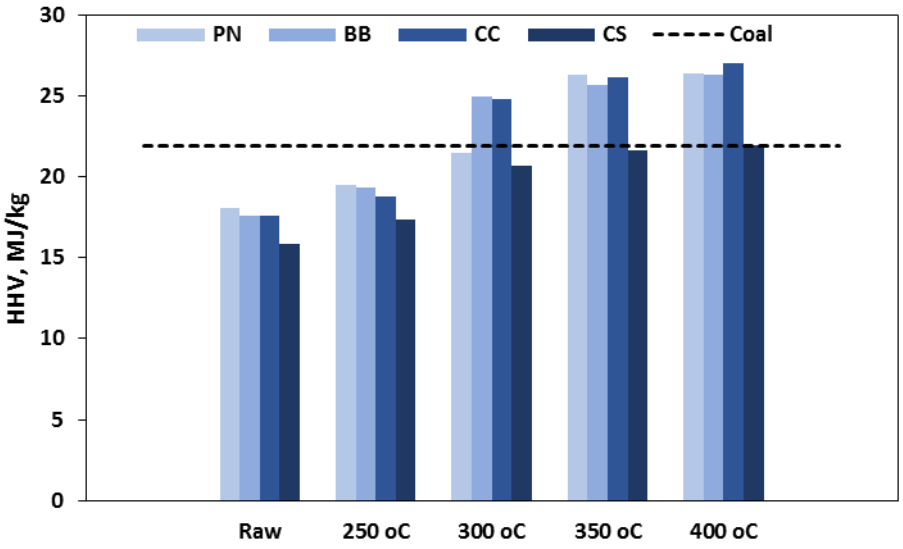

Figure 5-3: HHV comparison of coal, raw biomass and charcoal

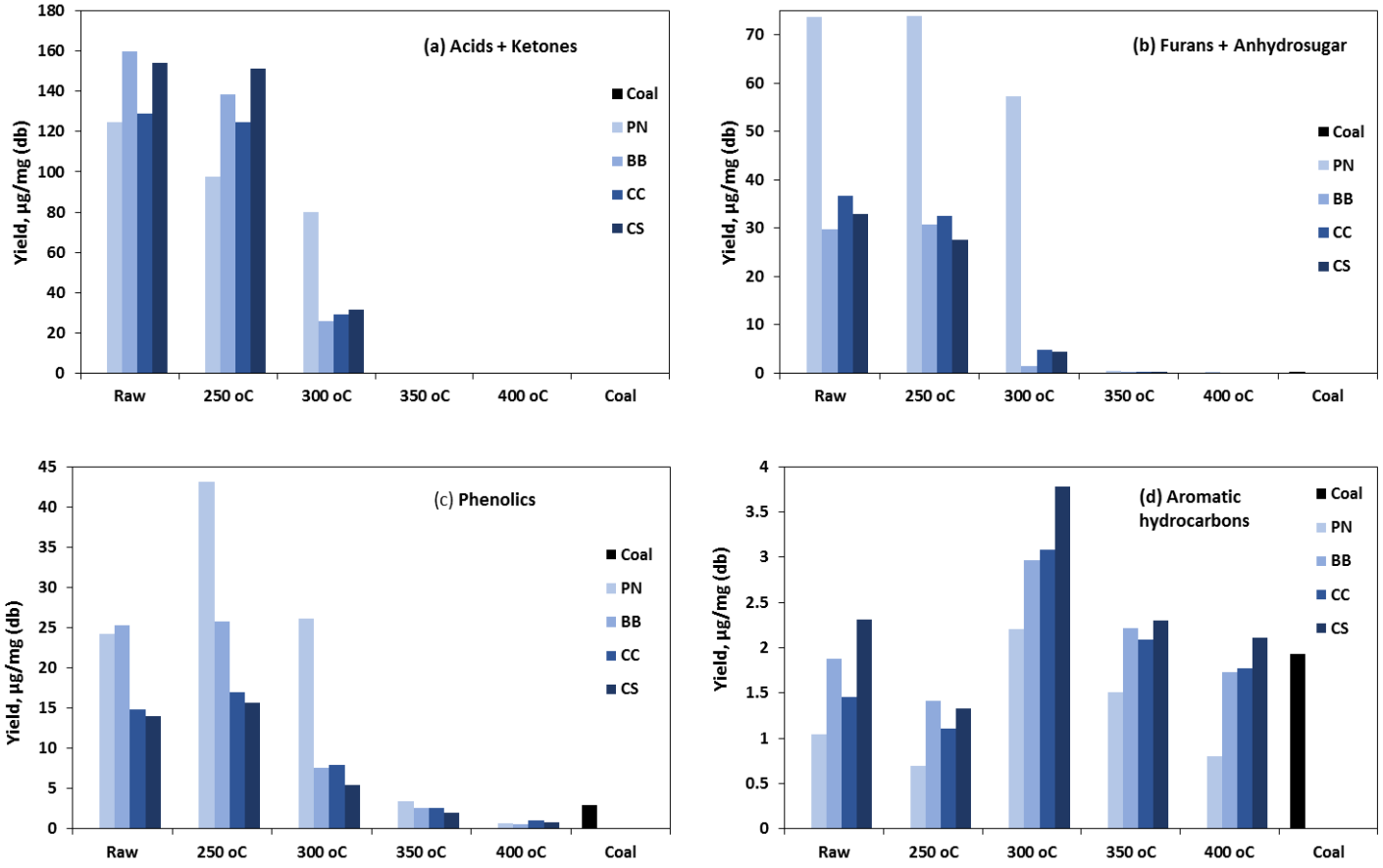

Figure 5-4: Yields of condensable volatiles

Chapter 6

Devolatilization characteristics and CO_2 gasification kinetics of biomass char and coal blends

This chapter is prepared as a manuscript for submission to the journal of Fuel

Title: "*Devolatilization characteristics and CO_2 gasification kinetics of biomass char and coal blends.*"

Authors: *Frank Nsaful, François-Xavier Collard, Johann F. Görgens*

Objective of dissertation in this chapter and summary of findings

Having determined a suitable biomass pretreatment condition for char production (chapter 5) the objective of this chapter was to assess the impact of the pretreated material (char) on the devolatilization and gasification characteristics of coal during co-gasification (objective 5). In this chapter biomass feedstocks were thermally pretreated to produce char and then blended with coal at different blending ratios to study the devolatilization characteristic and gasification parameters (objective 5) in comparison to the blending of raw biomass samples. Biomass pretreatment was done at the gram scale using the condition identified at the milligram scale in chapter 5. All devolatilization characteristic studies were done using the TGA. CO_2 gasification of fuels were also simulated in the TGA and the data used to establish gasification kinetic parameters. Insight into the devolatilization and gasification characteristics of char-coal and raw biomass-coal blends are provided.

Char-coal blends were shown to follow similar devolatilization profile as coal while two distinct stages were shown during the devolatilization of raw biomass-coal blends. However, no synergies

were detected during devolatilization of the various fuel blends. It was established that a char pretreated according to the preferred method, was suitable for coal substitution at a blending ratio of up to 20 wt%, as this gave similar reactivity during gasification when compared to using coal alone. The overall objective of the dissertation, i.e. biomass pretreatment for coal substitution, was therefore achieved.

Summary of authors' contributions

All experimental work were planned and performed by *Frank Nsaful*. He also analysed and did the interpretation of the experimental data and wrote the chapter. *François-Xavier Collard* contributed to the experimental planning, data interpretation and also reviewed the chapter. *Johann F. Görgens* assisted with data interpretation and reviewed the chapter.

Abstract

In this work the devolatilization characteristic and CO_2 gasification kinetics of biomass chars and their blends with coal were investigated. Pine, bamboo and corn stover biomass feedstocks were pretreated to produce char at 350 ^oC and 30 min hold time. The individual fuels and their blends with coal were compared based on devolatilization behaviour and gasification characteristics. In addition raw biomass feedstocks were also subjected to the same analysis to assess the impact of the thermal pretreatment. As a result of the pretreatment the fuel characteristics of the chars were found to be comparable to those of coal. As such their behaviours during devolatilization were characterized by conversion at higher temperature than the raw feedstocks, the latter being converted with the release of a significantly higher amount of volatiles. The char-coal blends followed similar devolatilization profiles as coal while the raw biomass-coal blends showed two distinct stages. A study of the fuels blends showed no synergy during devolatilization. CO_2 gasification characteristic established through isoconversional analysis showed that char blending at 20 wt% gave similar reactivity as compared to using coal alone. Hence char blending up to 20 wt% can be considered for co-gasification purposes.

Keywords: Biomass; Char; Coal; Co-gasification; Pyrolysis; TGA

6.1. Introduction

Global industrial growth has led to an increase in the demand for energy. Currently fossil fuels are major sources of energy in the world. However, these fuels are not renewable and their overuse is causing a depletion of such resources. In addition these fuels have a major contribution to the increased release of CO_2 and other greenhouse gases into the environment, thereby causing a rise in the problem of global warming [1,2]. Lignocellulosic biomass is a sustainable and renewable fuel source and is CO_2 neutral. Due to its sustainable carbon, biomass has the potential to be converted into chemicals, energy and energy products such as liquid fuels [3]. The application of biomass as an alternative fuel source will decrease the use of fossil-based fuels, ultimately leading to a decreased release of pollutant emissions and greenhouse gases [4,5].

Several ways exist for using biomass to generate bioenergy. Notably among these is the use of biomass blended with coal which is currently gaining much research attention [2]. Biomass and coal blends can find applications in co-combustion or co-firing [6–9] and co-gasification [10–13]. Previous studies have shown that co-processing coal and biomass for combustion application can decrease the SO_x and NO_x levels in the flue gas in addition to cutting down on greenhouse gas emissions [7,14]. This can be attributed to the low nitrogen and sulphur contents of biomass in comparison with coal. Pyrolysis or devolatilization is the first step of combustion and gasification processes [15–19]. By co-pyrolysing biomass and coal blends it was noticed that the conversion temperature of the mixture was reduced compared to using only coal [16]. The liquid and gas yields from co-pyrolysis of biomass and coal blend have also been shown to increase with the fraction of biomass in the blend [16,20]. In the co-pyrolysis study of Seo et al [11] it was found that the char from the blend had an increased proportion of micropores after pyrolysis. This created an increase of active sites within the char giving it a more reactive structure suitable for gasification. Concerning co-gasification, it has been observed that the syngas yield and its heating value were significantly increased when biomass and coal were co-gasified in a fluidized bed gasifier [10]. The increase was observed to be in line with the increase in the biomass fraction. Similarly Seo et al [11] found that an increase in the biomass fraction during biomass/coal co-gasification increased the amount of CH_4 and H_2 in the product gas. Also the cold gas efficiency and the carbon conversion were improved. Blending biomass and coal has also been observed to

improve the rheological properties of the fuel when used in a fluidized bed gasifier compared to using coal alone [21].

The above examples show some of the advantages of using biomass as blend with coal. However, in spite of these advantages, in comparison with coal, raw biomass is characterized by a high moisture and oxygen content, high O/C ratio, low bulk densities and heating value [5,22,23]. In addition, raw biomass has a hygroscopic nature, is heterogeneous and has poor grindability [5,22,23]. All these negative properties pose challenges to ensuring the efficient utilization of raw biomass. As such recent research has focused on improving or eliminating the negative properties of raw biomass [3]. Torrefaction and/or slow pyrolysis has widely been used as pretreatment methods to upgrade raw biomass properties. Both methods are thermal pretreatments carried out at temperatures of 200-300 ^{o}C for torrefaction [24,25] and between 300 and 500 ^{o}C for slow pyrolysis [26] generally under inert atmosphere and at low heating rate (<50 ^{o}C/min). These thermal pretreatment methods give biomass several added advantages such as decreased oxygen contents and O/C ratio [27], low moisture content [28,29], improved heating value[30], improved grindability [24,31] and a hydrophobic nature [32,33]. Thus making the thermally pretreated biomass (char) a suitable fuel for a wider range of applications.

Torrefaction and slow pyrolysis of biomass into a char product have been widely studied [3,34]. Similarly, numerous studies have been done on biomass and coal co-pyrolysis (co-devolatilization) with some reporting synergies in their interactions [19,20,35]. However, studies on the co-pyrolysis of thermally pretreated biomass (char) and coal blends are limited. Similarly studies on co-gasification of thermally pretreated biomass and coal blends are also limited. The present work studies the devolatilization characteristics and CO_2 gasification kinetics of coal and biomass char blends. Chars were prepared from pine, bamboo and corn stover biomass feedstocks and then blended with coal at varying blend ratios. The devolatilization and subsequent gasification of the chars and coal blends were then carried out in a thermogravimetric analyzer and the kinetic parameters were determined.

6.2. Materials and methods

6.2.1. Feedstocks

The biomass feedstocks used were corn stover (CS), pine *(Pinus radiata)* (PN) and bamboo *(Bambusa balcooa)* (BB), which were sourced from the Northern, Eastern and Western provinces, respectively. All biomass feedstocks were dried to less than 10 wt% moisture content, milled and sieved to 250–450 μm particle size range by means of Retsch mill (model ZM100) and a vibratory sieve shaker (model AS200). Table 6-1 lists the lignocellulosic chemical composition of the raw biomass feedstocks. The coal used in this study was a typical South African low grade sub-bituminous coal with a high ash content. Prior to it is use, the coal was pulverized and then sieved to 160–450 μm particle size range. Sub-samples of each feedstock for experiment were obtained using the standard method DD CEN/TS 14780:2005.

6.2.2. Char preparation

The preparation of biomass char samples was done through thermal pretreatment in a horizontal bench-scale fixed bed reactor. The reactor consists of a cylindrical stainless steel tube (0.76 m long, 60 mm O.D, 2 mm thickness) and was electrically heated. Temperature control was by means of a k-type thermocouple which constantly monitored the temperature within the reactor. For pretreatment, about 20 g of raw biomass was heated at 10 ^{o}C/min from room temperature to 350 ^{o}C and then held for 30 min. Nitrogen (99.5% purity, Afrox SA) at a flowrate of 500 ml/min was used as carrier gas to provide an inert atmosphere. To prevent the combustion of char, the nitrogen gas flow was maintained at the end of the reaction until the reactor temperature had reached 50 ^{o}C. The char was then collected and stored for further analysis.

6.2.3. Physico-chemical analysis

Higher heating value (HHV), proximate and elemental analysis were performed on coal, char and raw biomass samples. HHV was determined according to the ASTM standard D5865-11a using bomb calorimetry (CAL2K ECO bomb calorimeter – model 2013). Proximate analysis was performed according to the ASTM method E1131, by means of thermogravimetric analysis (TGA) (TGA/DSC 1-LF1100 system, Mettler Toledo) to determine the percentage composition of volatile

matter (VM), fixed carbon (FC) and ash in each sample. Elemental analysis (C, H, N, S) of samples was done using a Leco TruSpec Micro elemental analyzer. O content was determined by difference.

6.2.4. Devolatilization characteristics

The devolatilization behaviour of biomass (raw/char), coal and their blends were studied using a TGA reactor (TGA/DSC 1-LF1100 system, Mettler Toledo). A 10 mg sample was weighed into a sample holder and pyrolyzed from 30 ^{o}C to 600 ^{o}C at a heating rate of 10 ^{o}C/min, with a nitrogen (baseline 5.0, Afrox SA) flow of 70 ml/min. For blends, raw biomass or char samples were physically mixed with coal at biomass blend ratios (BBR) of 10, 20 and 50 wt%.

6.2.5. Gasification and kinetics

The atmospheric gasification of raw biomass, char, coal and blends was simulated in a TGA (TGA/DSC 1-LF1100 system, Mettler Toledo). 10 mg sample was first pyrolyzed under nitrogen gas (baseline 5.0, Afrox SA) flow of 70 ml/min. Sample was heated at 10 ^{o}C/min from 30 ^{o}C to 105 ^{o}C and held for 5 min to ensure moisture removal, then from 105 ^{o}C to 600 ^{o}C and further held for 20 min to ensure mass stability. At the end of the isothermal stage at 600 ^{o}C, the nitrogen flow was reduced to 20 ml/min (balance protective gas) and CO_2 at a flow of 80 ml/min was used for gasification. The sample was gasified from 600 ^{o}C to 1100 ^{o}C at different heating rates (5, 10, 15, 20 and 25 ^{o}C/min). A hold time of 7 min was maintained at 1100 ^{o}C to ensure complete conversion. The choice of CO_2 as the gasification agent was due to the operational limitations of the available TGA equipment (not adapted for the use of steam/oxygen as widely applied in industry). The non-isothermal data recorded for the CO_2 gasification region was used for kinetic studies.

6.2.6. Kinetic analysis

The non-isothermal CO_2 gasification kinetic analysis of biomass and coal blends was done using the differential isoconversional method of Friedman over the gasification temperature range (ie. 600-1100 ^{o}C). The non-isothermal kinetics of thermal decomposition of solid material is usually given as [36]:

$$\frac{d\alpha}{dt} = A\, exp\left(-\frac{E}{RT}\right) f(\alpha) \qquad 6\text{-}1$$

Where A is the pre-exponential factor (s^{-1}), E is the activation energy (kJ mol^{-1}), R is the gas constant (8.314 J K^{-1} mol^{-1}), T is the absolute temperature (K), t is time (s), $f(\alpha)$ is the hypothetical reaction model. The isoconversional method is model-free and as such does not require the selection of an appropriate reaction model $f(\alpha)$. Thus E is estimated at progressive values of the conversion α independent of the reaction model $f(\alpha)$ [37].

The conversion α in Equation 6-1 is defined as:

$$\alpha = \frac{m_o - m_t}{m_o - m_f} \qquad 6\text{-}2$$

Where m_o is the initial mass at the start of gasification (ie. the mass at the end of the isothermal stage at 600 °C), m_t and m_f are the mass at time t and the final mass at the end of gasification respectively.

For a constant heating rate β (°C/min) during gasification, $\beta = dT/dt$. Substituting β into Equation 6-1 and taking the logarithm yields:

$$ln\left(\frac{d\alpha}{dt}\right) = ln\left(\beta\frac{d\alpha}{dT}\right) = ln\,[A.f(\alpha)] - \frac{E}{RT} \qquad 6\text{-}3$$

The plot of $ln(d\alpha/dt)$ versus $1/T$ at the same degree of conversion from data taken from various heating rates will give a series of straight lines, each having a slope of $-E/R$ and intercept of $ln[A.f(\alpha)]$ corresponding to a particular degree of conversion. From these the activation energy and the pre-exponential factor at each conversion α can be obtained.

6.3. Results and discussion

For the purpose of the discussions below, the raw biomass samples (pine, bamboo and corn stover) are designated as PN_{raw}, BB_{raw} and CS_{raw} respectively. In the same way, the char samples from pine, bamboo and corn stover are denoted as PN_{char}, BB_{char}, and CS_{char} respectively.

6.3.1. Higher Heating Value, proximate and elemental analyses

The proximate, elemental and higher heating value (HHV) results for coal and untreated/treated biomass samples are shown in Table 6-2. It can be seen that the coal had the highest ash content (25.96 wt%). As expected, compared to raw biomass samples, the volatile matter (VM) of coal was very low (22.89 wt%) while its fixed carbon (FC) content was high (51.64 wt%). It is also seen from Table 6-2 that the raw biomass samples were characterized by much higher oxygen (O) content and lower carbon (C) content than coal. The composition of raw biomass samples in terms of VM (75.30–81.85 wt%), FC (16.01–21.45 wt%) and oxygen content (47.83–50.93 wt%) were consistent with usual reported values [38]. The high oxygen and low FC contents are the reasons for the relatively low HHV of raw biomass as shown in Table 6-2. Following thermal pretreatment, the biomass chars experienced significant reduction in VM and increase in FC contents. The FC contents of PN_{char}, BB_{char} and CS_{char} were more than 3 times higher than they were in the respective raw samples (ie. PN_{raw}, BB_{raw} and CS_{raw}). The sulphur (S) and the nitrogen (N) contents of the chars remained significantly lower than for the coal sample. Due to deoxygenation during thermal pretreatment, the carbon (C) content of chars were increased by as high as 71.59 % compared to the raw biomass samples, while the O content highest percentage decrease was 57.41%. Following the reduction in oxygen and the increase in FC and C contents as a result of thermal pretreatment, the HHV of biomass chars were higher in comparison to raw biomass and coal samples. The HHV of CS_{char} was much less than that of the other chars due to its high ash content (Table 6-2).

6.3.2. Devolatilization characteristics

6.3.2.1. Devolatilization characteristics of single fuels

The TGA and dTG devolatilization curves of coal and raw biomass single fuels obtained at 10 ^{o}C/min are shown in Figure 6-1. For the raw biomass fuels the start of thermal decomposition occurred at around 200 ^{o}C with the major weight loss taking place in the temperature range of 200-390 ^{o}C (Figure 6-1a-c) after which the weight loss became gradual and almost complete at 500 ^{o}C. For the major weight loss region of raw biomass (200-390 ^{o}C), the dTG curves of PN_{raw} and CS_{raw} were characterized by the presence of a shoulder (Figures 6-1a and c), at a temperature around 285 ^{o}C. This was due to the decomposition of hemicellulose while the second and highest peak occurring at a higher temperature (around 365 ^{o}C and 330 ^{o}C for PN_{raw} and CS_{raw} respectively) can

be attributed to cellulose decomposition. For BB_{raw} (Figure 6-1b) only the cellulose peak can be seen while the hemicellulose peak was hard to detect. The tailing end of the dTG curves of the raw biomass samples can be attributed to the slow decomposition of the char residue generated from the three components, with the main contribution from lignin. For coal single fuel the dTG curve (Figure 6-1d) shows that the major devolatilization occurred in the temperature range of 400-510 ^{o}C with the maximum rate occurring at around 455 ^{o}C. Considering the dTG curves (Figure 6-1a-d) the maximum devolatilization rates of raw biomass fuels were in the range 8.13-10.31 %/min (Figure 6-1a-c) which were one order of magnitude higher than that of coal (0.73 %/min, Figure 6-1d). This points to the structural differences between coal and raw biomass. While the maximum peaks for raw biomass resulted from the thermal decomposition of reactive oxygenated groups (especially from cellulose), that of coal with low oxygen content was much more stable. From Table 6-2 the VM of coal is seen to be very small compared to raw biomass hence the low devolatilization rate and high char yield of coal.

Considering the single biomass char fuels it can be seen that the decomposition occurred in a similar region as that for coal, starting at around 360 ^{o}C with the maximum devolatilization peak occurring at around 445 ^{o}C (Figure 6-2). As reported previously [39] the thermal pretreatment of raw biomass at >300 ^{o}C results in the significant removal of volatile matter, producing a much more stable char. Hence the peaks obtained for the biomass char fuels can be attributed mainly to the release of volatiles due to some rearrangement reaction during char formation process. The maximum devolatilization rates depicted in the dTG curves (Figure 6-2a-c) were in the range 1.01-1.44 %/min, which was closer to the value observed for coal. From Figure 6-1d the TGA curve shows that the solid residue yield from coal at the end of devolatilization was much higher than those of the raw biomass single fuels (Figure 6-1a-c) due to the high decomposition rates of the raw biomass. Similarly for the same reason the solid residue yield for the single char fuels (Figure 6-2) were also higher than that of the raw biomass samples.

6.3.2.2. Devolatilization characteristics of blends

In Figure 6-3 the dTG curves of raw biomass-coal and biomass char-coal blended fuels at different blending ratios are shown (100 wt% and 0 wt% refer to pure biomass or char fuel and pure coal fuel respectively). The TGA curves for the various blends are given in Figure C-1 (Appendix C).

Considering the dTG curves for raw biomass-coal blends (Figure 6-3a-c) it can be seen that for blend ratios of 10 wt%, 20 wt% and 50 wt% the distinct peaks related to biomass and coal fractions (as seen in Figure 6-1) were observable and the peak temperature position were also maintained. Blending however had an impact on the devolatilization rate and peak height. As observed in Figure 6-3a-c an increase in the biomass blend ratio resulted in an increase in the maximum devolatilization peak corresponding to biomass while reducing the maximum devolatilization peak corresponding to coal.

For the char-coal blends (Figure 6-3d-f) the profiles of all the blends fitted the shape of the coal curve especially for the 10 wt% and 20 wt% blends. A slight decrease in the peak position on the temperature axis can be observed as the fraction of char in the blend was increased. As seen in Figure 6-2 the peak temperature for char devolatilization was at 445 ^{o}C while in Figure 6-1d the peak for coal occurred at a temperature of 455 ^{o}C. Thus the peaks exhibited for the char-coal blends were as a result of the overlap of char and coal decomposition explaining why the peak temperature shifted towards the lower temperature range as the char fraction in the blend increased. In Figure 6-3d-f it can also be seen that the maximum devolatilization rate of char-coal blends increased with increase in the char fraction in the blend.

To check for possible interactions or synergies between raw biomass and coal or char and coal during the devolatilization of the blends, the experimental and calculated dTG and TGA curves of the various blends were plotted. Figure 6-4 shows the dTG plots while the TGA plots are shown in Figure C-2 (Appendix C). The predicted results were calculated as a function of the percentage weight contributions of each single fuel in the blend. In the absence of any interactions the devolatilization characteristics of the blends are expected to follow that of the individual fuels in the blend in an additive behaviour. In Figure 6-4, comparison of the experimental and the calculated dTG curves of the various blends are shown. It can be seen from Figure 6-4 that the experimental curves almost overlapped the calculated curves. This indicates that interactions or synergies were very minimal or non-existent for both the raw biomass-coal blend and char-coal blends.

6.3.3. Kinetic analysis

As stated earlier the differential isoconversional method of Friedman was used in this study to estimate kinetic parameters during the CO_2 gasification of raw/treated biomass, coal and their blends. Figures 6-5, 6-6 and 6-7 present the calculated apparent activation energy (E) of the fuels as a function of the conversion (α). The values of $ln[A.f(\alpha)]$ are given in Table C-1 (Appendix C). Due to the poor R^2 obtained at conversions below 0.1 and above 0.9, only the conversion range of 0.1-0.9 ($R^2 \geq 0.97$) was considered.

The apparent E results for raw biomass and coal individual fuels over the 0.1-0.9 conversion range are given in Figure 6-5. As seen in Figure 6-5a the apparent E of PN_{raw} increased from 203 kJ/mol (α=0.1) to a maximum of 259 kJ/mol at α of 0.3, after which there was a decline in E at higher conversion values reaching a minimum of 183 kJ/mol at α=0.9. Over the conversion range the average apparent E of PN_{raw} was 226 kJ/mol (Table C-1, Appendix C). For BB_{raw} (Figure 6-5b) E ranged from 161-224 kJ/mol with an average of 183 kJ/mol and was characterized by a progressive reduction in E as α increased. When considering CS_{raw} (Figure 6-5c) a different trend was observed. The apparent E decreased from 276 to 202 kJ/mol at α=0.6 before increasing to 255 kJ/mol at α=0.9. The average E of CS (239 kJ/mol) was the highest among the raw biomass samples despite its content of inorganics, which are likely to promote the conversion through catalytic effect. For coal (Figure 6-5d) the apparent E reached a minimum at α=0.2 (185 kJ/mol) and then increased gradually over the conversion range with an average of 216 kJ/mol.

The trends of apparent E for the char single fuels as depicted in Figure 6-6 were much different from what was observed for their parent raw biomass samples particularly for PN (Figure 6-6a). PN_{char}, after biomass pretreatment, had an increased reactivity during the early stages of CO_2 gasification as such a sharp decline in apparent E was observed over the 0.1-0.4 conversion range contrary to what was observed for PN_{raw}. For BB_{char} (Figure 6-6b) the apparent E range shifted to 153-216 kJ/mol with an average value of 175 kJ/mol, thus also showing improved reactivity. Such effect was also observed for CS_{char} (Figure 6-6c). This might be as a result of the formation of a more reactive pore structure during biomass thermal pretreatment. Such a phenomenon was reported in the study of Chen et al. [40]. It was found that torrefaction pretreatment of biomass led to the creation of pores with larger diameter inside the biomass.

The apparent E results of the coal and raw/treated biomass blends are detailed in Figure 6-7 and in Table C-1 (Appendix C). It can be seen from Figure 6-7 that for all blend ratios the addition of biomass/char did not change significantly the reactivity of the fuel especially for the blend ratio of 10 and 20 wt%, hence giving apparent E values within the same range. While for raw biomass and coal blends, no drastic change in E was observed even for a blend ratio of 50 wt%, more discrepancies were observed with the char samples. It can be seen that for char and coal blends at 50 wt%, the addition of char caused an increase in apparent E at lower conversion ($\alpha \leq 0.4$) especially for CS_{char}, while the opposite trend was observed at higher conversion values for BB_{char} and CS_{char} (Figures 6-7e and f). Based on the apparent E results of char and coal blends and raw biomass and coal blends it can be seen that in comparison with char, the addition of raw biomass could be considered in higher blending ratio, without significant effect on the fuel reactivity. However, due to the high volatile matter of biomass and the associated risk of tar condensation, an addition of raw biomass is not recommended. Regarding the addition of char, with improved fuel qualities due to thermal pretreatment (Table 6-2), a blending ratio of 20 wt% char will be suitable for coal substitution for co-gasification.

6.4. Conclusion

In this work, the devolatilization characteristics and CO_2 gasification kinetics of biomass chars (pretreatment at 350 °C) and their blends with coal were studied. In addition, the behaviour of raw biomass and coal blends was also studied for comparison. The devolatilization and gasification behaviours of each individual fuel were compared to their respective blends with coal at various blend ratios. The blending of the biomass-based fuels with coal gave no particular synergy during devolatilization. Following pretreatment, the devolatilization characteristics of the chars were found to be comparable to coal characteristics, with lower production of volatiles that are released at higher temperature. CO_2 gasification characteristics established through isoconversional analysis showed that char blends up to 20 wt% gave comparable reactivity as opposed to using coal alone. Hence, char blending at 20 wt% can be considered for gasification purposes.

References

[1] A. Franco, A.R. Diaz, The future challenges for “clean coal technologies”: Joining efficiency increase and pollutant emission control, Energy. 34 (2009) 348–354.

[2] K.M. Lu, W.J. Lee, W.H. Chen, T.C. Lin, Thermogravimetric analysis and kinetics of co-pyrolysis of raw/torrefied wood and coal blends, Appl. Energy. 105 (2013) 57–65.

[3] M.J.C. van der Stelt, H. Gerhauser, J.H.A. Kiel, K.J. Ptasinski, Biomass upgrading by torrefaction for the production of biofuels: A review, Biomass and Bioenergy. 35 (2011) 3748–3762.

[4] M. Sami, K. Annamalai, M. Wooldridge, Co-firing of coal and biomass fuel blends, Prog. Energy Combust. Sci. 27 (2001) 171–214.

[5] D. Medic, M. Darr, A. Shah, B. Potter, J. Zimmerman, Effects of torrefaction process parameters on biomass feedstock upgrading, Fuel. 91 (2012) 147–154.

[6] E. Kastanaki, D. Vamvuka, A comparative reactivity and kinetic study on the combustion of coal-biomass char blends, Fuel. 85 (2006) 1186–1193.

[7] J. Dai, S. Sokhansanj, J.R. Grace, X. Bi, C.J. Lim, S. Melin, Overview and some issues related to co-firing biomass and coal, Can. J. Chem. Eng. 86 (2008) 367–386.

[8] T.Y. Mun, T.Z. Tumsa, U. Lee, W. Yang, Performance evaluation of co-firing various kinds of biomass with low rank coals in a 500 MWe coal-fired power plant, Energy. 115 (2016) 954–962.

[9] M.V. V Gil, D. Casal, C. Pevida, J.J.J. Pis, F. Rubiera, Thermal behaviour and kinetics of coal/biomass blends during co-combustion, Bioresour. Technol. 101 (2010) 5601–5608.

[10] Y.G. Pan, E. Velo, X. Roca, J.J. Manyà, L. Puigjaner, Fluidized-bed co-gasification of residual biomass/poor coal blends for fuel gas production, Fuel. 79 (2000) 1317–1326.

[11] M.W. Seo, J.H. Goo, S.D. Kim, S.H. Lee, Y.C. Choi, Gasification characteristics of coal/biomass blend in a dual circulating fluidized bed reactor, Energy and Fuels. 24 (2010) 3108–3118.

[12] J.J. Hernández, G. Aranda-Almansa, C. Serrano, Co-gasification of biomass wastes and coal-coke blends in an entrained flow gasifier: An experimental study, Energy and Fuels, 24

(2010) 2479–2488.

[13] J. Rizkiana, G. Guan, W.B. Widayatno, X. Hao, W. Huang, A. Tsutsumi, A. Abudula, Effect of biomass type on the performance of cogasification of low rank coal with biomass at relatively low temperatures, Fuel. 134 (2014) 414–419.

[14] L. Duan, Y. Duan, C. Zhao, E.J. Anthony, NO emission during co-firing coal and biomass in an oxy-fuel circulating fluidized bed combustor, Fuel. 150 (2015) 8–13.

[15] H.. Vuthaluru, Thermal behaviour of coal/biomass blends during co-pyrolysis, Fuel Process. Technol. 85 (2004) 141–155.

[16] B. Moghtaderi, C. Meesri, T.F. Wall, Pyrolytic characteristics of blended coal and woody biomass, Fuel. 83 (2004) 745–750.

[17] E. Biagini, F. Lippi, L. Petarca, L. Tognotti, Devolatilization rate of biomasses and coal-biomass blends : an experimental investigation, Fuel. 81 (2002) 1041–1050.

[18] E. Kastanaki, D. Vamvuka, P. Grammelis, E. Kakaras, Thermogravimetric studies of the behavior of lignite-biomass blends during devolatilization, Fuel Process. Technol. 77–78 (2002) 159–166.

[19] Y.G. Pan, E. Velo, L. Puigjaner, Pyrolysis of blends of biomass with poor coals, Fuel. 75 (1996) 412–418.

[20] A.O. Aboyade, M. Carrier, E.L. Meyer, H. Knoetze, J.F. Görgens, Slow and pressurized co-pyrolysis of coal and agricultural residues, Energy Convers. Manag. 65 (2013) 198–207.

[21] T.R. McLendon, A.P. Lui, R.L. Pineault, S.K. Beer, S.W. Richardson, High-pressure co-gasification of coal and biomass in a fluidized bed, Biomass and Bioenergy. 26 (2004) 377–388.

[22] Q. Lu, X.C. Yang, C.Q. Dong, Z.F. Zhang, X.M. Zhang, X.F. Zhu, Influence of pyrolysis temperature and time on the cellulose fast pyrolysis products: Analytical Py-GC/MS study, J. Anal. Appl. Pyrolysis. 92 (2011) 430–438.

[23] M. Phanphanich, S. Mani, Impact of torrefaction on the grindability and fuel characteristics of forest biomass, Bioresour. Technol. 102 (2011) 1246–1253.

[24] B. Arias, C. Pevida, J. Fermoso, M.G. Plaza, F. Rubiera, J.J. Pis, Influence of torrefaction on the grindability and reactivity of woody biomass, Fuel Process. Technol. 89 (2008) 169–175.

[25] M. Broström, A. Nordin, L. Pommer, C. Branca, C. Di Blasi, Influence of torrefaction on the devolatilization and oxidation kinetics of wood, J. Anal. Appl. Pyrolysis. 96 (2012) 100–109.

[26] A.V. Bridgwater, Renewable fuels and chemicals by thermal processing of biomass, Chem. Eng. J. 91 (2003) 87–102.

[27] M.J. Prins, K.J. Ptasinski, F.J.J.G. Janssen, Torrefaction of wood. Part 2. Analysis of products, J. Anal. Appl. Pyrolysis. 77 (2006) 35–40.

[28] P. Rousset, C. Aguiar, N. Labbé, J.-M. Commandré, Enhancing the combustible properties of bamboo by torrefaction., Bioresour. Technol. 102 (2011) 8225–31.

[29] J.H. Peng, H.T. Bi, C.J. Lim, S. Sokhansanj, Study on density, hardness, and moisture uptake of torrefied wood pellets, Energy and Fuels. 27 (2013) 967–974.

[30] W. Yan, T.C. Acharjee, C.J. Coronella, V.R. Vásquez, Thermal pretreatment of lignocellulosic biomass, Environ. Prog. Sustain. Energy. 28 (2009) 435–440.

[31] A. Ohliger, M. Förster, R. Kneer, Torrefaction of beechwood: A parametric study including heat of reaction and grindability, Fuel. 104 (2013) 607–613.

[32] F.F. Felfli, C.A. Luengo, J.A. Suárez, P.A. Beatón, Wood briquette torrefaction, Energy Sustain. Dev. 9 (2005) 19–22.

[33] H. Li, X. Liu, R. Legros, X.T. Bi, C.J. Lim, S. Sokhansanj, Torrefaction of sawdust in a fluidized bed reactor, Bioresour. Technol. 103 (2012) 453–458.

[34] P. Basu, Biomass Gasification, Pyrolysis and Torrefaction: Practical Design and Theory,

2013.

[35] S.S. Idris, N.A. Rahman, K. Ismail, A.B. Alias, Z.A. Rashid, M.J. Aris, Investigation on thermochemical behaviour of low rank Malaysian coal, oil palm biomass and their blends during pyrolysis via thermogravimetric analysis (TGA), Bioresour. Technol. 101 (2010) 4584–4592.

[36] S. Vyazovkin, Computational aspects of kinetic analysis . Part C . The ICTAC Kinetics Project - The light at the end of the tunnel ?, Thermochimica Acta. 355 (2000) 155–163.

[37] T. Damartzis, D. Vamvuka, S. Sfakiotakis, A. Zabaniotou, Thermal degradation studies and kinetic modeling of cardoon (Cynara cardunculus) pyrolysis using thermogravimetric analysis (TGA), Bioresour. Technol. 102 (2011) 6230–6238.

[38] D. Neves, H. Thunman, A. Matos, L. Tarelho, A. Gómez-Barea, Characterization and prediction of biomass pyrolysis products, Prog. Energy Combust. Sci. 37 (2011) 611–630.

[39] W.H. Chen, P.C. Kuo, Torrefaction and co-torrefaction characterization of hemicellulose, cellulose and lignin as well as torrefaction of some basic constituents in biomass, Energy. 36 (2011) 803–811.

[40] Q. Chen, J.S. Zhou, B.J. Liu, Q.F. Mei, Z.Y. Luo, Influence of torrefaction pretreatment on biomass gasification technology, Chinese Sci. Bull. 56 (2011) 1449–1456.

Tables

Table 6-1: Lignocellulosic composition (wt% daf: dry ash-free basis) of raw biomass feedstocks

Component	Feedstock		
	Pine (PN)	Bamboo (BB)	Corn Stover (CS)
Lignin	29.87	25.48	16.53
Cellulose	40.94	39.39	36.70
Hemicelluloses	11.82	16.34	21.28
Extractives	5.19	12.96	17.53
Acetyl	1.89	3.32	3.06

Table 6-2: HHV, Proximate and Elemental analysis of coal and raw/treated biomasses

Feedstock	HHV (MJ/kg)	Proximate analysis (wt%), db[a]			Elemental analysis (wt%), daf[b]				
		VM	FC	Ash	C	H	N	S	O[c]
Coal	21.89	22.39	51.64	25.96	75.92	4.02	1.95	2.25	15.86
PN									
PN_{raw}	18.07	81.85	16.01	2.14	45.60	6.47	0.02	0.08	47.83
PN_{char}	26.25	35.84	60.95	3.21	73.94	4.53	0.22	0.00	21.30
BB									
BB_{raw}	17.60	76.11	21.45	2.44	44.41	6.32	0.44	0.14	48.69
BB_{char}	25.67	29.70	65.49	4.81	71.65	4.56	0.82	0.12	22.84
CS									
CS_{raw}	15.83	75.30	16.85	7.85	41.88	6.40	0.59	0.20	50.93
CS_{char}	21.66	31.25	51.67	17.08	71.86	4.87	1.33	0.24	21.69

[a] Dry basis
[b] Dry ash-free basis
[c] Determined by difference

Figures

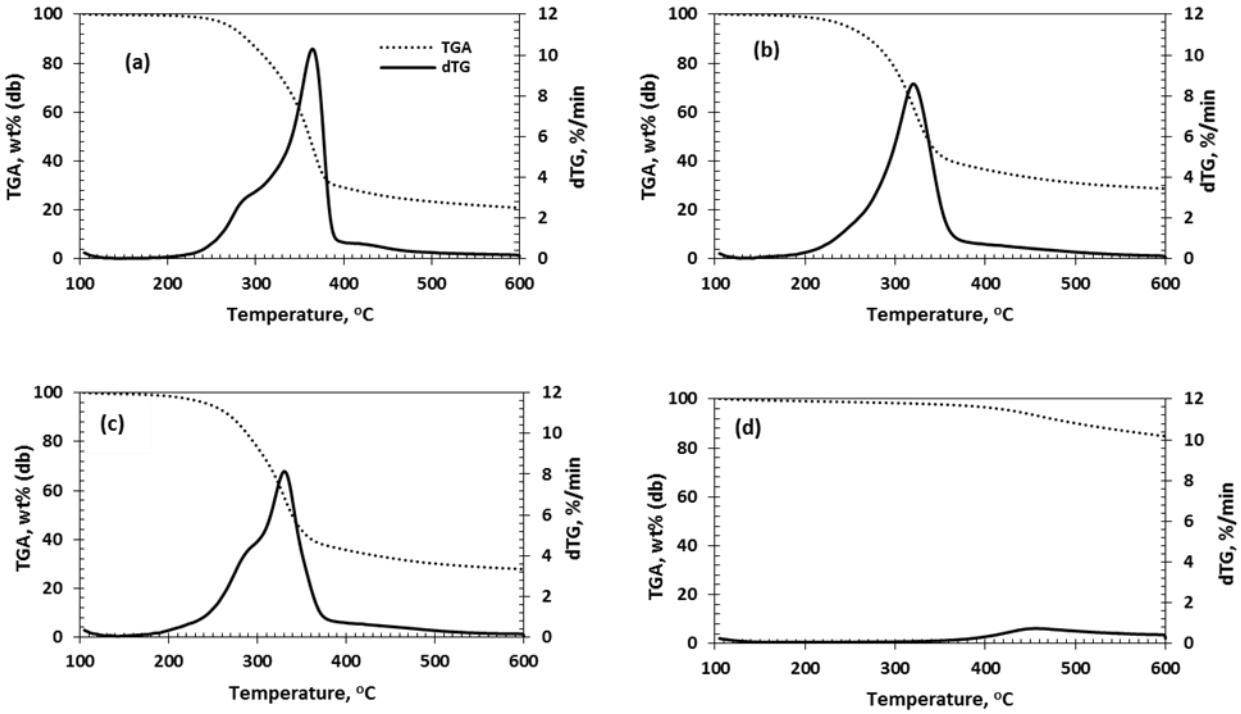

Figure 6-1: Devolatilization characteristics of raw biomass and coal (a) PNraw, (b) BBraw, (c) CSraw and (d)coal

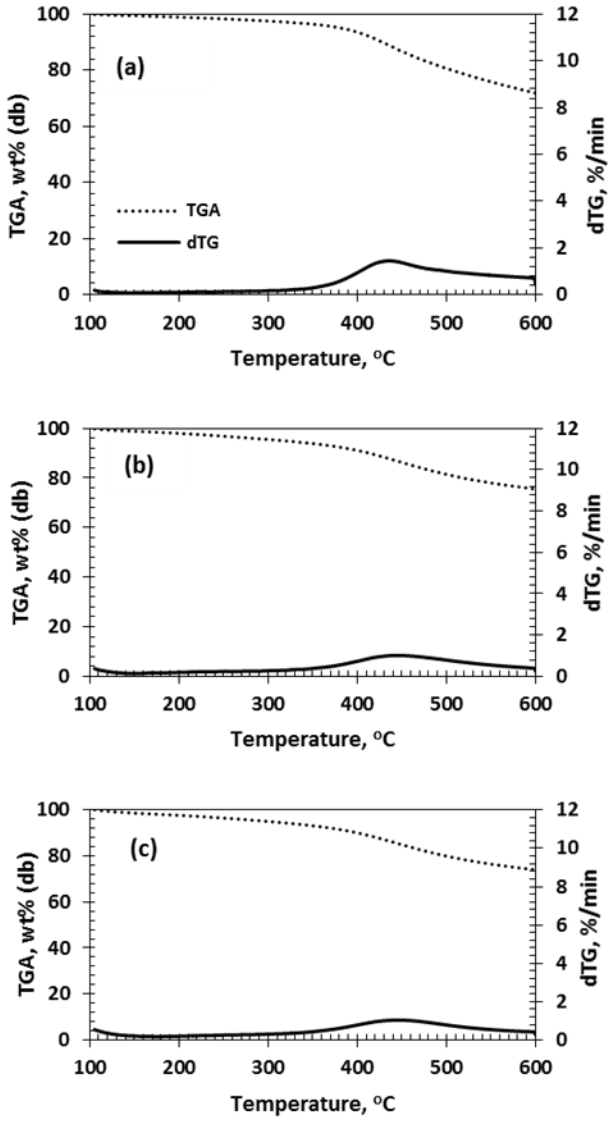

Figure 6-2: Devolatilization characteristics of biomass char (a) PNchar, (b) BBchar, (c) CSchar

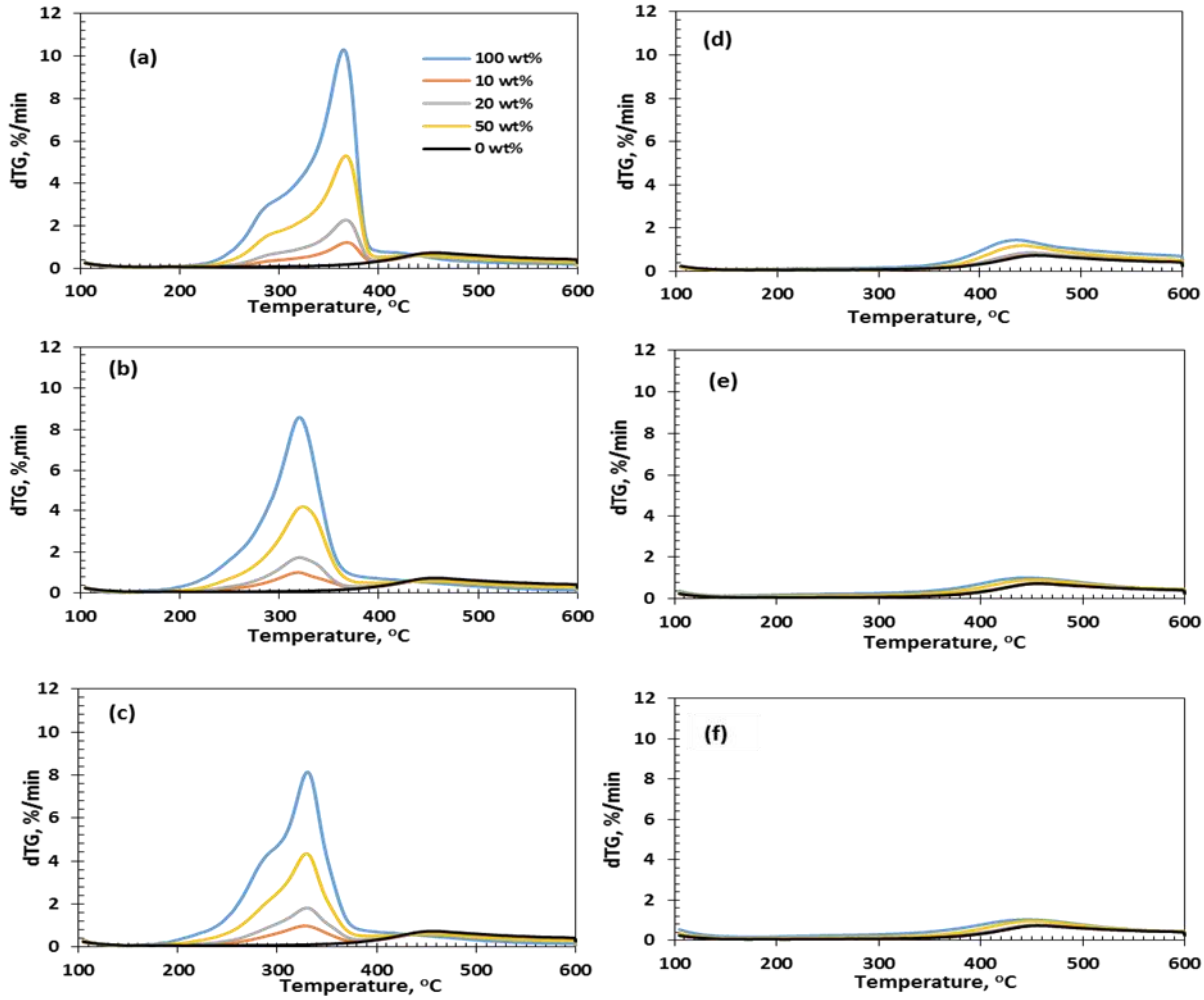

Figure 6-3: Devolatilization characteristics of raw biomass/char and coal blends (a) PNraw (b) BBraw, (c) CSraw (d) PNchar, (e) BBchar, (e) CSchar

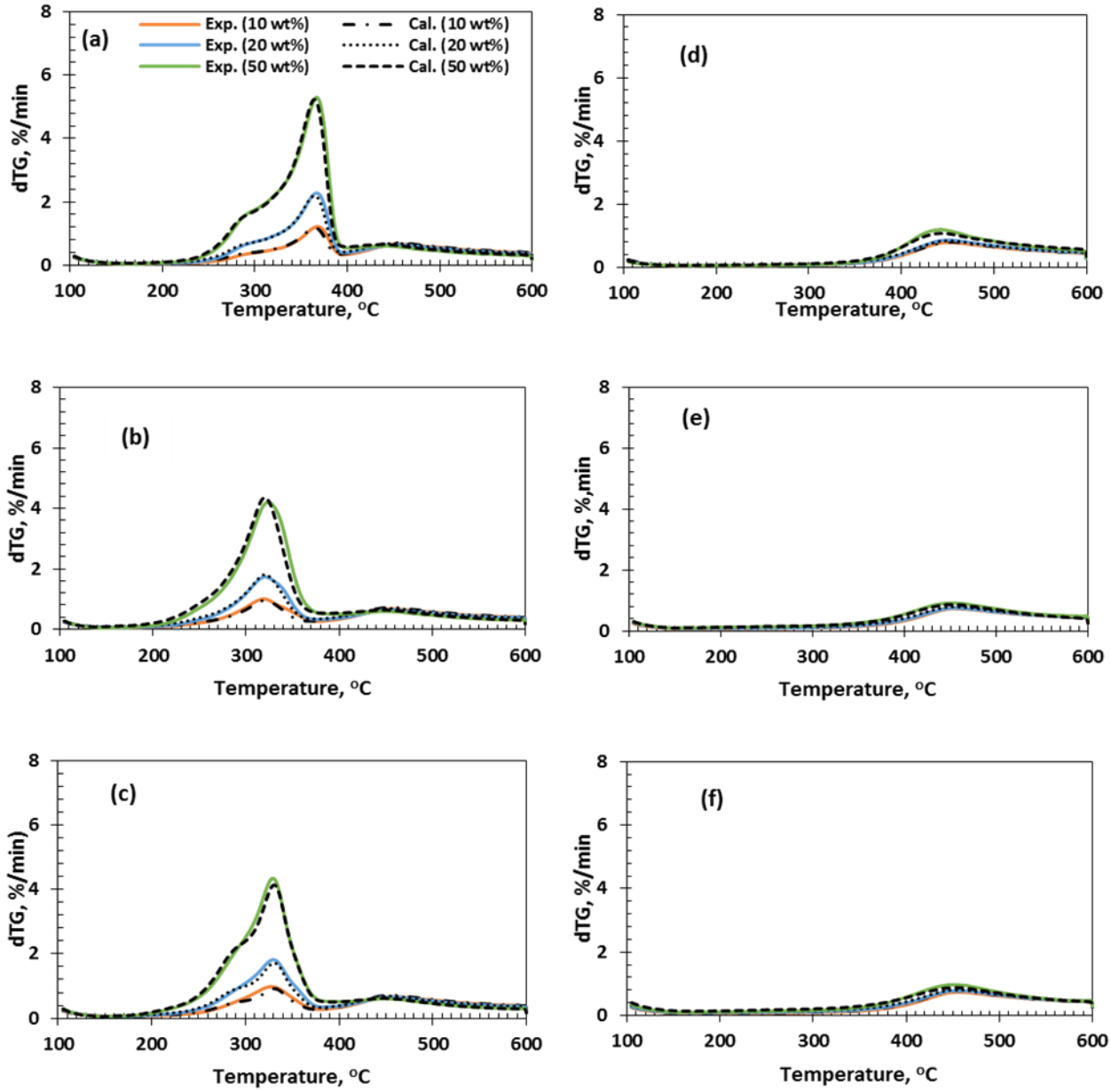

Figure 6-4: Comparison of experimental and calculated dTG curves of raw biomass/char and coal blends (a) PNraw (b) BBraw, (c) CSraw (d) PNchar, (e) BBchar, (e) CSchar

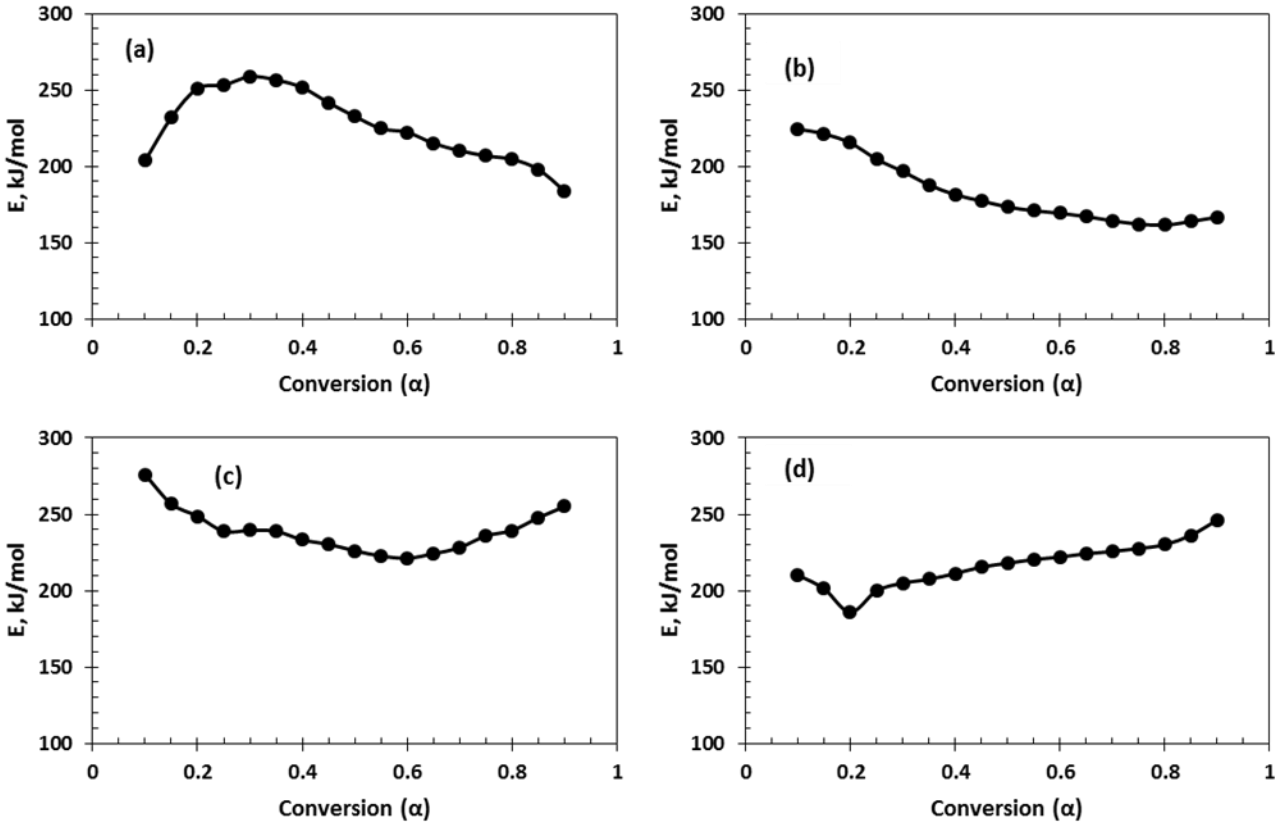

Figure 6-5: Isoconversional CO2 gasification parameters of raw biomass and coal (a) PNraw, (b) BBraw, (c) CSraw and (d)coal

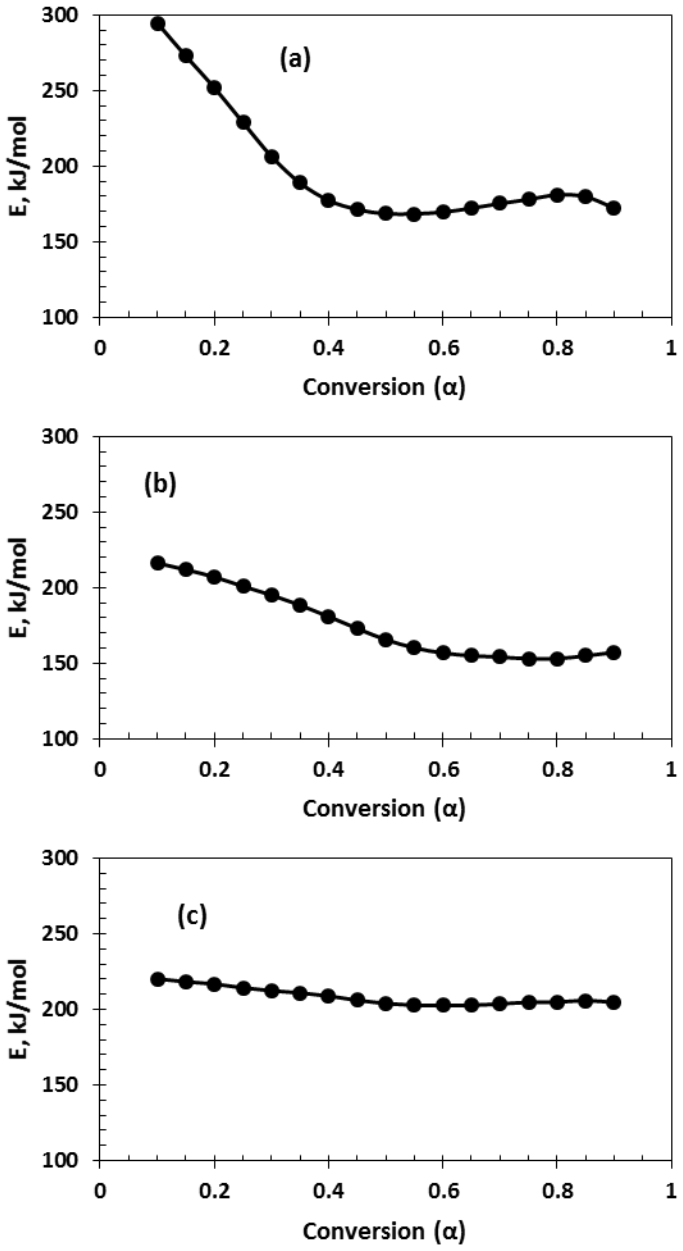

Figure 6-6: Isoconversional CO2 gasification parameters biomass char (a) PNchar, (b) BBchar, (c) CSchar

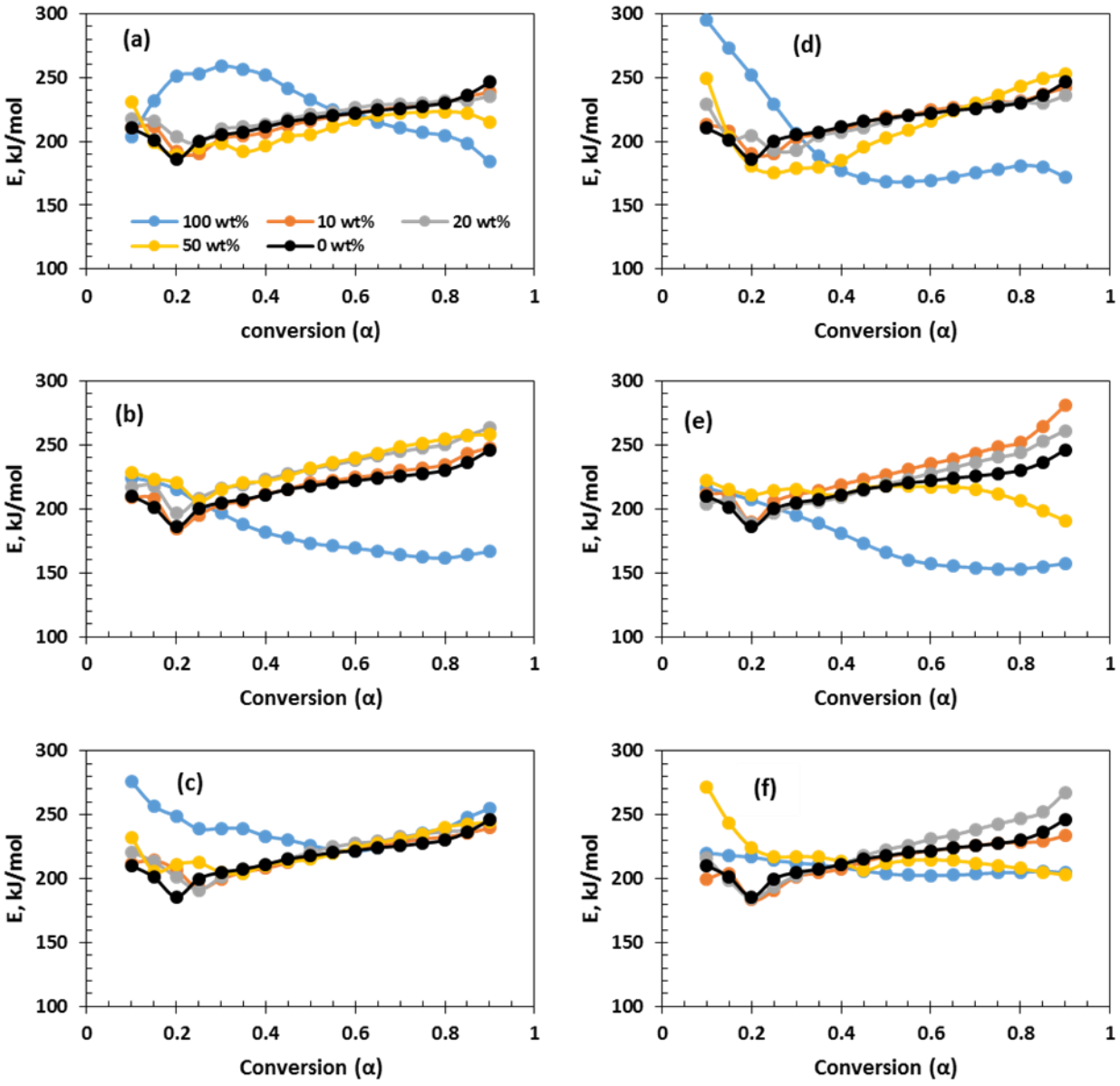

Figure 6-7: Isoconversional CO2 gasification parameters raw biomass/char and coal blends (a) PNraw (b) BBraw, (c) CSraw (d) PNchar, (e) BBchar, (e) CSchar

Chapter 7

Conclusions and recommendations

7.1. Conclusions

Lignocellulosic biomass offers opportunity for coal substitution in applications such as gasification. However, due to the nature of biomass, it is associated with poor fuel properties in comparison to coal and generates increased amount of oxygenated volatiles (tar precursors) during its co-gasification with coal, thereby negatively effecting the quality of gasification products. This challenge has limited the development of biomass-based gasification processes. Therefore lignocellulosic biomass has to be upgraded in order to efficiently utilize it with coal.

For this study, thermal pretreatment methods of torrefaction and slow pyrolysis were used as a means to upgrade biomass, thus producing an upgraded solid fuel (char) with reduced oxygen content and improved fuel properties more comparable to coal for use in co-gasification. However, though the thermal pretreatment was found to reduce the volatile matter content of biomass, there was a need to confirm that the composition of the volatiles released during the devolatilization stage of gasification was acceptable. To this aim, there was a need to develop an analytical technique to identify and quantify the organic volatiles released during devolatilization, the main challenge being for the char samples with relatively low volatile matter content. An analytical method incorporating the use of Thermogravimetric Analysis, thermal desorption and Gas Chromatography–Mass Spectrometry (herein referred as (TGA-TD/GC-MS)) was developed. Following some reproducibility tests, the composition of the oxygenated volatile compounds released from the devolatilization of the raw biomass feedstocks of this study (pine (PN), bamboo (BB), corn cob (CC) and corn stover (CS)) was studied and compared with literature. Through principal components analysis (PCA) of the results, it was established that the yields of the volatile compounds were correlated with the lignocellulosic chemical compositions. As the results were consistent with literature, the TGA-TD/GC-MS analytical method was validated and used for further work.

Following this, biomass thermal pretreatment was done at varying conditions of temperature (250-400 ºC) and hold time (30 and 60 min at the pretreatment temperature) at the milligram scale to study the influence of pretreatment conditions on char devolatilization volatile products distribution and the chemical changes occurring in the biomass during the pretreatment. Biomass pretreatment at different conditions of temperature and hold time revealed that the effect of temperature towards the transformation and volatile evolution mechanism of char was critical. The distribution of char devolatilization products was shown to be consistent with the extent of biomass transformation during thermal pretreatment. The biomass composition, particularly cellulose crystallinity, was also found to have an impact on the required temperature to achieve significant degradation. For biomass feedstock with high degree of crystallinity such as PN a pretreatment temperature greater than 300 ºC was required. Due to this stability, the pretreatment of such biomass at lower temperature (≤300 ºC) was not sufficient and led to the production of volatile products with high levels of furans and anhydrosugar during subsequent char devolatilization. For the other feedstocks of this study, a pretreatment temperature of 300 °C was sufficient to degrade the cellulose structure. From this result, it appears that when considering the use of a new lignocellulosic feedstock (for instance hardwoods not considered in this work), a similar type of study is recommended to determine the temperature required to ensure cellulose degradation.

In order to identify the preferred pretreatment conditions for char production for use in co-gasification, a comparison between coal and the char pretreated at different temperatures was made. The comparison was based on some relevant fuel properties (proximate and elemental composition and Higher Heating Value) and the composition of the oxygenated volatiles released during the devolatilization stage. . This study showed that a temperature of ≥350 ºC is required for biomass pretreatment when considering the production of biomass char for coal substitution in gasification applications. Chars produced at such temperature had superior fuel properties and generated volatiles consisting of aromatic hydrocarbons and phenolics that were comparable to volatiles from coal under similar conditions. For feedstocks with high lignin and/or high inorganic content a temperature of 400 °C could be considered.

Subsequently the pretreatment temperature of 350 °C was used to produce chars at the gram scale. These chars were then used together with coal at different biomass char blend ratios to study in a TGA the impact of the char addition on coal devolatilization and CO_2 gasification characteristics.

Regarding the devolatilization characteristics, though the coal and the chars released most of the volatiles on a similar temperature range, no synergy was detected. From CO_2 gasification kinetics results it was found that the devolatilization characteristics of the char blended with coal were similar to those of coal for 10 and 20 wt% char blend ratios.

7.2. Recommendations

This work confirmed the potential of using thermally pretreated biomass chars for coal substitution in gasification process. In order to confirm the influence of the pretreatment on reduced tar condensation, tests at pilot scale should be implemented. The composition of the compounds released during the devolatilization should be similar to what was observed in TGA, but differences in quantities can be expected, as usually observed when scaling-up. Also while the use of TGA is useful especially for kinetic studies of solid product decomposition, the condition in the TGA are far from ideal industrial conditions of the gasifier. It is recommended that a further study be taken on char/coal gasification in a real gasifier.

In this work, the different stages of gasification (devolatilization and action of the oxidizing agent) were studied separately. For practical reason, the gasification stage was simulated with CO_2, though different oxidizing agents are more often used (O_2 or steam). In the gasification reactor, the compounds generated during devolatilization are likely to further react with the oxidizing agent (volatiles gasification). Such conversion is likely to lead to even lower yield of tar precursors. Tests at pilot scale should confirm that it is possible to partially substitute coal with biomass chars without any particular operational issue.

Finally, it is recommended that a techno-economic study regarding large scale implementation be conducted in order to estimate the full effect of the biomass pretreatment on the gasification process both in terms of energy efficiency and economic viability. In addition the impact on the overall mass and carbon balances when integrating biomass thermal pretreatment technology into a gasification process must also be considered. From this study, it was clear that increasing the pretreatment temperature led to the production of a char with improved quality. While char quality is of paramount importance, a trade-off must be made between quality and the overall mass yield. Higher pretreatment temperature will mean higher energy consumption and a reduced mass yield of the solid pretreated material for use in the subsequent gasification process which will negatively

affect the overall mass balance and in turn the carbon balance of the integrated process. Therefore the preferred pretreatment temperature should be determined depending on the char blending ratio and the properties of the considered lignocellulosic feedstock. The use of the other pyrolysis products (bio-oil and gas) can be considered to provide the heat required in order to make the pretreatment process energy self-sufficient and also improve the overall carbon and mass balances of an integrated pretreatment and gasification process.

Appendix A

Table A-1: Correlations matrix – Active and Supplementary Variables

Variable	Char	H lignin	G lignin	5-HMF	Furfural	2-Methylfuran	2(5H)-Furanone	Phenol, 2,6-dimethoxy-	Levoglucosan
Char	1.00	0.89	-0.58	-0.75	-0.82	-0.08	-0.35	0.13	-0.70
H lignin	0.89	1.00	-0.43	-0.80	-0.94	0.13	-0.61	0.24	-0.77
G lignin	-0.58	-0.43	1.00	0.84	0.58	0.78	0.54	0.72	0.85
Phenol, 2,6-dimethoxy-	0.13	0.24	0.72	0.39	-0.03	0.87	0.33	1.00	0.43
Levoglucosan	-0.70	-0.77	0.85	0.99	0.87	0.44	0.83	0.43	1.00
5-HMF	-0.75	-0.80	0.84	1.00	0.89	0.42	0.80	0.39	0.99
Furfural	-0.82	-0.94	0.58	0.89	1.00	0.07	0.73	-0.03	0.87
2-Methylfuran	-0.08	0.13	0.78	0.42	0.07	1.00	0.21	0.87	0.44
2(5H)-Furanone	-0.35	-0.61	0.54	0.80	0.73	0.21	1.00	0.33	0.83
Methyl acetate	0.91	0.97	-0.31	-0.66	-0.86	0.26	-0.42	0.41	-0.61
Formic acid	-0.98	-0.86	0.70	0.83	0.83	0.22	0.43	0.04	0.78
Acetic acid	0.95	0.90	-0.56	-0.80	-0.82	-0.02	-0.47	0.07	-0.75
Acetol	0.95	0.79	-0.37	-0.54	-0.64	0.12	-0.12	0.31	-0.47
Propanoic acid	0.46	0.45	-0.89	-0.87	-0.57	-0.68	-0.69	-0.73	-0.89
[1]Lignin	-0.27	-0.16	0.91	0.71	0.35	0.88	0.53	0.91	0.73
[1]Extractives	0.77	0.54	-0.93	-0.82	-0.61	-0.65	-0.39	-0.51	-0.79
[1]VM	-0.92	-0.80	0.83	0.90	0.82	0.40	0.51	0.25	0.87
[1]FC	0.59	0.89	-0.19	-0.65	-0.87	0.31	-0.71	0.32	-0.66
[1]AC	0.79	0.47	-0.80	-0.65	-0.48	-0.55	-0.15	-0.37	-0.60
[1]C_5	0.24	0.32	-0.83	-0.80	-0.51	-0.72	-0.76	-0.80	-0.84
[1]C_6	-0.33	-0.40	0.86	0.85	0.58	0.70	0.79	0.76	0.88
[1]Acetyl	0.31	0.53	-0.69	-0.85	-0.69	-0.45	-0.90	-0.55	-0.89

[1] Supplementary variables

Table A-1 continued

Variable	Acetol	Methyl acetate	Formic acid	Acetic acid	Propanoic acid	[1]Lignin	[1]Extractives	[1]VM	[1]FC	[1]AC	[1]C_5	[1]C_6	[1]Acetyl
Char	0.95	0.91	-0.98	0.95	0.46	-0.27	0.77	-0.92	0.59	0.79	0.24	-0.33	0.31
H lignin	0.79	0.97	-0.86	0.90	0.45	-0.16	0.54	-0.80	0.89	0.47	0.32	-0.40	0.53
G lignin	-0.37	-0.31	0.70	-0.56	-0.89	0.91	-0.93	0.83	-0.19	-0.80	-0.83	0.86	-0.69
Phenol, 2,6-dimethoxy-	0.31	0.41	0.04	0.07	-0.73	0.91	-0.51	0.25	0.32	-0.37	-0.80	0.76	-0.55
Levoglucosan	-0.47	-0.61	0.78	-0.75	-0.89	0.73	-0.79	0.87	-0.66	-0.60	-0.84	0.88	-0.89
5-HMF	-0.54	-0.66	0.83	-0.80	-0.87	0.71	-0.82	0.90	-0.65	-0.65	-0.80	0.85	-0.85
Furfural	-0.64	-0.86	0.83	-0.82	-0.57	0.35	-0.61	0.82	-0.87	-0.48	-0.51	0.58	-0.69
2-Methylfuran	0.12	0.26	0.22	-0.02	-0.68	0.88	-0.65	0.40	0.31	-0.55	-0.72	0.70	-0.45
2(5H)-Furanone	-0.12	-0.42	0.43	-0.47	-0.69	0.53	-0.39	0.51	-0.71	-0.15	-0.76	0.79	-0.90
Methyl acetate	0.89	1.00	-0.86	0.90	0.27	0.01	0.48	-0.76	0.81	0.48	0.10	-0.19	0.30
Formic acid	-0.90	-0.86	1.00	-0.94	-0.59	0.42	-0.86	0.97	-0.56	-0.84	-0.39	0.47	-0.42
Acetic acid	0.89	0.90	-0.94	1.00	0.56	-0.32	0.75	-0.91	0.64	0.72	0.34	-0.42	0.42
Acetol	1.00	0.89	-0.90	0.89	0.24	-0.05	0.64	-0.80	0.47	0.73	-0.02	-0.07	0.04
Propanoic acid	0.24	0.27	-0.59	0.56	1.00	-0.93	0.81	-0.74	0.31	0.62	0.94	-0.96	0.86
[1]Lignin	-0.05	0.01	0.42	-0.32	-0.93	1.00	-0.79	0.61	0.01	-0.63	-0.93	0.92	-0.73
[1]Extractives	0.64	0.48	-0.86	0.75	0.81	-0.79	1.00	-0.94	0.19	0.96	0.65	-0.70	0.51
[1]VM	-0.80	-0.76	0.97	-0.91	-0.74	0.61	-0.94	1.00	-0.50	-0.88	-0.57	0.64	-0.56
[1]FC	0.47	0.81	-0.56	0.64	0.31	0.01	0.19	-0.50	1.00	0.04	0.29	-0.35	0.60
[1]AC	0.73	0.48	-0.84	0.72	0.62	-0.63	0.96	-0.88	0.04	1.00	0.41	-0.46	0.24
[1]C_5	-0.02	0.10	-0.39	0.34	0.94	-0.93	0.65	-0.57	0.29	0.41	1.00	-1.00	0.93
[1]C_6	-0.07	-0.19	0.47	-0.42	-0.96	0.92	-0.70	0.64	-0.35	-0.46	-1.00	1.00	-0.94
[1]Acetyl	0.04	0.30	-0.42	0.42	0.86	-0.73	0.51	-0.56	0.60	0.24	0.93	-0.94	1.00

[1] Supplementary variables

Appendix B

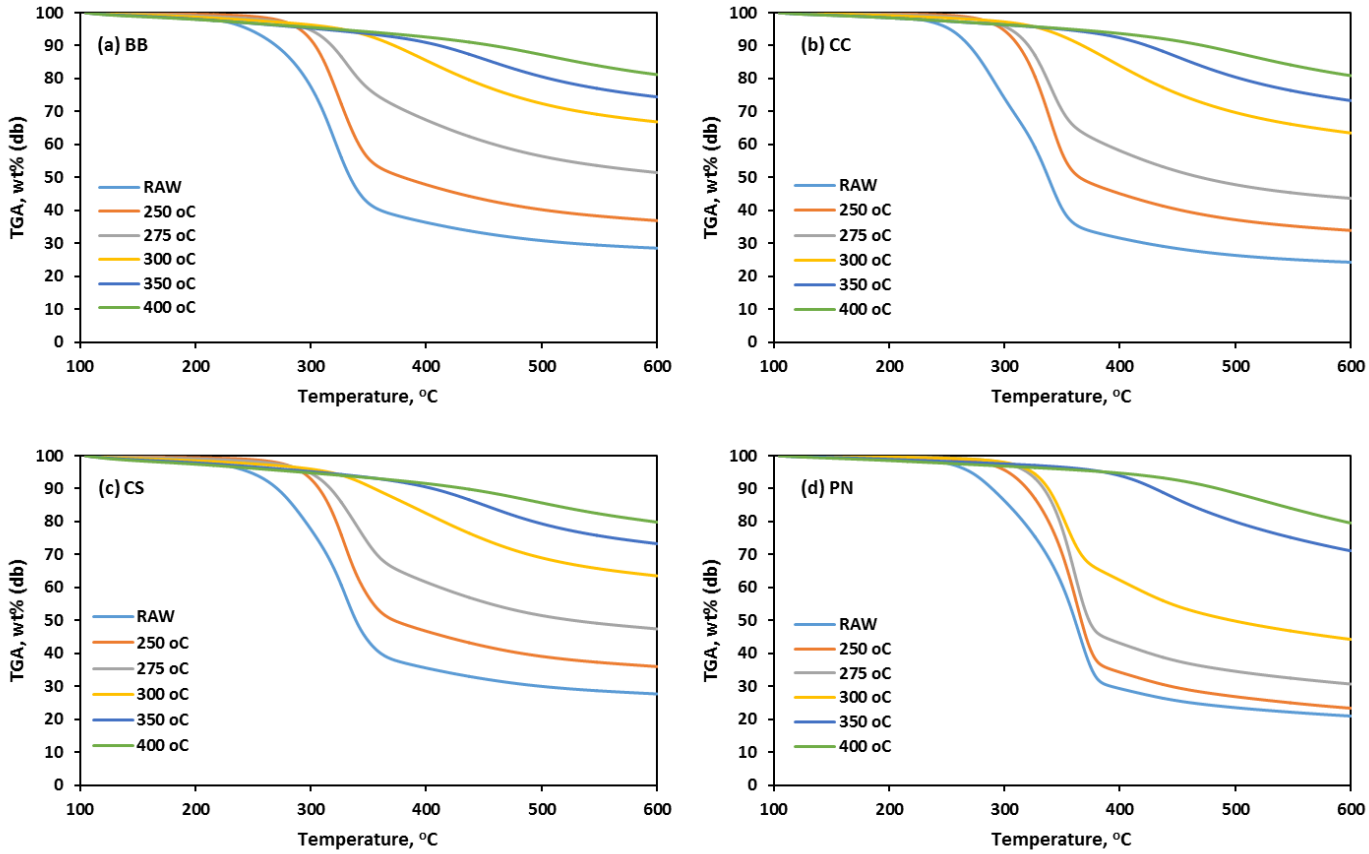

Figure B-1: Thermogravimetric Analysis (TGA) of biomass samples pretreated at different temperatures (60 min Hold Time) during devolatilization

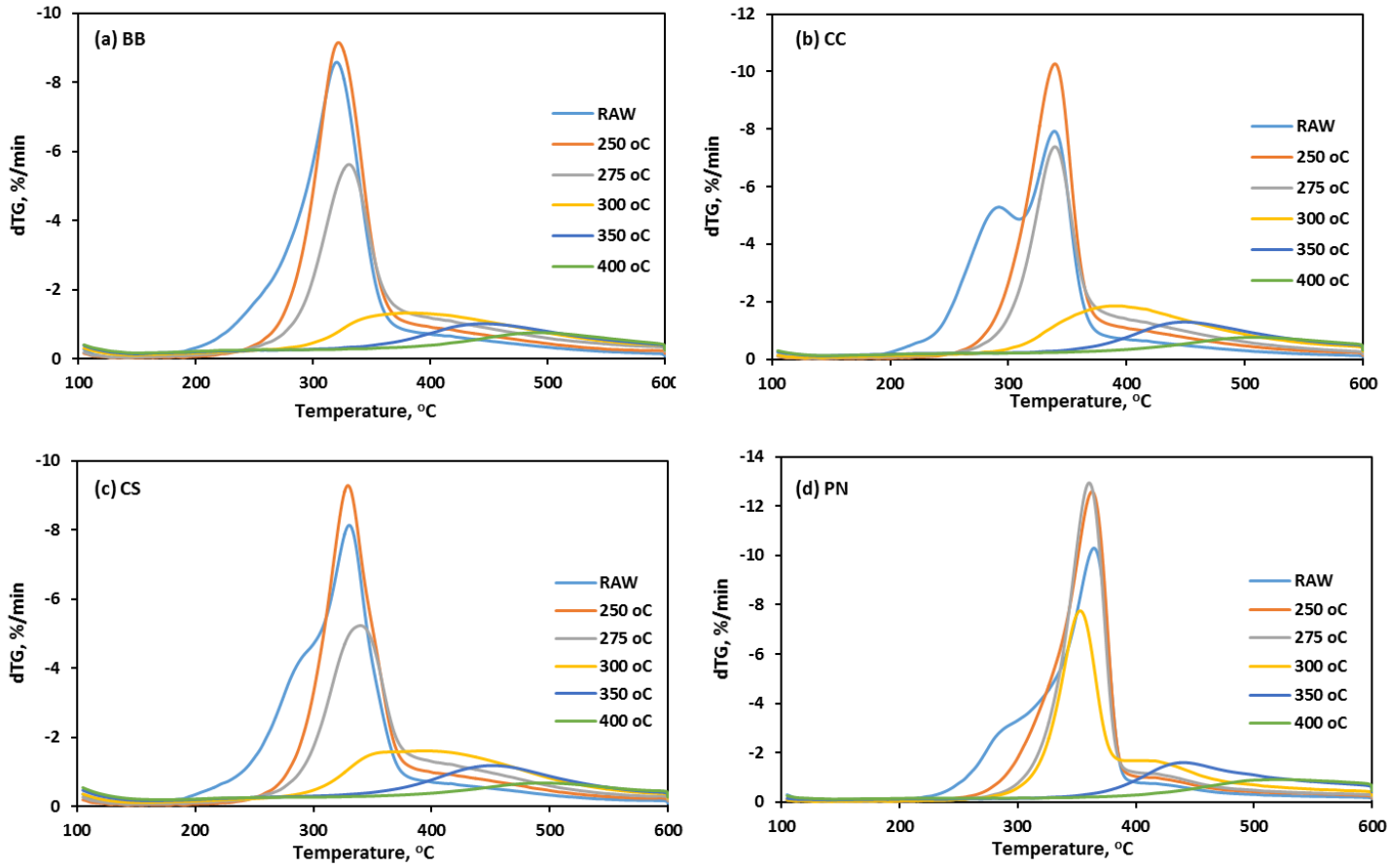

Figure B-2: Derivative thermogravimetric (DTG) curves of biomass samples pretreated at different temperatures (60 min Hold Time) during devolatilization

Table B-1: Yields (µg/mg, dry basis) of devolatilization volatile products from raw and thermally pretreated biomass (Pine, Corn cob and Corn stover) – (nq: not quantified)

Compound	Raw	Char								
		250 ºC		275ºC		300 ºC		350 ºC		400 ºC	
		30 min	60 min	30 min	60 min	30 min	60 min	30 min	60 min	30 min	60 min
PINE (PN)											
Acids											
Formic acid	27.43	10.22	10.89	7.98	7.75	8.14	6.73	0.00	0.00	0.00	0.00
Acetic acid	62.01	52.41	54.03	45.45	44.16	40.79	33.60	0.00	0.00	0.00	0.00
Propanoic acid	2.61	2.57	2.90	2.33	2.52	0.00	0.00	0.00	0.00	0.00	0.00
Sub-total	**92.05**	**65.20**	**67.82**	**55.76**	**54.42**	**48.93**	**40.32**	**0.00**	**0.00**	**0.00**	**0.00**
Ketones											
2,3-Butanedione	4.77	3.63	3.84	3.64	3.42	3.14	2.81	0.00	0.00	0.00	0.00
Hydroxy acetone	21.62	21.97	21.27	21.95	21.19	21.93	10.45	0.00	0.00	0.00	0.00
2-Cyclopenten-1-one	1.58	2.38	2.32	1.93	2.26	2.56	2.58	0.00	0.00	0.00	0.00
2-Hydroxy-3-methyl-2-cyclopentene	4.76	4.37	3.66	2.80	3.46	3.47	2.53	0.00	0.00	0.00	0.00
Sub-total	**32.73**	**32.36**	**31.09**	**30.32**	**30.33**	**31.10**	**18.37**	**0.00**	**0.00**	**0.00**	**0.00**
Furans											
2-Methylfuran	1.74	4.78	4.63	4.02	4.02	4.30	3.55	0.32	0.31	0.00	0.00
Furfural	9.55	10.12	10.02	8.04	7.48	8.35	6.55	0.00	0.00	0.00	0.00
Furfuryl alcohol	25.94	15.91	14.40	13.67	13.04	11.42	7.58	0.00	0.00	0.00	0.00
Benzofuran	0.02	0.11	0.13	0.12	0.13	0.14	0.15	0.13	0.14	0.11	0.12
5-Methyl furfural	1.82	1.13	1.16	1.27	1.54	1.29	1.04	0.00	0.00	0.00	0.00
2(5H)-Furanone	6.06	10.63	10.49	7.23	8.09	6.44	4.45	0.00	0.00	0.00	0.00
5-Hydroxymethylfurfural	7.39	4.29	4.16	4.06	3.89	3.82	3.15	0.00	0.00	0.00	0.00
Sub-total	**52.51**	**46.96**	**44.99**	**38.42**	**38.19**	**35.76**	**26.46**	**0.44**	**0.45**	**0.11**	**0.12**
Anhydrosugar											
Levoglucosan	21.20	26.99	27.73	24.22	22.24	21.51	22.04	0.00	0.00	0.00	0.00
Phenolics											
Phenol	0.54	1.01	0.83	0.76	1.03	1.32	1.56	0.97	1.44	0.38	0.45
Guaiacol	2.35	4.00	3.83	3.12	3.54	3.96	3.72	0.64	0.82	0.04	0.05
o-Cresol	0.17	0.49	0.38	0.38	0.52	0.71	0.76	0.41	0.73	0.06	0.10
Maltol	2.67	2.25	2.40	2.05	2.49	2.89	1.76	0.00	0.00	0.00	0.00
m&p-Cresol	0.12	0.44	0.30	0.30	0.44	0.63	0.79	0.39	0.69	0.08	0.11
Creosol	2.39	4.94	4.27	3.66	4.31	4.83	4.85	0.48	0.67	0.05	0.07
4-Ethyl-phenol	0.09	0.12	0.14	0.06	0.08	0.13	0.15	0.07	0.12	0.02	0.02
2,4-Xylenol	0.02	0.05	0.04	0.03	0.05	0.09	0.11	0.06	0.12	0.01	0.01
2-Methoxy-4-vinylphenol	3.63	6.16	4.34	2.63	2.67	2.34	1.83	0.06	0.07	0.02	0.03
Eugenol	0.43	0.50	0.31	0.19	0.19	0.18	0.15	0.00	0.00	0.00	0.00
4-Propyl guaiacol	0.13	0.20	0.13	0.11	0.13	0.17	0.16	0.02	0.02	0.00	0.01
2,6-Dimethoxy phenol	5.01	7.58	5.90	5.24	6.09	6.60	4.89	0.31	0.33	0.00	0.00
trans-Isoeugenol	5.00	9.19	6.05	4.06	4.02	0.00	0.00	0.00	0.00	0.00	0.00

Isoeugenol	1.13	5.99	4.80	2.91	2.58	1.98	1.40	0.06	0.07	0.03	0.11
Apocynin	0.53	0.16	0.15	0.35	0.32	0.34	0.21	0.02	0.02	0.02	0.02
Sub-total	**24.21**	**43.07**	**33.87**	**25.86**	**28.46**	**26.16**	**22.33**	**3.47**	**5.10**	**0.72**	**0.98**
Aromatic hydrocarbons											
Benzene	0.32	0.36	0.31	0.28	0.34	0.43	0.46	0.32	0.41	0.25	0.32
Toluene	0.54	nq	nq	0.75	0.90	1.18	1.38	0.74	1.20	0.34	0.59
Ethylbenzene	0.00	0.08	0.09	0.09	0.09	0.10	0.11	0.08	0.10	0.07	0.07
p-xylene	0.13	0.18	0.24	0.22	0.27	0.35	0.42	0.23	0.38	0.10	0.16
o-xylene	0.04	0.05	0.05	0.05	0.06	0.07	0.09	0.05	0.07	0.02	0.03
Naphthalene	0.02	0.03	0.03	0.03	0.04	0.07	0.07	0.09	0.08	0.03	0.19
Sub-total	**1.04**	**0.70**	**0.73**	**1.42**	**1.70**	**2.20**	**2.54**	**1.51**	**2.24**	**0.80**	**1.36**
Total Volatile Yield	**223.74**	**215.28**	**206.23**	**175.99**	**175.35**	**165.66**	**132.07**	**5.43**	**7.79**	**1.63**	**2.46**
CORN COB (CC)											
Acids											
Formic acid	22.48	22.78	20.26	5.74	3.05	0.00	0.00	0.00	0.00	0.00	0.00
Acetic acid	71.33	56.52	53.14	46.55	42.04	25.45	24.68	0.00	0.00	0.00	0.00
Propanoic acid	6.10	3.99	3.61	2.91	2.70	0.00	0.00	0.00	0.00	0.00	0.00
Sub-total	**99.91**	**83.29**	**77.01**	**55.19**	**47.78**	**25.45**	**24.68**	**0.00**	**0.00**	**0.00**	**0.00**
Ketones											
2,3-Butanedione	5.13	6.91	6.90	5.82	6.23	1.71	2.02	0.00	0.00	0.00	0.00
Hydroxy acetone	18.48	28.03	25.50	26.39	13.86	0.00	0.00	0.00	0.00	0.00	0.00
2-Cyclopenten-1-one	2.47	4.11	4.27	4.59	5.00	1.83	2.09	0.00	0.00	0.00	0.00
2-Hydroxy-3-methyl-2-cyclopentene	3.00	2.47	2.39	2.56	2.44	0.40	0.06	0.00	0.00	0.00	0.00
Sub-total	**29.08**	**41.51**	**39.07**	**39.36**	**27.53**	**3.95**	**4.17**	**0.00**	**0.00**	**0.00**	**0.00**
Furans											
2-Methylfuran	1.39	3.89	4.09	5.07	4.89	2.02	2.36	0.22	0.28	0.00	0.00
Furfural	6.58	8.02	7.36	6.90	6.11	0.00	0.00	0.00	0.00	0.00	0.00
Furfuryl alcohol	17.82	11.31	10.34	10.12	8.94	0.71	0.72	0.00	0.00	0.00	0.00
Benzofuran	0.02	0.13	0.13	0.13	0.14	0.13	0.14	0.12	0.12	0.00	0.00
5-Methyl furfural	0.86	0.71	0.77	0.75	0.84	0.45	0.00	0.00	0.00	0.00	0.00
2(5H)-Furanone	3.37	4.83	5.23	4.61	3.97	0.67	0.28	0.00	0.00	0.00	0.00
5-Hydroxymethylfurfural	4.00	0.60	1.17	0.51	0.00	0.00	0.00	0.00	0.00	0.00	0.00
Sub-total	**34.05**	**29.49**	**29.09**	**28.09**	**24.89**	**4.00**	**3.51**	**0.34**	**0.40**	**0.00**	**0.00**
Anhydrosugar											
Levoglucosan	2.59	2.99	2.41	2.62	2.53	0.84	0.25	0.00	0.00	0.00	0.00
Phenolics											
Phenol	2.22	4.13	4.21	4.46	5.06	3.14	4.72	1.47	2.02	0.71	0.46
Guaiacol	2.25	2.69	2.55	2.42	2.27	1.09	1.32	0.08	0.07	0.00	0.00
o-Cresol	0.21	0.72	0.77	0.92	1.10	0.68	1.25	0.35	0.58	0.14	0.07
Maltol	1.23	0.87	1.48	1.44	1.60	0.27	0.00	0.00	0.00	0.00	0.00
m&*p*-Cresol	0.26	0.81	0.86	0.94	1.27	0.85	1.56	0.40	0.63	0.16	0.08
Creosol	0.40	0.92	0.95	1.03	1.03	0.51	0.69	0.03	0.03	0.00	0.00
4-Ethyl-phenol	0.33	0.64	0.66	0.64	0.76	0.46	0.98	0.15	0.25	0.03	0.01

2,4-Xylenol	0.00	0.06	0.07	0.07	0.09	0.07	0.15	0.03	0.07	0.01	0.01
2-Methoxy-4-vinylphenol	5.65	3.27	2.51	1.46	1.45	0.33	0.33	0.00	0.00	0.00	0.00
Eugenol	0.05	0.00	0.00	0.00	0.00	0.00	0.00	0.00	0.00	0.00	0.00
4-Propyl guaiacol	0.04	0.03	0.03	0.04	0.04	0.02	0.03	0.00	0.00	0.00	0.00
2,6-Dimethoxy-phenol	1.31	2.08	1.70	1.39	1.27	0.37	0.42	0.02	0.02	0.00	0.00
trans-Isoeugenol	0.56	0.00	0.00	0.00	0.00	0.00	0.00	0.00	0.00	0.00	0.00
Isoeugenol	0.17	0.59	0.47	0.36	0.36	0.11	0.14	0.00	0.00	0.00	0.00
Apocynin	0.18	0.09	0.08	0.11	0.13	0.04	0.05	0.01	0.00	0.00	0.00
Sub-total	**14.83**	**16.91**	**16.35**	**15.26**	**16.42**	**7.94**	**11.65**	**2.54**	**3.67**	**1.05**	**0.63**
Aromatic hydrocarbons											
Benzene	0.37	0.40	0.39	0.50	0.50	0.45	0.53	0.44	0.37	0.38	0.39
Toluene	0.79	nq	nq	1.97	2.13	1.78	2.18	1.08	1.36	0.91	0.61
Ethylbenzene	0.03	0.13	0.13	0.15	0.16	0.12	0.16	0.10	0.12	0.08	0.00
p-xylene	0.18	0.43	0.48	0.58	0.65	0.43	0.70	0.31	0.44	0.27	0.22
o-xylene	0.05	0.11	0.13	0.15	0.17	0.10	0.17	0.07	0.09	0.04	0.00
Naphthalene	0.03	0.05	0.05	0.08	0.08	0.20	0.10	0.09	0.25	0.08	0.07
Sub-total	**1.46**	**1.11**	**1.17**	**3.43**	**3.69**	**3.09**	**3.83**	**2.09**	**2.64**	**1.77**	**1.28**
Total Volatile Yield	**181.92**	**175.29**	**165.09**	**143.96**	**122.83**	**45.27**	**48.09**	**4.97**	**6.70**	**2.82**	**1.92**
CORN STOVER (CS)											
Acids											
Formic acid	10.86	16.02	13.94	6.48	2.81	0.00	0.00	0.00	0.00	0.00	0.00
Acetic acid	89.90	77.30	66.19	50.65	37.28	26.81	26.05	0.00	0.00	0.00	0.00
Propanoic acid	6.15	4.34	4.86	4.08	3.54	0.00	0.00	0.00	0.00	0.00	0.00
Sub-total	**106.91**	**97.66**	**84.98**	**61.21**	**43.63**	**26.81**	**26.05**	**0.00**	**0.00**	**0.00**	**0.00**
Ketones											
2,3-Butanedione	6.88	8.93	8.56	7.17	5.45	1.95	2.12	0.00	0.00	0.00	0.00
Hydroxy acetone	31.80	36.71	37.61	27.60	17.57	0.00	0.00	0.00	0.00	0.00	0.00
2-Cyclopenten-1-one	4.20	4.89	5.05	4.90	4.10	2.54	2.65	0.00	0.00	0.00	0.00
2-Hydroxy-3-methyl-2-cyclopentene	4.47	2.93	3.08	2.56	1.88	0.39	0.15	0.00	0.00	0.00	0.00
Sub-total	**47.35**	**53.45**	**54.30**	**42.23**	**29.00**	**4.88**	**4.92**	**0.00**	**0.00**	**0.00**	**0.00**
Furans											
2-Methylfuran	1.28	3.52	3.62	4.09	3.65	1.57	1.93	0.19	0.23	0.00	0.00
Furfural	6.25	8.64	7.89	6.61	5.50	0.00	0.00	0.00	0.00	0.00	0.00
Furfuryl alcohol	13.67	4.63	4.72	3.33	1.78	0.76	0.76	0.00	0.00	0.00	0.00
Benzofuran	0.00	0.13	0.13	0.14	0.13	0.12	0.13	0.00	0.00	0.00	0.00
5-Methyl furfural	1.02	0.72	0.79	0.86	0.75	0.42	0.00	0.00	0.00	0.00	0.00
2(5H)-Furanone	4.90	7.06	6.79	5.13	3.32	0.85	0.00	0.00	0.00	0.00	0.00
5-Hydroxymethylfurfural	3.58	0.62	0.99	0.61	0.00	0.00	0.00	0.00	0.00	0.00	0.00
Sub-total	**30.68**	**25.31**	**24.92**	**20.76**	**15.12**	**3.72**	**2.81**	**0.19**	**0.23**	**0.00**	**0.00**
Anhydrosugar											
Levoglucosan	2.29	2.38	1.95	2.22	1.45	0.79	0.31	0.00	0.00	0.00	0.00
Phenolics											
Phenol	3.01	3.50	3.66	3.47	3.29	2.31	3.56	1.19	1.52	0.54	0.37

Guaiacol	1.88	1.90	1.78	1.52	1.19	0.60	0.69	0.02	0.02	0.00	0.00
o-Cresol	0.53	0.70	0.76	0.86	0.90	0.67	1.06	0.34	0.46	0.12	0.07
Maltol	1.42	0.85	1.23	1.52	1.39	0.10	0.00	0.00	0.00	0.00	0.00
m&*p*-Cresol	0.47	0.68	0.72	0.86	0.95	0.63	1.06	0.32	0.45	0.12	0.07
Creosol	0.32	0.55	0.50	0.55	0.50	0.27	0.32	0.01	0.01	0.00	0.00
4-Ethyl-phenol	0.48	0.49	0.50	0.50	0.66	0.33	0.55	0.13	0.20	0.03	0.02
2,4-Xylenol	0.00	0.06	0.06	0.06	0.09	0.05	0.07	0.02	0.04	0.01	0.00
2-Methoxy-4-vinylphenol	3.34	2.44	1.79	1.01	0.83	0.16	0.14	0.00	0.00	0.00	0.00
Eugenol	0.04	0.05	0.00	0.00	0.00	0.00	0.00	0.00	0.00	0.00	0.00
4-Propyl guaiacol	0.02	0.04	0.03	0.04	0.04	0.01	0.02	0.00	0.00	0.00	0.00
2,6-Dimethoxy-phenol	1.69	2.01	1.41	1.21	0.97	0.20	0.18	0.01	0.01	0.00	0.00
trans-Isoeugenol	0.66	1.42	0.00	0.00	0.00	0.00	0.00	0.00	0.00	0.00	0.00
Isoeugenol	0.11	0.85	0.43	0.40	0.36	0.08	0.07	0.00	0.00	0.00	0.00
Apocynin	0.06	0.09	0.07	0.13	0.10	0.02	0.01	0.00	0.00	0.00	0.00
Sub-total	**14.04**	**15.61**	**12.95**	**12.14**	**11.27**	**5.43**	**7.75**	**2.03**	**2.72**	**0.82**	**0.53**
Aromatic hydrocarbons											
Benzene	0.48	0.49	0.52	0.57	0.52	0.66	0.64	0.44	0.49	0.50	0.48
Toluene	1.31	nq	nq	2.23	2.13	2.14	2.68	1.06	1.60	1.03	0.84
Ethylbenzene	0.05	0.14	0.15	0.16	0.16	0.15	0.18	0.10	0.12	0.08	0.07
p-xylene	0.35	0.51	0.56	0.65	0.63	0.57	0.80	0.38	0.51	0.35	0.29
o-xylene	0.09	0.13	0.14	0.16	0.16	0.14	0.20	0.09	0.12	0.07	0.00
Naphthalene	0.03	0.06	0.06	0.08	0.08	0.11	0.10	0.22	0.10	0.09	0.26
Sub-total	**2.31**	**1.33**	**1.43**	**3.85**	**3.68**	**3.78**	**4.61**	**2.30**	**2.93**	**2.11**	**1.95**
Total Volatile Yield	**203.59**	**195.74**	**180.54**	**142.41**	**104.16**	**45.41**	**46.45**	**4.52**	**5.88**	**2.93**	**2.47**

Appendix C

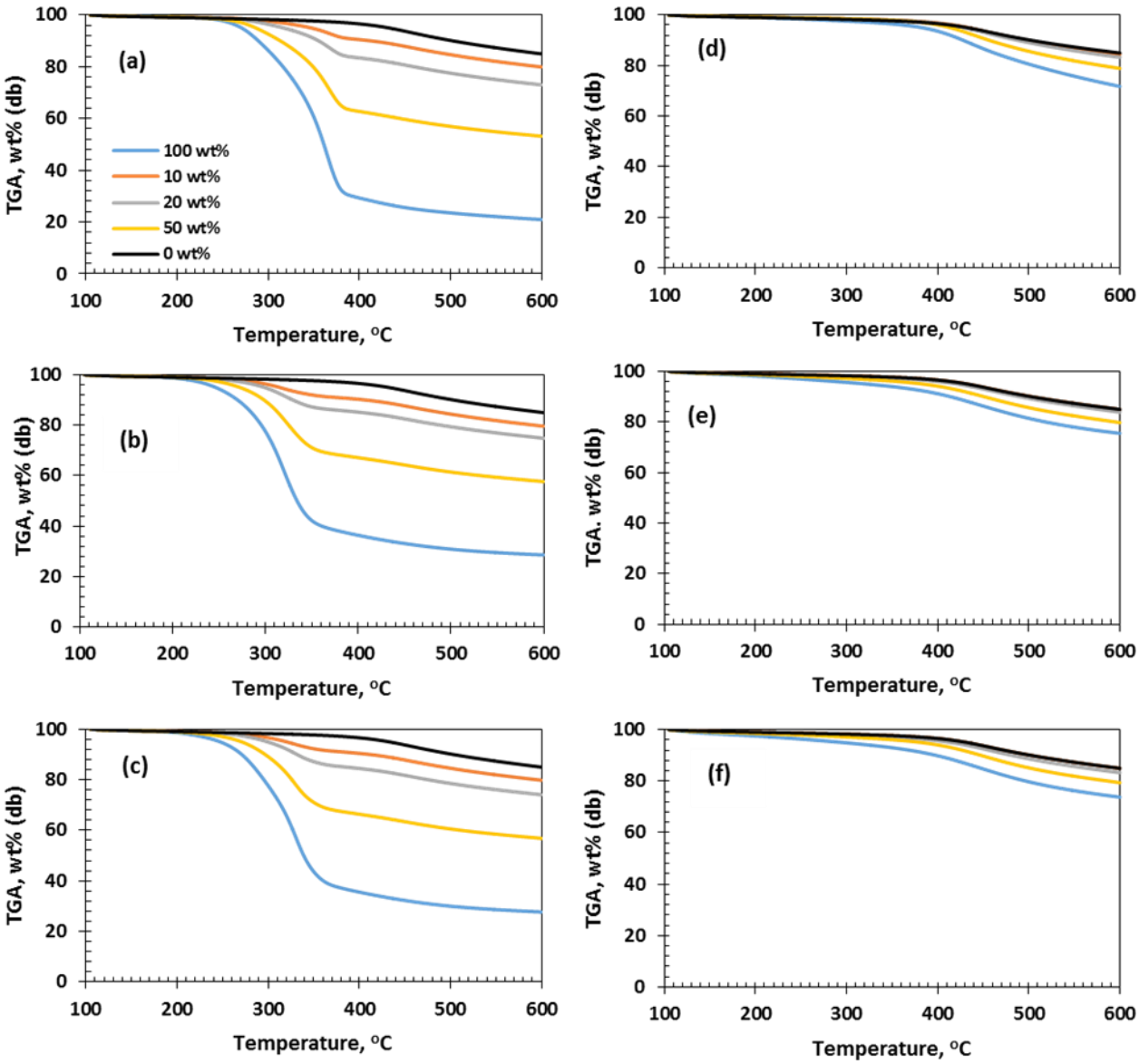

Figure C-1: Devolatilization characteristics of raw biomass/char and coal blends (a) PN_{raw} (b) BB_{raw}, (c) CS_{raw} (d) PN_{char}, (e) BB_{char}, (e) CS_{char}

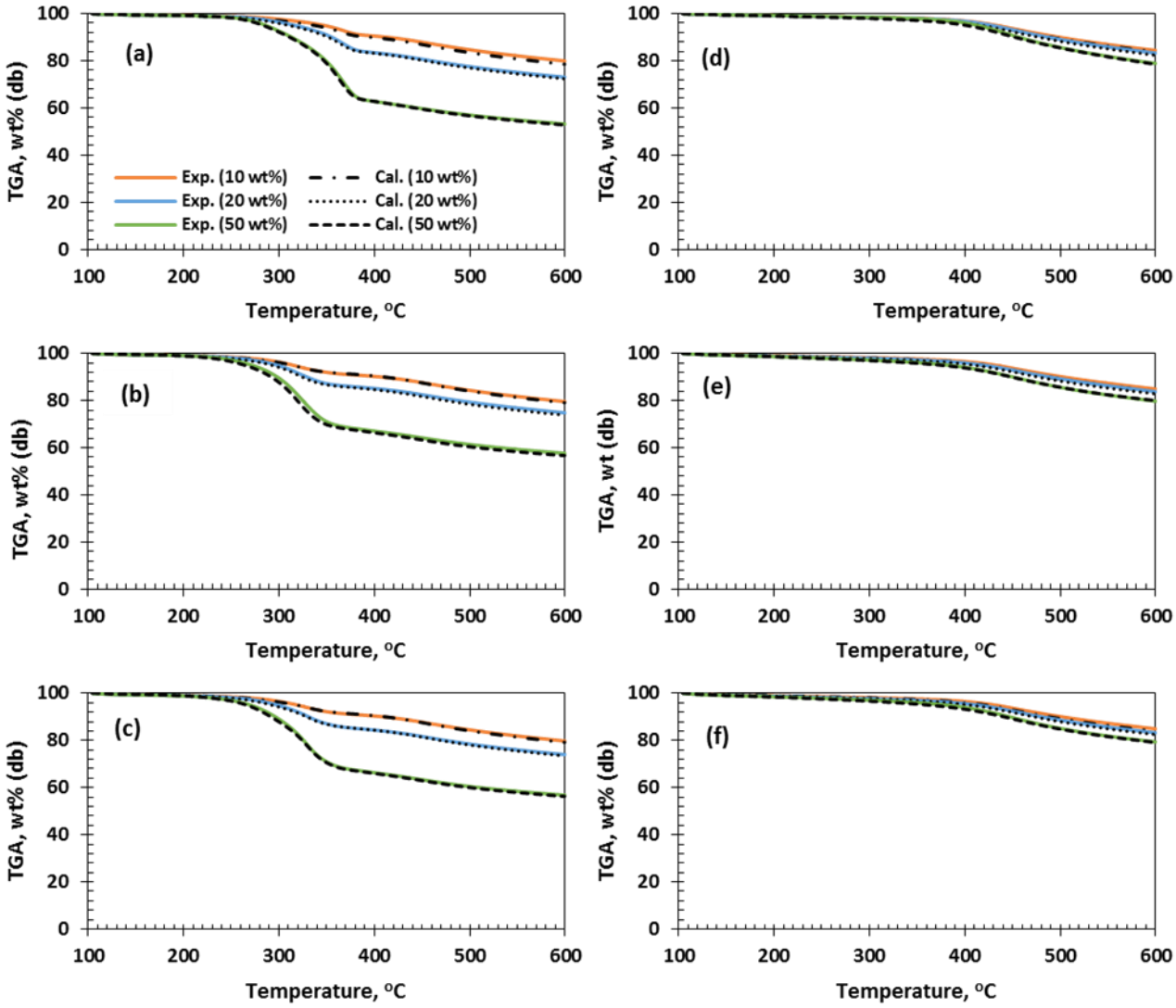

Fig. C-2: Comparison of experimental and calculated TGA curves of raw biomass/char and coal blends (a) PN_{raw} (b) BB_{raw}, (c) CS_{raw} (d) PN_{char}, (e) BB_{char}, (e) CS_{char}

Table C-1: Kinetic parameters

		100 wt%			10 wt%			20 wt%			50 wt%		
	α	E (kJ/mol)	Ln(A·f(α))(1/s)	R^2	E (kJ/mol)	Ln(A·f(α))(1/s)	R^2	E (kJ/mol)	Ln(A·f(α))(1/s)	R^2	E (kJ/mol)	Ln(A·f(α))(1/s)	R^2
PNraw													
	0.10	203.72	14.65	0.986	210.88	13.46	0.971	217.82	14.22	0.968	230.79	15.94	0.987
	0.15	232.02	17.64	0.993	211.21	13.51	0.999	216.14	14.04	0.995	199.01	12.67	0.988
	0.20	250.98	19.58	0.996	191.83	11.67	0.999	203.34	12.81	1.000	189.79	11.75	0.983
	0.25	253.24	19.76	0.999	190.34	11.53	0.998	198.08	12.31	0.999	195.17	12.24	0.995
	0.30	258.75	20.29	0.998	202.20	12.63	1.000	209.32	13.36	1.000	198.28	12.51	0.996
	0.35	256.60	20.03	0.999	204.34	12.80	0.999	211.15	13.49	1.000	191.72	11.85	0.998
	0.40	251.57	19.47	0.999	207.16	13.02	0.999	213.62	13.67	1.000	196.27	12.23	0.999
	0.45	241.67	18.43	0.998	212.33	13.44	1.000	217.39	13.96	1.000	203.82	12.89	0.999
	0.50	232.72	17.48	0.998	216.16	13.72	1.000	221.16	14.24	1.000	205.60	12.98	0.999
	0.55	224.75	16.63	0.998	219.50	13.95	1.000	222.98	14.32	1.000	211.31	13.43	1.000
	0.60	222.28	16.33	0.998	222.37	14.13	1.000	226.16	14.52	1.000	216.59	13.82	1.000
	0.65	215.06	15.55	0.998	224.85	14.25	1.000	228.53	14.63	1.000	219.85	14.01	1.000
	0.70	210.31	15.02	0.998	226.75	14.31	1.000	229.11	14.56	1.000	222.01	14.08	1.000
	0.75	206.89	14.61	0.998	228.42	14.32	1.000	229.79	14.48	1.000	222.82	14.01	0.999
	0.80	204.61	14.30	0.997	230.58	14.34	1.000	231.94	14.50	1.000	223.36	13.87	0.999
	0.85	197.98	13.51	0.995	235.12	14.54	1.000	231.90	14.27	1.000	221.81	13.49	0.998
	0.90	183.84	11.93	0.991	238.57	14.55	0.999	235.64	14.31	0.999	215.36	12.58	0.998
	Avg	226.29			216.04			220.24			209.62		
PNchar													
	0.10	294.61	23.56	0.987	213.25	13.80	0.972	228.66	15.48	0.978	249.35	17.97	0.994
	0.15	272.65	21.12	0.998	208.22	13.27	0.997	202.83	12.87	0.982	203.33	13.26	0.982
	0.20	251.77	18.91	1.000	190.24	11.54	0.999	204.44	12.99	0.998	180.38	10.92	0.986
	0.25	228.85	16.52	0.998	190.58	11.57	0.999	192.66	11.84	1.000	175.39	10.39	0.994
	0.30	206.37	14.20	0.996	202.79	12.71	1.000	193.20	11.87	0.999	178.61	10.66	0.999
	0.35	188.85	12.41	0.995	205.13	12.89	1.000	204.26	12.88	1.000	179.96	10.76	1.000
	0.40	177.34	11.23	0.997	209.19	13.22	1.000	207.40	13.13	1.000	184.82	11.18	0.999
	0.45	171.29	10.61	0.998	214.35	13.64	1.000	210.77	13.38	1.000	195.25	12.12	1.000
	0.50	168.52	10.32	0.999	219.09	14.01	1.000	216.21	13.82	1.000	202.80	12.77	1.000
	0.55	168.40	10.30	0.999	220.41	14.04	1.000	220.07	14.10	1.000	208.54	13.23	1.000
	0.60	169.55	10.39	0.998	224.35	14.31	1.000	221.88	14.17	1.000	215.56	13.79	1.000
	0.65	172.15	10.63	0.997	226.54	14.40	1.000	225.12	14.36	1.000	223.41	14.41	1.000
	0.70	175.25	10.91	0.997	227.96	14.41	1.000	228.12	14.52	1.000	230.17	14.90	1.000
	0.75	177.96	11.15	0.997	230.52	14.49	1.000	229.06	14.46	1.000	235.95	15.28	1.000
	0.80	180.95	11.42	0.996	231.46	14.40	0.999	230.91	14.45	1.000	243.21	15.74	1.000
	0.85	179.77	11.27	0.995	236.97	14.67	1.000	230.09	14.15	0.999	249.36	16.04	1.000
	0.90	172.19	10.47	0.994	241.97	14.82	1.000	235.73	14.35	1.000	252.76	15.98	1.000
	Avg	197.44			217.24			216.55			212.28		

Table C-1 cont.

		100 wt%			10 wt%			20 wt%			50 wt%		
	α	E (kJ/mol)	Ln(A·f(α))(1/s)	R^2	E (kJ/mol)	Ln(A·f(α))(1/s)	R^2	E (kJ/mol)	Ln(A·f(α))(1/s)	R^2	E (kJ/mol)	Ln(A·f(α))(1/s)	R^2
BBraw													
	0.10	224.44	17.34	0.991	208.85	13.25	0.970	217.43	14.06	0.974	228.67	15.48	0.984
	0.15	221.29	17.12	0.992	207.85	13.18	0.998	217.57	14.11	0.999	223.57	14.99	0.984
	0.20	215.38	16.61	0.994	184.74	10.99	0.999	196.54	12.12	0.999	220.43	14.68	0.991
	0.25	204.72	15.59	0.994	195.38	12.01	0.999	208.18	13.23	1.000	206.26	13.30	0.995
	0.30	196.70	14.85	0.994	203.46	12.75	1.000	215.75	13.92	1.000	215.06	14.11	0.994
	0.35	187.91	14.03	0.994	206.04	12.96	1.000	218.74	14.16	1.000	220.24	14.55	0.995
	0.40	181.46	13.44	0.994	211.59	13.42	1.000	222.89	14.49	1.000	221.72	14.63	0.995
	0.45	177.36	13.07	0.994	215.69	13.74	1.000	227.50	14.86	1.000	225.90	14.96	0.995
	0.50	173.39	12.70	0.992	220.33	14.10	1.000	231.50	15.15	1.000	231.59	15.41	0.995
	0.55	170.95	12.47	0.990	222.27	14.20	1.000	234.44	15.34	1.000	236.36	15.76	0.995
	0.60	169.29	12.30	0.988	224.74	14.33	1.000	238.03	15.57	1.000	239.73	15.97	0.996
	0.65	167.14	12.07	0.988	226.69	14.41	1.000	241.82	15.81	1.000	243.80	16.23	0.997
	0.70	164.32	11.74	0.988	229.82	14.57	1.000	244.81	15.96	1.000	248.53	16.53	0.997
	0.75	162.22	11.46	0.989	231.77	14.61	1.000	247.93	16.09	1.000	251.72	16.66	0.998
	0.80	161.52	11.28	0.989	234.72	14.69	0.999	250.26	16.11	1.000	254.92	16.76	0.998
	0.85	163.93	11.35	0.989	242.97	15.21	0.999	257.36	16.50	1.000	257.70	16.75	0.998
	0.90	166.74	11.34	0.991	247.90	15.33	0.998	263.54	16.70	0.999	257.98	16.38	0.997
	Avg	182.87			218.52			231.43			234.37		
BBchar													
	0.10	216.32	16.03	1.000	211.83	13.47	0.984	204.28	12.75	0.997	222.39	15.21	0.997
	0.15	211.93	15.68	1.000	210.25	13.36	0.999	206.11	12.97	1.000	215.13	14.48	0.998
	0.20	207.12	15.26	1.000	189.60	11.41	0.998	188.90	11.35	0.996	211.08	14.09	0.996
	0.25	200.94	14.69	1.000	205.40	12.91	0.999	196.61	12.08	0.997	214.54	14.41	0.998
	0.30	195.15	14.17	1.000	211.41	13.46	1.000	203.47	12.71	0.998	215.64	14.50	0.998
	0.35	188.50	13.57	1.000	214.05	13.66	0.999	205.60	12.87	0.997	211.83	14.11	0.999
	0.40	180.94	12.89	1.000	219.04	14.07	1.000	209.45	13.18	0.997	211.23	14.02	0.999
	0.45	173.04	12.17	0.999	223.12	14.39	1.000	214.66	13.60	0.997	216.49	14.48	0.998
	0.50	165.71	11.50	0.999	226.60	14.63	1.000	219.28	13.96	0.998	217.90	14.57	0.997
	0.55	160.30	11.01	0.999	230.90	14.95	1.000	223.33	14.25	0.998	217.78	14.50	0.997
	0.60	156.90	10.70	0.999	235.37	15.26	1.000	228.01	14.59	0.998	217.34	14.39	0.995
	0.65	155.07	10.53	0.999	239.03	15.48	1.000	232.24	14.86	0.998	217.20	14.31	0.994
	0.70	154.16	10.43	0.999	243.61	15.77	1.000	236.69	15.14	0.998	215.62	14.08	0.992
	0.75	153.17	10.29	0.999	248.36	16.04	1.000	240.43	15.32	0.998	211.77	13.63	0.991
	0.80	153.21	10.20	0.999	252.07	16.18	0.999	243.89	15.44	0.998	206.26	12.99	0.991
	0.85	154.99	10.22	0.998	264.84	17.08	0.999	252.82	15.99	0.996	198.49	12.10	0.994
	0.90	157.28	10.15	0.998	281.02	18.16	0.998	261.34	16.37	0.993	190.92	11.09	0.997
	Avg	175.57			229.79			221.59			212.45	13.94	1.00

Table C-1 cont.

		100 wt%			10 wt%			20 wt%			50 wt%		
	α	E (kJ/mol)	Ln(A·f(α))(1/s)	R^2	E (kJ/mol)	Ln(A·f(α))(1/s)	R^2	E (kJ/mol)	Ln(A·f(α))(1/s)	R^2	E (kJ/mol)	Ln(A·f(α))(1/s)	R^2
CSraw													
	0.10	276.02	23.10	0.967	212.00	13.57	0.975	220.89	14.53	0.980	232.48	15.99	0.986
	0.15	256.88	20.86	0.988	214.36	13.83	0.997	213.31	13.77	0.998	206.13	13.31	0.994
	0.20	248.84	19.91	0.995	206.94	13.13	0.999	201.41	12.64	1.000	211.42	13.81	0.999
	0.25	238.90	18.80	0.999	192.42	11.75	0.999	191.24	11.68	0.998	212.52	13.92	1.000
	0.30	239.53	18.84	1.000	199.53	12.40	0.999	201.11	12.60	0.999	205.08	13.20	0.999
	0.35	238.94	18.74	0.999	205.48	12.93	1.000	207.68	13.19	0.999	204.42	13.12	0.998
	0.40	233.26	18.12	0.999	208.10	13.13	1.000	210.26	13.39	0.999	210.57	13.67	0.998
	0.45	230.37	17.79	0.999	212.71	13.50	1.000	215.79	13.85	0.999	213.34	13.88	0.998
	0.50	226.19	17.31	0.999	216.97	13.83	1.000	220.73	14.24	1.000	215.05	13.99	0.998
	0.55	222.73	16.91	0.999	220.52	14.07	1.000	224.78	14.53	1.000	219.52	14.33	0.998
	0.60	221.29	16.69	0.999	223.23	14.23	1.000	227.75	14.71	1.000	224.45	14.71	0.998
	0.65	224.20	16.91	0.999	225.68	14.35	1.000	229.07	14.73	1.000	228.15	14.95	0.999
	0.70	228.28	17.21	0.998	228.23	14.47	1.000	232.61	14.93	1.000	231.14	15.11	0.999
	0.75	235.90	17.85	0.998	231.14	14.59	1.000	235.07	15.01	1.000	234.89	15.30	0.999
	0.80	239.46	18.03	0.997	232.55	14.54	1.000	237.03	15.01	1.000	240.43	15.62	0.999
	0.85	247.80	18.62	0.995	235.65	14.60	1.000	238.37	14.90	1.000	242.80	15.58	0.999
	0.90	255.11	19.01	0.993	239.69	14.65	1.000	245.89	15.26	0.999	244.28	15.34	0.999
	Avg	239.04			217.95			220.76			222.16		
CSchar													
	0.10	220.18	16.53	0.997	199.87	12.37	0.960	216.22	14.04	0.973	272.05	20.63	0.995
	0.15	218.31	16.26	0.999	203.80	12.77	0.998	198.49	12.24	0.994	243.61	17.60	0.994
	0.20	216.78	16.07	0.999	183.56	10.86	0.998	184.35	10.92	0.999	224.36	15.59	0.992
	0.25	214.29	15.79	0.999	190.66	11.56	0.998	193.67	11.84	0.999	217.33	14.84	0.995
	0.30	212.36	15.57	0.999	201.62	12.60	0.999	202.41	12.68	1.000	217.40	14.80	0.998
	0.35	210.88	15.39	0.999	204.56	12.85	0.999	207.43	13.14	1.000	216.79	14.71	0.999
	0.40	208.87	15.15	0.999	207.81	13.11	1.000	211.53	13.49	1.000	213.32	14.35	0.999
	0.45	206.00	14.82	0.999	213.14	13.55	1.000	217.76	14.03	1.000	206.47	13.67	1.000
	0.50	203.90	14.56	0.999	217.27	13.87	1.000	222.85	14.44	1.000	211.87	14.15	0.999
	0.55	202.75	14.39	0.999	219.51	14.01	1.000	226.29	14.69	1.000	214.29	14.34	0.999
	0.60	202.66	14.32	0.999	221.88	14.14	1.000	231.01	15.04	1.000	214.84	14.33	0.999
	0.65	202.72	14.26	0.999	223.80	14.22	1.000	234.16	15.23	1.000	214.23	14.21	0.998
	0.70	203.63	14.26	0.999	225.79	14.29	1.000	238.52	15.51	1.000	212.32	13.94	0.998
	0.75	204.69	14.26	0.999	227.80	14.33	1.000	242.90	15.77	1.000	210.52	13.65	0.998
	0.80	204.86	14.15	0.999	228.48	14.22	1.000	246.88	15.95	1.000	208.00	13.25	0.997
	0.85	205.87	14.08	1.000	229.33	14.07	1.000	251.99	16.17	1.000	205.18	12.76	0.997
	0.90	204.61	13.71	1.000	233.74	14.16	1.000	267.42	17.22	1.000	203.17	12.22	0.998
	Avg	208.43			213.68			223.17			217.99		

Table C-1 cont.

Coal	α	E (kJ/mol)	Ln(A·f(α))(1	R^2
	0.10	210.29	13.39	0.974
	0.15	201.24	12.54	0.999
	0.20	185.95	11.10	0.996
	0.25	199.90	12.43	0.998
	0.30	204.96	12.88	0.999
	0.35	207.46	13.08	0.999
	0.40	211.28	13.38	0.999
	0.45	215.50	13.71	1.000
	0.50	217.97	13.87	1.000
	0.55	220.41	14.01	1.000
	0.60	222.02	14.07	1.000
	0.65	224.25	14.16	1.000
	0.70	225.68	14.17	1.000
	0.75	227.62	14.21	1.000
	0.80	230.16	14.26	1.000
	0.85	236.35	14.61	0.999
	0.90	246.32	15.21	0.999
	Avg	216.90		